Graduate School Form 30
Updated 1/15/2015

PURDUE UNIVERSITY
GRADUATE SCHOOL
Thesis/Dissertation Acceptance

This is to certify that the thesis/dissertation prepared

By Hasan Onan Demirel

Entitled
MODULAR HUMAN-IN-THE-LOOP DESIGN FRAMEWORK BASED ON HUMAN FACTORS

For the degree of Doctor of Philosophy

Is approved by the final examining committee:

Vincent G. Duffy
Chair

Mark R. Lehto

Nathan W. Hartman

Senay Purzer

To the best of my knowledge and as understood by the student in the Thesis/Dissertation Agreement, Publication Delay, and Certification Disclaimer (Graduate School Form 32), this thesis/dissertation adheres to the provisions of Purdue University's "Policy of Integrity in Research" and the use of copyright material.

Approved by Major Professor(s): Vincent G. Duffy

Approved by: Abhijit Deshmukh 11/05/2015

Head of the Departmental Graduate Program Date

MODULAR HUMAN-IN-THE-LOOP DESIGN FRAMEWORK BASED ON HUMAN FACTORS

A Dissertation

Submitted to the Faculty

of

Purdue University

by

Hasan Onan Demirel

In Partial Fulfillment of the

Requirements for the Degree

of

Doctor of Philosophy

November 2015

Purdue University

West Lafayette, Indiana

This work is dedicated to Ataturk and to my parents...

ACKNOWLEDGMENTS

This dissertation becomes reality with the kind support and help of many individuals. My deep gratitude goes first to my family. I can not thank enough to them for their unconditional love and support. I would not have been able to get to this stage without their presence and sacrifices.

I am deeply indebted to my advisor Dr. Vincent G. Duffy for giving me the encouragement, motivation and the opportunity to pursue my graduate studies at Purdue University. His feedback and guidance through professional and personal development has been invaluable. It has been a pleasure to work with my committee. I thank my dissertation committee members Dr. Mark Lehto, Dr. Nathan Hartman and Dr. Senay Purzer for their support and guidance throughout my dissertation.

My appreciation also extends to Dr. Barrett Caldwell, Dr. Gavriel Salvendy, Dr. Steven Landry and Dr. Dan Surber. Their feedback, mentorship and intellectual stimulation on my life has been substantial. I would also like to thank Statistical Consulting Service (SCS), especially to Dr. Michael Yu Zhu and Ching-Wei Cheng for their guidance and assistance in developing statistical design of my study.

I am grateful to my friends, who have all helped me to get where I am today. I would like to thank them for their friendship and all invaluable memories.

I have been giving unique opportunities at Purdue, and taken advantage of them. This includes growing-up, learning and living at this campus over ten years. Throughout these years I have been touched by so many individuals, whom I can not name them individually. I acknowledge faculty, staff and friends at Purdue School of Industrial engineering who became a part of my journey.

I would finally like to acknowledge Caomengxing, Abhijatya Gupta and Sameer Bhardwaj (Appendix-C) from GrabCad community for their valuable contributions to open-source vehicle modeling.

TABLE OF CONTENTS

LIST OF TABLES

LIST OF FIGURES

Figure Page

Figure Page

Figure Page

Figure Page

Figure Page

SYMBOLS

m	mass
A_θ	A-Pillar Obscuration Angle
B_θ	B-Pillar Obscuration Angle
C_θ	C-Pillar Obscuration Angle
CD_θ	C-Pillar Obscuration Angle used in this study
A_0	Head-Turn Angle associated with A-pillar obscuration zone
B_0	Head-Turn Angle associated with B-pillar obscuration zone
C_0	Head-Turn Angle associated with C-pillar obscuration zone
CD_0	Head-Turn Angle associated with C-pillar obscuration zone used in this study
kg	kilogram
g	gravitational constant
N	Newton
in	inche
cm	centimeter
MPa	megapascal

ABBREVIATIONS

ANOVA	Analysis of Variance
HFE	Human Factors Engineering
CAD	Computer Aided Design
CAE	Computer Aided Engineering
CATIA	Computer Aided Three-dimensional Interactive Application
CFD	Computational Fluid Dynamics
DHM	Digital Human Modeling
HCD	Human-Centered Design
ED	Engineering Design
EEC	European Economic Committee
HSLA	High Strength Low Alloy
FEA	Finite Element Analysis
FEM	Finite Element Modeling
FMVSS	Federal Motor Vehicle Safety Standards
ICC	Intra Class Correlation
ID	Industrial Design
IRB	Institutional Review Board
LCD	Liquid Crystal Display
MANOVA	Multivariate Analysis of Variance
MoCap	Motion Capture
NCAP	New Car Assessment Programme
PLM	Product Life-cycle Management
QFD	Quality Function Deployment
SAE	Society of Automotive Engineers

SUV	Sport Utility Vehicle
UK	United Kingdom
USA	Unites States of America
VPD	Virtual Product Development
VR	Virtual Reality
VE	Virtual Environment
VB	Virtual Build
WMA	Weighted Moving Average

NOMENCLATURE

2D	Two-dimensional
3D	Three-dimensional
A-Pillar	Front pillar zone
B-Pillar	Side pillar zone
C-Pillar	Rear pillar zone
CD-Pillar	Rear pillar zone referred in this study
Human-in-the-loop	Proposed design framework
Old (Current) Pillar	Represents current solid pillars
New (Proposed) Pillar	Pillar model proposed used in this study
Cooper-Harper Test	A type of an aircraft handling test
L4/L5	Lower 4^{th} and 5^{th} lumbar section

ABSTRACT

Demirel, Hasan Onan Ph.D., Purdue University, November 2015. Modular Human-in-the-loop Design Framework Based on Human Factors. Major Professor: Vincent G. Duffy.

Human-in-the-loop design framework introduced in this dissertation utilizes Digital Human Modeling (DHM) to incorporate Human Factors Engineering (HFE) design principles early in design process. It embodies scientific methods (e.g., mathematics) and artistic approaches (e.g., visualization) to assess human well-being and overall system performance. This framework focuses not only on ergonomics assessments but also actual design process including, but not limited to, concept development, structural integrity and digital prototyping. It addresses to three major limitations found in HFE literature and practices:

1. Poor HFE communication between product designers

2. Poor HFE practice inside product design cycle

3. Lack of HFE awareness in systems approach

The efficacy of the framework is tested through a design study, where an automobile pillar design with see-through gaps was evaluated for its potential in reducing look-but-failed-to-see obscuration errors. Two human-subject experiments and a simulation experiment were conducted to examine the fidelity and value of this framework. A blend of statistical (ANOVA/MANOVA), and visual (heat-maps) studies were performed to analyze eye-tracking data. Statistical results obtained from subjects' feedback (questionnaires, Cooper-Harper test) and structural data (finite element analysis) were combined with eye-tracking data analysis. Results show that human-in-the-loop design framework: 1. demonstrates high test-retest reliability, 2.

has potential to overcome HFE design problems associated to conventional design methodologies, and 3. can detect safety and reliability related problems early in design process. Key findings about the design study include: 1. proposed pillar model provides improved visual field to drivers and 2. subjects rated visibility, safety and aesthetics related design attributes of proposed pillar model higher than current pillar models.

Design is an integrative mechanism of scientific methods and artistic approaches, which has been the major driver of human prosperity. Everything is done by, for, or against humans through the inherent activity of design. Thus, considering human needs, abilities and limitations in design process is inevitable. However, this is either neglected or not equally considered when compared to other design contributors. *Human-in-the-loop design framework* germinates a hybrid design environment to integrate form (industrial design) and functional (engineering design) requirements of product development - from conception to creation - with human element at the focus.

1. INTRODUCTION

Design is considered as one of the central activities in engineering [1]. It is often associated with creation and making [2, 3]. It is a primary human endeavor, and inextricably linked to human progress. Design occupies our lives, from dawn to dusk, everything is designed by humans - intentionally or not [4, 5]. Today, sustaining a modern society would be unimaginable without design [6, 7].

This thesis is based upon the historical foundations that design is one of the most important factors that not only fuels but also drives the human progress. Human element is at the center of all design activities. However modern design methods have shortcomings in embodying human needs, abilities and limitations into design process [8–13]. With the ever increasing complexities associated to designing products, processes and environments, consideration of human element early in design process becomes more prominent.

Human-in-the-loop design framework described in this thesis provides a systematic approach on how to integrate human element early into design process. It encapsulates scientific (engineering design), artistic (industrial design) and human-centered (human factors) nature of design process. In contrast to human-centered design guidelines, human-in-the-loop framework provides actual design platform, which blends engineering design and industrial design methods/tools together. It focuses on multiphysics simulations to incorporate human needs, abilities and limitations through Digital Human Modeling approach. The main goal is more to motivate and inspire than exhaustively cover every research article on human-centered design process. To that end, the primary emphasis is to explain the general principles of human-in-the-loop design framework, and demonstrate its theoretical and practical contributions on how to integrate human aspects early into the design process.

This chapter will start with a brief review on historical foundations and importance of design in human progress. Then, a detailed literature review will be provided about what human-centered design is - including human factors, engineering, and industrial design aspects associated with product development process. Finally, a section on shortcomings in human factors design process will be explored. The motivation is to inspire the field as a whole, not just from a sense of scientific curiosity, but from an engineering excitement on how to transfer findings of the experiments to practical designs. Human-in-the-loop design framework brings substantial theoretical and practical contributions to scientific community, which, eventually, could contribute to human well-being and prosperity.

2. LITERATURE REVIEW

2.1 Historical Foundations of Design in Human Progress

Life is a progress. The urge towards attaining well-being and prosperity is inevitable. Historical landmarks of human progress show that the central tendency of civilizations is primarily not a statement of being, but evolved around the quest of doing (making and creation) [1,14]. There is a tremendous value proposition given towards making or creating something new that brings potential benefit to society [15]. That something new could be a product and a process (engineering), an artistic work (arts), a body of knowledge (science) or combination of both [16].

The tendency of progress through making something new is different than the philosophical or intellectual pursuit of existence. It excludes theological or spiritual search of finding meaning of life in general. It is about the aggregated will, which instinctively pushed societies forward, towards improvement in the human condition. That is, humans can become better in terms of quality of life through progression. One other alternative to progression is stagnation, which eventually leads to extinction. Whether it is explained best by scientific approaches (e.g., theory of evolution) or perceived within system of beliefs (e.g., optimism), the well-being of humans as well as the prosperity of humankind depends on progression.

Part of human progress is very systematic and rational. Amongst all the drivers of human progress, scientific methods (through engineering) has been the most influential on creation of modern societies. Today, human progress highly depends on how we utilize body of techniques to investigate a phenomenon, acquire knowledge, falsify and integrate previous knowledge, then transferring knowledge to set of problem solving methodologies, products, environments or processes. In contrary, a part of the human progress is unstructured and ambiguous, which is rooted to attributes

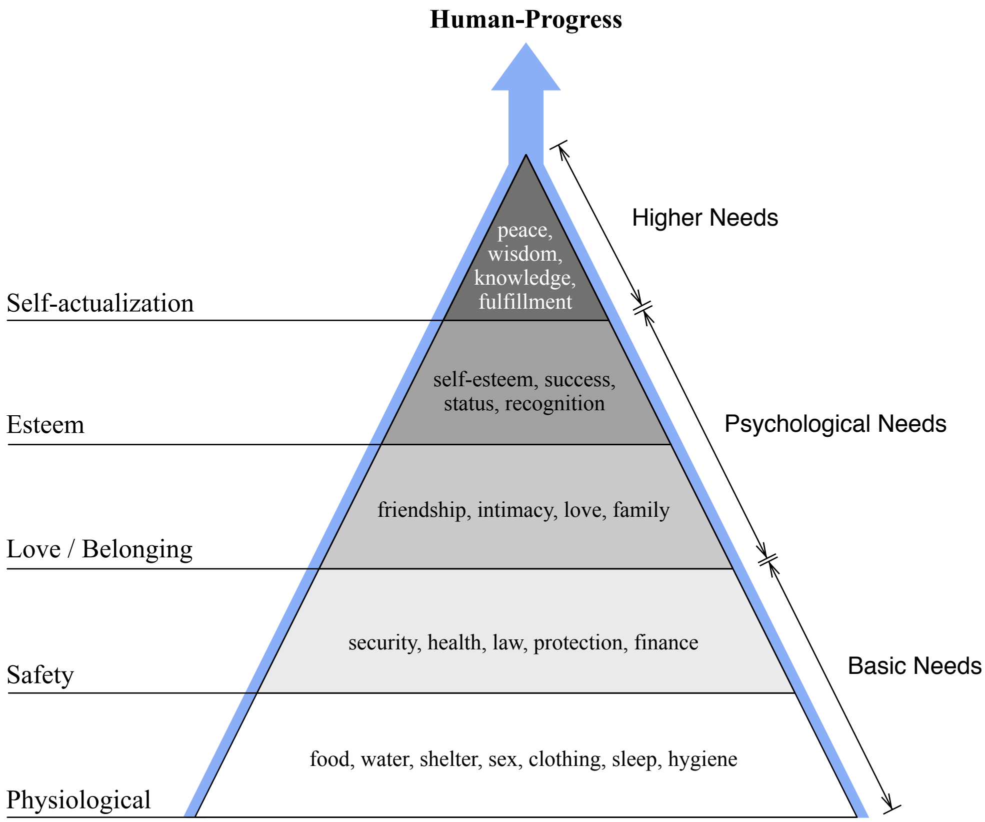

Figure 2.1. Human progress is composed on rational and irrational components. Maslow's *'Hierarchy of Needs'* provide some of the foundations that explain the mechanism behind human progress, which is rooted to human motivation - a balancing game of satisfying basic, psychological and higher needs [17].

of human psychology such as existence, happiness, belongingness (Figure 2.1). Archaeological studies uncovered that early people designed primitive homes (caves) as a method of protection and shelter [2, 3]. They also designed wall paintings and various ornaments to communicate and make their shelters more comfortable, where they feel belonged and content. Even at the early ages, design activities showed a tendency of blending rational and irrational motivations to satisfy human needs. As the time progresses, from prehistoric ages until today, people reflect on new ideas and alter their process of making. Yet, the motivation of satisfying basic needs and fulfilling higher needs still hold paramount. Given the same motivation exists today, people design structural members of high-rise buildings and decorate interiors with wall paintings. The inner-dynamics of human progress has been relatively unchanged, but the processes associated with designing evolves dynamically [4]. Thus, the motivation of blending rational (e.g., basic needs - *protection*) and unstructured (e.g., higher needs - *peace*) needs is an inseparable part of human progress, which also constitutes the driving force behind designing. Maslow's *'Hierarchy of Needs'* perhaps provides one of the most intuitive approaches in portraying the mechanism behind human progress, which is deeply rooted to the theory of human motivation (Figure 2.1). Maslow's hypothesis suggests that once basic needs of survival (safety, food, shelter) are satisfied, the mechanism shifts towards more intrinsic and higher level of needs such as belonging, esteem, and self-actualization [17]. Thus, human motivation towards progress is an amalgamation of basic and higher level of needs, which are synthesized within our physiological and cognitive worlds, and bounded by the laws of nature.

The art of synthesizing this collective knowledge and expertise to satisfy our basic to higher needs define the aptitude of human progress. Thus, this art is design, which is inextricably link to making and creating [2, 3]. It is a ubiquitous character of every human [3]. From a cook preparing a fine tasting dressing, to an engineer manufacturing a high temperature cooking utensil - all are part of designing. Design controls our whole life, affects everybody, at all times, perpetually [19]. We live in it. Our efficiency at work, comfort at living spaces, speed of traveling, chance of survival in a surgery, our prosperity depends on it. Entire human history is built on the process of *'designing'*, not only tools and shelter for survival but artifacts: from the most tangible items - compasses, refrigerators, airplanes - to the most abstract forms - plans, problem-solving, hypotheses [20].

In summary, design is a reflection to human motivation. A greater part of human progress depends on the activity of design (Figure 2.2). Throughout the history, humans, both as individuals and societies, have made progress through design [18].

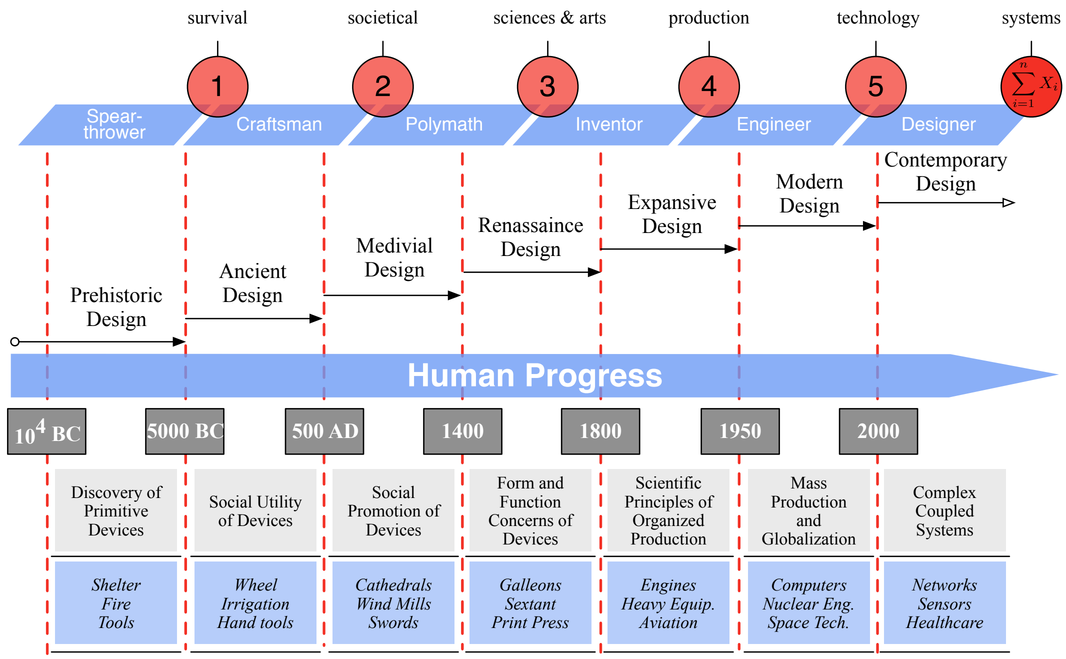

Figure 2.2. Evolution of design and landmarks of human progress are portrayed on a timeline. The urge of satisfying basic needs and fulfilling higher needs relatively unchanged since early ages. However, process/strategies of designing has continuously evolved parallel with the changes in human motivation. Today, *Contemporary Design* embraces a body of collective knowledge and expertise accumulated since the Prehistoric era. Evolution of design shares some similar pathways with 'Engineering-in time' discussed by Harms [18].

Results have not always been smooth or positive, and the path often been painful and inadvertent. Progress is not autonomous and does not guarantee to a direct improvement. However, aside all the struggles, widely accepted improvements have attained from increasing life expectancy to faster and safer transportation. The good news is that scientific and engineering knowledge is in a geometric growth. With the turn of the millennium, the developed world has seen the healthiest, safest and most productive civilization in history [21]. Unimagined breakthroughs attained in a large measure to scientific discoveries and advancements in engineering. Now, the inconvenient truth is that the world becomes more connected, crowded, and resource limited than ever - which challenges the efficacy of current design methodologies.

2.2 On Holism, Emergence and Modularity

The fundamental complexity associated with human-centered design arises from the emergent and holistic nature of human progression. Humans make connections with every facet of life. The vast array of entities that has relations with human progression is ultimately composed of natural and human-made systems. Human-made systems are those in which humans created through synthesis of resources found in nature. Natural systems are those that existed by natural processes. All human-made systems becomes a part of the natural world once they are brought into existence. Thereby, human progression is perpetually evolving within a continuously expanding ecosystem. This ecosystem embraces all entities (natural and human-made) associated with human progression, which are embedded in a complex hierarchy (Figure 2.3). The ecosystem is composed of smaller sub-systems that are modularly integrated. Human progression takes a place within this complex coupled ecosystem. To that end, design is about wholeness. It works in harmony with entities of the ecosystem, embraces a wide range of domains to develop solutions (e.g., methodologies, products, processes) that serve benefit to people. In the context of design process, these entities can range from resources (e.g., raw material) and tools (e.g., computers, machines) to information (e.g., engineering requirements), stakeholders (e.g., users), and policies (e.g., environmental policies). Each entity exists independently, modularly interlinked, and collectively makes up the ecosystem. Due to its complexity and inseparable nature, we assign random properties and explain the ecosystem in statistical terms. Thus, the modular system can not be entirely simplified or fully-understood but reasonably structured and predicted.

For traditional craft-based societies, designing was not different than making. Basic needs were often satisfied through unstructured processes that did not require the consideration of interactions between multi-dimensional entities. Psychological and higher needs were only an interest of significantly fortunate classes (e.g., royalties, clerics), but a common concern of society. Thus, designing process was highly

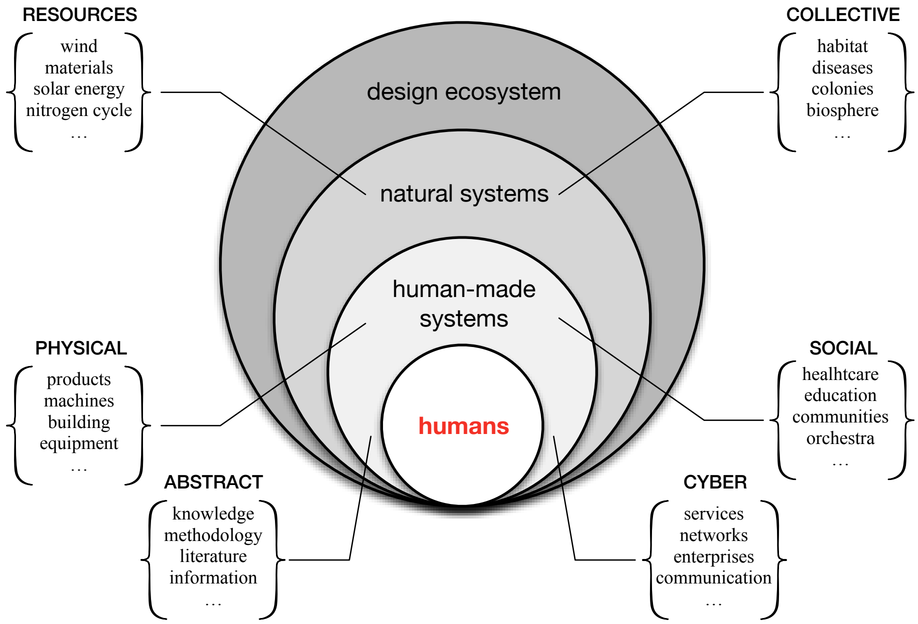

Figure 2.3. Natural system embraces all entities that make up the human-made system. Design artifacts are initially created within human-made systems and then becomes part of the natural world. Design ecosystem encompasses all multi-dimensional entities that are part of the natural system, including abstract ones.

specific across a single or few entities, which only possessed small number of interactions with other entities. These interactions were relatively easy to observe and their realization did not necessitate any scientific method (e.g., experimentation and probabilistic theory). Thus, design process did not require any thorough planning, conception and/or modeling. Any tool or equipment that gets the job done in favor of the user could fulfill the design objectives. The process of making a clay pottery was solely based on the skills and expertise of a single craftsman, who often did not work in strict timelines of delivery nor concerned about the product's life-cycle. The craftsman did not worry about socio-ethical (e.g., environmental effects) implications of his end-product. Throughout the human progress, motives of human needs have shifted from modest propositions (basic needs) to multi-dimensional complex schemes (higher needs). In modern industrial societies, activities of designing become a balancing game of decision making under uncertainty. Today, designing an aircraft is utterly different than a craftsman making a clay pottery. Entire design process, from raw material selection to recycling, top-level goals as well as component level attributes, must be considered before committing to production. Modern design involves significant intellectual and technical preparation, which incorporates planning, conception and realization of various entities from resources (e.g., humans, finance, time, raw material) and technical knowledge (e.g., economics, engineering, logistics) to environmental policies and marketing [22–25]. Today, designers need take a holistic approach and consider of a wide range of entities that independently exist, and must work in harmony [26, 27]. Complex design projects often require a good blend of scientific knowledge (e.g., probabilistic theory) and artistic skills (e.g., aesthetics), as well as consideration of limited resources (finance, time, materials) with their socio-ethical implications (e.g., sustainability).

In summary, managing such a complex embedded ecosystem require an inclusive approach with the capability of concurrently monitoring what goes in and out of the system. Without considering holistic, emergent and modular characteristics of this complex ecosystem, design solutions are inadequately realized.

2.3 What is Design?

Design is neither a pure science, nor a true representative of arts, perhaps combination of both or a synthesis of scientific and artistic approaches [2,3]. Many authors have tried to explain what design is. Often, efforts failed to provide a well-rounded definition. In fact, this is all expected because design involves both objective and subjective pursuits towards realization of ideas into tangible (e.g., products, environments) and/or intangible (e.g., problem solving methodologies, plans) entities. It is a six letter word with so many meanings, which explains why looking for a unique definition may not be helpful to grasp what design is - yet, could be impossible to state what it is not. Whether it is practiced by a craftsman or an engineer, design is ubiquitous to everyone. It is fueled by the human motivation, executed by humans and serves for humanity - both the designer and the user are humans. This multifaceted nature requires not only taking functional (e.g, sciences) and form (e.g. arts) aspects into account, but also focusing on the human well-being and the overall system performance [28].

Design is human centered (e.g., physiology and cognition) and addresses to our multi-dimensional level of needs (Maslow's Hierarchy of Needs). It is composed of structured (e.g., scientific - *power output of an engine*) and unmethodical (e.g., artistic - *styling of a vehicle*) worlds. It defines parameters of economical growth (e.g., creativity and innovation), creates new cultures (e.g., social media), connects resources (e.g., raw material), translates ideas to products (e.g., cars, airplanes), improves well-being of humans (e.g., assistive technologies), and provides solutions to grand challenges (e.g., sustainability) [29–32].

Design can be thought as an integrative mechanism of scientific methods and artistic approaches, which utilizes combination of technical, cognitive and social processes to respond our problems [2, 3]. It is a quest of searching for the most creative and exclusive solutions to a problem, and make sure that each solution satisfies boundary requirements to make it safe, useful, practical, and reliable [33].

Design is a goal directed reasoning, which can be methodologically schemed, but cannot be universally formulated [34]. It is a melting pot of objective and subjective pursuits. Successful designs need to be not only functional, reliable and safe but also creative, novel and fulfilling. This perspective makes design a holistic field, where one requires to gather complex bodies of knowledge to solve a specific problem [6, 35, 36]. Thus, curiosity and skillset of a versatile person (Renassaince man or polymath) is appreciated within design process. This is often correlated to a person who possesses a profound knowledge and expertise in at least few or more fields related to design (e.g., engineering, arts, biomechanics, architecture). Individuals who can demonstrate technical competence of an engineer with aesthetics concerns of an artist are often referred as good designers. Notable names such as Shen Kuo, Leonardo da Vinci, Mimar Sinan, Nasuh Al-Matraki, Isambard Kingdom Brunel, Benjamin Franklin, Nikola Tesla, James Dyson and Jonathan Ive are some of the pioneers and known figures who drew technical expertise in multiple fields with keen interest in creating/making artifacts.

Design in 21^{st} century is a different phenomenon than what polymaths were involved in past centuries. Today, designers work in coherence with multi-dimensional sectors with strict turnover times, high quality expectations and financial constraints. Solution space is designated by the effective understanding and utilization of not only scientific and artistic expertise but also technical communication, resource management, economics and environmental policies. Designing better products heavily rely on systematic realization of knowledge and collective expertise of design teams, rather than based on individual skills or talent of a virtuous (polymath). However, expertise in multiple fields are still essential character what makes a good designer. Holistic perspective still has paramount importance and only gained more significance.

Since design covers such a vast array of multi-disciplinary domains, combining every entity under a single framework is relatively out of reality. However, one can focus on the inner domains that have direct interactions with design process, and expands as the design scope enlarges. This dissertation focuses on design in the more limited sense - designing human-centered products. Figure 2.4 demonstrates some of the multi-disciplinary domains that have loose and direct relations with human-centered design.

In this dissertation, the exposition of design rationale is split into a troika structure: Engineering Design, Industrial Design and Human Factors Engineering. The unique integration of these three domains contribute to development of a new design methodology called *'human-in-the-loop design framework'*.

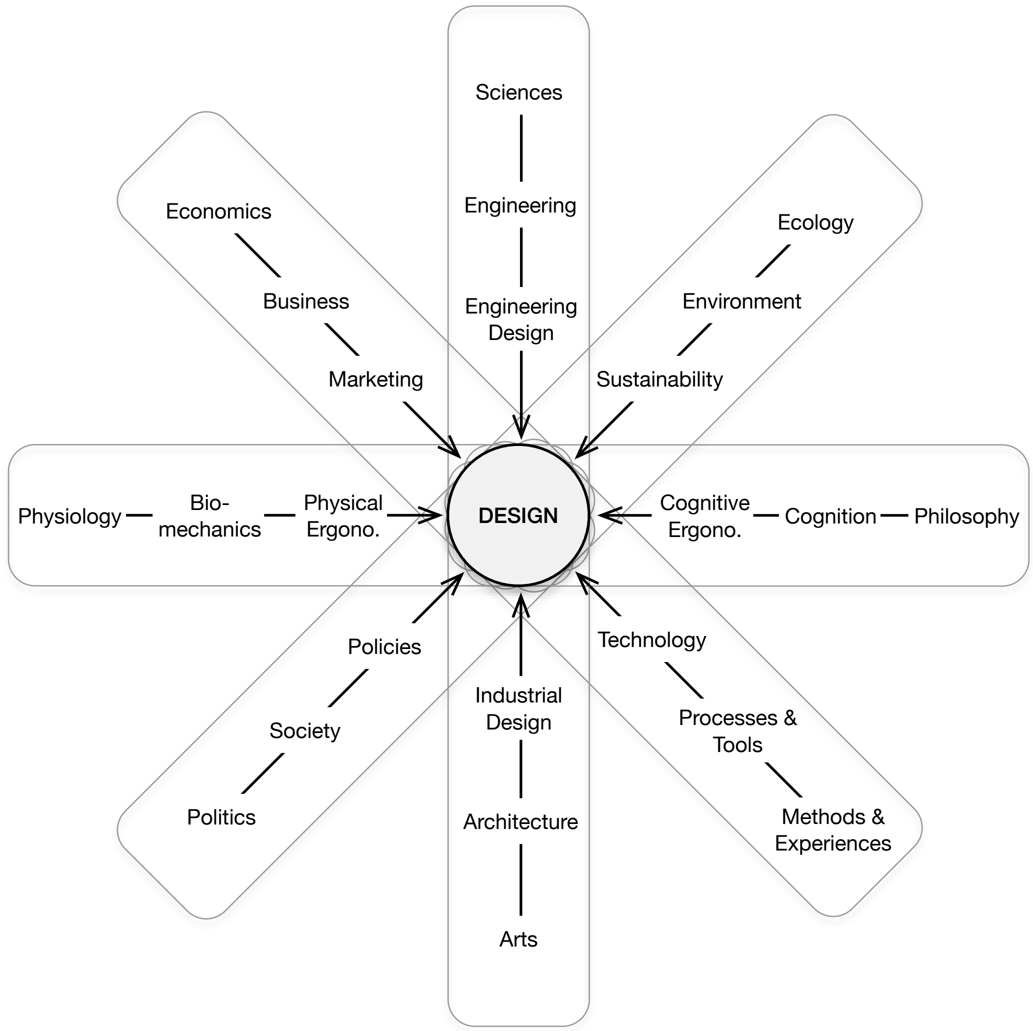

Figure 2.4. Modern design is a synthesis of multi-disciplinary domains. Various domains interact during product development process. Human-in-the-loop design framework makes connections with these domains through integrating engineering design, industrial design and human factors disciplines. Outer domains show generalized/abstract disciplines that have relatively loose connections with human-in-the-loop design framework, whereas inner disciplines are more concentrated and reflect direct relations. A robust human-centered design methodology should consider collective existence of these multi-disciplinary domains.

2.3.1 Engineering design

Design activities in the field of engineering is mostly regarded as the analytic processes (mental work) [37, 38]. It is a game of decision making and optimization, where engineers contemplate on what should be built and which strategies should be sought among several alternatives. The goal is to satisfy customer needs through well-directed engineering requirements within a resource limited environment. It is a collective envelope of planning, modeling, analysis and manufacturing to determine the final form given the functions defined by stakeholders [28, 39]. In engineering design domain, emphasis is given to the functionality of products. Functions are often defined by technical, economic, safety, social, environmental or regulatory constraints, which shape the boundaries of the design process [40].

Drafting and sketching are often referred as standard tools of engineering design process. Engineers use drafting techniques for generating concepts and communicating ideas. However, design work in engineering discipline is heavily based on mental work [4, 41]. Although drafts are important part of the design practice, they are not the end-product of engineering design, rather tools for generating the intended design tasks. Engineering design uses a structured methodology, which can be iteratively modified, systematically improved and replicated with precision. Modeling and analysis activities dominate engineering design process [42]. Instead of an artist's or a craftsman's intuitive approach, scientific methods rely on the investigation of potential paths for error and failures before making actual products. Numerous what-if scenarios related to safety, structural integrity, comfort and cost of products are assessed through physical mockups or digital prototypes. Often, cost, quality and time to market are the most common measures of an effective design. These multi-disciplinary measures require a systematic control of the design interventions from conception to recycle [39, 43].

In modern engineering design applications concurrent approach dominates conventional practices. Digital design software are utilized as common components of engineering design process. Computer Aided Design (CAD) tools form the backbone of design process (Figure 2.5). There are numerous digital methods (e.g., Product Life-cycle Management) provide systems approach on product design from conception to recycling. Scope of such tools differ depending on the nature of design (e.g.,

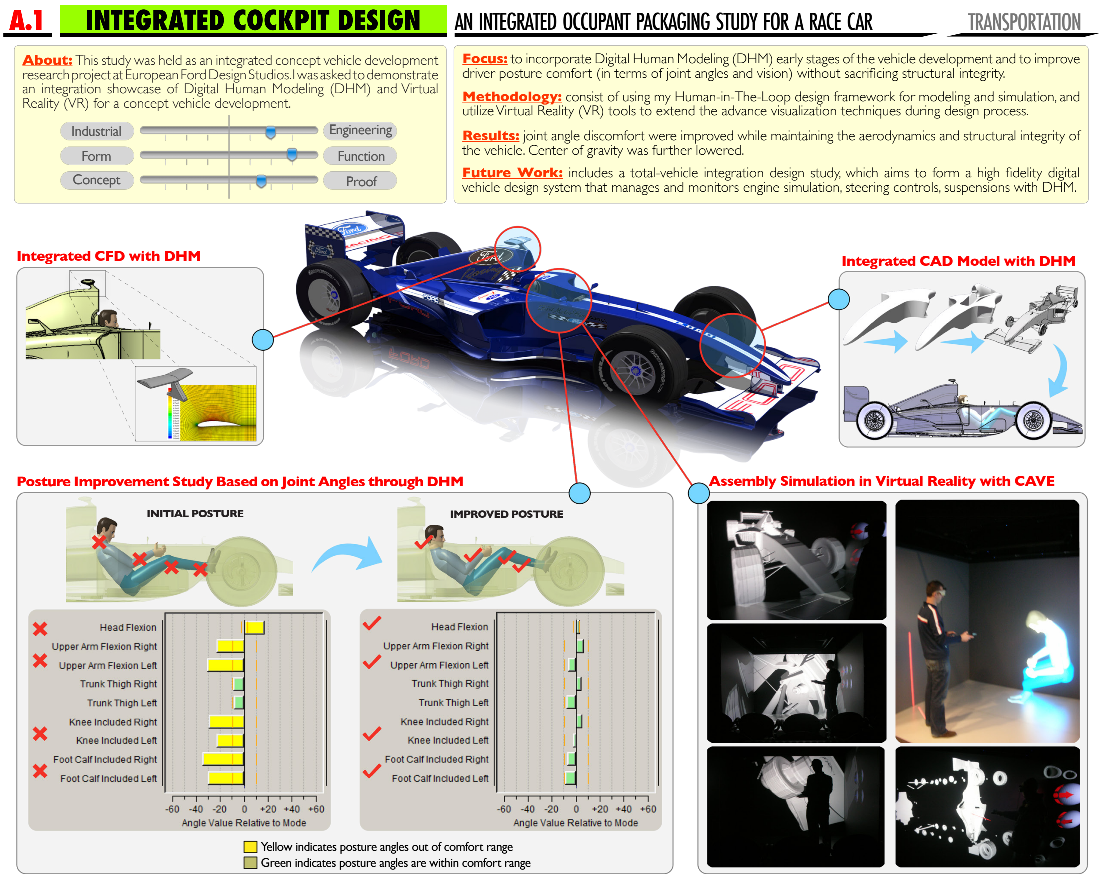

Figure 2.5. An engineering design study demonstrates how multi-disciplinary domains (Computational Fluid Dynamics, CAD modeling, Occupant packaging and Virtual Reality) are integrated for a race car cockpit development. Emphasis is given to the functional attributes of the design process. Final form is a synthesis of all functional attributes that make up the end-product. Yet, form aspects of the end-product have strong connections with the performance and/or functionality of the overall system (e.g., aerodynamics of the race car).

apparel vs. aerospace design), the size of the project (e.g., coffee maker vs. airplane) and stakeholders (e.g., small firm vs. large company). Systematic design procedures increase the likelihood of reaching rational solutions through the optimization of various parameters that contribute to design process.

In summary, engineering design use scientific principles, tools and technology to create products in the definition of structure, machine or system to perform operations safely with minimum resources and maximum efficiency [44, 45]. It focuses on generating final form based on functions driven by customer needs and engineering requirements.

2.3.2 Industrial design

Industrial design is mostly associated with artistic and creative side of the design process. It provides benefits to users in terms of product aesthetics and ergonomics. Industrial design is an important component of value-added process. It primarily affects the uniqueness (product differentiation) of the product [46–48]. The degree of uniqueness often arises exclusively from the appearance (form/shape/topology). Dimensions, proportions, flow and geometry exclusively reflect visual cues of a product, which has direct interactions with how a product is perceived by customers [6,49–51]. Industrial designers require a sound technical understanding of materials, manufacturing processes and user needs. Industrial design process heavily relies on the subjective judgment of individuals to generate creative solutions [52].

A good industrial design process improves product appeal and customer satisfaction through adding desirable features, minimizing ergonomics problems and providing higher usability outcomes (better human-product interactions) [53]. These benefits not only affect the market share but also creates a consistency with the corporate identity [54]. Within industrial design domain, emphasis is given to form aspects of products. Often the most influential factor that attracts customers to a product is aesthetics, which is a collective body of form attributes such as: topology, geometry, color, shape, textures, and dimensions (Figure 2.6). Together, these qualities create perception of appreciation or criticism. Customers are inclined to products that are functionally sound and aesthetically pleasing. Aesthetics attributes can generate emotional and logical satisfaction (or repulsion). Emotional qualities are composed of subjective attributes of 'likes' and 'dislikes', which are closely related to enjoyment or appreciation. Similarly, features that do not play along with customers' subjective perception may create repulsion [33]. Logical qualities are often related to universal perception, which are rooted deeply to cultural or learned behaviors. A red sports car often evokes perception of speed. Rounded shapes reflect dynamism and flow.

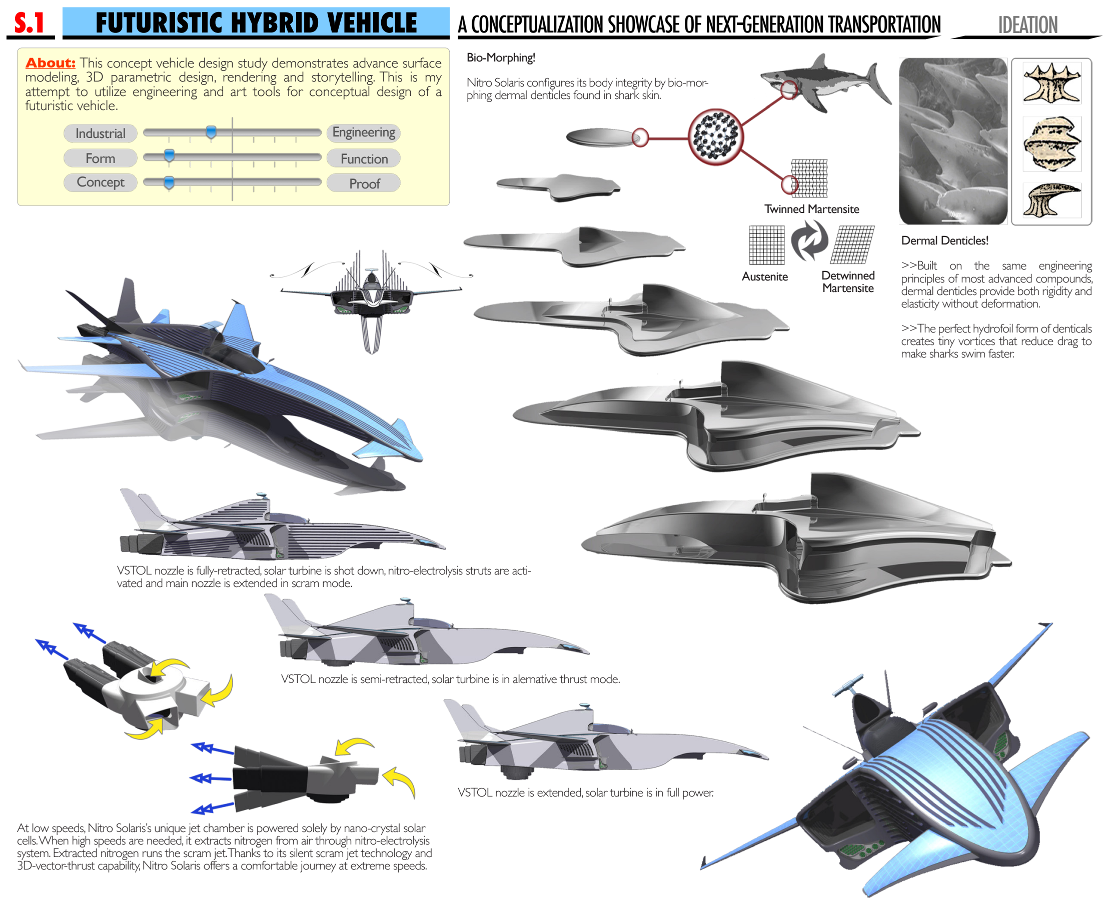

Figure 2.6. An industrial design concept study shows how abstract ideas are transformed into three-dimensional (3D) models through surface and free-form modeling.

Higher quality of a product also depends on how industrial design practice is represented within the product development process [50, 51, 55–58]. Today, with the common use of CAD software, industrial design aspects of products can be integrated directly into concept development phase. Designers can generate surface models and three-dimensional representations of products on a computer environment and rapidly generate design alternatives. A typical concept product development process includes investigation of customer needs, conceptualization, refinement of concepts, digital prototyping, and finally integration to engineering/manufacturing. Before concept models are integrated to engineering/manufacturing, a great deal of time and human resources are dedicated to prototyping phase. Prototyping in the context of industrial design assists designers to discover the perception of actual dimensions and hidden ergonomics aspects of human-product interactions. Today, some of the prototyping is done on computers, which eliminates expenses associated with physical prototyping. Even though digital tools dominate design process, hand drawings (e.g., quick sketches) and physical prototyping (e.g., clay modeling) are still required and practiced in various industrial design applications.

In summary, industrial design is a creative pursuit on aesthetics and ergonomics [59]. Form, proportion, style, composition, balance and harmony define visual appearance of a product. Ease-of-use, positive emotions and safety are vital components of industrial design practices. Together, they play a major role in overall product quality and market success.

2.3.3 Human factors engineering

Human Factors Engineering (HFE) is a multi-disciplinary domain with a broad scope and wide range of applications. It is the primary discipline that consider human element in engineering systems. HFE contemplates on human interactions with other humans, artifacts and the environments [60]. The discipline is different than most of the human-centered scientific disciplines (e.g., anthropology, cognitive sciences, psychology...etc.), which often focuses on human physiology and cognition. Purpose of these disciplines are to understand and model human behavior. HFE utilizes the knowledge gained from these disciplines to design and evaluate products, services, tasks, environments and systems. Therefore, HFE is both a theoretical and an applied discipline, and mostly associated with engineering and industrial design domains due to its design emphasis [61–66]. Despite the historical differences in the context and application areas, *'Human Factors Engineering'* and *'Ergonomics'* often reflect a very similar subject matter and used without distinction [44, 67].

The main focus of HFE is design of optimal products and systems [68]. This involves developing both research and application framework to build a knowledge base about human needs, abilities and limitations, then apply this knowledge to the design of human-machine systems that are safe to operate and comfortable to use [69]. In the context of HFE design, compatibility between human and artifact defines the functional requirements. HFE design principles play a major role in mapping these functional requirements to overall system requirements (design constraints, cost, time, safety).

HFE provides opportunities for multi-disciplinary collaboration with other disciplines (e.g., engineering, industrial design). It gathers data from sciences, arts, technology and biomechanics to provide design solutions to problems relating to man and the machine [70, 71].

In summary, HFE has direct affects on well-being and quality of life [12,68,70,72, 73]. Within the design context, improving human well-being and quality of life are usually achieved by reducing hazard, discomfort and fatigue while maximizing utility, usability, safety, etc. of systems and/or products, which all share a medium with humans [44, 67]. Today, HFE theory and practice not only require to include human physiology and cognition, but also embrace design parameters such as functionality, form, cost, time, and regulations. This extends the scope of HFE from a contemporary design approach to a more hybrid form of a design, which requires a holistic coverage of numerous design entities (Figure 2.7). In this context, the very top-level goals are to increase human well-being and quality of life by optimizing interactions between the human and the artifacts.

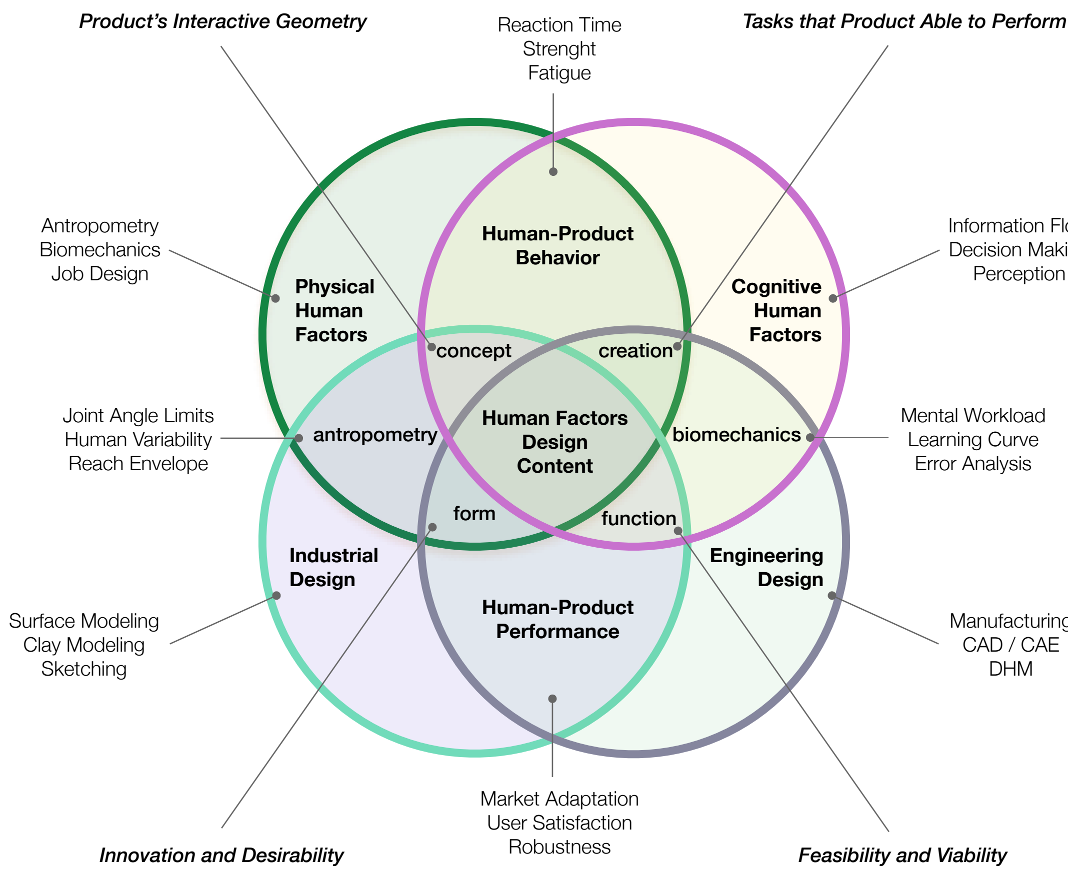

Figure 2.7. Venn diagram summarizes interacting disciplines within HFE domain. The main focus of the HFE is design of optimal products and systems. HFE design content makes connections to engineering and industrial design through physical and cognitive human factors.

2.4 Shortcomings in Design from Human Factors Stand Point

Over the years, global marketing competition, range of technologies and sophistication of products increased considerably. In parallel to these changes, customers are inclined to an innovation driven purchasing perspective. Today, products that go into market are expected to gather a good blend of appealing form and robust functionality with ease of use, cost effective maintenance, high level of safety and comfort [74]. These design attributes are all correlated with human needs, abilities and limitations. However, due to complexities and variations of the human element, additional complications arise in the design process. To that end, understanding the actual human needs, abilities and limitations are an essential component of the product design practice, which plays a crucial role with other success indicators such as time to market, cost reductions, safety, and comfort/usability [74–77]. Designers are known for their ambition to consider of human element during design process. However, academic and practical evidence shows that human factors of product design is either neglected or omitted during design process [8, 10, 11, 68, 78, 79]. In contrast, consideration of human element must be a top priority. Ignoring human aspects of design brings costly human error and poor performance. As means of providing a summary of HFE related shortcomings, fundamental problems are broken-down into three sub-sections, where each sub-section addresses a specific HFE related problem.

2.4.1 Poor human factors communication between product designers

The needs, abilities and limitations of humans may carry some rational (objective) and irrational (subjective) attributes depending on the product of interest [78]. Therefore, design engineers and industrial designers need to communicate within an integrated medium. Both disciplines are highly concerned about human element when it comes to human-centered product design [33,80,81]. However, due to differences in curriculum, social norms and field practice, a seamless integration is missing. Artistic judgment of industrial designers and/or structural approach of design engineers are either missing or dominating each other in product design process [52, 67, 82].

There is a need of a collective effort from both sides, which directs technical, cognitive and social expertise to address challenging design problems [65, 83]. HFE provides a common ground for both disciplines [6, 33]. Engineering and industrial design focus on the human element with a mutual interest but within a compartmentalized environment. Each domain has its own field of interest in safety, reliability and usability attributes of designs process [30]. However, there is a gap exist between two worlds - even though human element is a common interest. Engineering

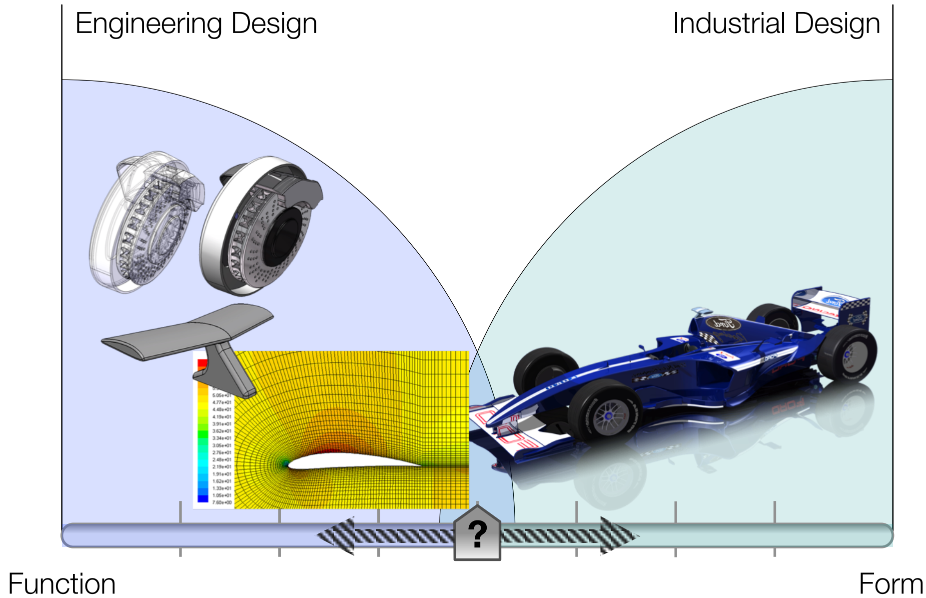

Figure 2.8. Contribution of design engineers and industrial designers depend on the context of the design project. Despite the difference, each domain shares similar ambition and concerns towards human-centered design problems. The slider represents a virtual fulcrum between form and function aspects of the product design. Designers should incorporate expertise and tools from each domain interchangeably.

and industrial design professionals must work in harmony to address human needs, abilities and limitations in their product design practices. This approach assures a holistic and well-rounded design coverage, which allows consideration of ergonomics principles early in design process [84]. It has potential to increase the successful synthesis of form and function while making connections to other design contributors (e.g., management, manufacturing) (Figure 2.8).

2.4.2 Inadequate human factors practice in product design process

Studies and expertise show that good ergonomic practice is important for an effective and a safe working environment. Poor ergonomic practice can result in not only physical injuries but also significant financial and reputation losses. However, the literature review reveals that most of the designers do not regard HFE principals during design of products [67, 68, 74, 75]. Often, designers consider HFE principles at late stages of product design as a post-evaluation method (Figure 2.9). Also, not enough fundamental interest is paid to HFE principles comparing to mechanical engineering or software programming [77, 85]. However, if designers employ a better design practice through HFE and follow a human-centered design approach, failures due to poor design practice would decrease [68, 77, 85].

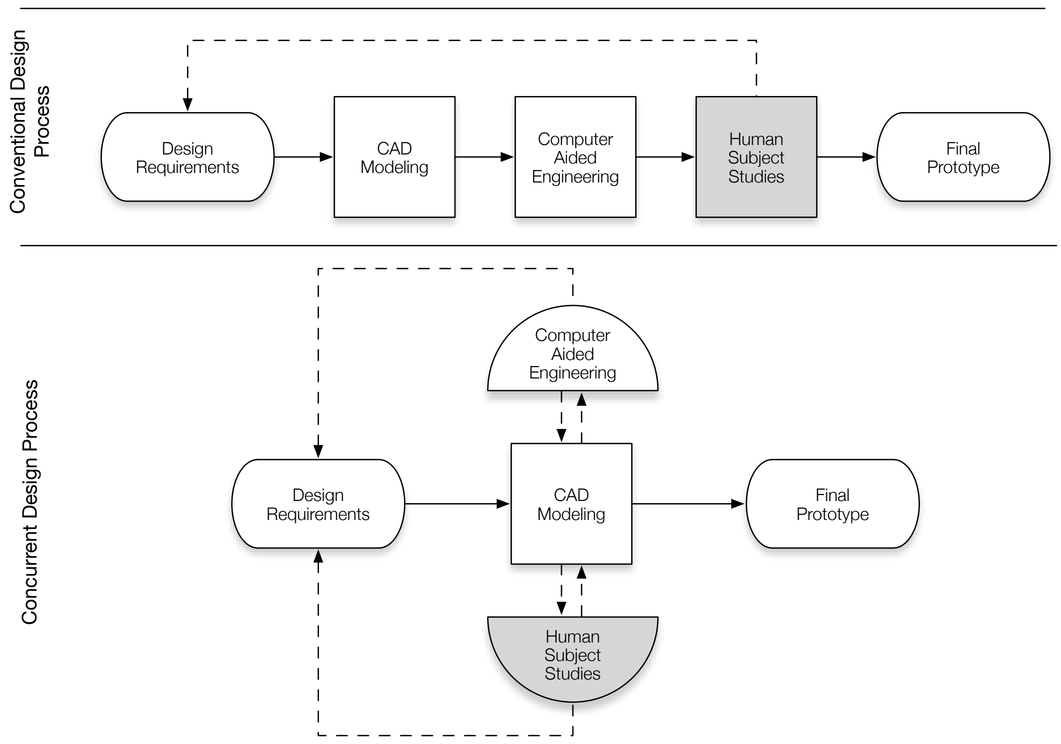

Figure 2.9. HFE is often conceived as a method of post-processing ergonomics evaluation. In contrast, HFE design principles should be concurrently integrated to earlier design process. Considering HFE principles at later stages of product design is associated with higher costs of design modification. A parallel approach enables discoveries of design errors earlier in comparison to conventional serial design process.

Studies show that only two percent of decisions taken during design process follow a systematic decision making, and the rest 98% were decisions based on past experience and intuition. This evidence points out that most of the time designers follow a case-based trial-and-error procedure. They work with unmethodically driven design ideas, and then see if they work for a specific design problem [44,67]. Later, they make slight design changes and evaluate results to see any progress is made. During this associative and negotiating cognitive work, human needs, abilities and limitations are sometimes omitted or not get sufficient attention. The nature of subjective decision making do not allow a systematic control of how decision will affect design process (e.g., manufacturability), satisfaction of users (e.g., comfort, safety) and profitability (e.g., cost, recycling).

Although, design characteristics regarding human element are not easy to classified universally, it is still possible to put many human aspects of design attributes (comfort, fatigue, vision, etc.) into a much systematic and structured order. This may eliminate some of the irrational/erroneous decisions taken in conceptual design phase.

2.4.3 Lack of human factors awareness in systems engineering

Systems Engineering (SE) is a fairly new discipline comparing to other traditional engineering disciplines such as civil and mechanical engineering. Therefore, the role and the practice of HFE (especially in terms of product design) inside system engineering approach is not clearly defined [86, 87]. Systems approach is initially developed in biological sciences and further refined by engineers. The popularity of systems approach increased during World War II when it was recognized as a tool for logistics and operations management. It also served as a tool for modeling complex human behavior in military environment. This discovery gave a rise to recognition of systems approach in engineering domain, especially in HFE. Its integration to human factors domain holds paramount, however its utilization as a design approach is still subject to question [44, 68].

In addition, HFE domain has traditionally been treated as a separate domain from engineering and have not fully integrated inside design cycle. However, the domain covers very important aspects of product design (e.g., anthropometry, biomechanics, industrial/mechanical engineering, industrial design, kinesiology, physiology and psychology) and must be fully integrated into design cycle [44, 77].

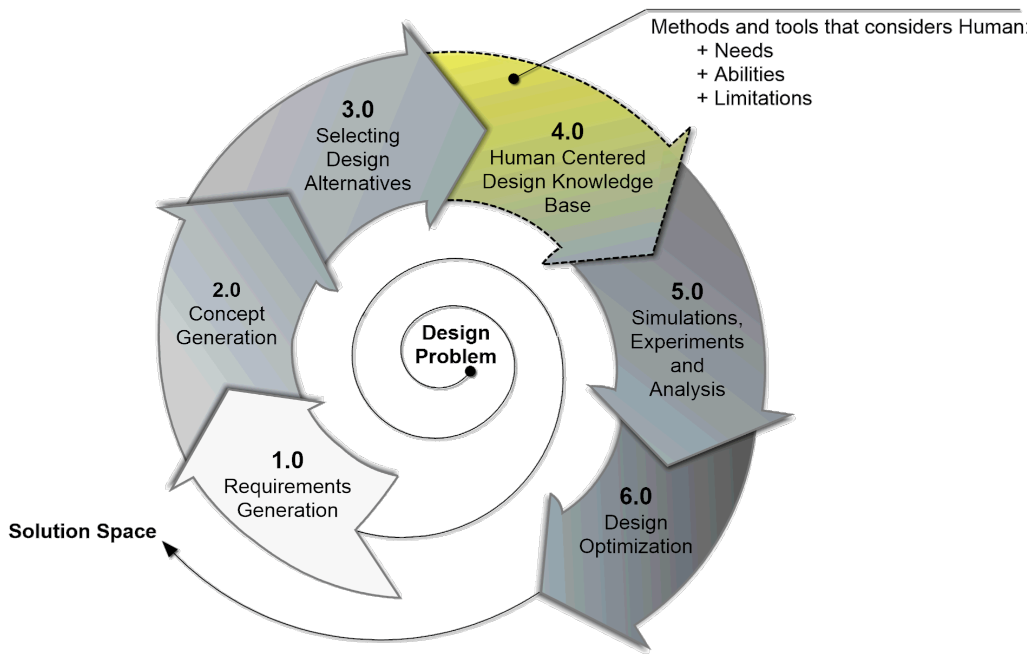

Figure 2.10. Human aspects of design process is either neglected or omitted. A robust product design system must be pursued to incorporate human needs, abilities and limitations systematically.

The fundamental tenet of HFE is to integrate knowledge about physiological and cognitive aspects of humans to the optimal design of products. Instead of focusing on a particular system component or element in isolation, HFE offers a synergetic (holistic) approach to recognize the overall efficiency of the system by optimizing human-well being and overall system performance [44, 88] (Figure 2.10). This is the pursuit of creating an effective symbiosis between human and the system components so that system members can work in a complementary fashion.

The holistic characteristics of HFE naturally provides a multi-disciplinary collaborative approach, which considers not only human-artifact interactions but also embraces entire life-cycle of products. It can also provide a systematic monitoring that covers conception and disposal of products. Meanwhile, systems perspective builds connections with stakeholders functional, physical and operational performance requirements as well as economics, logistics and marketing constraints.

Although systems theory shares a great interest with human well-being and overall system performance, understanding and practicing the HFE design principles within systems engineering has not fully realized. Inside systems engineering cycle HFE methods are mostly used as check points or evaluation steps rather than design guidelines. Since the main objective of HFE is to consider needs, abilities and limitations of products, then, systems principles should be integrated early in the design cycle of products.

2.5 The Need for A Systematic Human-Centered Design Process

2.5.1 Embracing form and function centered on human element

It is natural to conceive that human-centered design domain positions itself on the foundations systems concept, which is deeply rooted to philosophy of holism and emergence. In contrast to reductionist approach, the systems thinking recognizes that the whole is more than the sum of its parts. This approach is driven by the necessity to understand the interactions between integrative levels of nested entities. Biological sciences had a long history of inquiring nature as a body of collective entities that work together to accomplish a greater purpose - survival (existence). Hegel was amongst the first who recognizes that the unity that exists in a complex system can not be predicted or deduced from behavior in the lower-level of components. Even though every sub-level parts of a system are linked to each other, whether in a weak or strong emergence, their performance require consideration of the whole. This perspective does not devalue the sub-system level importance. Specialization at sub-levels of the system, such as component level expertise, is still required and hold paramount interest in design process. In contrast, systems perspective provides a top-down approach to recognize the comprehensive functionality of collective body of sub-systems (components or entities). In other words, focusing solely on each nut and bolt that goes into the airplane assembly does not guarantee the prediction of aerodynamic coefficient. One needs to consider not only sub-level components, but also synthesis of components that makes the whole airplane. The unique behavior (e.g., aerodynamic coefficient) of the finished airplane is independent (or loosely-coupled) from the surface topology of a single bolt, but directly related to the assembly of thousands of bolts, which their collective existence affects the overall topology, so the aerodynamics coefficient. Thereby, systems approach provides both synthesis and decomposition, from bottom-up and top-down, at component and assembly level. Figure 2.11 shows a comphrehensive example of how form and function aspects of a design study could effect human well-being and the overall system performance.

Within design process, a system can be summarized as aggregation of entities organized in structured ways to accomplish design objectives. In general sense, a system is formed through interactions of entities (e.g., raw material, machines), have external boundaries (e.g., environmental policies) and work for a common design goal/purpose (e.g., design objectives). All of these entities communicate and interact to achieve systems goals with in an environment that is formed by boundaries and should respond to changes [44]. This approach focuses on the effectiveness of the system as a whole, while still considering the harmony of sub-system level components. The process is decomposed in an interactive fashion, from general macro functions, to molar functions and then to micro functions. At each stage, constraints that bound the design process are cross-checked with the design objectives.

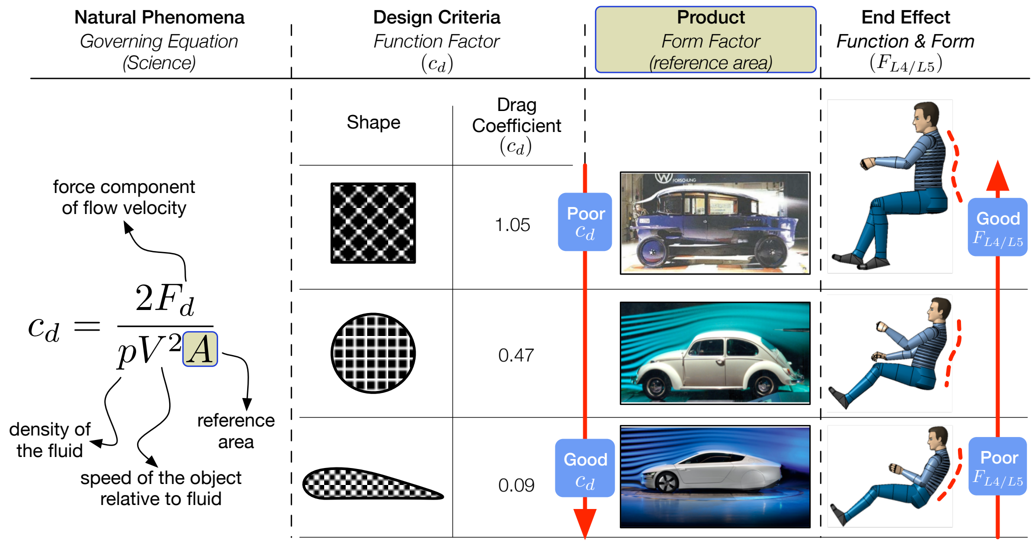

Figure 2.11. Modern vehicles are designed around the motivation of fuel economy. Gas mileage depends on the coefficient of drag, which is directly related to the overall topology/surface geometry of the vehicle. As the vehicles become more streamlined (lower drag coefficient), cabin space becomes tighter and confined, which has severe affects on driver's posture. Drivers often take a posture where lumbar area is not supported. The gap between lumbar area and the seat causes chronic pain. Unless bucket seats or lumbar support systems are provided, drivers take a reclined position. Poor posture results in high compression forces occur between 4^{th} and 5^{th} lumbar section of drivers due to awkward (extreme reclining) sitting angles. As the drag coefficient (C_d) decreases, driver's posture becomes poorer (high $F_{L4/L5}$). This may not be a critical problem on a short distance highway cruising. However, when the effects of road bumps and longer cruising are combined, poor posture not only creates discomfort but also results with a prolong back-pain. In addition, poor posture leads to severe back and neck injury in case of a traffic accident. Without the presence of a human-centered systematic design framework, it could be highly infeasible to predict the connection between equations governing the aerodynamics flow and its effects on driver safety, comfort and performance.

2.5.2 Systematically filtering best idea(s) to reach meta model(s)

The process of designing requires systematic (structured and methodical) approach to manage a complex body of entities. Although one can argue that structuring the design process is a way of suppressing creativity. On the contrary, structured approach supports creative pursuits in design process without sacrificing imagination and inspiration. It provides a structural road-map to consider both mechanics and management aspects of the product development and methods to monitor growth and decline of assets throughout a system's entire life-cycle [86]. This approach assists designers to reduce error and increase safety, efficacy and marketability of products. Best ideas from a pool of alternatives can be systematically evaluated and then filtered according to attributes (design goals and constraints). Without the presence of a such systematic procedure, subjective judgement can rarely be effective in complex design environment (Figure 2.12). One can think of systems approach as a top-down problem solving methodology, which focuses on the overall purpose of the problem area with emphasis on mechanics, management and organizational skills [87, 89]. It could be also proposed as a bridge between many disciplines (e.g., mechanics, operations) to monitor the life-cycle of products. In modern design processes, any procedure that dwell in unstructured processes for the sake of creative pursuits are destined to fail. The sheer complexity of technical, operational, logistic and resources of product design process require concrete course of actions [36, 90]. Systematic design process can only serve to improve the successful decision making rates, which eventually increase the creativity of a talented designer. Without a structured approach, design process is obsolete.

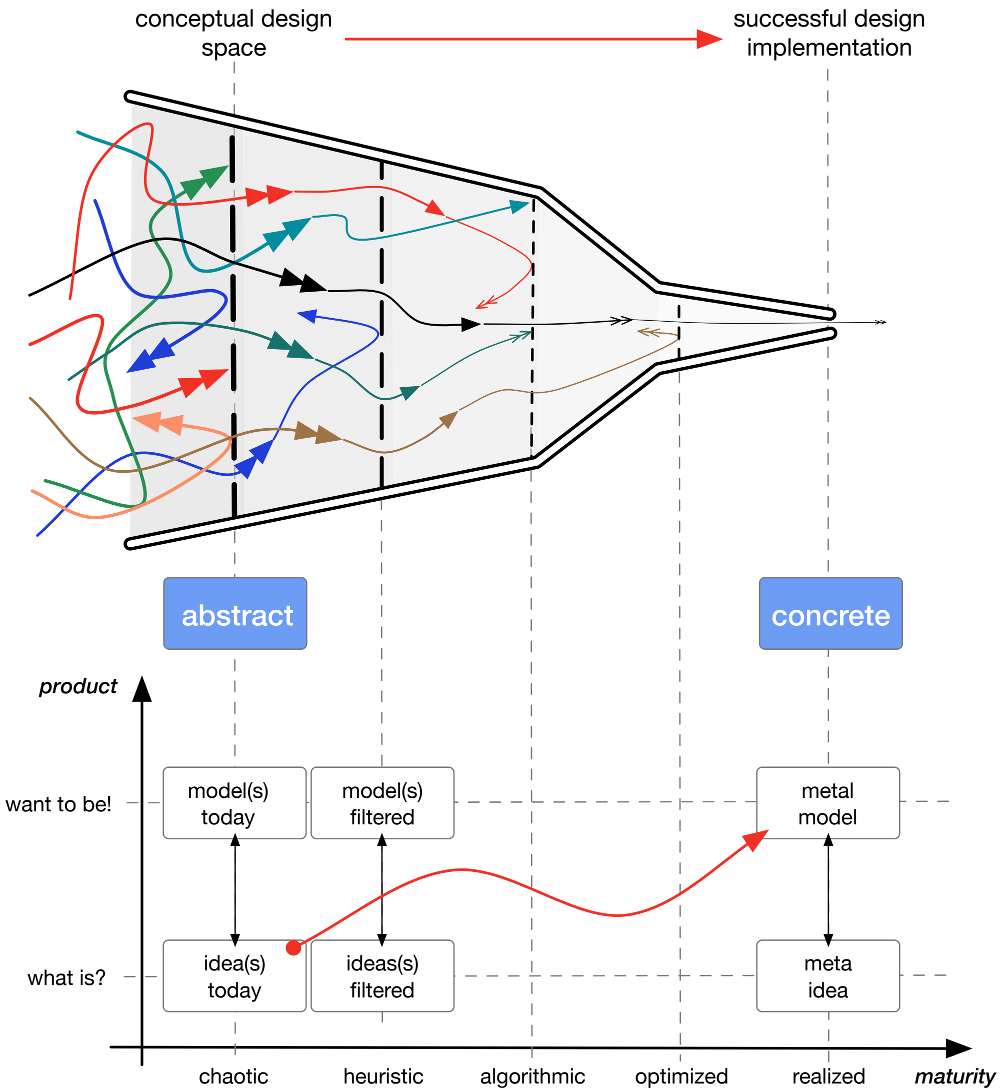

Figure 2.12. Design process includes trade-off between various design parameters. As a result, a group of ideas are refined and reduced into best ideas (from abstraction to concrete). This process can be imagined as a filtration operation, where conceptual (coarse) ideas are filtered and refined into implementations (fine). Reaching to a future meta model from idea(s) today require a systematic filtration process. This can be conceptualized as a funnel model, which refines best ideas amongst a group of alternatives, systematically.

3. HUMAN-IN-THE-LOOP DESIGN FRAMEWORK

The main objective of Human Factors Engineering (HFE) is design of optimal products and systems [68, 91]. The domain is concerned about the interactions between humans and the entire system - including all entities that make up the system (e.g., products, machines, computers). It focuses on human needs, abilities and limitations to sustain, or ideally improve, human-system interactions. It is hard to imagine any scientific discipline rather than HFE that has better overlapping interest and objectives with human-centered design strategies.

Human Factors Engineering domain has diverse knowledge base and supports a wide range of disciplines. It provides ergonomics assessment methods and tools, which can assess safety, comfort, performance, and compatibility of human-product interactions. One of the advanced HFE methods that could create a paradigm shift in design domain is Digital Human Modeling (DHM). It has the potential to be a merger between form and functionality aspects of product design process with focusing on human needs, abilities and limitations.

In this thesis, DHM is proposed as a middle-ware to integrate Design, HFE and Systems Engineering/Approach. The primary objective is to develop a human-centered design framework that introduces HFE principles early in product design phase. Secondarily, the framework forms a holistic design scope through embracing emergent design methodologies and tools. In combination, the design framework contemplates on form and function aspects of design process from conception to creation with human needs, abilities and limitations are being central interests.

3.1 What is Digital Human Modeling?

Complex functions of the human body, both physical and cognitive aspects, can be digitally represented, simulated and/or analyzed through DHM tools [77, 92]. DHM uses digital humans as representations of workers inserted into a simulation or virtual environment to facilitate the prediction of performance and/or safety. DHM includes visualizations of the human with the mathematics and science in the background [7, 10, 11, 77] (Figure 3.1). It helps organizations design safer and efficient products while optimizing the productivity and cost [93]. Engineering design practices that utilize DHM have the potential to enable engineers to incorporate HFE principles earlier in the design process [74,77,94,95]. One of the advantages of DHM applications is their integration flexibility with Computer-Aided Engineering (CAE) packages and digital design technologies such as motion capture, eye-tracking and virtual reality [10, 11, 77, 96].

Traditionally, DHM applications have been utilized by manufacturing and design industry. One of the first DHM applications was implemented by the U.S. military for cockpit design in which virtual drivers were used to assess the safety and the performance of the prototype vehicles. The use of DHM reduced the need of expensive and bulky physical mockups [74, 97–99]. Popularity of DHM applications has increased in past decade and many companies have realized the effectiveness of DHM tools for ergonomics evaluation [100]. Recently, technological developments and advancement in the CAE software expanded the application areas of DHM [92,101]. There are multiple DHM platforms introduced as part of CAD and CAE packages, which include digital ergonomics and biomechanical assessment tools to evaluate injury, safety and comfort related design attributes [102–104].

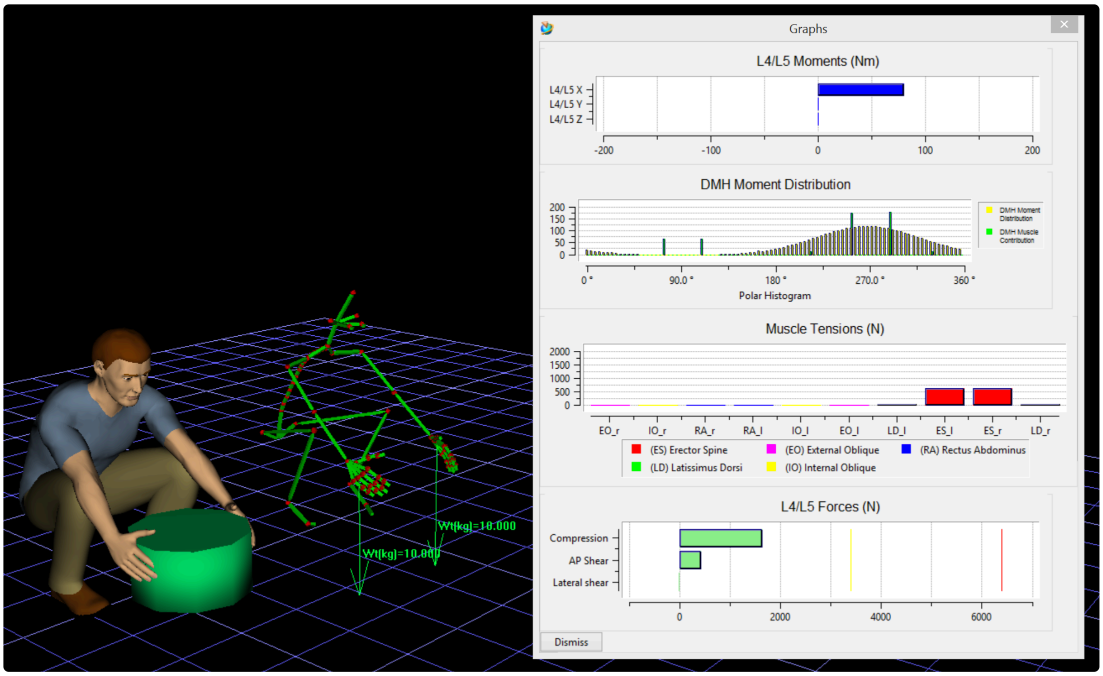

Figure 3.1. DHM includes visualizations of the human with the mathematics and science in the background. This figure shows identical manikins with surface and skeletal model separately. Surface human model includes overall topology that represents body sections with realistic rendering. Skeletal human model shows musculoskeletal relations, kinematics properties, physiological attributes, and embedded equations thats run biomechanics calculations. Analysis modules can include force and moment distributions associated with upper and lower limbs, which are linked to anthropometric libraries. Kinematics related data can either retrieved from pre-recorded motion data or directly obtained from a motion capture system. Pop-up window on the right demonstrates forces and moments associated with a generic lifting task. A 10kg virtual vector load is assigned palm centers of each hand. Analysis output shows moment and force distributions on the lower 4^{th} and 5^{th} section of the lumbar section (L4/L5). Analysis incorporates applied load, anthropometric attributes and associated posture. The capability of blending mathematics/science with visual aspects of human body creates abundance of opportunities for designers to generate evaluation techniques that can go beyond the traditional coverage of human-centered design strategies.

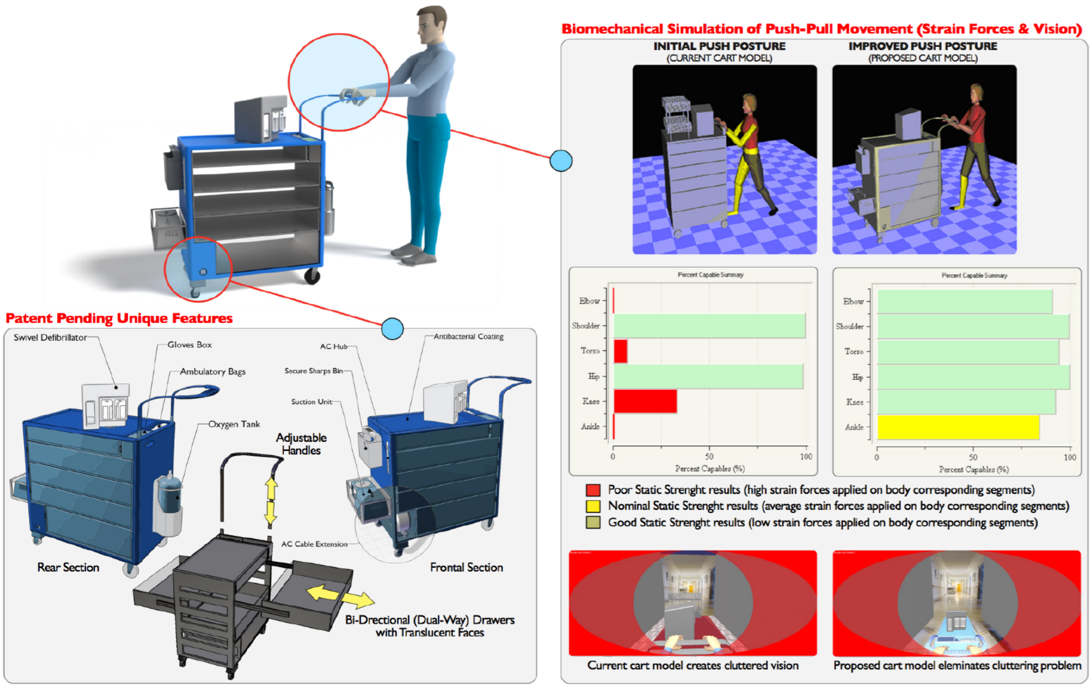

Figure 3.2. DHM can be used not only as an ergonomics evaluation tool but also a method to embrace form and function during product development. A hospital code cart design study shows how biomechanics assessment process can be integrated to test product design alternatives (Current cart model vs. Improved cart model). This approach integrates form aspects of industrial design with functional aspects of engineering design early in the product development phase. Financial costs and excess time required for physical prototyping can be reduced. This approach allows generating ergonomics analysis in a fraction of less time.

3.2 How does Digital Human Modeling Provide an Integration between Building Blocks of the Framework

The proposed design framework not only integrates Design, Human Factors and Systems Engineering, but also provides a systematic understanding of human element inside the product development process. It embraces cross-functional knowledge and expertise through building connections with various disciplines (such as anthropometry, biomechanics, industrial engineering, mechanical engineering, industrial design, kinesiology, physiology, psychology and others) [105]. This multidisciplinary approach allows modular integration to second and third party design methodologies and technologies (Figure 3.2).

One of the advantages of DHM applications is in their integration flexibility with concurrent engineering methodologies such as Product Life-cycle Management (PLM), Virtual Product Development (VPD), and Computer-Aided Engineering (CAE) packages [96]. Trial-and-error on physical prototypes may resolve some of the design complexions, however it has limiting factors such as visualization, simulation, time and cost. Time-to-market and cost of a product are critical for success in global competition [77]. These versatile group of multi-faceted factors must be considered early in the design process to have a safe, efficient and profitable product [106–108]. It is important for designers (and manufacturers) to accomplish a competitive edge during creation and marketing of products through reducing design timescales, overall costs and time to market [74, 95]. These complex goals need systematic product development strategies, which embraces mechanics and aesthetics of design process while considering manufacturing, marketing, management and recycling phases of the product development. In this context, absence or poorly consideration of HFE principles can result in poor quality standards, which may lead to customer dissatisfaction, safety and hazard concerns. Companies often end up in product recalls and lawsuits, which eventually result in reputation loss. Concurrent engineering tools provide an integrated platform to monitor technical and managerial aspects of the product development [109], however fail to consider human element early in the design process.

DHM integrated with concurrent engineering tools enable designers to check if people of different age, gender, size and strength characteristics can safely and effectively perform tasks inside computer simulation environment. Furthermore, Virtual Reality (VR) tools could be used inline with DHM to provide a higher level of fidelity. Through VR environment, user-product interactions can be assessed regarding comfort and safety without the need of full-scale physical prototypes [74, 110, 111]. A design platform that allows direct connections to DHM can assists designers to evaluate both aesthetics (visualizations - *concept sketching and rendering*) and functionality (mathematics - *simulation and analysis*) of product innovation. DMH can also provide a common medium to connect subjective judgment and divergent (inspirational) nature of industrial designers with objective and convergent (structural) nature of the design engineers [67, 105].

DHM forms an ideal medium for integrating designers and engineers early in the design process. It also promotes a more holistic design approach through embracing emergent design methodologies and technologies, which can assist designers to consider human element throughout the design-cycle. Thus, DHM can bring additional time and cost savings on top of the savings associated to concurrent design methodologies. Figure 3.3 shows cost associated with conventional, CAE and DHM integrated engineering design methodologies. Because of its interdisciplinary focus, quantitative nature and flexibility of integration with other design platforms, DHM becomes a potential problem solving tool to various multi-disciplinary design challenges.

3.3 Theoretical Building Blocks of Human-in-the-loop Design Framework

3.3.1 The framework is holistic and emergent: Virtual Build Structure

A structure called 'Virtual Build' was first proposed by Ford Automotive Company [112]. Virtual Build (VB) methodology demonstrated a promise on integrating research on DHM, Motion Capture (MoCap) and Virtual Environment (VE) for ergonomics evaluation of products and processes. The methodology is composed of a physical or a virtual environment that represents a real workstation or a product. Human motion data either comes from MoCap system, a motion prediction model or a manikin posture through manual anthropometric setup [77]. If MoCap method is used, actual representation of subject's motion and posture can be captured and attached to a representative manikin created on computer environment. This method allows capturing actual human motion data without the need of predictive modeling. If motion capture system is not used, then information related to descriptive task

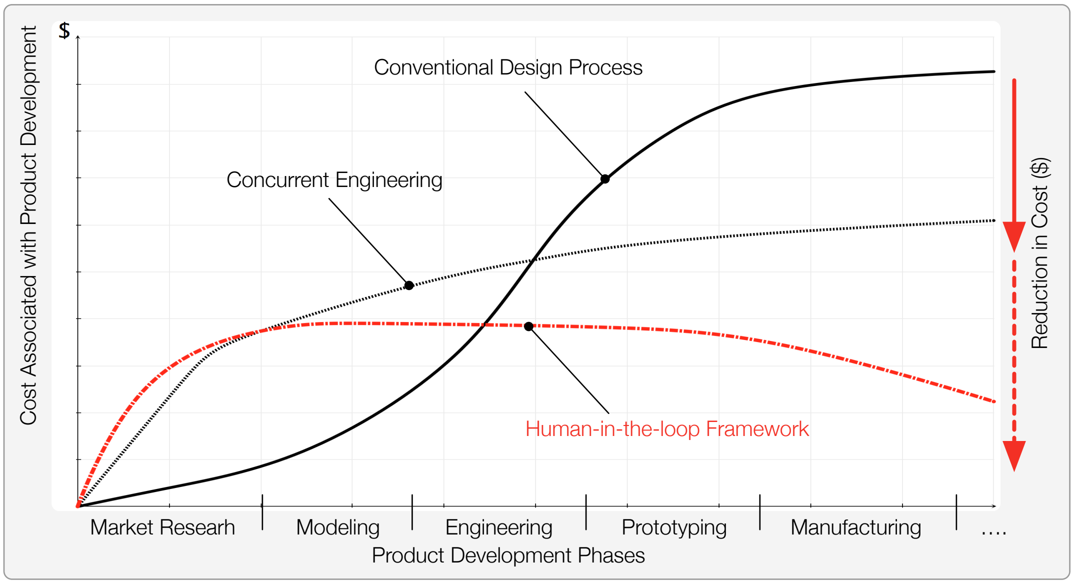

Figure 3.3. DHM can reduce cost associated with physical prototyping or mockups [101]. In addition, identifying problems of human-product interactions early in design phase can reduce additional costs arises from product incompatibility. If errors reduced early in the design phase, cost associated to product modifications at later phases can be further reduced. Thus, DHM provides additional cost savings on top of cost savings established by CAE strategies. Solid red arrow indicates estimated cost savings when concurrent engineering tools (e.g., CAE) used without DHM. Dashed red arrow shows further savings when DHM is integrated to concurrent design tools.

parameters (e.g., push-pull distance, lift-lower height, external loading) needed to be input through manually or via predictive models. [77, 113, 114].

There are various virtual design methods similar to VB structure. However, often these methods are solely used for post-design ergonomics evaluation of products. Thus, VB methodologies can be regarded as ergonomics approaches - not as direct design methods. Human-in-the-loop design framework demonstrated in this thesis study is a modified version of VB structure, which does not only function as an ergonomic assessment tool but also acts as an actual design methodology. Figure 3.4 shows a generic framework where flow of human motion data is connected to ergonomics assessment tool.

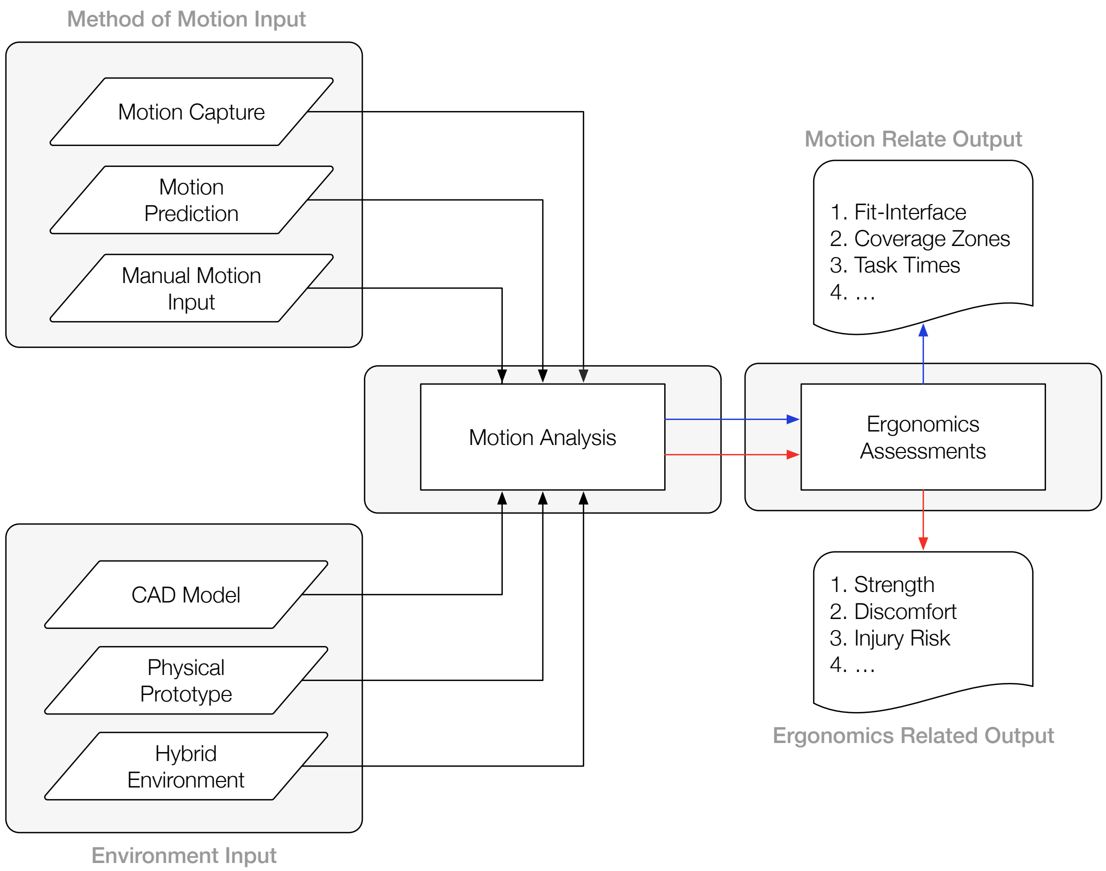

Figure 3.4. Virtual Build design methodology integrates DHM, MoCap and VE for ergonomics evaluation of products [112]. Similar to VB, various traditional design methodologies are often used as ergonomics evaluation methods. This approach (post-design ergonomics assessment) is associated with high cost and extended time-to-market when design modifications are addressed at later stages of product development.

Through human-in-the-loop design methodology product/process design can be analyzed prior to production. This approach provides an expansion to Virtual Build structure used by Brazier towards a more global design platform with human-centered focus [112]. The framework not only integrates DHM, MoCap and VE, but also allows building connections with emerging HFE design tools/methods such as CAD, CAE, PDM and PLM. These technologies are known for their individual potential in resolving HFE related design challenges, however, their integration with a global design framework is still require further research and development [77].

3.3.2 The framework is built around human needs, abilities and limitations: Human-Centered Design

Human-Centered Design (HCD) integrates various technical and non-technical fields of design expertise to enhance well-being of humans through improving product-user interactions. Results often include improved usability, safety and performance. Definition of HCD may differ depending on the context, however the domain focuses on methods that continuously improve the product-human interactions based on users needs, abilities and limitations [67, 105]. Although above definition shares similarities with HFE, HCD is not a scientific domain but a design methodology. It captures variation between users and accommodate these differences efficiently in product design with the goal of satisfying users from different physical and cognitive backgrounds.

In addition to the above, the growing interest in human-centered design practices reiterate the importance of human safety, usability and performance. This motivates engineers to understand human needs, abilities and limitations to design products, services, and experiences people truly value as individuals and as a culture [77]. Researching to find better analytic models to address human variability in design process is also a core challenge for designers. Incorporating human variability into the design process creates design alternatives that serves to accommodate a diverse human needs [115].

The backbone of the human-in-the-loop design framework is supported by DHM tools which provide a human-centered focus for designing products and services. Physiological and cognitive human needs, abilities and limitations can be modeled in DHM environment. In addition, DHM provides a seamless integration with CAE tools to assess ergonomics adequacy of products and services. This approach supplies a continuous monitoring capabilities to designers. User attributes could be cross-checked

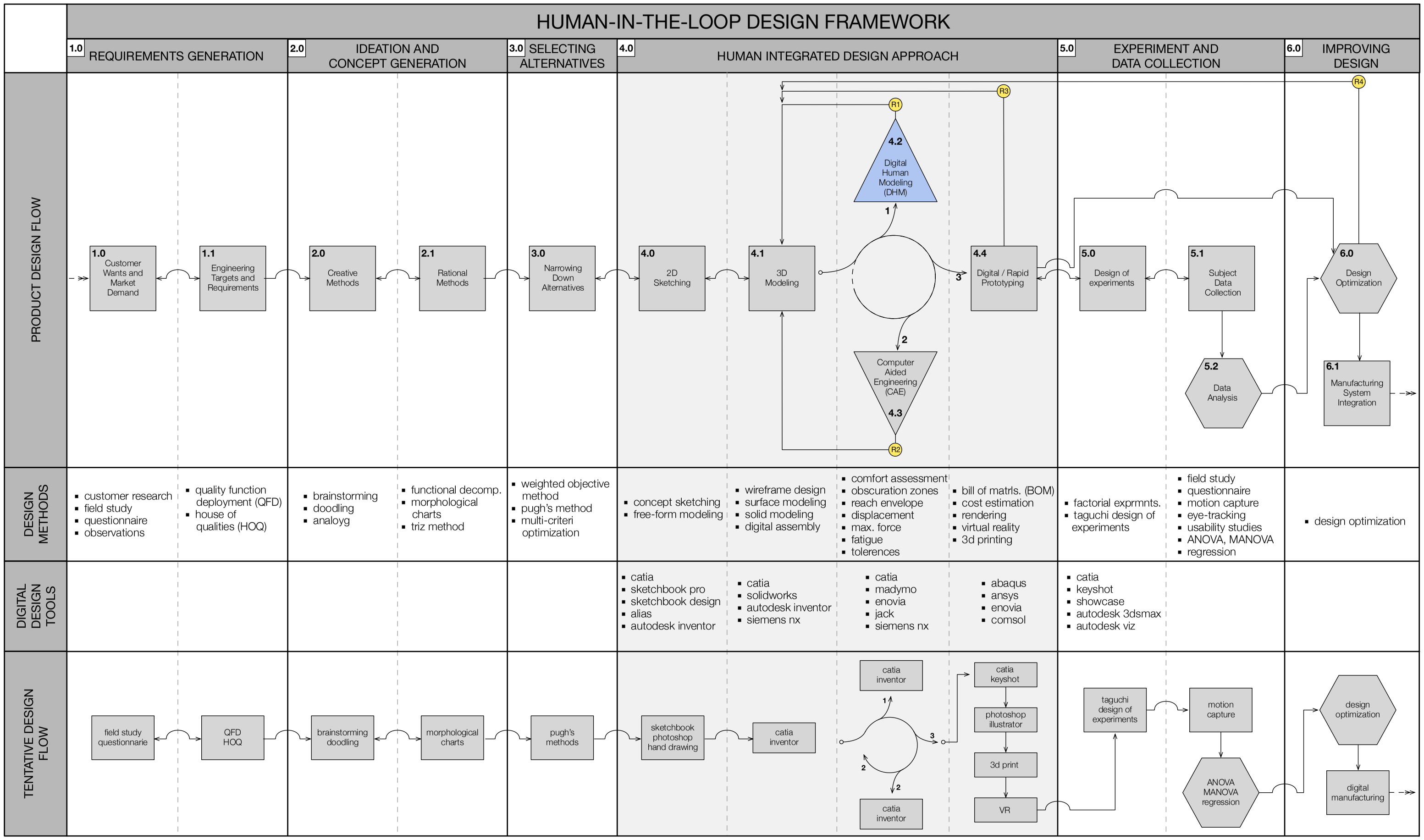

Figure 3.5. A macro-level view of the human-in-the-loop design. The framework integrates early stages of design framework with modeling and analysis phases.

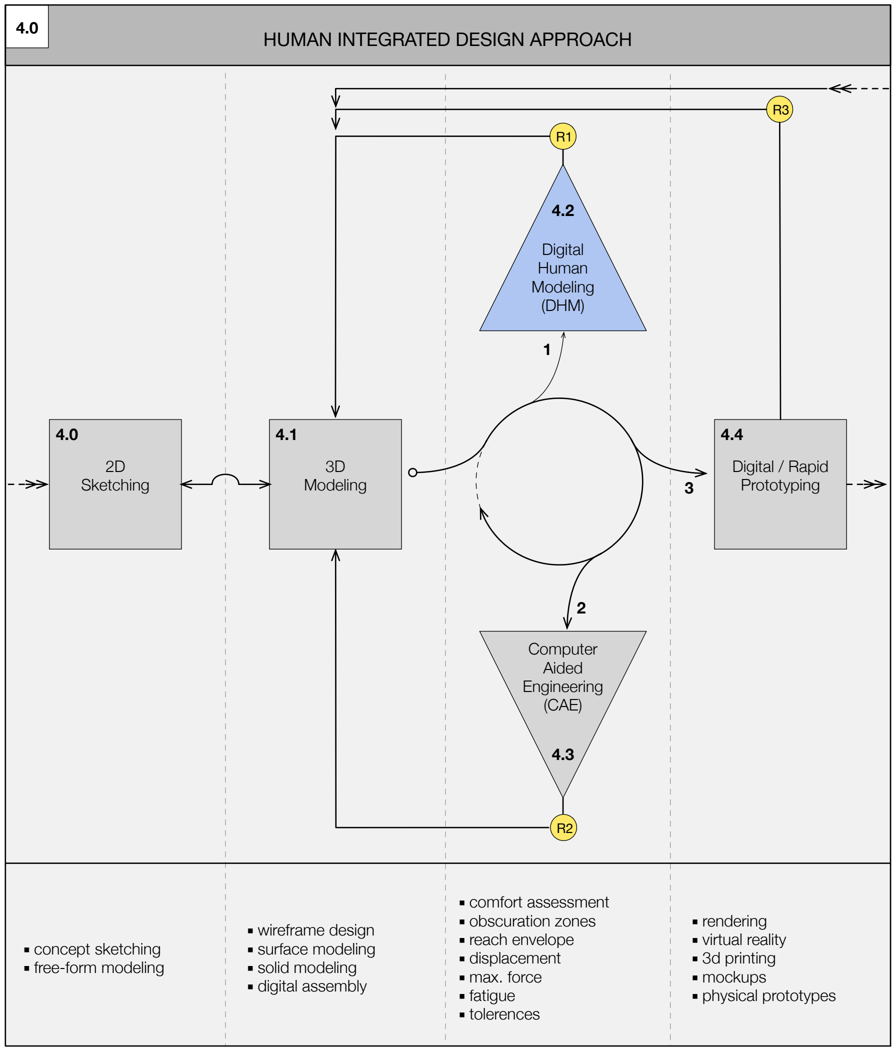

Figure 3.6. In conventional design strategies, HFE design principles are often applied sequentially at later stages of product development as a post-evaluation method. This approach is associated with high costs and excessive time-to-market. In contrast, human-in-the-loop design framework offers a parallel approach, which considers human-element early in product development phase. Within human-in-the-loop design framework, conceptual design ideas iteratively modified through DHM and CAE in a parallel sequence - before ever getting into prototyping phase. This way, human needs, abilities and limitations are considered early in the design process. Design errors or human-product incompatibilities can be captured before prototyping begins.

with design requirements. Figure 3.5 shows a macro-level of the human-in-the-loop framework, from conceptual design to manufacturing. Figure 3.6 shows a more detailed meso-level outlook of the human-in-the-loop framework with DHM and CAE simultaneously applied to the design process.

3.3.3 The framework is emergent: Modular Integration

Product design domain highly depends on physiological and cognitive needs of humans, and expands through the dynamic trends in technology, engineering, economics, arts and social interactions. This broad perspective brings the need of considering both technical and non-technical aspects of the product development, which embraces form and function, as well as non-technical design attributes.

A successful design platform need to allow the utilization of previous methodologies and expertise while providing means of integration with technical and non-technical parameters from engineering aspects of design to artistic concerns, and from technological advancements to resources and finance. [52, 109, 116]. Because of the holistic and complex nature of the design process, one can not come up with a single equation or a universally accepted rule for a good design strategy. Instead, the goal in the context of human-centered design is to provide a synergic design framework, which encompasses available tools and methods and continue to expand as new tools and methods emerge. This approach provides flexibility of allowing additional new technologies, design tools and methods on top of existing ones (Figure 3.7).

Human-in-the-loop design framework is built in a way to allow modular integration of different tools and methods from various scientific fields, non-technical domains, technologies and design methods. Some of these entities are demonstrated in current DHM tools, however access to most of them are limited [117, 118]. Each tool can be integrated in different stages of the design cycle (e.g., conception, modeling, simulation....etc.) to enhance different stages of product development. These tools can be integrated to the framework through multi-physics platforms (Finite Element Analysis, Computational Fluid Dynamics, Photo-realistic rendering packages.)

Therefore, the modular structure approach accommodates different design methodologies and technology tools at different stages of product development. Figure 3.8 shows how design entities can be integrated as modular blocks for under different categories. Content of each category may differ depending on the technological and domain requirements as well as context of the design of interest. The key here is that most of these entities can be simulated/integrated into DHM software packages. With the advancement in DHM research, additional HFE methods (physiological and cognitive) can be added to design framework.

3.4 Fundamentals of Human-in-the-loop Design Framework

Human-in-the-loop framework is a modified verison of 'Virtual Build' structure, which brings HFE design principles earlier to product design process (Figure 3.5) [94]. Previous Virtual Build studies focused solely on ergonomics evaluation and human factors assessment of products and/or systems [113, 114]. This framework focuses not only ergonomics assessments but also actual design process including, but not limited to, concept development, structural integrity and digital prototyping. It provides scientific insight (ergonomics, biomechanics) and artistic approach (rendering, visualization) on product-user interactions.

Data related to human attributes can come from manual or digital sources. For example, human posture data can either come from a manual antropometric setup or from various digital systems (MoCap, eye-tracker, a motion prediction model). If manual methods are used, descriptive task parameters (e.g., push-pull distance, lift-lower height) are inserted manually to generate ergonomics evaluations. CAD model can be updated parametrically depending on the changes required after each ergonomic and structural assessments. Affects of changes on CAD model in terms of ergonomics and structural integrity can be cross-checked simultaneously.

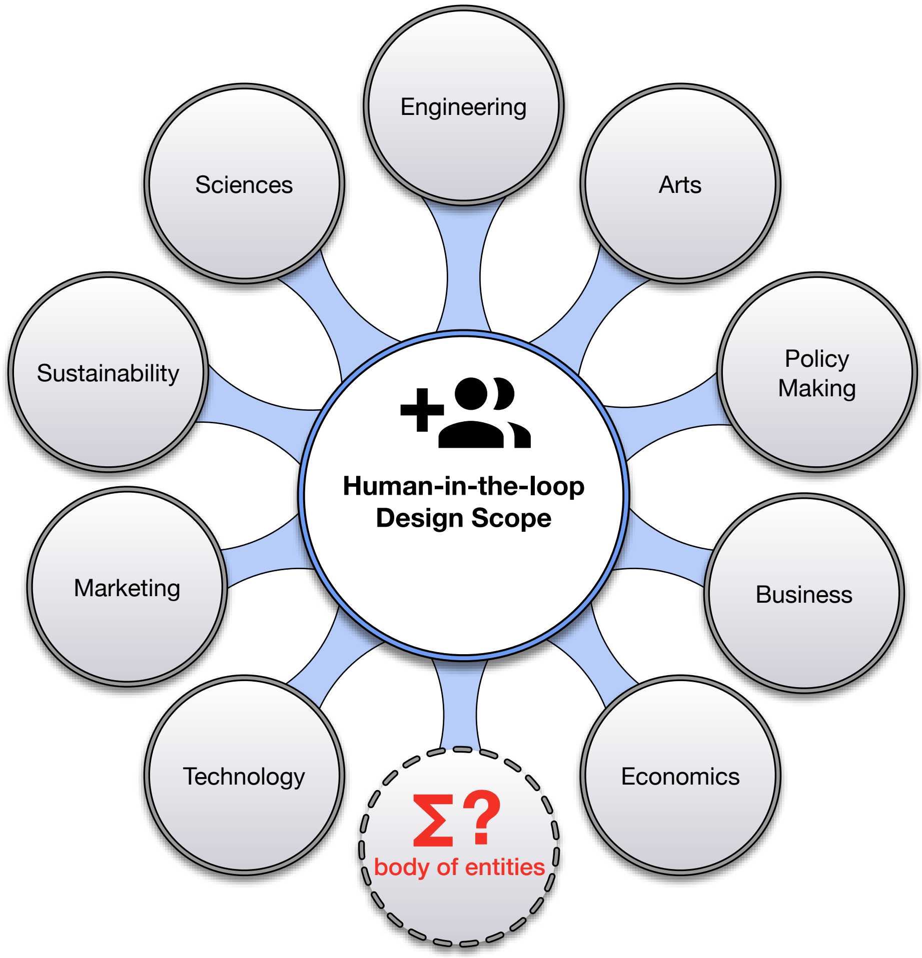

Figure 3.7. Human-in-the-loop framework expands through modular integration of multi-disciplinary disciplines. A design methodology should not solely consider technical aspects of design process. Design embraces various domains, disciplines and methodologies. This multi-disciplinary nature brings a holistic approach into the product design process, which builds connections with a wide range of professions from marketing, policy-making, engineering to business. Each entity that represents a specific discipline is integrated into the framework through different mechanisms. Technical entities (engineering, technology) can be integrated via multi-physics simulation applications. DHM can work back-and-forth with various CAE packages, where it can share data with multi-physics applications such as Finite Element Analysis, Fluid Dynamics, Photo-realistic rendering. Non-technical entities can be integrated through user-questionnaires (marketing), quality standards (e.g., ISO), policies (policy-making), and photo-realistic rendering (arts).

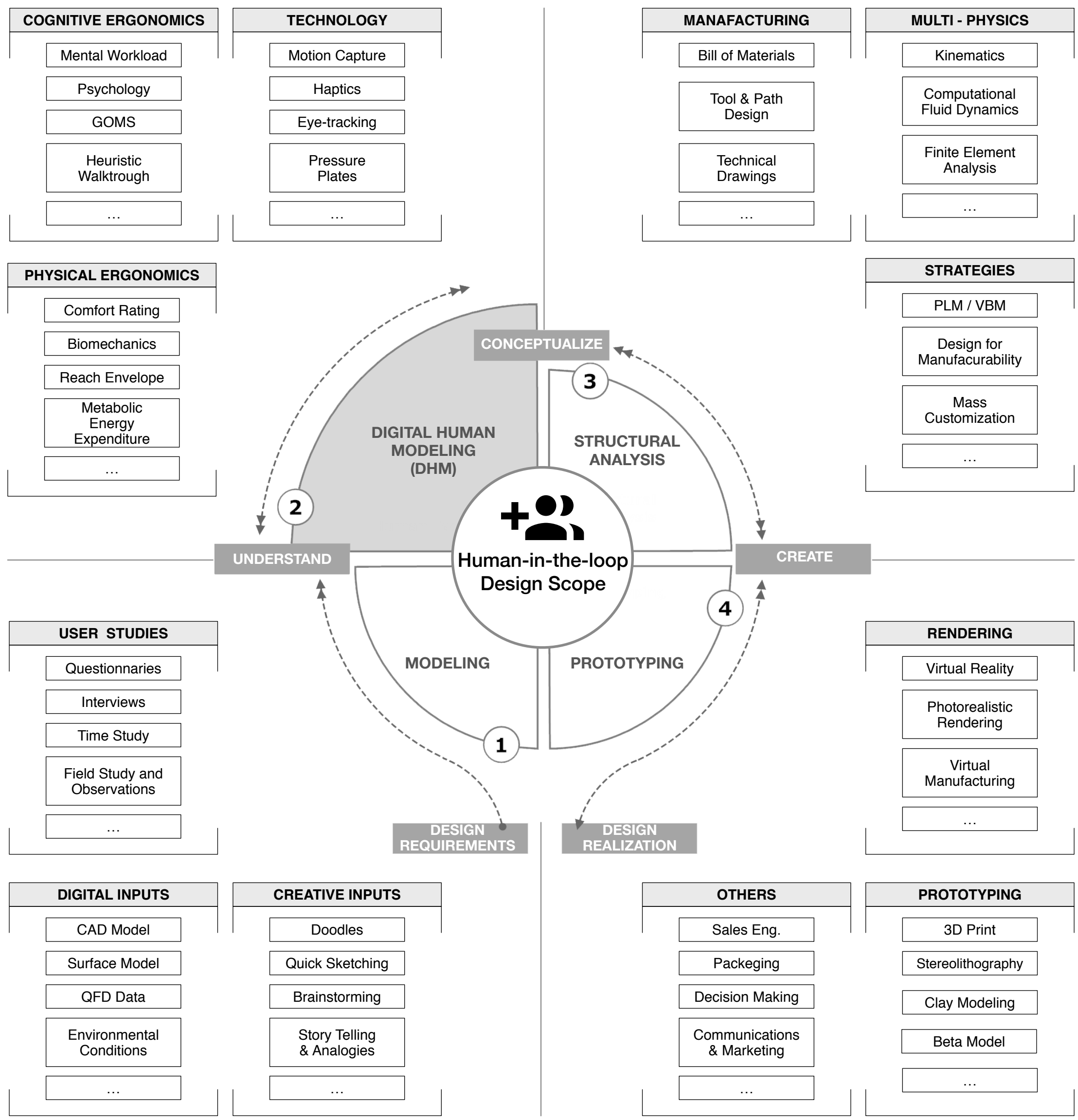

Figure 3.8. Human-in-the-loop design framework embraces various tools, methods and technologies in a modular fashion. Each toolkit can be added/plugged to the framework. DHM acts as a merger between modular entities. Each toolkit communicates back-and-forth, iteratively, to realize a product - from sketching to ergonomics assessments, structural integrity and prototyping. Figures demonstrates how various toolkits can be integrated to the human-in-the-loop framework under different design context.

There are few variants of VB structure that bridge DHM and MoCap for ergonomic research [111, 119]. Different than those studies that use DHM as a method of post-processing analysis tool, this framework utilizes DHM to bring human needs, abilities and limitations earlier into design process. DHM is used as an actual product design tool rather than as a method of ergonomics evaluation executed at the very late stages of product development.

In this study, human-centered design approach forms the foundation of the design strategy. It is composed of four product development phases (Understand, Conceptualize, Create and Realize) and four Constraints (Costumer Requirements, Human Capabilities and Limitations, Physical Requirements and Process Requirements). Design flow works in clockwise (from Understand to Realize) and in ascending order (from 1 to 4) respectively, to establish a design hierarchy. This hierarchy provides a systematical process flow to understand customer requirements, generate concept ideas, then create digital models and finally realize a high-fidelity digital model. The framework utilizes this hierarchal strategy to map user requirements with engineering constraints and find potential pathways to satisfy overall design goals (Figure 3.9). Each building block acts like an individual part of an embedded system, where ascending blocks provide design decision filters to the information sent from lower blocks.

Human-in-the-loop design framework functions similar to an Quality Function Deployment (QFD) system, where Customer Attributes (WHATs) are mapped to Engineering Requirements (HOWs) [120]. In QFD, WHATs provide customer's (supplier's, maintenance personnel's) desires and HOWs provide engineering (design and supplier) characteristics to satisfy (or ways to achieve them) WHATs within available resources. These elements (WHATs and HOWs) eventually define goals and constraints of the design system, which together form the available design space [121,122]. Goals are different than constraints. Goals define the ultimate design objectives (all potential design alternatives) and constraints draw up the boundaries, which form the feasible design space. Not all initial goals can be achieved. In other words what

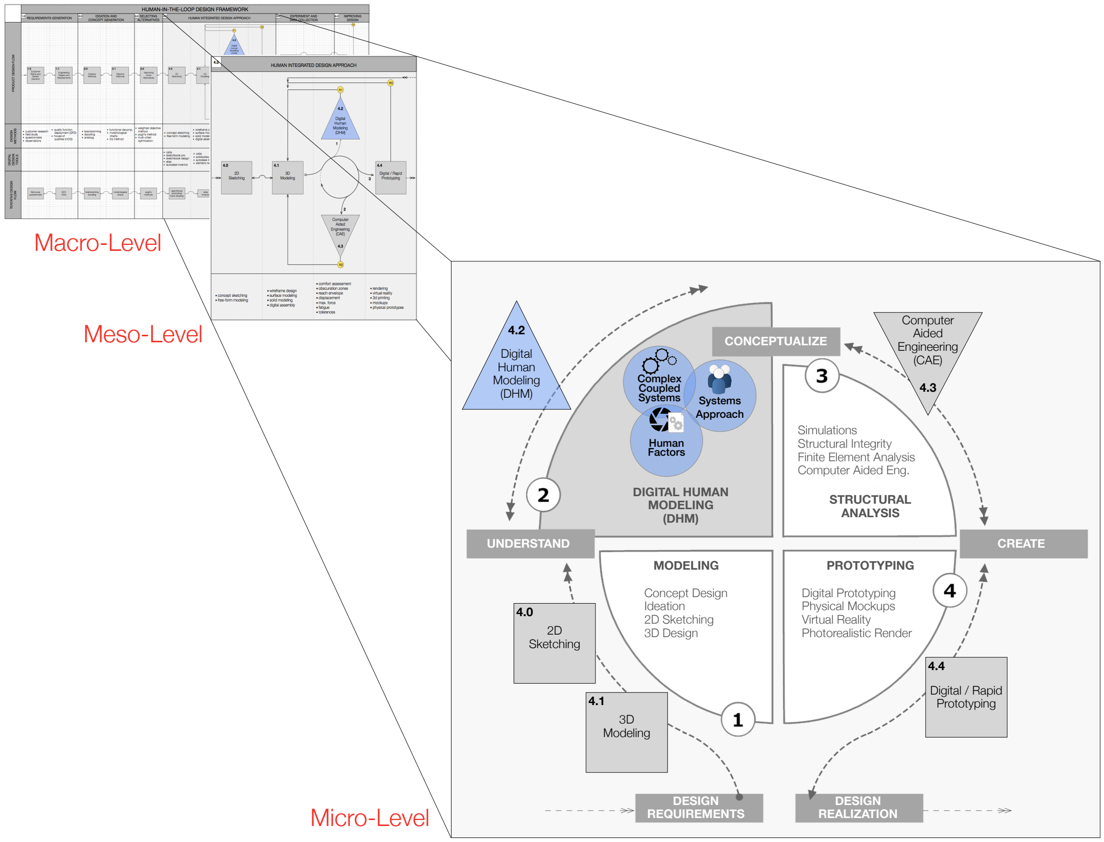

Figure 3.9. Image shows extended overview of the human-in-the-loop design framework, from macro-level to micro-level. At micro-level the framework functions similar to the VB methodology discussed in previous chapters. In contrast to VB, human-in-the-loop framework does not only functions as a post-processing ergonomics analysis tool. It is actually an integrated part of a concurrent product design and development system (macro-level). This approach creates a holistic coverage of design entities while keeping human needs, abilities and limitations at focus throughout the design process.

customer's wish can sometimes be misleading or technically not feasible. Often, Engineering Requirements form the boundaries that shape up all feasible/alternative ideas. In this context, DHM defines human-aspects of Engineering Requirements. Without the use of DHM techniques, engineers utilize manual checklists or expert opinion, which often fail to systematically generate a list of realistic Engineering Requirements. How people interact with products, both physiologically and cognitively, goes beyond the scope of simple checklists and expertise. The use of DHM as a core member of design cycle assists engineers in iterating various what-if scenarios parametrically without the need of extensive use of physical prototypes or mockups. Without such design strategy, decision making during design process would be misleading and erroneous, which often resulted in high costs, hazard or dissatisfaction.

3.4.1 Phases of the human-in-the-loop design process

Product design process starts with identifying or understanding consumer needs, abilities and limitations. Understanding the problem area is essential to create sound design requirements. After this step, engineering requirements are linked with knowledge base where each requirement can guide designers to generate necessary design alternatives. Later, alternative (concept) models can be modeled and simulated to check various design specific what-if scenarios. Best model(s) from pool of alternatives can be refined to create the most feasible prototype model(s) that meet engineering requirements while satisfying as much customer needs [120]. Finally, concept product is selected and beta product for manufacturing and production are finalized at Realization stage. More information is provided below for each design phase.

- <u>Understand:</u> This is the initial product development phase where user needs, abilities and limitations are identified and checked with the knowledge base. This phase is the most critical amongst other stages, which requires at most attention to carefully identify design challenges. Designers often omit or ignore human aspects of design process at the earlier stages of design process, which ends up being a cost driver at the later stages of product development.

- <u>Conceptualize:</u> After design requirements are identified, concept models can be generated. These models should reflect designers' creativity while satisfying design requirements. At the end of this phase, concept models should be filtered to obtain prototype model(s), which represent the best models amongst a pool of design alternatives.

- Create: Prototype model(s) further go into more refinement process, which includes structural modeling and multi-physics simulations. If higher fidelity can not be achieved with available multi-physics simulations, physical prototyping, field tests and experiments should be sought.

- Realize: At this stage final prototype should be further refined to meet manufacturing, maintenance, production and packaging requirements. Depending on the complexity of a product or the nature of the design project, a final prototype can be a fully digital model, a physical prototype or a combination of both.

3.4.2 Goals and constraints

Within human-in-the-loop framework, upper blocks function as a filter for the lower blocks. In Customer Requirements step, customer attributes are identified by designers. These attributes may exceed physical and cognitive capabilities of users. Therefore, Human Capabilities and Limitations block acts like a filter for the design alternatives generated in previous stage. This step only allows attributes that are capable to be performed by users. Later, qualified customer attributes are mapped to Physical Requirements, which are used to generate the form and functions associated with conceptual design model. At this stage of the design process, only human-product interactions that are feasible pass to the next stage. In Process Requirements stage concept model is further refined and working prototype is finalized. More information is provided below for each phase.

- Customer Requirements: The foundation of the design development is to understand customers wants and needs. This step provides a vast number of customer needs and desires on a new product or modifications for an existing product. Human centered products should be designed to reflect customers' needs while satisfying engineering requirements. This is also a very important step to define the design scope. Surveys show that poor product design definition is a factor in 80% of market delays [43].

- Human Capabilities and Limitations: This step filters customer requirements and provide limitation to those that exceed human physiology and/or cognition (e.g., control button distance exceed maximum reach of 75% male). Ignoring or omitting the human aspects of design is a costly mistake and should be avoided with all the cost. Products that do not reflect human capabilities and limitations are not appreciated by customers and result in compatibility issues, safety problems and market failures.

- Physical Requirements: In this step customer attributes and human characteristic are mapped to each other to provide a conceptual design that satisfies users characteristics from a wide range of population. Also, technical attributes such as form, functionality, and material selection are generated and checked with compatibility requirements.

- Process Requirements: After generating the conceptual models (or working prototypes), products are further refined by usability studies and experiments. In this step, available resources (suppliers, marketing...etc.) are mapped and the working prototype is finalized for production.

3.5 How Does Human-in-the-loop Framework Function?

At the core of the framework DHM functions as an analytical design/analysis tool as well as a communication medium between contributors of each stages of the design. In this study, HCD approach retains user needs, abilities and limitations at sight throughout the design cycle. Goals and Constraints link HFE knowledge and methods with design requirements. Varying HFE methods and technology tools are added to adequate stages of the product development through modular approach. Variations and combinations of methods and technologies used inside the framework depend on the nature of the design study. A consumer product design may not require advance simulations. On the other hand, an aircraft design may demand multi-physics simulations, as well as extended physical experiment and prototyping.

Thus, the domain of interest dictates what tools to be integrated to the framework. In either case, DHM blends form and function of aspects of products with humans at the center, and builds connections with other design entities.

Human subject data either comes from digital libraries or collected through manual methods. Digital libraries include kinematics, anthropometrics and posture related human attributes. If manual methods are used, attributes can be linked design framework through various data collection methods (MoCap, eye-tracker, sensors). Similarly, environment input could be a fully digital CAD model, immersive VR environment, a physical prototype or a hybrid model (a physical model with limited digital probes). DHM blends human data and environment input and generate analysis that constitutes mathematical (e.g., biomechanics) and visualization (e.g.,rendering) outputs.

Within human-in-the-loop design work-flow concept model(s) go in digital test that iteratively forces what-if design scenarios. This portion of the design framework uses multi-physics simulation tools to answer what-if scenarios. In case multi-physics tools are not capable of providing required answers to what-if questions asked by designer, physical experiments and field tests should be conducted for further understanding and refinement, if necessary. The need for physical prototyping often results due to complexity of design projects where product or process requires higher levels of human-product interactivity [111]. At this stage designer should make the decision of either fully relaying on simulation tools or collecting human subject data through physical experiments. The choice of either method or degree of relaying on one method depends on the level of human product interaction. If multi-physics simulation tools provide sufficient fidelity, then digital prototypes would be a sound strategy. At this stage, DHM can be utilized without the need of physical experiments or full-scale prototyping. When simulation tools loses the fidelity, then human subject experiments through physical models becomes an ideal path to follow (Figure 3.10).

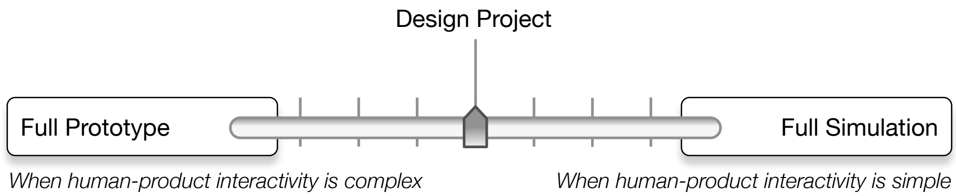

Figure 3.10. The need for full-scale modeling or full-simulation in a design project is shown in a continuum. Depending on the complexities of human-product/process interactions, DHM simulations can either be used as stand-alone (simulation) or linked to data capturing tools (prototyping) [111]. The degree of the using either full or a moderate simulation/prototyping depends on the nature of the design project.

The need for digital prototypes or full-scale models also define the scope of the design project. Often, one can split design projects as either industrial design or engineering design oriented. In the case where abstraction and conceptualization are concerned, industrial designers heavily involve with the generation of design ideas, which are often require low fidelity models that rely on form aspects of design. In contrast, engineering design projects require high fidelity models that are based on functionality of products with validation (proof). DHM has the advantage of working back-and-forth with either extremes, and can accommodate form and functionality requirements of design projects (Figure 3.11).

Within human-in-the-loop design approach, contributors of the product development, whether it's a group of industrial designers, design engineers or managers, can interact with the design process in any given time. The framework connects technical (engineers) and non-technical experts (managers) as well as third party contributors (suppliers) together. It allows parametric modification of dimensions, tasks and environments. Results due to changes on CAD models and CAE simulations can be simultaneously updated, and changes on ergonomics and structural evaluations can be monitored accordingly. This work-flow creates opportunities for optimizing design alternatives through iterative changes (what-if scenarios). In addition, holistic cov-

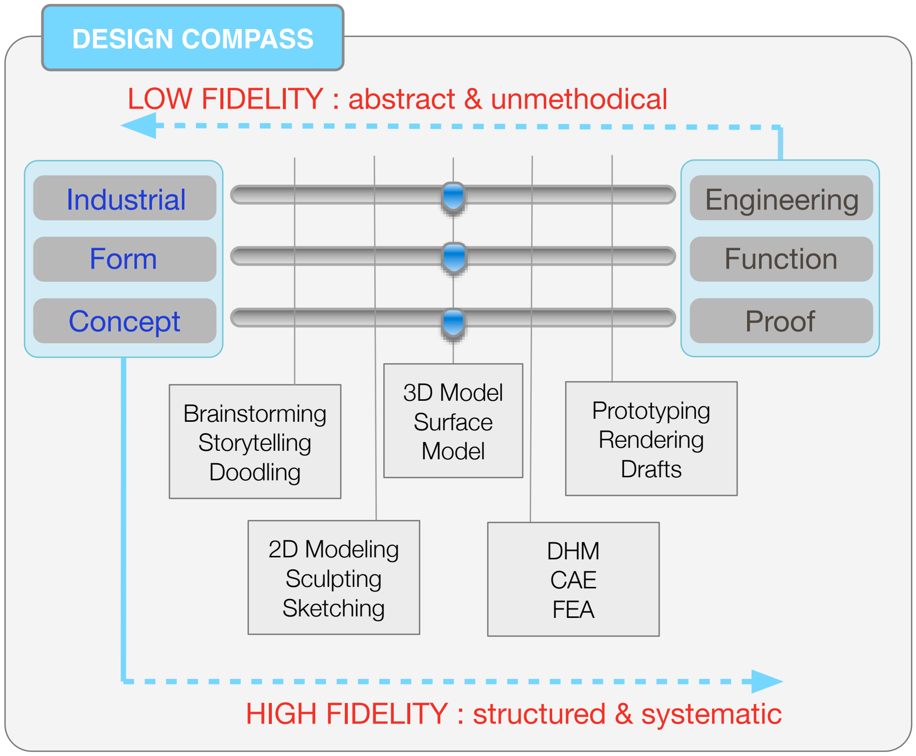

Figure 3.11. Depending on the design study, either Industrial Design or Engineering Design can dominate each other. In product design studies, often Industrial Design or Engineering Design contribute equally. DHM can function either way by blending form and function aspects of design attributes centered at human needs, abilities and limitations.

erage of design disciplines and modular integration of various tools and technologies can provide unexplored spaces for creativity (Figure 3.12).

There are three design studies summarized in following section. Each study focuses on different design objectives that require integration of distinctive human subject data (either manually, automated or through hybrid methods). Experimental procedures of these studies are not covered in details. Only figurative design story is demonstrated to provide a breadth of the human-in-the-loop design framework, and to demonstrate how it could be applied to different design studies. First design story represents a reverse engineering of a hospital code cart design, which follows a detailed visual design story in the order of: schematic layout, product design phases

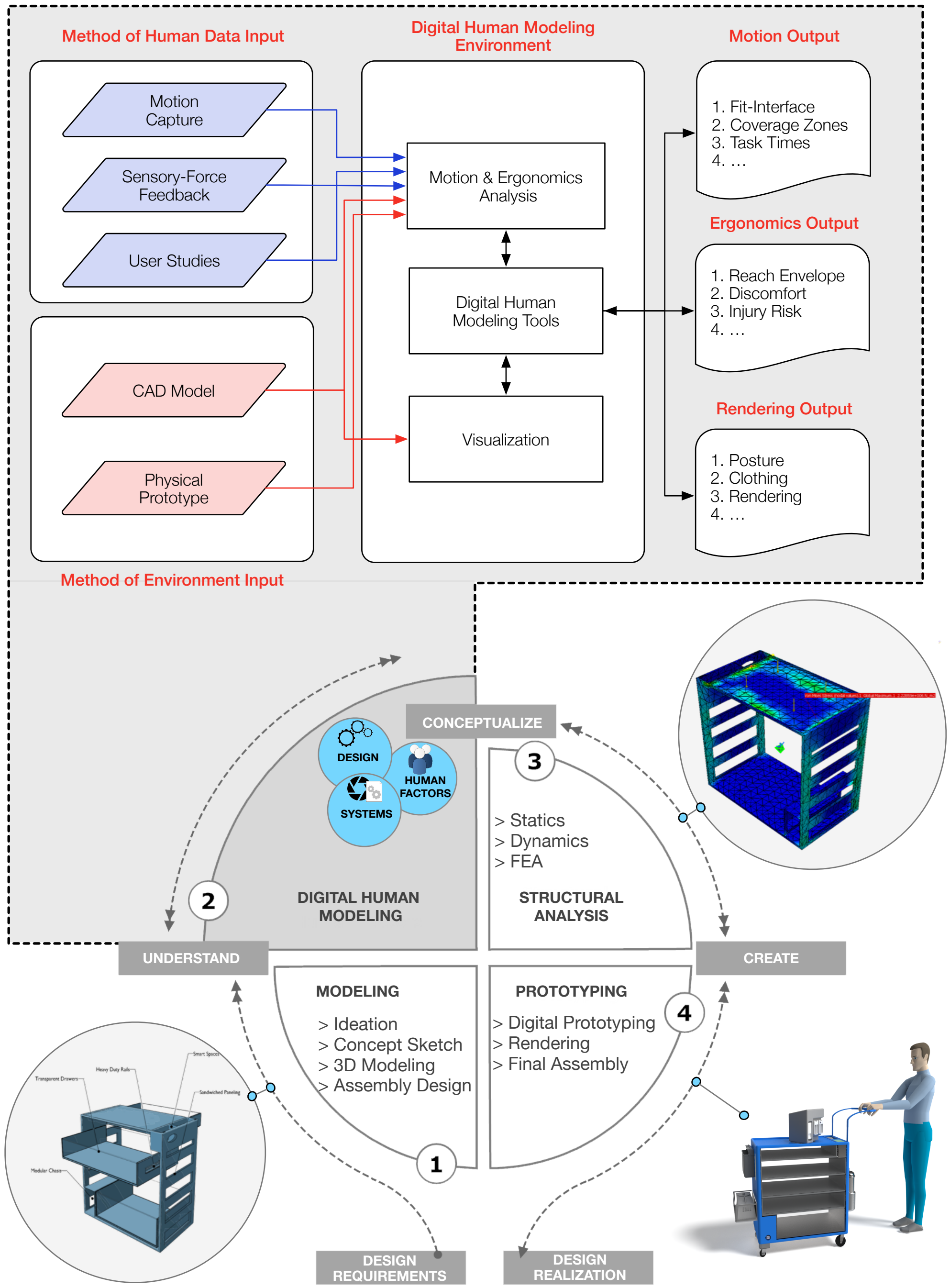

Figure 3.12. The framework merges human subject data with a full scale CAD model and a low-fidelity physical prototype to generate three different outcomes: motion, ergonomics analysis and rendering. Through this approach human aspects of design data was integrated to realize a code cart that reflects user needs, abilities and limitations. DHM provided tools to validate ergonomics and visualization aspects of the human-product interactions.

and summary. Second study provides a concise visual synopsis of a Formula-1 race car cockpit design, which blends form aspects with functional development. Final study focuses on the conceptual development of a futuristic vehicle with emphasis given to artistic conception. Figure 3.13 provides a summary of human-in-the-loop studies with associated design content.

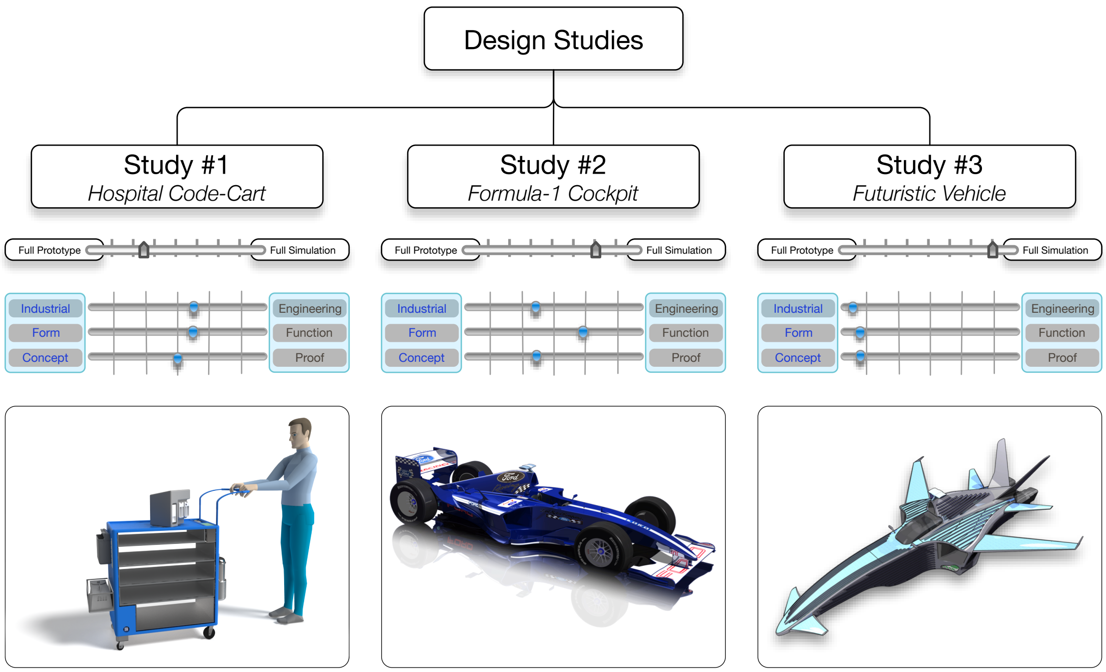

Figure 3.13. Three design studies summarized to show how human-in-the-loop design framework could work in projects with different design scope. Each project represents different levels of industrial design and engineering design contribution. Design scales and design compasses reflect information about the level of contribution.

3.5.1 Reverse engineering a code cart

This design study embodies two theme areas: product design and design research. Main objective of this project was to design a better code cart and to integrate haptic feedback into design process (Figure 3.14). Although it seems that the study had two separate areas of focus, human-in-the-loop design framework was used as a testbed to evaluate design research (haptic feedback) through a practical design study (code cart design).

Product design in this study focused on reverse engineering a hospital code cart according to needs, abilities and limitations of nurses. Emphasis was given on creating a light-weight, maneuverable and a versatile code cart (Figure 3.15). The main HFE objective was to test whether new design proposes an improved L4/L5 compression force readings on lumbar section during a push-pull task. In addition, subjective feedback of users about the cart design was collected to further accommodate design attributes (e.g., bi-directional drawers, adjustable handle) that nurses were expecting on an ideal code cart design [77].

The design research question focused on integrating a haptic feedback mechanism (sensory-force feedback) for ergonomic evaluation of products during design phase (Figure 3.16). Ultimately, the above methodology was evaluated through a push-pull experiment (a physical and a virtual push-pull experiment) in which two different product designs (a market available code cart and the prototype code cart) were evaluated for ergonomic adequacy under different loading conditions (Figure 3.17). Also, a questionnaire was given to subjects to assess their subjective opinion on whether the prototype cart was more preferred than current cart [77].

Human-in-the-loop design framework integrated haptic-feedback and motion capture with a digital and a low-fidelity physical prototype model. DHM modules were used for generating percent capable, compression and comfort evaluations. CAD code-cart model went through several multi-physics assessments including: FEA for top loading scenario, weight estimation and center-of-gravity calculations (Figure 3.18). After defining parameters that satisfies user needs and engineering requirements, a photo-realistic rendering of the concept cart model was generated (Figure 3.19). Figure 3.20 and Figure 3.21 provide a human-in-the-loop design summary. Starting by next section, information about how human-in-the-loop framework was applied to this project was provided in details.

Schematic layout and data flow

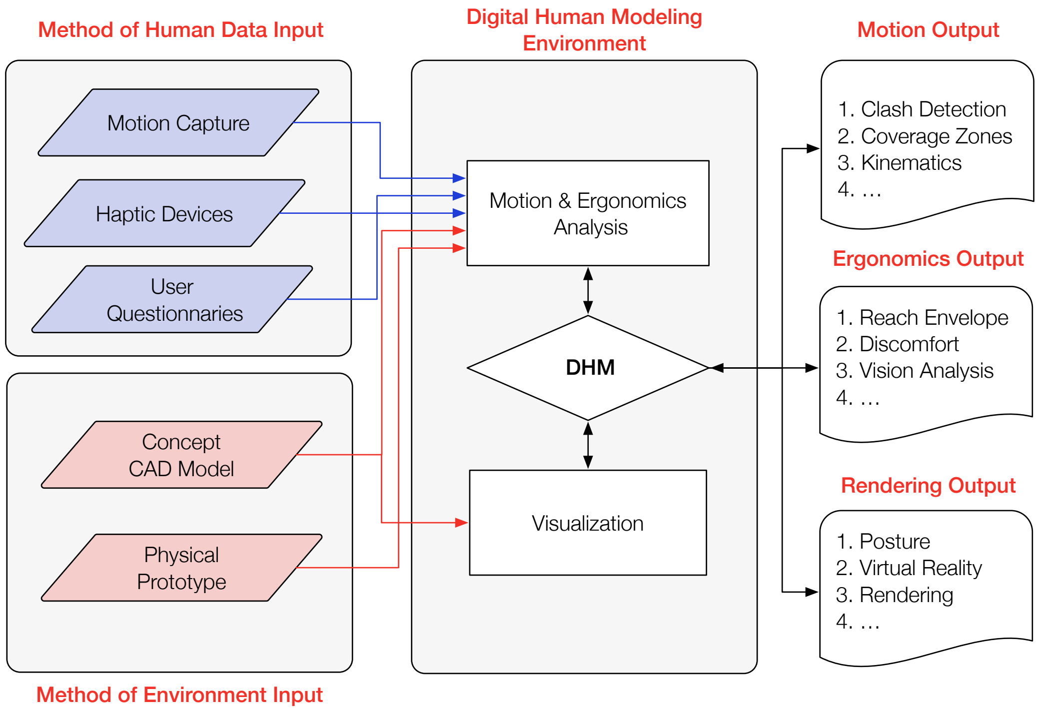

Figure 3.14. Human-in-the-loop design framework merges MoCap, haptic devices (sensory force-feedback) and subject questionnaire (user studies) data with a full scale CAD model and a low-fidelity physical prototype to generate three different outcomes: motion, ergonomics and visualization. Through this approach both objective (motion and pressure) and subjective (questionnaire) aspects of design data were integrated to realize a concept code cart model that reflects user needs, abilities and limitations. DHM provided tools to validate ergonomics and visualization aspects of human element within design process. Human-in-the-loop design framework provide multi-disciplinary creative pursuits for industrial designer and design engineers to work together on the same design project without isolation. Form and functional aspects of product development can be monitored, modified, tested and furthered refined in a parallel sequence, with human needs, abilities and limitations are kept at the center. In addition, qualitative nature of design process can also be integrated through user feedback, questionnaires and field studies. This approach offers a more systematic method to evaluate of what customer wants.

Product design stages

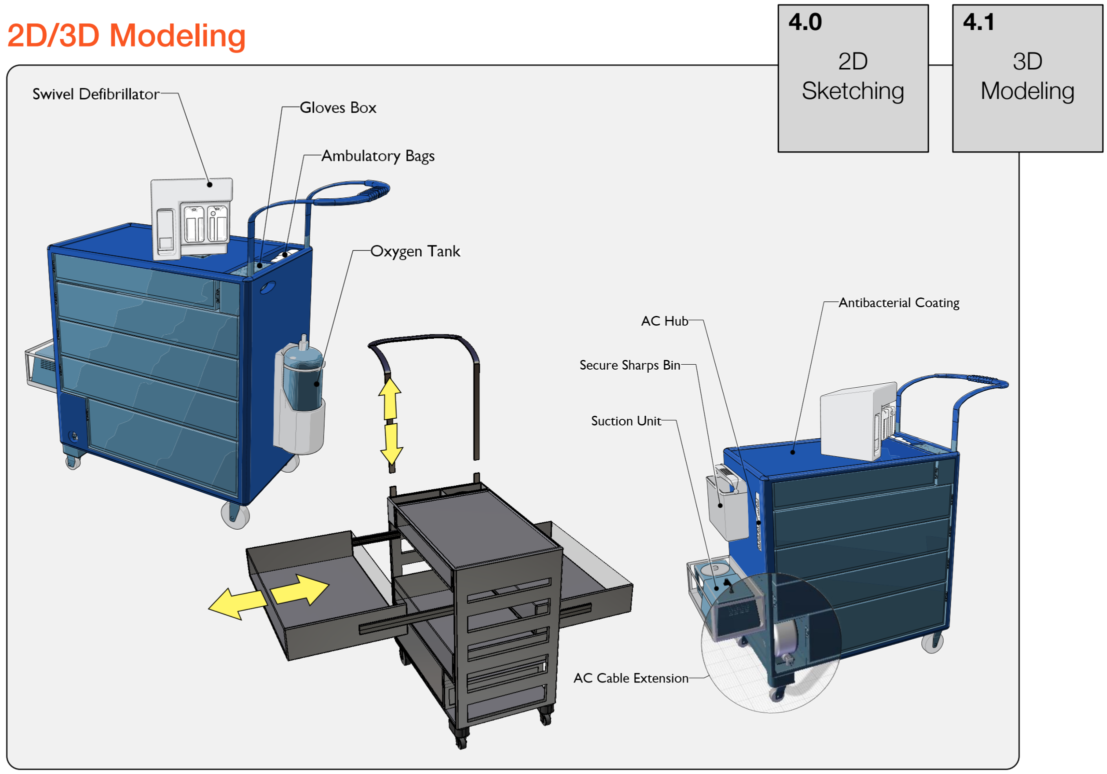

Figure 3.15. Design process started with identifying key features that are essential for nurses. These features were gathered after on-site observations and questionnaires data collected from nurses. This approach reflected what was missing in current code carts and what could be included in the concept design in terms of improving nurses' comfort and performance. Features such as retractable handles and dual-way access drawers, as well as swivel defibrillator and AC plug were amongst the most that provided versatility and ease of use to nurses. These conceptual ideas were further refined through QFD, functional decomposition and Pugh's charts. Finally, a representative conceptual model that includes surface and solid models were developed as a CAD assembly. After this stage, CAD model was linked to DHM to get validation in terms of its ergonomics compatibility. Meanwhile, structural tests were conducted on multiple what-if scenarios. After running various biomechanics and FEA simulations, conceptual features were modified, some features were disregarded, and new features were added.

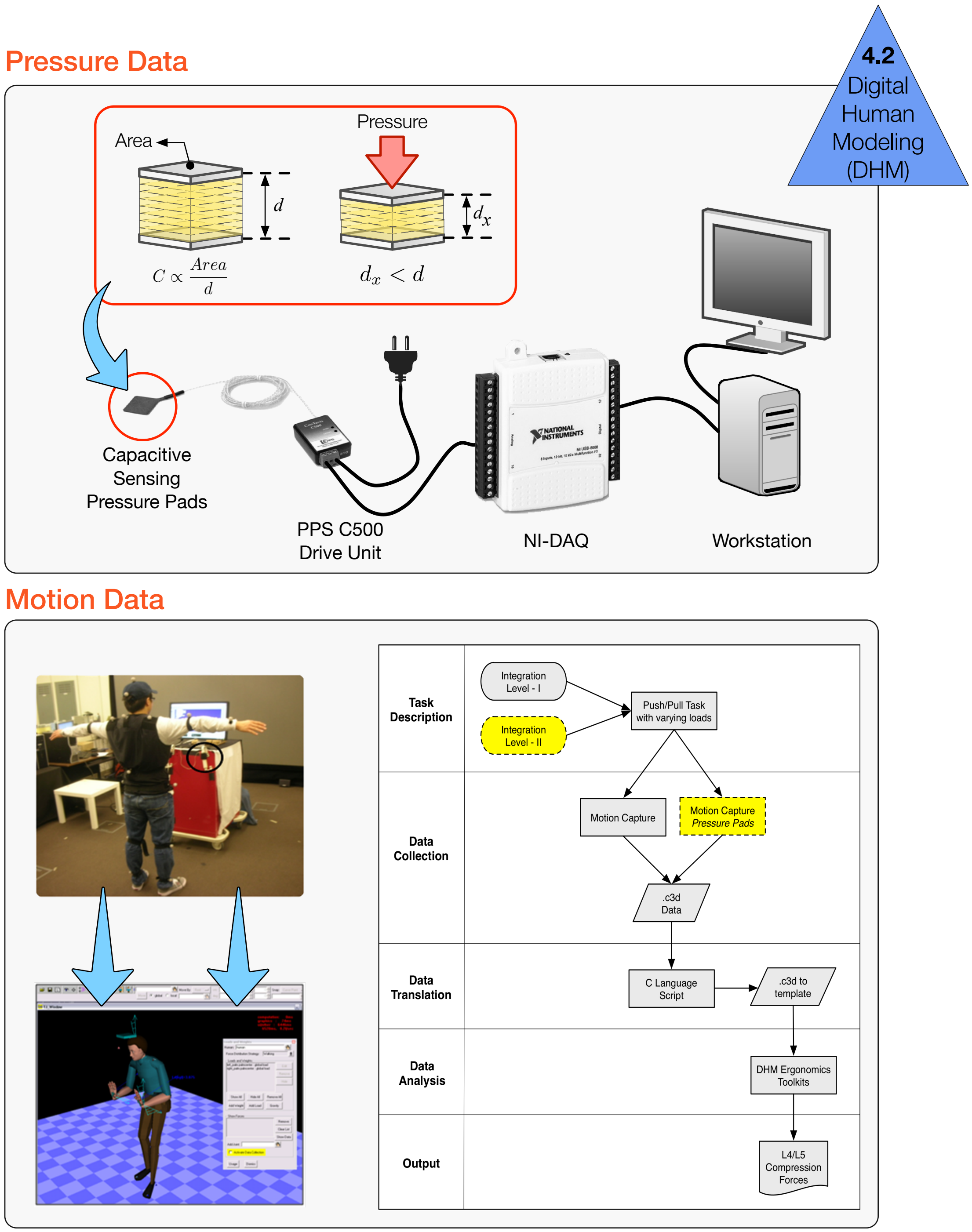

Figure 3.16. At this stage haptic (force-feedback data) and motion data were integrated to create digital representation of users in computer environment. Low-fidelity prototype cart model was used as physical probe to gather realistic information about push-pull forces required by nurses. Data collected were sent to DHM for conducting ergonomics analysis.

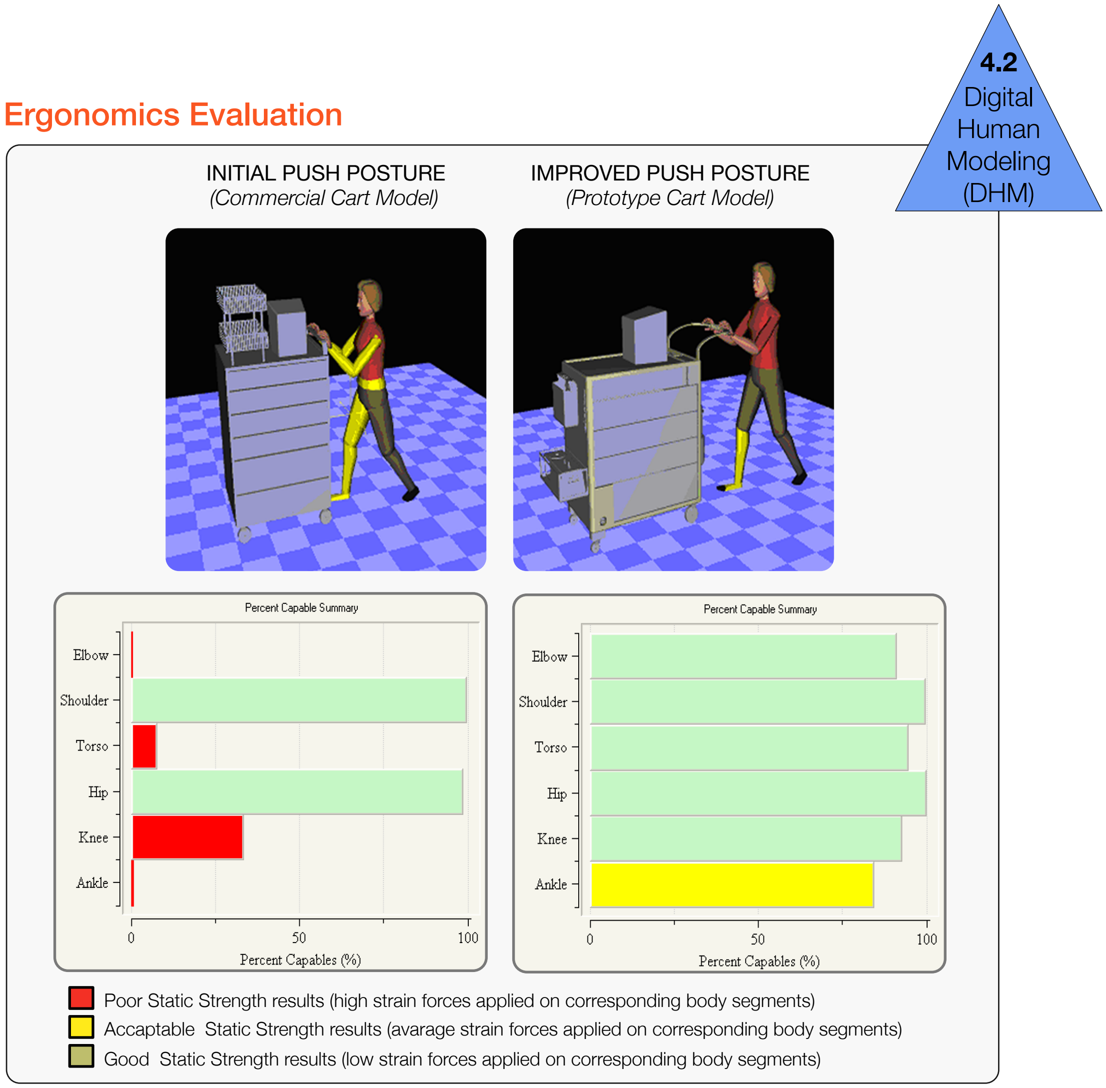

Figure 3.17. After haptic and motion data were incorporated with CAD model, various ergonomics analysis were conducted to evaluate human-product interactions. Manikins that represented different percentile of populations were tested for their capabilities in pushing-pulling the cart with various loading scenarios. Performance of nurses between current code cart model and concept design were compared in terms of ergonomics adequacies. In this figure percentage capability analysis was performed for 50th percentile female when pushing current and concept cart with identical external loads. Once can see that current cart model created a wider range of accommodation. Almost every nurse can conduct a pushing task without exerting a large force readings on their joints. In contrast, only few nurses can complete the same push test when they used current code cart.

Structural Analysis

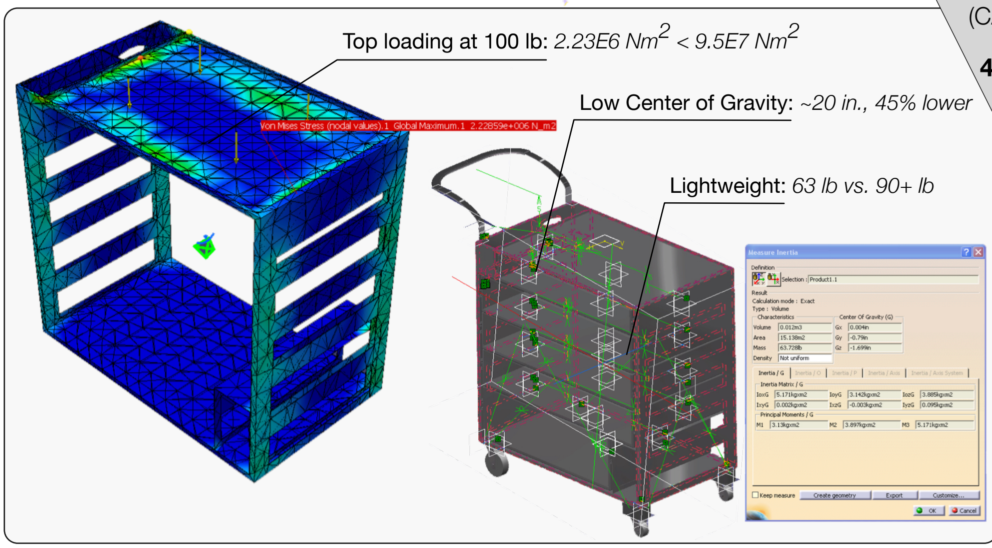

Figure 3.18. Structural analysis demonstrates lower center of gravity, weight reduction and good structural integrity in top-loading scenario.

Photo-realistic Rendering

Figure 3.19. CAD model and digital manikins used in engineering design analysis were also used for design visualization purposes to enhance industrial design process.

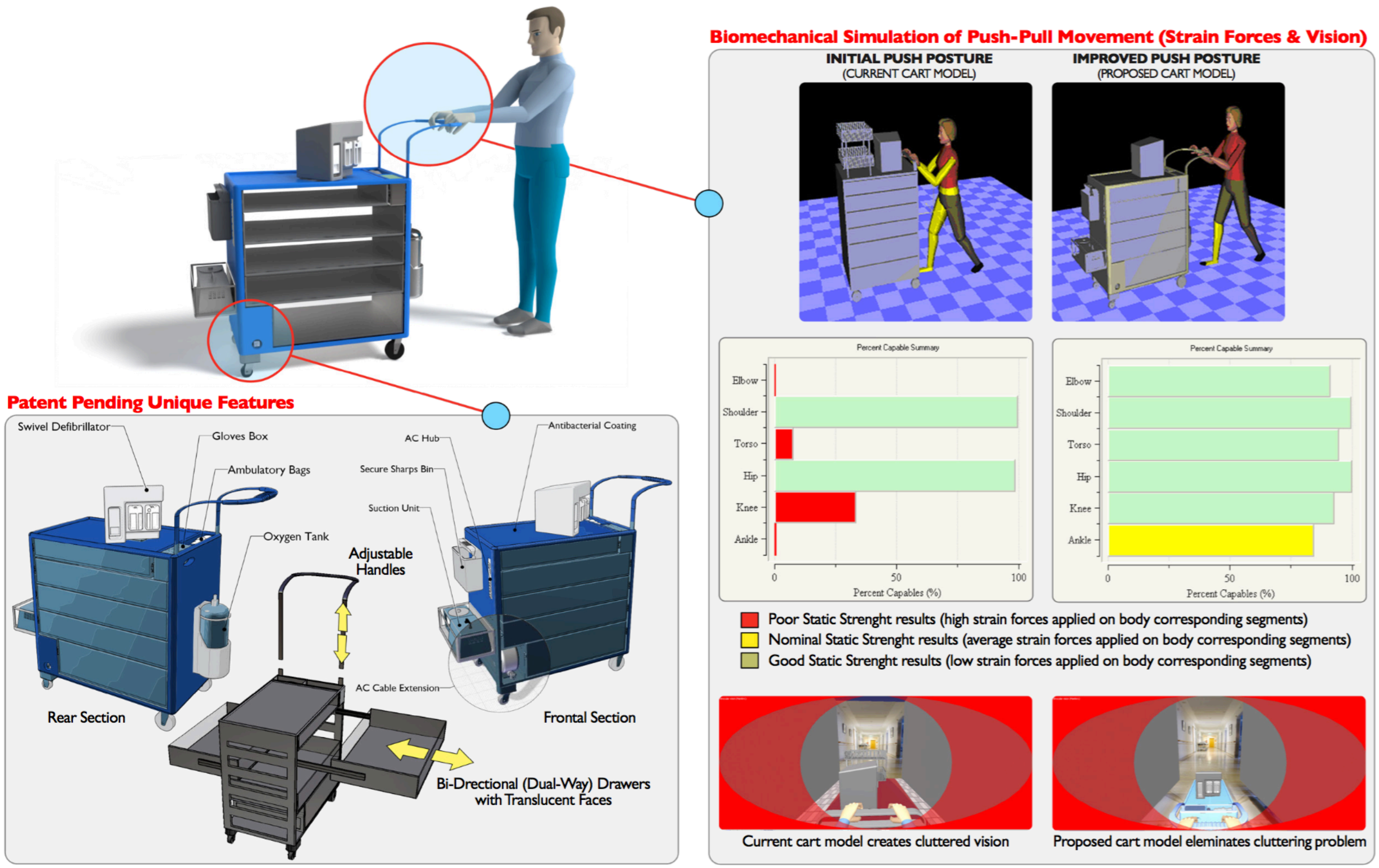

Figure 3.20. Integrated stages of product development are shown from concept modeling to biomechanics analysis. At each stage human element is kept at the center of the design process.

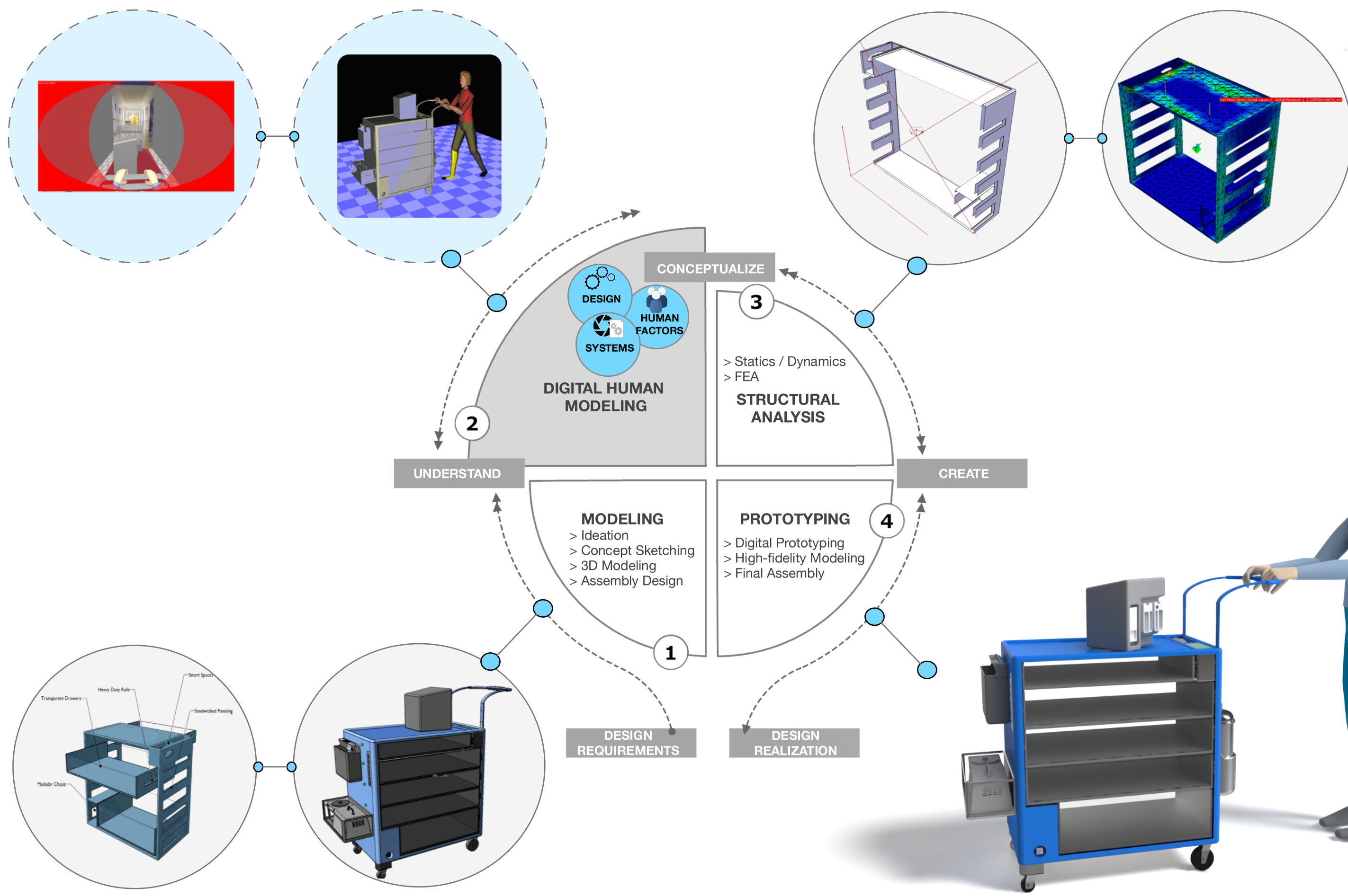

Figure 3.21. Summary of the human-in-the-loop design framework shows how different stages of design process are synthesized within a single design platform. Form and function aspects of design are centralized around the human element - from conceptual design to photorealistic rendering.

3.5.2 Integrated cockpit design of Formula-1 race car

Main objective of this study was to develop a cockpit design for a Formula-1 car through human-in-the-loop design process (Figures 3.22). Driver's cockpit was the central theme in the design process, where driver's joint angles were optimized to sustain a comfortable posture inside a confined space (cockpit) (Figures 3.23). This project demonstrates capabilities of human-in-the-loop design framework in a full-digital environment. Figure 3.24 shows overall summary of human-in-the-loop framework from conceptual development to photorealistic rendering, which encapsulates functional as well as the form aspects of design process.

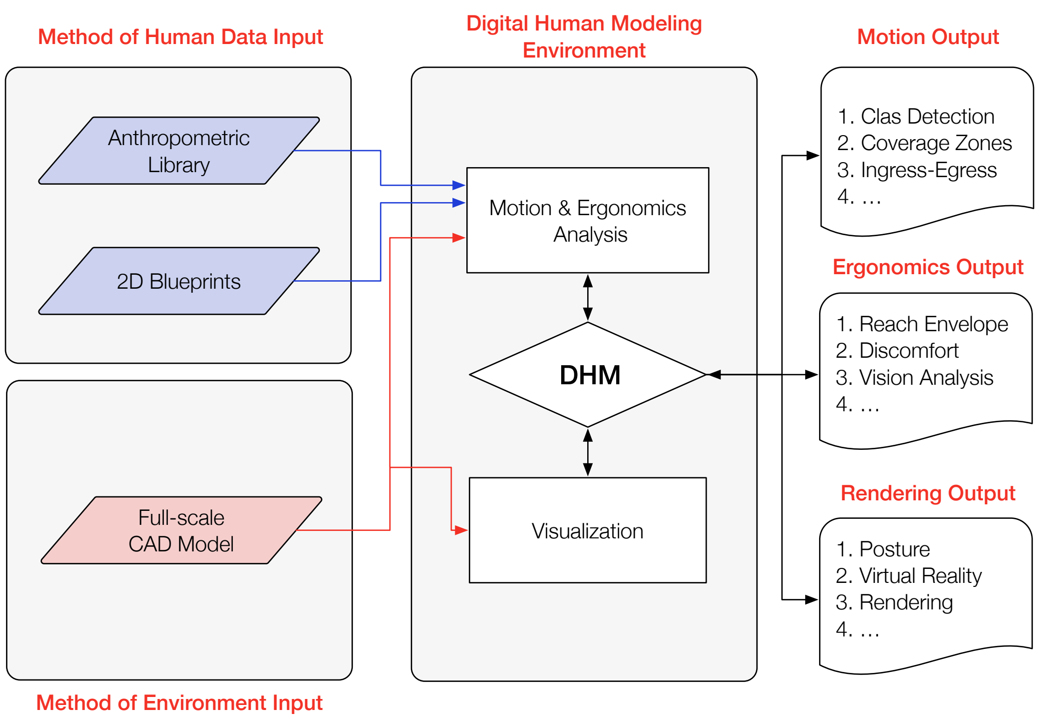

Figure 3.22. Human-in-the-loop framework merges anthropometrics data with 2D vehicle blueprints and a full-scale CAD model. Major outcomes are summarized under motion, ergonomics and rendering. DHM blends function and form aspects of vehicle design and provides tools to validate ergonomics as well as visualization aspects of human element in cockpit development.

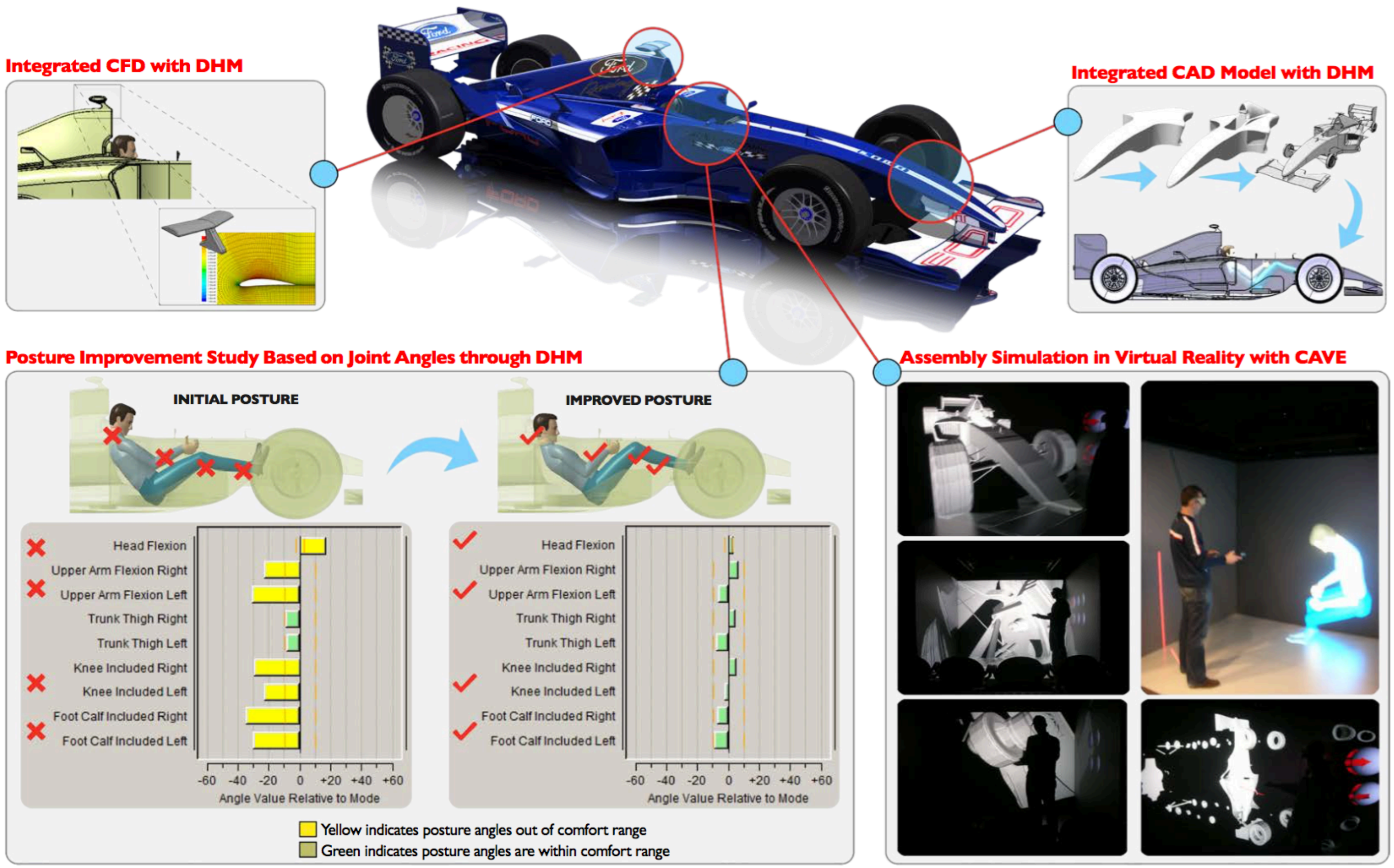

Figure 3.23. Integrated stages of vehicle development from CAD modeling to CFD analysis, and from VR and DHM were summarized. At each stage human element is kept at the center of the design process.

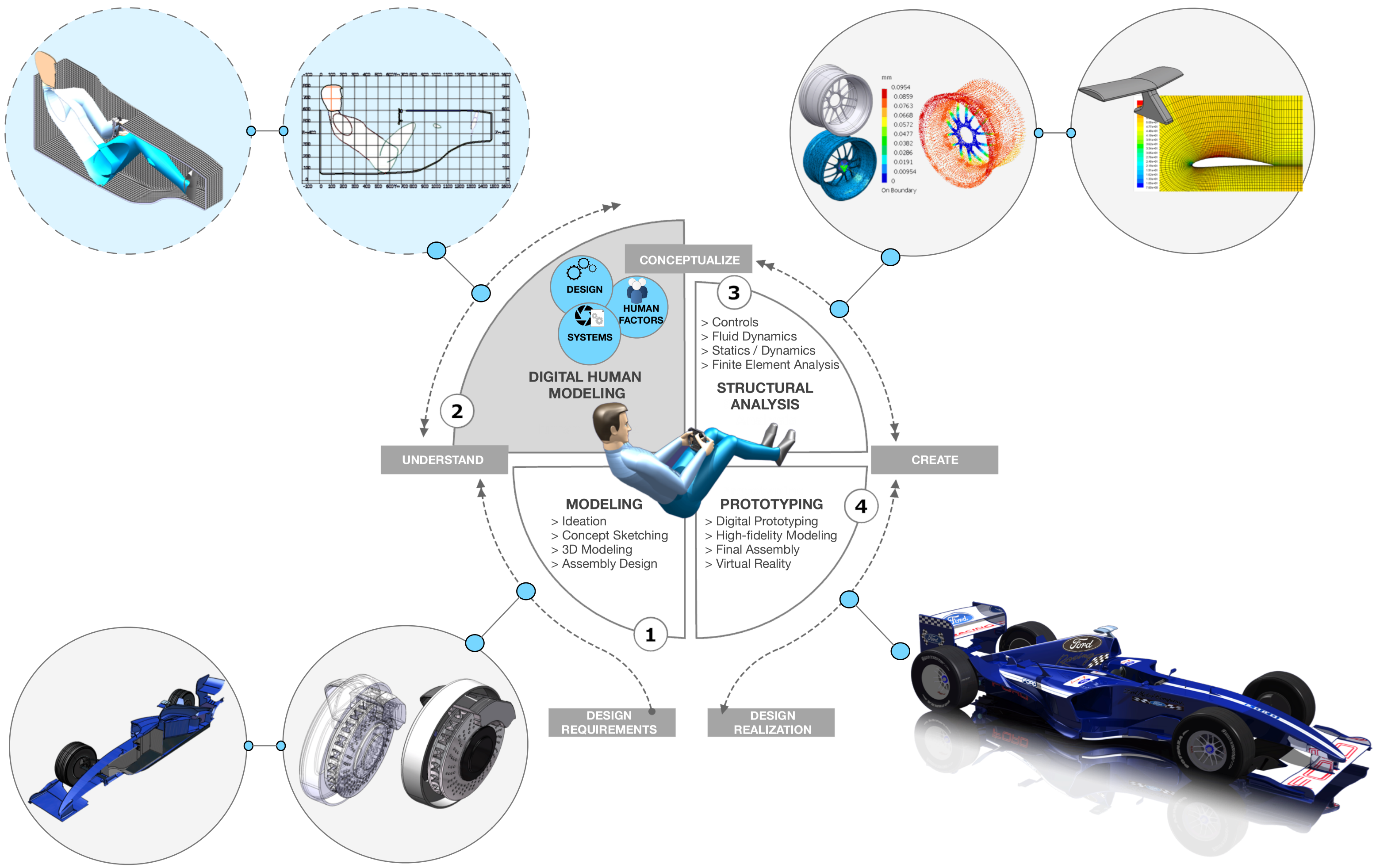

Figure 3.24. Summary of the design actions taken during the design process were summarized within human-in-the-loop design framework. This approach integrates form and function aspects of design centralized around the human element.

3.5.3 Futuristic transportation design

Formula-1 design project represented a fully-digitized engineering design study without any subject data collection. Digital anthropometric data and vehicle blueprints were used to generate driving postures. This study does not include any human data collection. Manikin and the monocoque cockpit data from Formula-1 study was used. The design objective in this study was creating an artistic conceptual model of a futuristic vehicle (Figures 3.25). Emphasis was given to industrial design (Figures 3.26). This project demonstrates how human-in-the-loop design framework can function even with artistic development of products (Figures 3.27).

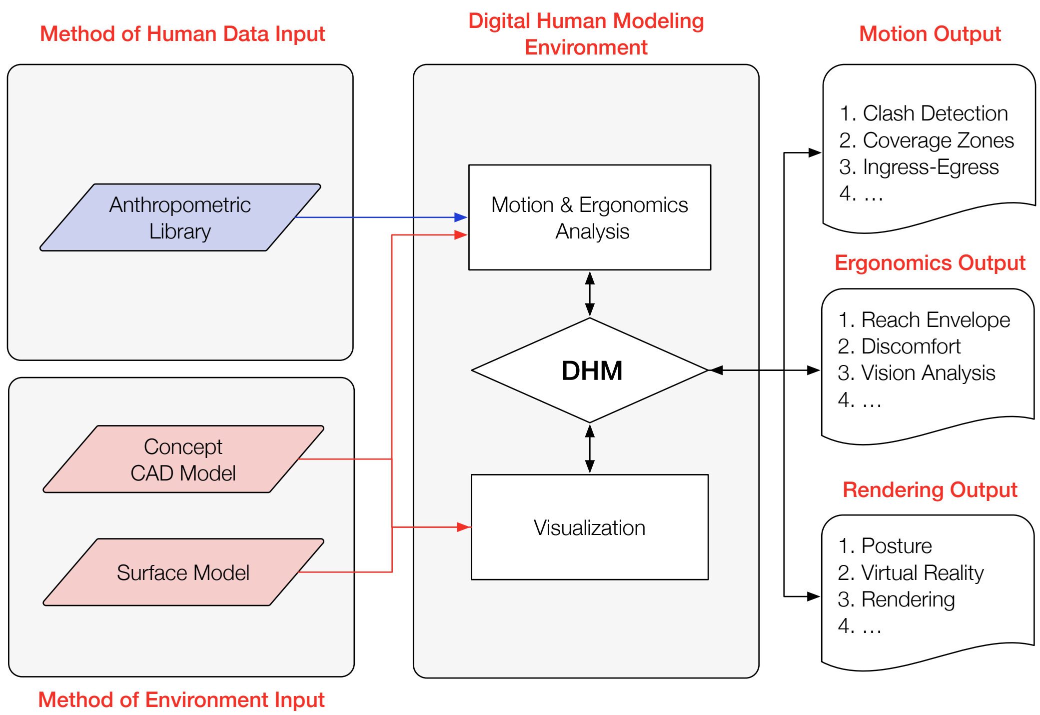

Figure 3.25. Digital manikin and CAD model from Formula-1 study was carried to this project. Digitized posture data from anthropometric libraries were linked with CAD model and surface model to generate a futuristic vehicle concept. CFD simulation was conducted to evaluate aerodynamics performance of the concept vehicle. Major DHM outcomes were mostly visualization focused, however, ergonomics and biomechanics outcomes can also be generated - if needed.

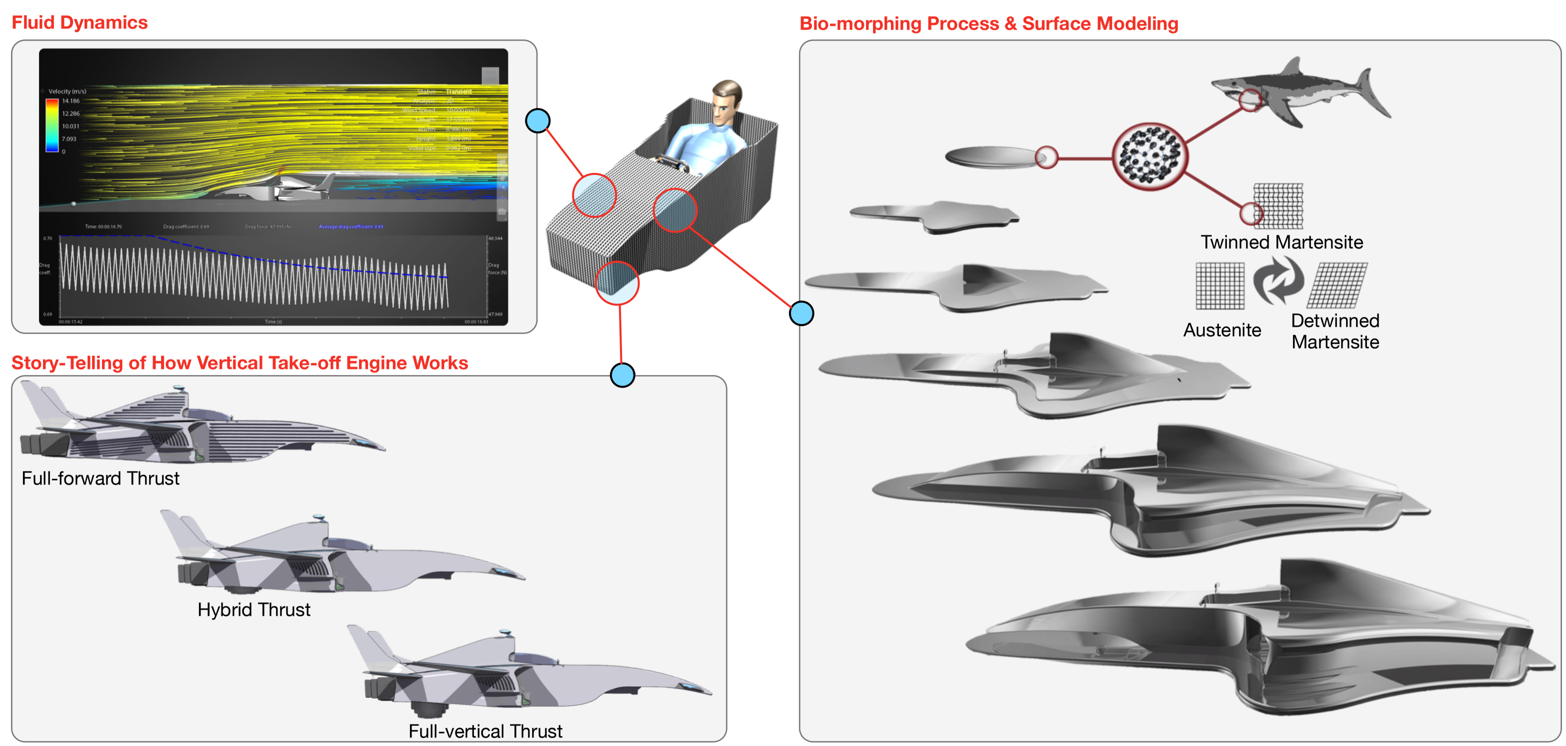

Figure 3.26. Integrated stages of futuristic vehicle development from storytelling to CFD analysis are summarized. The vehicle was developed through an inside-out approach, by taking the manikin and monocoque cockpit as the central theme.

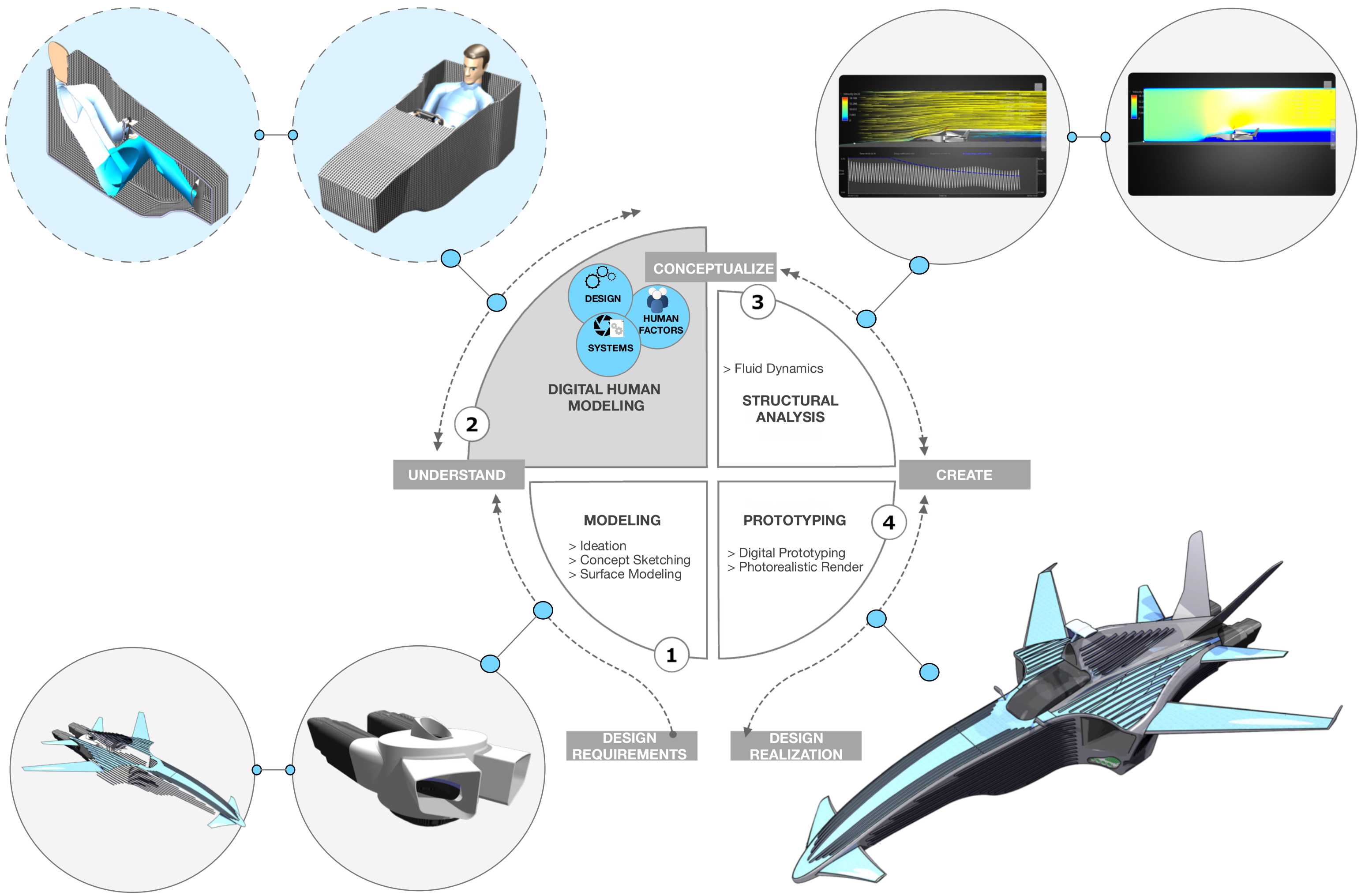

Figure 3.27. Concept vehicle development stages were summarized within human-in-the-loop design process. Surface modeling and conceptual development was linked to cockpit design and fluid dynamics analysis. Finally, a photorealistic output was rendered.

4. DESIGN STUDY

A systematic design framework that captures human needs, abilities and limitations has been missing in design research. Although few platforms offer some limited DHM based human-simulation coverage, utilization of these methods as part of product design framework has some limitations. Often, DHM is used a post-design ergonomics evaluation tool. Utilization of DHM as a direct design tool (similar to CAD or CAE) has not been at the central interest of designers. This dissertation proposes DHM as a direct design tool, rather than a post-processing ergonomics evaluation methodology. Human-in-the-loop design framework is built based on DHM. It integrates design (industrial and engineering), HFE and systems approach. Some of the details of this approach has been introduced through three design studies covered in Chapter 2: code-cart design, F-1 cockpit design and futuristic vehicle design (Figure 2.13). These studies provided a brief information about the capabilities of human-in-the-loop design framework and how the framework can be used for systematically blending industrial and engineering design principles with human-element at the center.

This chapter introduces a more comprehensive design research method, which not only demonstrates capabilities of human-in-the-loop framework in product design but provides a scientific validation to the framework. In this experiment, human-in-the-loop framework is proposed both as a testbed to integrate human element into design research and to validate the use of DHM toolkits in product development. Design methods used in this study are:

- Human subject data collection through an eye-tracker device
- Human subject data collection through user input, Cooper-Harper test and questionnaires

- Finite Element Analysis for structural integrity assessments

In this experiment, a combination of different design approaches, technologies and data collection methods were integrated within human-in-the-loop design framework. This multi-disciplinary design approach demonstrates holistic, emergence and modular characteristics of the framework. This experiment involves an automobile pillar design study, which makes connections with form and functional aspects of industrial and engineering design process. DHM was used as a bridge to connect form and functional attributes of automobile design with needs, abilities and limitations of humans. Efficacy of human-in-the-loop design framework was validated through human-subject data collection. Chapter 4 and Chapter 5 provide a detailed introduction to the design study, which includes statement of design problem, objectives, hypothesis and measures.

4.1 Statement of the Design Problem

The importance of occupant safety is one of the most vital aspects of product development and marketing in automotive industry. Today, it is a must to have to meet minimum safety requirements (EURO NCAP, SAE...etc.) to ensure protection of occupants, pedestrians and other traffic elements [123]. Within a very competitive technology driven environment, focusing solely on minimum requirements is not a smart way of winning a substantial reputation in the market. Companies strive to establish strict safety standards to sustain a high safety reputation, which leads to large market share. Since 1970's, manufacturers, private institutions and academia have introduced new technologies to increase the overall safety of ground transportation. Some of the well-known ways of increasing automobile safety (crash worthiness) are applying high strength steel to the chassis, introducing multiple airbags and developing advance body structures.

State of art energy-absorbing and/or energy-dissipating techniques are well-known for their success in reducing occupant injuries. However assisting technologies in reducing the risk of having a collision have not been successfully integrated to vehicle design when compared to energy-absorbing and/or energy-dissipating techniques. Majority of new safety technologies are focusing on minimizing the injury to the occupant during accident actually occurs. It is very important to decrease the severity of injuries and casualties through these techniques, but preventing vehicular accidents before they even occur should be a high priority item [123]. One of the important ways of improving safety of ground transportation is to offer a block-free or an optimized visual field, which can increase driver's reaction time for positive identification of other vehicles, road alerts and pedestrians [123,124]. Literature review and current vehicle design trends show that visual field obscuration is a major problem and pillar geometry is a critical design element in vehicle packaging [125]. In this context, not sufficient attention is paid for improving visual obscuration due to pillar geometry when compared to improvements in cockpit entertainment, efficient engines, alternative fuels, and weight reduction. Literature review shows that A-pillars (also B, CD pillars) provide a visual block and may lead to accidents [126, 127]. However very limited research has was done on this topic.

4.2 Literature Review on Automobile Pillars

4.2.1 Safety and product design connections to driver's visual field

This design study focuses on methods for ensuring driver's field of vision to reduce obscuration related discomfort and accidents. Unobstructed field of forward, side and rear vision is essential to see other vehicles, pedestrians, road signals, bends and curves, road conditions, and other important information. Ability to see these information as quick as possible without misdoubt is critical for reacting on time. On-time-reaction (or reacting as quick as possible) is vital for increasing chances of accident prevention through proper steering, breaking and/or maneuvering [123].

One of the vital and essential characteristics of vehicle packaging is providing a good field of vision to the driver. Presence of any obscuration zones (steering wheel, mirrors, pillars, dashboard...etc.) should be minimized to increase visual quality and comfort [124]. Design of cockpit environment as well as other parts of the vehicle that reduces driver's field-of-vision should be carefully evaluated before the vehicle is ever launched to market. At this point, ignoring visual needs, abilities and limitations of people would clearly decrease the safety and performance of the overall vehicle.

When field of vision is concerned, opaque objects near to eye provides the most potential dangerous occlusions through generating a permanent blockage. The frame surrounds the driver and passengers called 'pillars' are the primary obscuration element in an automobile. Drivers mostly eliminate the occlusion generated by such blockage elements by moving the head on lateral plane. However, this technique does not necessarily circumvent or reduce the potential loss in visual field. The permanent presence of pillars exerts a continues blockage and threaten safety [123, 124, 126, 127].

4.2.2 Functionality of pillars

Safety for occupants

Pillars provide the structural frame that surrounds the occupant in a vehicle. Glass surfaces between pillars provide a shell for outside environment and permit good view of the road. Pillars provide a structural barrier between occupants and outside environment, which protects the driver and passengers if involved in an accident [124, 126]. Some luxury cars are also occupied with additional airbags hidden in A, B and CD pillar zones to provide extra protection to occupants when involved in a collision. Soft padding on and around pillars provide comfortable ingress and egress of vehicles.

Structural integrity

The overall forces act on a vehicle in case of a head-on collision and a roll-over accident directly absorbed by pillars. Pillar design has direct contributions on overall crash-worthiness of vehicles, especially in head-on collisions and roll-over (roof-crush). The crumble zone in front section of a vehicle is directly related the strength absorption capability of A-pillars. Pillars also have minor impacts on handling since they contribute the overall height of the vehicle. Differences in height and chassis design have effects on inertia of the vehicle, which becomes a an important handling factor in cornering and high-speed maneuvers [123, 124, 126, 127].

Aerodynamics

The overall exterior design of cars are getting streamlined in past decades to reduce aerodynamic coefficient, noise and vibration. This is a much common practice as the price of fuel becomes a major concern. Also, streamlined cars are becoming more popular with the introduction of hybrid and electrical vehicles. These vehicles rely on low drag resistance to increase performance (total distance driven with a single charge). Pillars provide smooth surfaces for easing the air flow [123, 124, 126, 127]. Therefore, A-pillar dimensions are getting larger in lateral plane as the overall vehicle body design gets more streamlined. In addition, shape of CD pillars are getting smoother to minimize the drag caused by trunk geometry. This becomes more visible in hatchback type vehicles, where engineers use wider pillars to accommodate trunk space under the rear window.

Aesthetics and style

One of the important marketing and cultural norm of vehicle design is aesthetics and styling. For many car enthusiast styling is the most important aspect of buying a new car. Pillars contribute a big portion of styling cues through providing a section formation between lower and upper part of the vehicle as well as between front and rear doors. Shape and curvature of glass surfaces are direct factors that define location and geometry of pillars.

4.2.3 Types of automobile pillars

There are four major pillars (A,B,C and D) associated with today's automobile design. Among those A and B pillars are most important in structural integrity and passenger safety in head-on, side and roll-over accidents. Most of the commuter cars have A, B, C pillars (Figure 4.1). D pillars are found in station wagons, large family cars and in Sports Utility Vehicles (SUV). Style, shape and size of pillars depends on overall geometry of the design, crash-worthiness and aerodynamics needs of the vehicle.

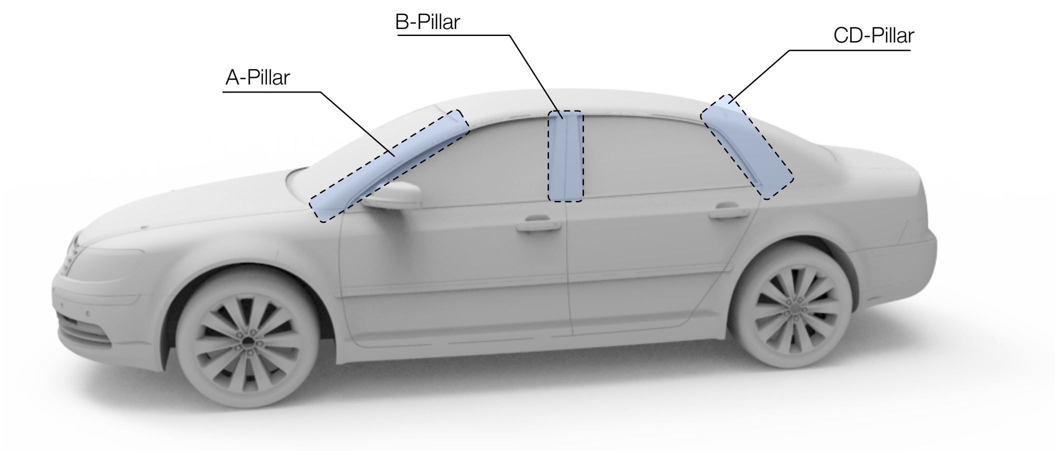

Figure 4.1. There are three major pillars (A, B and C) found in a family (sedan) car. The very last column found on station-wagon cars is named D-pillar. In this study, the very last column is represented by *'CD pillar'*.

4.2.4 Review of obscuration problems caused by pillars

The major sensory input used by drivers to maneuver and control their vehicle is the visual perception. It was estimated that vision provides 90% of the sensory input during driving [127]. Haslegrave discusses that binocular vision can have a considerable affects on obscuration caused by objects in the near field of the view [128, 129]. Studies show that if binocular vision is 40% or less, the risk of accidents increase due to loss in correct detection and identification of objects. Poor binocular vision decreases the ability of avoiding obstacles or making correct maneuvers [127].

It was also pointed that peripheral visual field loss significantly contributes to real-world accidents and risk of having accidents increases with severity of visual field loss [130]. In this context, subjects with peripheral field loss show the tendency of compensating visual looses with lateral eye movement. This may also include lateral movement of the neck to increase the visual field, which may increases the reaction time [129, 130].

Literature review also showed that peripheral visual detection distances decrease considerably as the peripheral visual angle away from fovea (or line of sight) increases [130]. This is important in cases when early detection is needed, such as negotiating a curve or detecting a vehicle in intersection point [131].

It was also observed that incorrect identification of road environment or looked-but-failed-to-see-errors are also a common causes of accidents. The term defines that the driver had actually looked in the direction where the other parties were (cars, pedestrians, road signs..etc.) but failed to see or correctly identified them. Permanent obstacles close to eye can cause loss of visual field or provide lapse of cognitive expectation (failure to scan for a particular class of road user). This eventually contribute to incorrect identification of information while driving [127].

A-pillars have been identified as the main obscuration to the visual field for the driver. Body pillars on transportation vehicles propose the issue of vision obscuration during lane changes, in city driving, parking and cornering. Recent studies show that pillar size and pillar angle have significant effects on obscuration during lane changes, which have fatal and/or financial consequences (lawsuits, hospitalization) [125].

A study by Matthew Reed's showed that A-pillars that are closer to the forward line of sight result in high-obscuration regions that are close to the vehicle travel path. This is linked to increased risk of crashes involving pedestrians during vehicle cornering and turning maneuvers [132]. It was also noted, but not finalized, A-pillar geometry may influence the turning trajectory, which can be a contributing factor for pedestrian accidents at intersections and/or curves [130, 132]. A similar study also showed that passenger cars have blind spots on the left side due to A-pillar and concluded that there are visibility requirements currently in place for passenger cars [133].

It was found that A-pillars potentially restrict essential visibility of road signs, other vehicles, and pedestrians [126]. A similar study showed that detection of distant targets are effected by pillar width greater than the observers inter-ocular distance [133].

Also, a recent study provides some initial assessments on potential safety importance of the location of B-pillars during lane-change crashes. It was found that B-pillars located near for-aft position of the driver tend to be over-involved in lane-change crashes [127, 134].

According to the studies done by the Department of Transport of UK, look-but-failed-to-see accidents are contributing 20% of all road accidents. Unfortunately, contribution of A-pillar obscuration on failed-to-see accidents was not specified in this study. However, it was suggested by experts that motorbikes were often obscured from view by nearside A-pillar. In theory, A-pillars should be designed in a way to allow optimum vision to avoid looked-but-failed-to-see accidents [135].

It was also found that thickness of the pillars have effects on failing to see an object. Some manufacturers offer slim pillar design to increase the field of vision. It was noted that slim A-pillar can provide better field of vision in comparison to thick A-pillars [123, 124].

In summary, one can find that pillar obscuration (especially in A-pillars) are of potential importance in situations where the vehicle is closing in to another vehicle in the intended line of travel and manuvering/cornering at in-city traffic [125]. B and CD pillars may also decrease the range of visibility during in-city driving, parking, cornering and backing-up. In each case, increase in thickness as well as lateral pillar angle causes obscuration zones.

4.2.5 Types of pillar obscuration

Figure 4.2 represents the obscuration zones formed by A, B and CD pillars of a generic passenger car [123]. D pillar obscuration zone is not presented in this image, however the very last pillar (C-pillar) in SUVs or station-wagons propose a D-pillar-like obscuration problem. Angles between eyelipse centroids are referenced to industry recommendations documented in SAE J941 manikin setup. According to the SAE J941 manikin, each pillar forms a pillar obscuration angle denoted as A_θ, B_θ and C_θ [136]. It should be kept in mind that each pillar zone would have be different angles and locations depending on overall vehicle geometry, as well as anthropometric differences of drivers and driver's seat location (forward-backwards, height).

A-pillar obscuration

According to the EEC 77/649 (European Economic Committee), the A-pillar angle of obstruction should not exceed 6^o [137]. This regulation strictly questions the safety of operating vehicles when obstruction angle is bigger than 6^o. Studies note that only one-third of production vehicles meet this standard [123, 124].

B-pillar obscuration

Although awareness on B-pillar obscuration is relatively insignificant when compared to A-pillar obscuration, manufacturers try to eliminate wide obscuration zones by optimizing B-pillar thickness through high strength steel frame construction. Studies show that B-pillar obscuration is more common in four-door type vehicles when comparing to two-door vehicles, due to shorter A-B pillar distance. In other words, B-pillars of four-door cars are much closer to drivers compartment than two-door ones, which create larger obscuration zones. This finding gets more prominent if front seat is adjusted backwards, which is a common practice for tall drivers [125, 134].

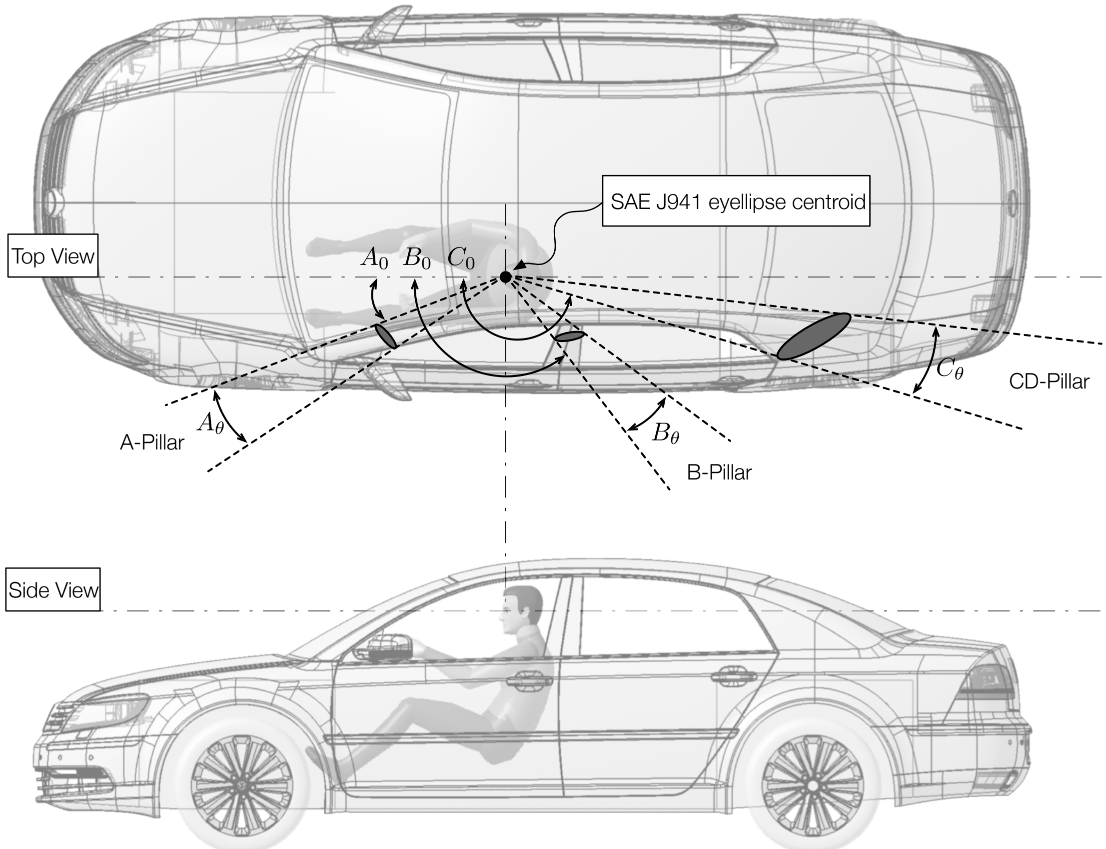

Figure 4.2. At Top View, shaded areas on each pillar zone represents portions of the pillars that obscure driver's line-of-sight. The primary parameter that affects the size of obscuration is the thickness of the pillar. Secondarily, the angle that pillar makes with the lateral plane has minor affects on obscuration. Thus, obscuration zone is a variable phenomenon, which reflects combined affects of seating location, posture of driver and overall vehicle design. SAE J941 manikin offers recommended design standards and dictates pillar obscuration as being a critical packaging parameter. In SAE J941, obscuration angles associated with each pillar zone are denoted as A_θ, B_θ and C_θ. Location of the head-turn associated with each pillar is referred as A_0, B_0 and C_0. The size of each angle depends on the dimensions of pillar thickness. Thus, each vehicle has different field of obscuration associated with the vehicle packaging.

CD-pillar obscuration

The field of vision research in automobile design mostly focuses on forward vision of the vehicles. Literature review shows that C and D pillar obscuration did not take much attention as safety and design concern. Few studies show that there is no clear prediction of a relationship between the location of C-pillars and lane change crashes. However, more data should be collected before coming up with a conclusion. There is still a concern about the potential relevance of C-pillars and lane change crashes in situations where the vehicle's intended lane of travel is closing to another vehicle [123, 125, 129].

When it comes to rear field of vision, C and D pillars are especially important in parallel parking and backing up. This becomes a major concern while trying to see small objects and pedestrians close to rear section of the vehicle. Large vehicles (SUVs) with thicker pillars create a more prominent problem. Although rear field cameras found in luxury vehicles assist driver while backing up, they still lack of monitoring rear left and right sections of the vehicle. Even though a true rear view coverage is provided through a camera system, this method can add extra cognitive challenges to drivers. One need to look at a back up camera and need to be aware of what is going on around vehicle perimeter, simultaneously.

5. METHODOLOGY

5.1 Why is This Experiment Needed?

Literature review outlined in Chapter 1 and Chapter 2 showed that a systematic consideration of human element in design system with a holistic coverage is either ignored or only recognized with limitations. There are limitations in engineering design literature in terms of integrating HFE design principles early into product development process. Often, HFE design principles are not truly regarded as direct contributors of the design process when compared to other contributors such as computer science, graphics design and mechanical engineering. DHM offers an extended coverage to the problem area through introducing HFE principles early in the design process, however utilization of DHM as a design package is not fully explored. In contrast, most of the designers consider DHM as a post-processing method for ergonomics evaluation of products. One of the major limitations that extenuates the adoption of DHM as a design package is the absence of a design framework that can link human needs, abilities and limitations with other design contributors.

Chapter 3 provided a detailed literature review on pillar obscuration problem. It is one of the indicators of poor HFE practice in automotive design domain. Some of the shortcomings of the obscuration problem arise from the fact that human needs, abilities and limitation are either neglected or not thoroughly considered in vehicle packaging. Among all the visual field related problems in vehicle packaging, pillar obscuration found to be the most problematic, which may lead to serious injuries and fatal accidents. However not much attention has been paid in comparison to recent technology improvements such as entertainment consoles, engine upgrades, alternative fuels, weight reduction and navigation.

This experiment focuses on visual analysis of obscuration phenomena caused by automotive pillars. A detailed study that explores the affect of pillar design on drivers performance is conducted. Human-in-the-design framework is used a testbed to provide a high-fidelity design work-flow to incorporate form and functional aspects of design process centered on physical and cognitive needs, abilities and limitations of humans. Human-in-the-loop design framework is proposed as a method to link HFE design principles early in the design process through DHM. Pillar design experiment is conducted as a real-life design study to validate the design approach introduced in human-in-the-loop design framework.

5.2 Design Objectives

This study provides a brief introduction to the pillar obscuration problem and proposes an alternative design solution. The proposed design is intended to decrease looked-but-failed-to-see errors and provides additional reaction time to drivers to avoid possible collisions with other vehicles, traffic objects or pedestrians. There are three main objectives proposed in this study. Each design objective is represented through three separate experiments. Key items to meet design objectives are:

1. Identify Obscuration Problems through Eye-tracking Experiment:
   Obscuration zones associated with front field will be evaluated for current and proposed pillar designs through an eye-tracking experiment. Improvements on field of vision will be measured in terms of accumulated number of eye-gazes, total duration of eye-fixations and success of detecting of traffic objects.

2. Develop Driver's Questionnaire:
   Traffic Object Detection form will be filled up by subjects as they go through static driving simulation. The goal is to detect performance of subjects in correctly detecting traffic objects. Cooper Harper test and pillar design review questionnaires will be distributed to subjects to measure which pillar model gets higher (better) reviews from subjects. Results (user ratings) associated to

proposed pillar model will be compared to ratings of current pillar model in terms of visual, safety and aesthetic attributes.

3. Construct Finite Element Analysis to Check Structural Integrity:
   A Finite Element Analysis (FEA) will be constructed to check the structural integrity current and proposed pillar models under roof-crush loading test. Results (maximum stresses and displacements) of pillar models will be compared with benchmark values of Federal Motor Vehicle Safety Standards (FMVSS).

5.3 Hypotheses

Design objectives in this thesis formed around four hypotheses that explore the validity and reliability of the human-in-the-loop design framework. These hypotheses also investigate effects of proposed pillar model on traffic object detection and structural integrity of the overall vehicle. Details about hypotheses will be covered in Chapter 5. Hypotheses associated with human-in-the-loop framework are:

1. Hypothesis #1 *(H1)* = For visual field analysis, correlation of visual field results (within subjects) between six trials should be at least in high correlation ('Good' or 'Excellent'), where Intra-Class Correlation (ICC) index falls in range of $0.6<ICC<1.0$.

2. Hypothesis #2 *(H2)* = For each subject, visual detection of road elements with Proposed Pillar (New Pillar) design and with Current Pillar (Old Pillar) design are significantly different.

3. Hypothesis #3 *(H3)* = Proposed Pillar (New) design is significantly better than Current Pillar (Old) design in terms of concept design criteria; forward (A-pillar), side (B-pillar) and rear field (CD-pillar) visibility.

4. Hypothesis #4 *(H4)* = Mean values of maximum forces and displacement values for front, side and rear loading on Proposed Pillar (New) design are not significantly different than Current Pillar (Old) design.

5.4 Overview of Experimental Setup

There were three experiments performed in this study (Figure 5.1). Experiment-I and Experiment-II use the same simulation components with a slightly different data collection strategy. Experiment-I is a visual detection/obscuration zone experiment, which includes subject data collection through an eye-tracking device. In this experiment, subjects performed visual detection tasks of traffic objects in a stationary driving simulator environment, where static images of an automobile interior (driver's point-of-view of windshield) and a traffic scene were projected on a LCD monitors. Specifically, subjects were asked to detect traffic objects (pedestrians, bicycles and motorcycles) on A-pillar obscuration zone for two types of pillar models: Old Pillar and New Pillar. Old Pillar model represents solid pillars that drivers see in regular cars. New Pillar model represents a modified version of solid pillars with see-through gaps. In Experiment-II, same static traffic objects and images represented the simulation environment were projected on LCD display. In contrast, subjects asked to detect traffic objects for A, B and CD pillars with two different pillar models (New and Old Pillar) without an eye-tracker device. Subjective feedback and driver's performance related data were collected through three assessment methods: Object Detection Form, Cooper-Harper Test and User Questionnaires. Finally, Experiment-III was conducted to evaluate structural differences between Old and New Pillar model. Finite Element Analysis (FEA) study was used as a method to validate the structural integrity of the vehicle frame according to Federal Motor Vehicle Safety Standards (FMVSS) of roof-crush resistance test (article No-216) [138]. Experiment-III did not include any subject data collection. It was executed in a computer simulation environment with digital manikins representing 95^{th} percentile of male population.

5.5 Common Components of the Experiment

This study proposes a novel pillar design model to increase driver awareness and reaction time for positive identification of other vehicles, pedestrians and other road

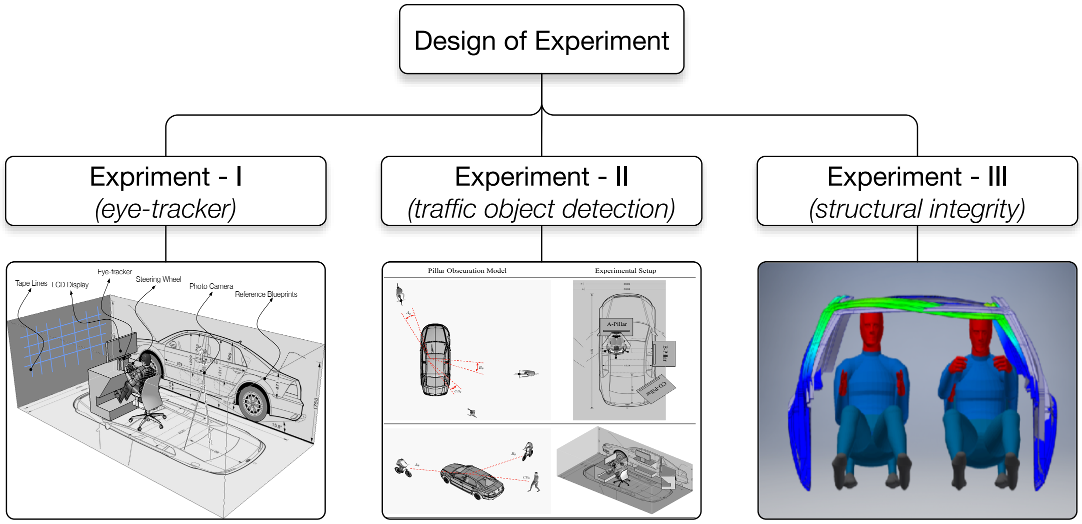

Figure 5.1. This study includes three types of experiments: Eye-tracker subject-data collection, Questionnaires subject-data collection and structural integrity. Experiment-I includes human subject data collection through a static simulator and an eye-tracker device. Experiment-II uses various subjective data collection methods to capture subject's perception and performance related data without the eye-tracker device. Experiment-III is a FEA to validate the structural integrity of New Pillar design under FMVSS roof-crush test.

elements. A see-through pillar design is conceptualized with openings that let drivers to see pillar obscuration zone found in solid pillars. Proposed pillar model provides visibility improvements through minimizing obscuration zones. In theory, the concept idea has the potential to be a successful pro-active safety feature in modern cars, however validation is required to assess the fidelity of the theory and implementation. A set of objective and subjective experiments are designed to gain a thorough understanding about the pillar obscuration phenomena and its physical and cognitive affects on drivers performance. The goal is to provide a see-through-space for drivers to improve their visual zone, which would ultimately have positive affects on driving safety.

5.5.1 Reference vehicle, pillar models and body frame

Throughout this experiment two pillar models are used: Old Pillar and New Pillar. Old Pillar model represents a generic solid pillar found on regular cars. New Pillar model is a modified (reverse-engineered) version of Old Pillar with see-through spaces providing a minimized obscuration area to driver. Each pillar has exactly same dimensions and surface finish. The only difference is the holes that were cut-out on New Pillar model.

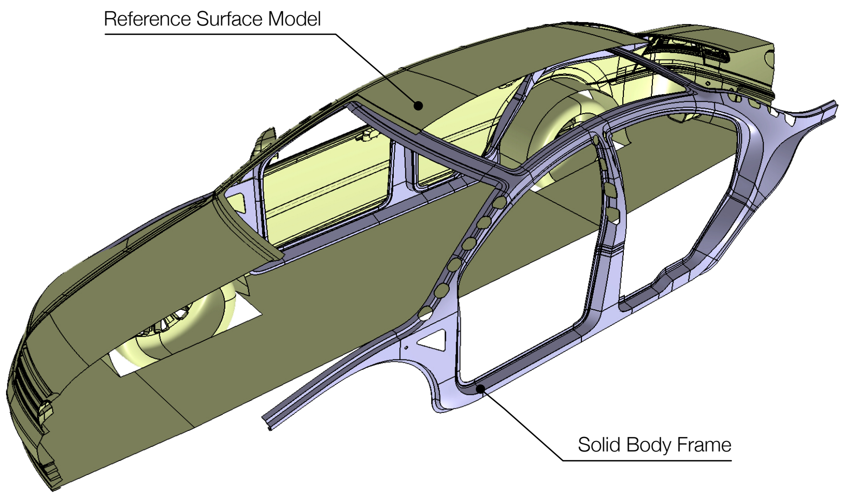

Figure 5.2. Body frame that acts as a chassis was constructed based on referenced CAD surface geometry. Image shows inner skeletal section (body frame) and outer surface model.

The shape of the see-through holes could be different depending on the functional and form aspect of vehicle packaging. In this experiment a four-door family sedan is used as a reference vehicle. CAD model of the car was based on a Volkswagen family sedan named 'Phaeton'. Pillar models were constructed with referenced to geometry and dimensions of Phaeton model provided in open-source blueprint and surface models (Appendix C) [139–142]. These models were used as wire-frame references and means of representing overall vehicle dimensions. Based on these reference geometry, modifications were made to create surface and solid CAD designs associated to new and old pillar models as well as the body-frame.

Although each vehicle has different pillar dimensions, the CAD model used in this study carries very similar pillar dimensions with some popular four door family sedans (Honda Accord, Nissan Altima, Mazda 6, etc.). Thus, similar pillar dimensions provide a more comprehensive understanding on pillar-obscuration phenomena. CAD model was used as the reference vehicle geometry throughout this study. In Experiment-III, a solid inner frame (chassis) was constructed based on the reference surface model. Figure 5.2 shows CAD models associated with A, B and CD pillars. Elliptical see-though shapes were cut-out to construct New Pillar model, which is a one-to-one replica of a regular solid pillar model (Figure 5.3).

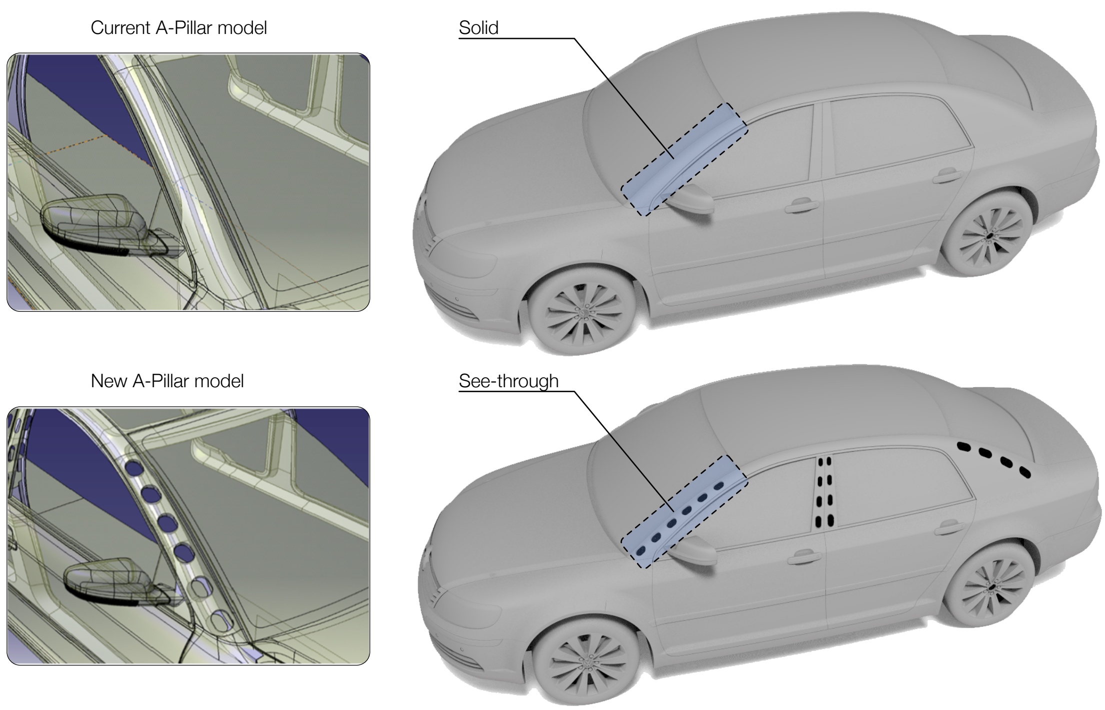

Figure 5.3. Two types of pillar models associated with A, B and CD pillars. Current Pillars are composed of solid bodies, whereas New Pillars are composed of see-through spaces.

5.5.2 Pillar obscuration and driver posture setup

Providing see-through pillars on vehicle packaging could help drivers to anticipate hard-to-see points that fall within angle of obscuration (A_θ, B_θ and CD_θ). This design challenge was tested through a group of obscuration scenarios that represented a real traffic condition. Three types of pillar obscuration scenarios were conducted in this study. To address each pillar obscuration scenario, three digital manikins coming from 95^{th} percentile male population were created through CATIA's anthropometric library. Each manikin was assigned to the associated A, B and CD pillar obscuration scenario. These scenarios are covered in details throughout next section.

Orientation of driver's seating location and postures associated with A, B and CD pillar obscuration were generated according to actual vehicle packaging dimensions, which were based on blueprints [139]. Posture assignment incorporates some of the vehicle packaging elements including seat section, steering wheel, accelerator and footrest. Thus, a realistic CAD model with high-fidelity postures were incorporated to represent obscuration problem in a realistic traffic situation. Figure 5.4 demonstrates steps taken for generating a manikin with referenced packaging dimensions.

5.6 Overall Procedure and Summary of Data Collection

Throughout this experiment subjects were asked, with the help of the experimenter, to take a comfortable driving posture in front of a static driving simulator, and complete a series of short traffic object detection experiments. Before the experiment started, subjects were asked to work on an eye-tracker calibration task. This task included making a normal eye contact with an eye-tracker device in front of the front-facing LCD monitor. Traffic object detection experiments were based on visual detection tasks, where subjects worked on detecting traffic objects that were projected to LCD monitors. There were three different pillar types (A, B and CD pillars) associated with two different pillar models (Old and New pillar models). Subjects were asked to detect traffic objects that were located behind the pillar area - or

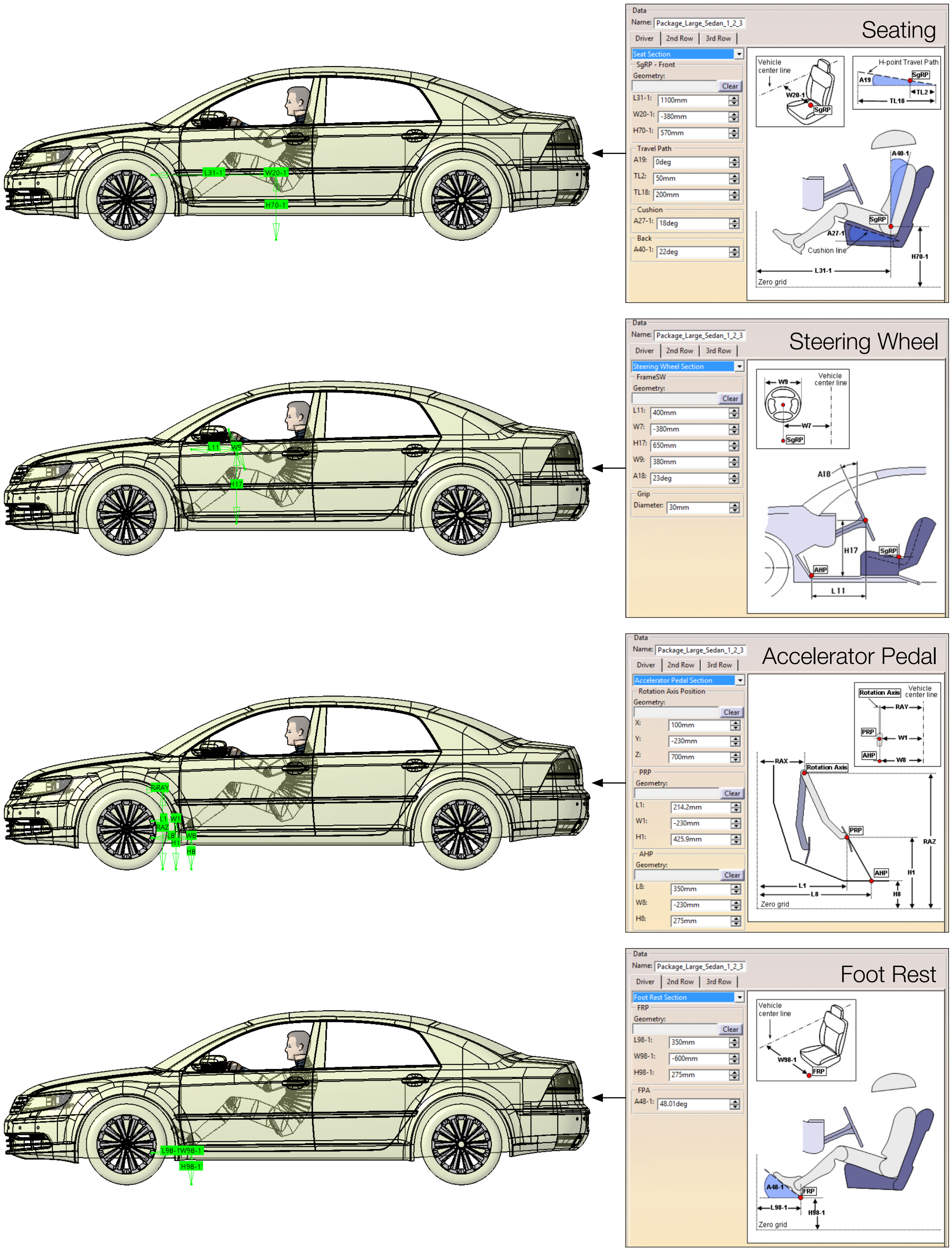

Figure 5.4. Driving posture associated with actual vehicle packaging takes into account some of the cockpit elements such as seating, steering wheel, accelerator pedal and foot-rest.

within the obscuration angle. Static traffic objects were projected in randomized order. After each subject completed Experiment-I, he/she proceeded to Experiment-II with a short break. Experiment-II included filling up Object Detection form and a Cooper-Harper Test associated with each pillar type (A, B and CD). Finally, subjects were asked to complete a two user experience questionnaires. First questionnaire was composed of two sets of sub-questionnaires, which are designed to assess pillar models used in this experiment. The last questionnaire was intended to collect data about subject' pillar obscuration related daily driving experiences. Experimental procedures and equipment used in this experiment were approved by Purdue Institutional Review Board (IRB) (Appendix-A). Procedures followed during the experiment were:

1. Subjects were asked to provide height and weight related data on human subject log. This step was intended for screening for exclusion and constructing referenced DHM manikin. This manikin was used in generating driving posture (Figure 5.4) and FEA analysis.

2. Subjects were asked to take a comfortable driving posture according to their seat adjustments. This included raising-lowering and tilting the seat.

3. Experiment started with eye-tracker calibration. This included a step-by-step eye-gazing to gather subject's eye motion behavior. Eye tracker was only used for A-pillar traffic object detection tasks.

4. After eye tracker calibration was completed, subjects worked on various visual detection tasks. As the computer simulator turned on, subjects were asked to make field-of-sight observations on static images projected to the LCD monitor. During simulator experiment, there were three different types of pillars corresponding to two different pillar models. There were two different traffic objects projected behind the pillars. Traffic objects were composed of what a driver could normally see on public road (vehicles, pedestrians, bicycles). Pillar model, pillar type and traffic objects were randomized. Each task was repeated six times.

5. Each simulator task took around three seconds. Subjects were asked to follow automated simulation with each traffic scenario shuffles automatically after three seconds. Subjects take a short break after completing Experiment-I.

6. In Experiment-II, subjects filled up Traffic Object Detection Forms as static simulation images shuffle randomly with three seconds between each other.

7. For each pillar model (Old and New), subjects were asked to fill up a modified Cooper-Harper test after completing each A, B and CD pillar Object Detection Form experiment, sequentially.

8. After simulator tasks, subjects were asked to fill up three short questionnaires.

9. After all simulator tasks and questionnaires were completed, subjects were required to sign off human subject log, and exited the experiment.

Table 5.2 shows estimated duration associated to each task. In this experiment, there were a total of 72 Object Detection Forms, 6 Modified Cooper-Harper Tests and 3 user questionnaires were used. Each subject was required to go-through all phases demonstrated in Figure 5.5 to successfully complete the experiment.

In this experiment, each subject was asked to finish a calibration task (takes around 5 minutes) and worked on object detection (obscuration test) experiments for 2 traffic objects for 3 pillar types (A, B and CD) and 2 pillar models (Old and New Pillar). Each task was replicated six times. Thus, each subject went through 72 (2 x 3 x 2 x 6) tasks, corresponding to: *pillar model* x *pillar type* x *traffic object* x *replication.* Obscuration tasks took around 1.5 minutes (3 seconds per task). There were a total of 72 Object Detection Forms (each takes 15 seconds), 6 Modified Cooper-Harper Tests (each takes 1-2 minutes) and 3 questionnaires (each takes 3-5 minutes) given to each subject.

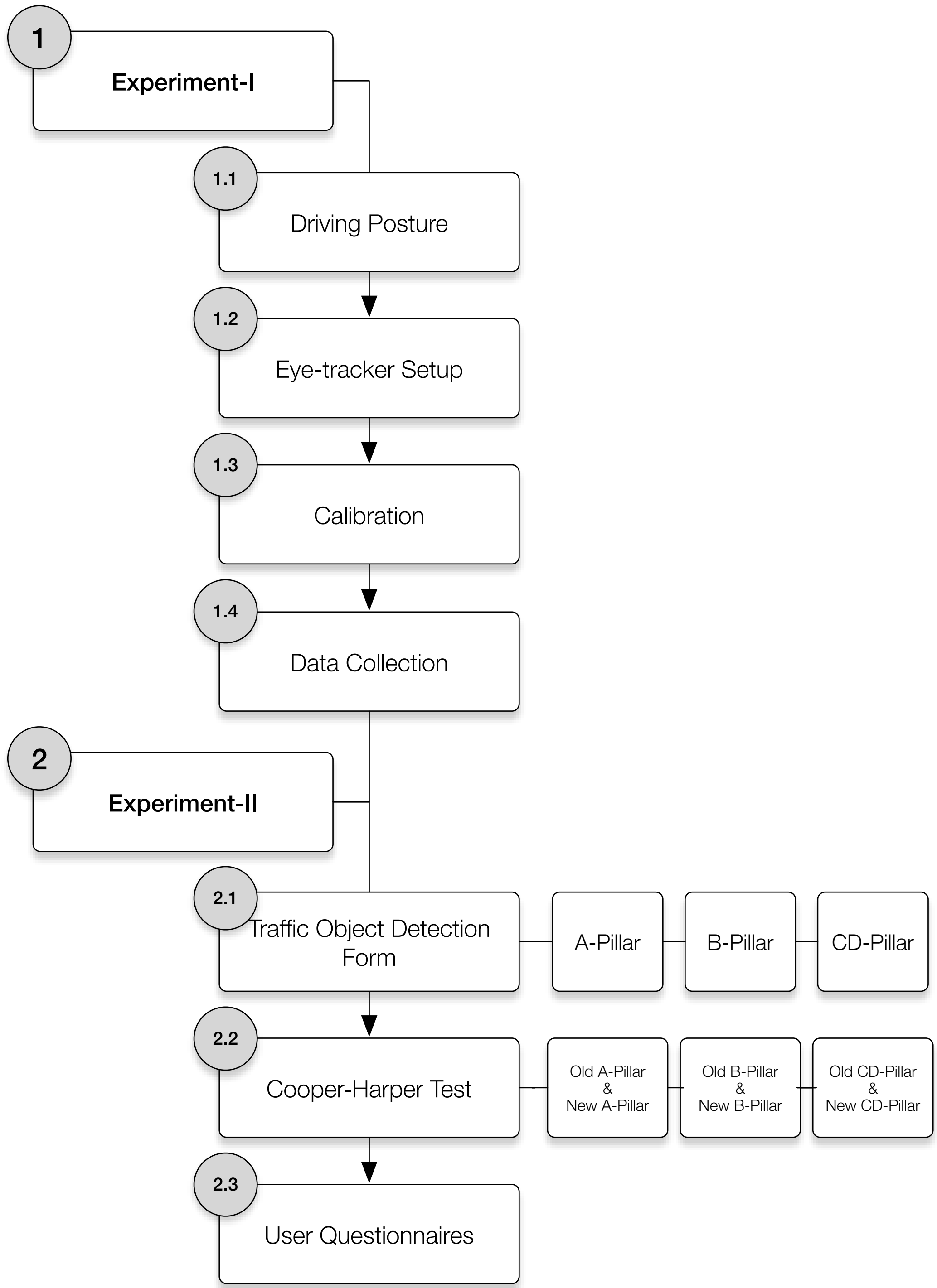

Figure 5.5. Subject-data collection flow associated with Experiment-I and Experiment-II. Experiment-III did not involve any data collection from subjects.

Table 5.1
Estimated specific times and total time associated with each task

Task Breakdown	Individual Times	Replications	Total Time
Calibration	5 minutes	1	5 minutes
Eye-tracking	3 seconds	24	1.5 minute
Obscuration Task	3 seconds	72	4.5 minutes
Object Detection Form	15 seconds	72	20 minutes
Cooper Harper Test	2 minutes	6	12 minutes
Questionnaire	5 minutes	3	15 minutes
			≈60 minutes

5.7 Overview of Variables and Data Types

There were three experiments conducted in this study. Each experiment was composed of multiple variables. Experiment-I and Experiment-II involved human-subject data collection. In Experiment-I, subjects' eye-movements were collected through an eye-tracker device. Eye-movements data had three variables: Fixation Duration, Coordinates-X and Coordinates-Y. Experiment-II composed of three sub-experiments: Traffic Object Detection form, Cooper-Harper tests and user questionnaires. Variables associated with Experiment-II were: Object Detection, Performance, Ease of Detection, Design Review and User Feedback. In Experiment-III, Finite Element Analysis (FEA) was conducted to assess the structural integrity of pillar designs under FMVSS roof-crush test. FEA analysis was evaluated by Displacement and Stresses. Table 5.2 summarizes types of data, variables, units, and hypotheses associated with experiments conducted.

Table 5.2
Types of data, variables, units, and hypotheses associated with experiments conducted in this study

Variables	Units	Expt.-1	Expt.-2	Expt.-3	Hypotheses
Fixation Duration	Milliseconds	•			H1, H2, H3
Coordinates-X	Pixels	•			H1, H2, H3
Coordinates-Y	Pixels	•			H1, H2, H3
Object Detection	Binary		•		H1, H2, H3
Performance	Binary		•		H1, H2, H3
Ease of Detection	Rating/Score		•		H1, H2, H3
Design Review	Rating/Score		•		H1, H2, H3
User Feedback	Rating/Score		•		H1, H2, H3
Displacement	Millimeters			•	H4
Stresses	Newtons			•	H4

5.8 Random Error and Systematic Error

Every experiment that involves data collection through a measurement device is subject to produce unintentional errors, which generate statistical fluctuations in collected data. Often, these errors result from experimenters inability to replicate the identical conditions during data collection. The degree of presence and frequency of such errors can predict the success of the measurement. These errors occur throughout the experiment, and allocate all chance factors that are associated with the measurement. We can classify measurement error in two major categories: random and systematic errors [143, 144].

Random errors are caused by unknown, uncontrolled and unpredictable changes in the data collection process. Any unknown variation in the measuring device (e.g., electronic noise) can affect the precision of collected data.

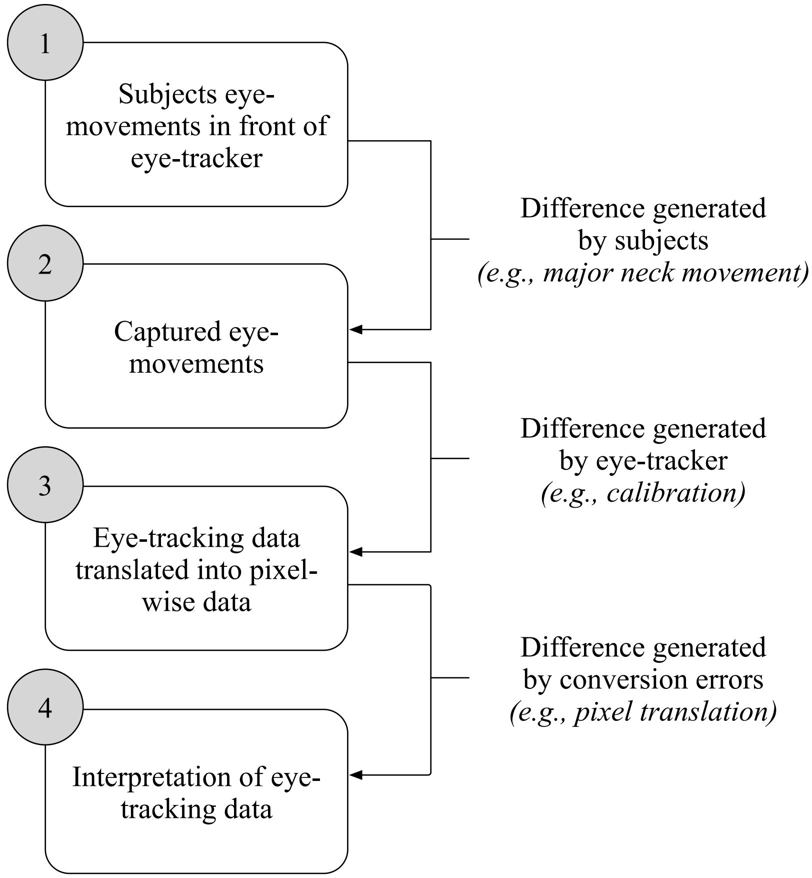

Figure 5.6. Potential random and systematic error pathways associated with eye-tracking experiment.

Systematic errors, similar to random errors, are also generated without intention. However, they often happen due to erroneous use of instruments and/or uncontrolled environmental conditions, which affect the accuracy of data collection.

It is practically not feasible to eliminate all random and systematic errors generated during data collection. In this experiment, the eye-tracker device (e.g., calibration and noise) and human subjects (e.g., positioning and posture) can be considered as potential contributors of such errors (Figure 5.6), which might have a systematic biasing effects on data collection. In order to minimize the biasing effect of uncontrolled errors, every experiment step and equipment calibration were carefully examined and executed systematically throughout each experiment.

Validity and reliability of data collection depend on the amount of random and systematic errors occur in an experiment. A measure that generates low random error and low systematic error should be considered acceptable, as it is both valid and reliable [77, 145]. Starting by the following section, methods and assumptions that examine validity and reliability of the data are covered in details.

5.9 Summary of Statistical Techniques

A summary of independent variables and dependent variables in as well as random and standard error were summarized in previous sections. A detailed information about (M)ANOVA and ICC were documented. This section summarizes statistical techniques used for analyzing data, as well as methods and goal of measurement (Table 5.4). Starting by Chapter 6, each experiment is analyzed in details through utilizing statistical methods described in this section.

Table 5.3: Summary of methods of measurement, goal of measurement, statistical, numerical and visual methods associated with hypotheses

Experiments	Method of Measurement	Goal of Measurement	Statistical, Numerical and Visual Methods
Experiment-I	Eye-tracker	Areas of Interest	Descriptive Statistics
			Bar Graphs
			Heat-maps
			Burnout Images
		Validity	ANOVA
			MANOVA
		Reliability	ICC
			Cronbach's Alpha

continued on next page

Table 5.3: *continued*

Experiments	Method of Measurement	Goal of Measurement	Statistical, Numerical and Visual Methods
Experiment-II	Detection Form	Detection Performance	Descriptive Statistics
			Bar Graphs
	Cooper-Harper	Design Improvement	Descriptive Statistics
			Line Graphs
	Questionnaire	User Preference	Descriptive Statistics
			Bar Graphs
		Internal Consistency	Cronbach's Alpha
Experiment-III	FEA	Structural Integrity	Descriptive Statistics
			Stress & Displmnt.
			Bar Graphs
		Correlation	ICC
			Pearson

6. EXPERIMENT - I

6.1 Introduction

6.1.1 Overview

Experiment-I involves a human data collection in a static driving simulator (Figure 6.1). Simulation setup was composed of a large monitor, steering wheel, pedals and adjustable seat. Subjects were asked to take a driving position in front of a large monitor, which represents the driver's side of the windshield and dashboard area. Driver's point-of-view of a traffic scenario was projected as still images. Subjects worked on visual detection tasks to identify traffic objects found behind A-pillar area through eye-gazing on the monitor. Purpose of this experiment was to collect eye-gazing data of drivers through a eye-tracking device. Research question posed whether pillar models and/or traffic objects have effects on eye-tracking data.

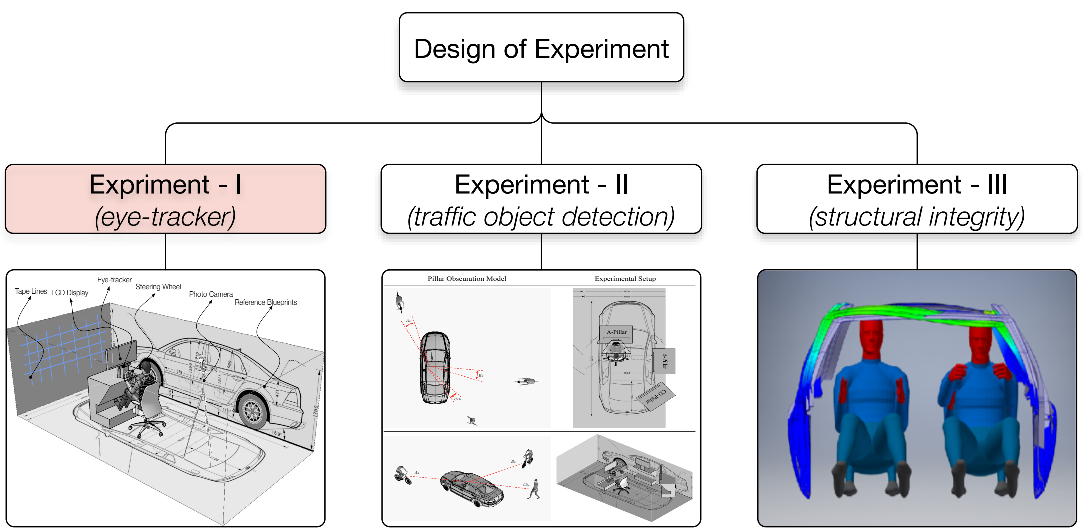

Figure 6.1. Experiment-I is a human subject data collection experiment through an eye-tracker device and a static simulator setup.

6.1.2 Connections to human-in-the-loop design framework

Experiment-I demonstrates how human related data could be connected into human-in-the-loop design framework. In this specific design study eye-tracker device with a static simulator setup was used as means of collecting human subject data. Shaded area in red Figure 7.2 shows how data collected through eye-tracker and simulator setup was integrated to DHM. Similarly, Figure 7.3 demonstrates a visual synopsis of how Experiment-I was integrated to DHM within human-in-the-loop framework.

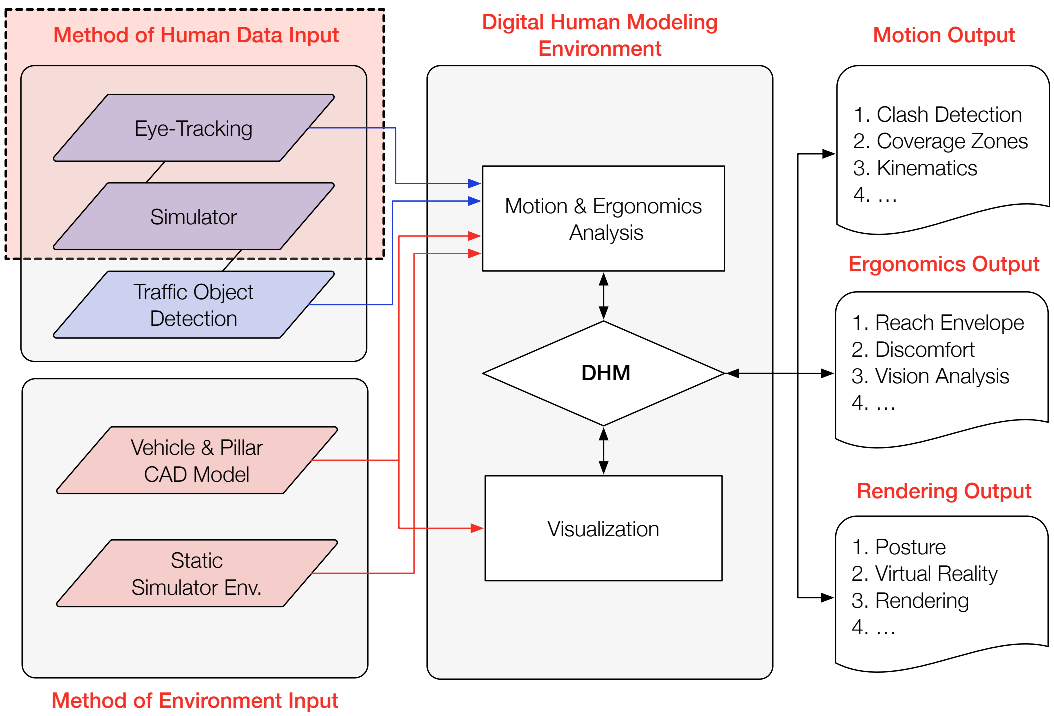

Figure 6.2. Shaded area in red (with dashed lines) represents how Experiment-I was integrated to data flow process within human-in-the-loop framework. Experiment-I gathered human subject related data through an eye-tracker device and a static simulator.

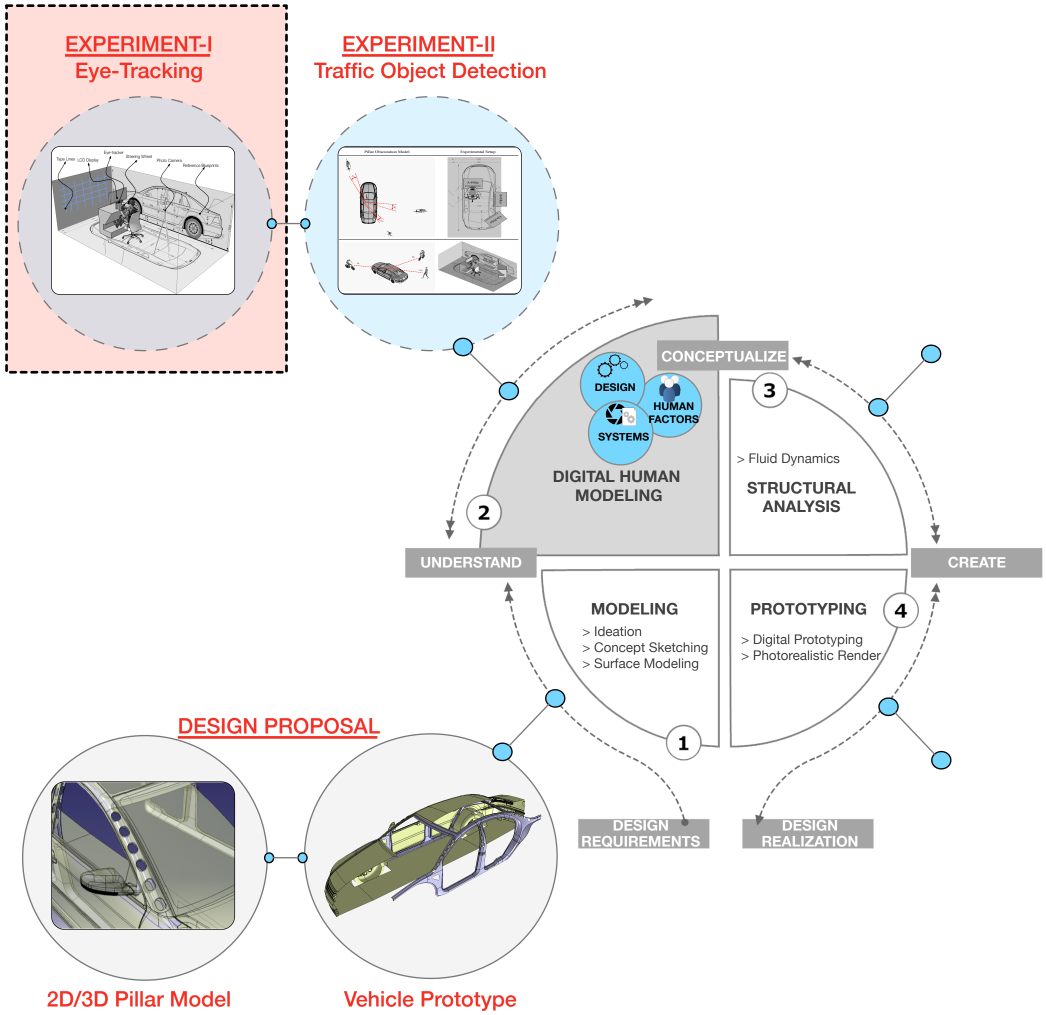

Figure 6.3. Shaded area in red (with dashed lines) represents whic portion of the human-in-the-loop design framework was used to integrate human aspects of data during design process.

6.2 Experimental Setup

6.2.1 Eye-tracker and simulator setup

An eye-tracker device from EyeTribe (The EyeTribe Tracker) was used as a method to capture pixel correspondences of eye movements of subjects on a large monitor [146]. Static images that represent what a driver would be seeing when driving an automobile were projected to LCD monitor as static images (Figure 6.4).

Eye-tracker device has a sampling rate of 60Hz and can capture eye movements with accuracy of 0.5 to 1 degrees. It uses a super-speed USB 3.0 port for power and data transfer. Throughout this experiment a 9-point calibration template was used for calibrating a 24 inches LCD monitor.

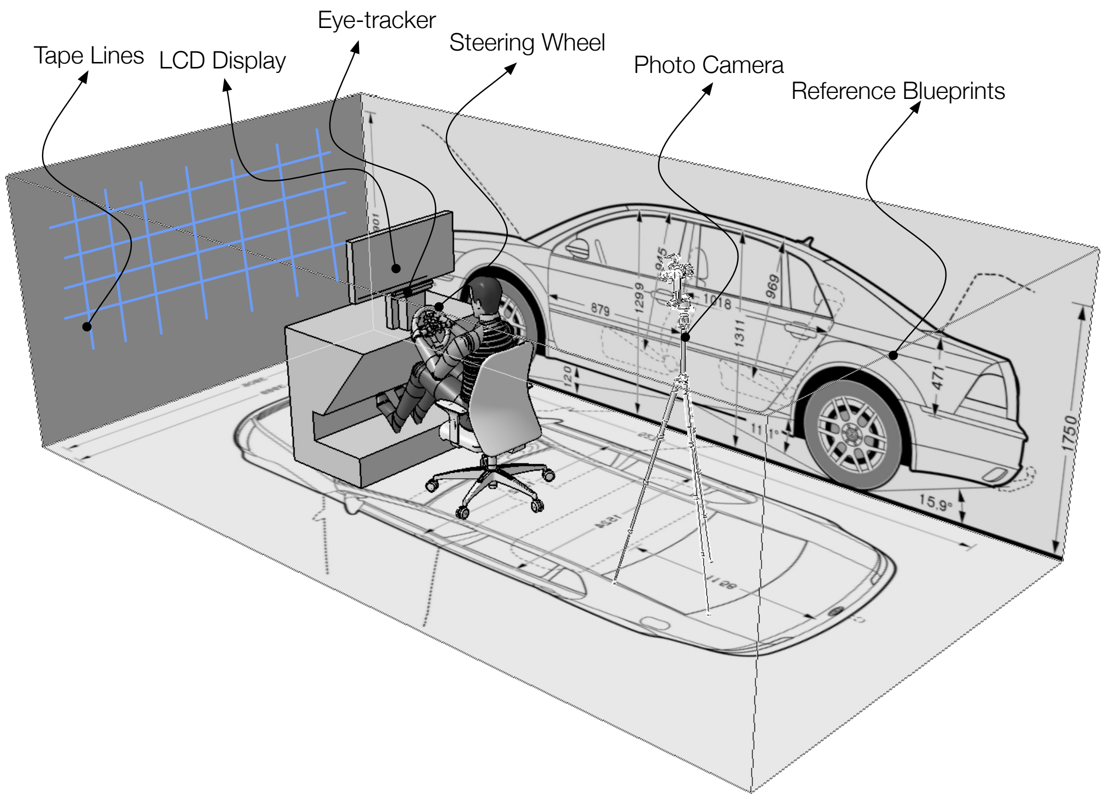

Figure 6.4. Simulation setup in Experiment-I consisted of an eye-tracker, an LCD display, a Logitech gaming steering wheel with pedals, a generic adjustable office seat and a photo camera. Eye-tracking device was used for capturing subject's eye-movements. Static images that represented driver's point-of–view of the windshield were projected on a LCD display. A Logitech steering wheel with pedals, and a generic adjustable chair were provided to subjects. Location of experimental components and seating position of the subjects were based on actual blueprints. Subjects had the flexibility of adjusting seat position (back-and-forth, incline) within the boundaries shown on blueprints.

During data collection, subjects sat on an adjustable seat roughly 50cm away from the eye-tracker device. Subjects were able adjust seat location (back and forth, up and down, recline). Seat location was bounded by the referenced interior layout taken from CAD vehicle model (blueprint) (Figure 6.4).

In addition, a photo camera on a tripod setup was used for capturing head and upper body position of subjects in reference to tapelines that were stuck on a front-facing wall. These images were solely used for gaining understanding about driver's posture.

6.2.2 Traffic objects

There were a total number of 24 (2 x 2 x 6) static images representing 2 traffic objects (either a bicycle or a pedestrian) located behind the A-pillar zone for 2 pillar models (Old and New) with 6 replications. Each image stayed on the monitor for three seconds. After three seconds, simulation setup proceeded to the next image. Images were randomly shuffled.

Total number of images shown in driving simulator split between Old Pillar and New Pillar model, where subject either saw a solid pillar (Old Pillar) or a see-through pillar (New Pillar), accordingly.

Table 6.1: Traffic scenarios for A-pillar obscuration for two pillar types with trials

Pillar Model	Pillar Type	Traffic Objects	Trials
Current Pillar	A	Pedestrian	6
		Bicycle	6
New Pillar	A	Pedestrian	6
		Bicycle	6

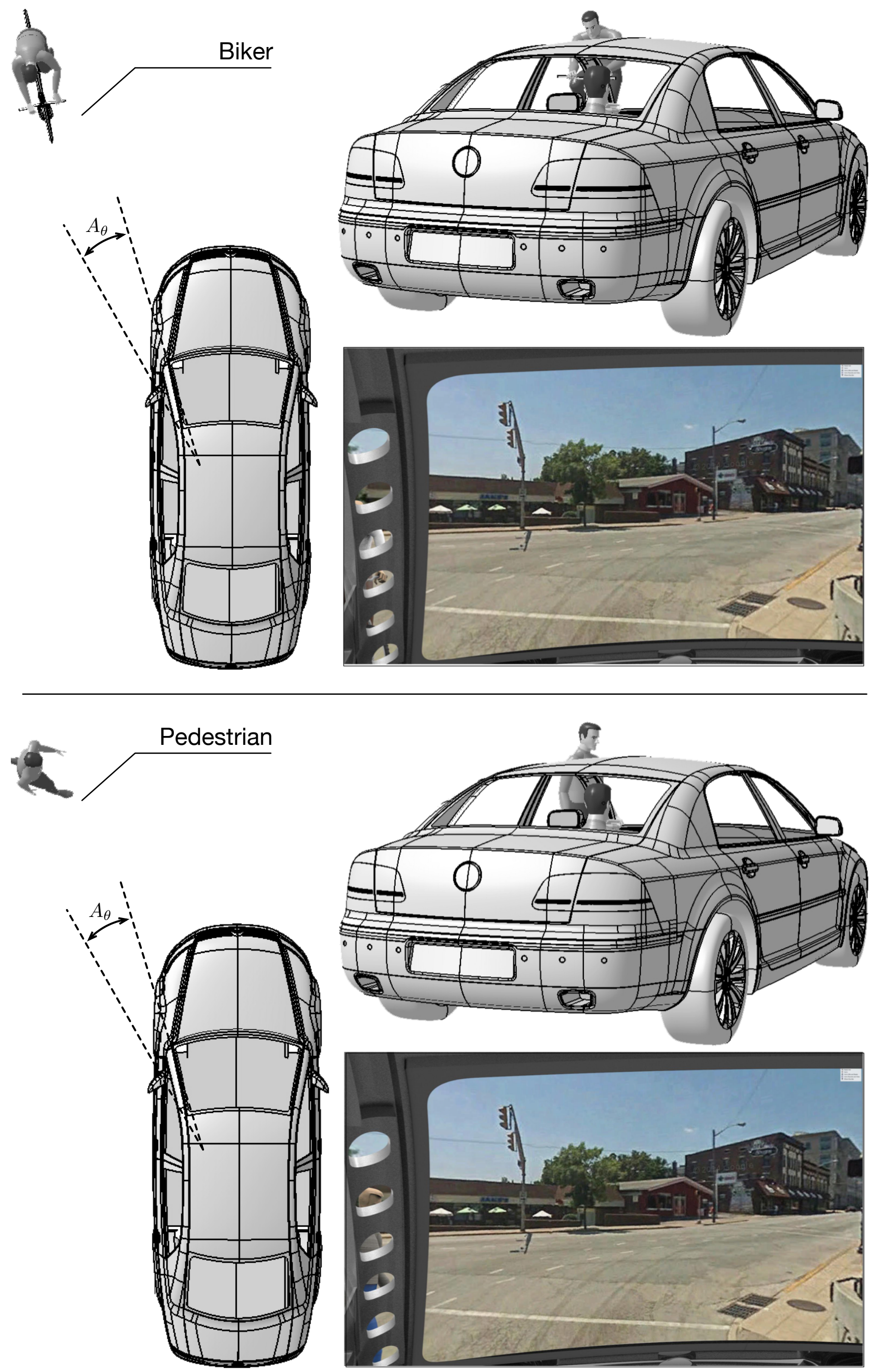

Figure 6.5. Two traffic objects were used interchangeably. Images represented a pedestrian or a biker were projected in a randomized order during static driving simulation. Each traffic object was located within the A-pillar obscuration angle (A_θ).

Figure 6.5 shows visual setup of traffic objects according to the vehicle's location. Each traffic object falls within obscuration angle of A_θ. Either a biker or a pedestrian was placed within obscuration angle. Static images on the lower-right corner for each traffic object demonstrates the street view of what driver's would be seeing during simulation. These images were based on the Google Map street view images explained in previous chapter. Figure 6.5 only demonstrates how a biker and a pedestrian were situated at the pillar obscuration zone for New Pillar design. During Experiment-I, the exact traffic objects but for solid pillar were also presented to subjects in conjunction to see-through pillar.

6.3 Procedure

Throughout Experiment-I static driving simulator setup presented in Figure 6.4 was used and eye-tracker device was utilized for capturing subject's eye-movements through static images projected on a LCD monitor. Each image represented a traffic scenario associated with two different traffic objects for two pillar models. This experiment solely focused on A-pillar obscuration. Data flow is summarized in Figure 6.6. Specific procedures to follow in Experiment-I were:

1. Subjects were asked to take a comfortable driving posture according to their seat adjustments. This includes raising-lowering and tilting the seat.

2. Eye-tracker device was adjusted to accommodate subject's seating preference and checked if it was able to capture eye-movements. (Subjects binocular field-of-vied should be inside the active green zone, which represents active area of eye-tracking.)

3. Experiment started with eye-tracker calibration. This includes a step-by-step setup to gather individual eye motion behavior. Subjects were asked to follow a moving red dot between 9 points shown on the screen.

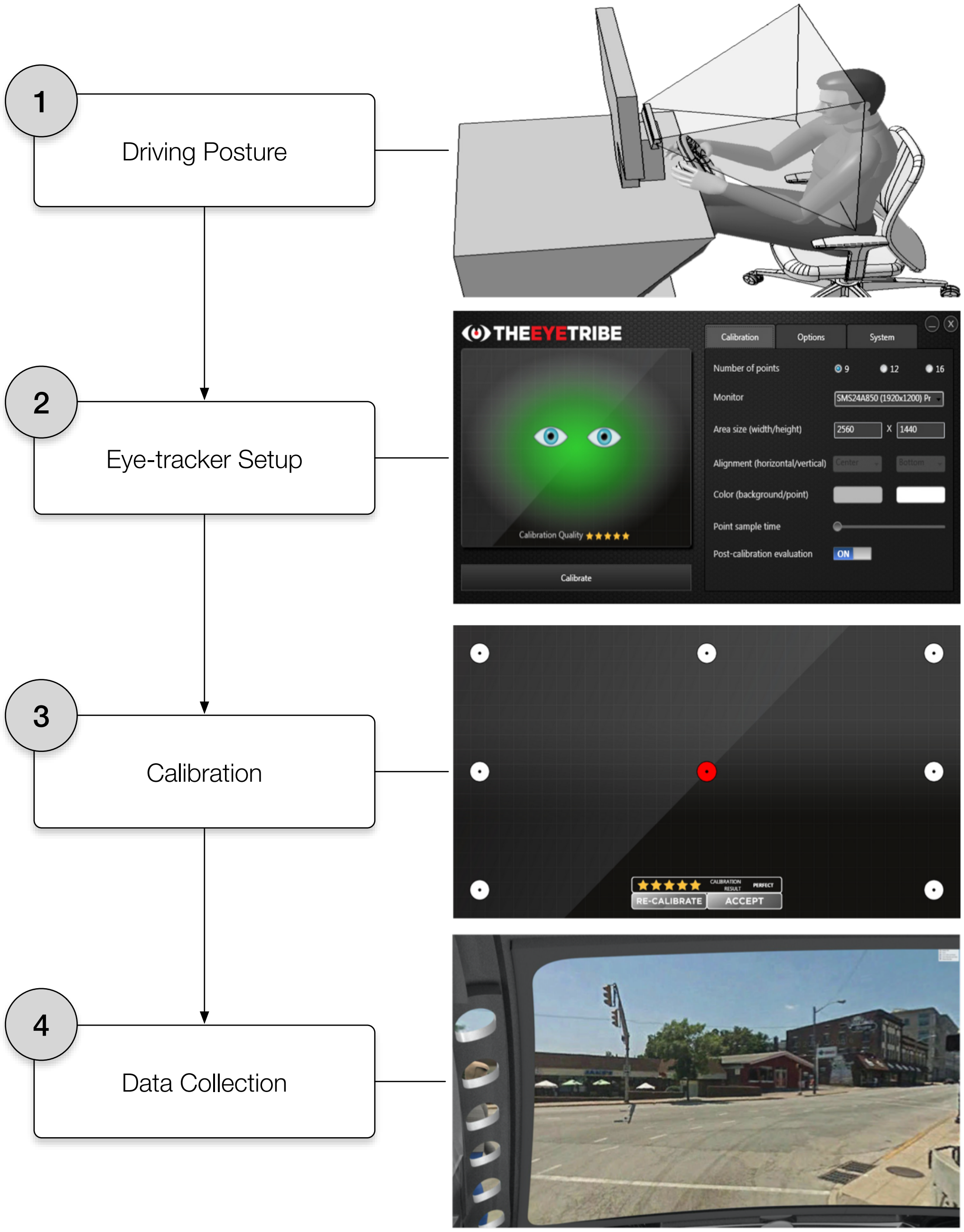

Figure 6.6. Experiment-I involves a static driving simulator to capture eye-movements of subjects. It starts with subjects taking a driving posture, orienting eye-tracker device according binocular field, followed by calibration and finally with data collection.

4. After eye-tracker calibration was completed, subject worked on various visual detection tasks. As the computer simulator turned on, subjects were asked to make field-of-sight observations of traffic objects projected to the LCD monitor. During simulator experiment, there were two types traffic objects (biker or pedestrian) corresponding to two different pillar models (Old of New Pillar model). Traffic environment was composed of what a subject could normally see when he/she is driving on a public road (Figure 6.5). Pillar model, pillar type and traffic objects were projected in randomized order. A total of 24 images were used throughout this experiment. Each image only stays on LCD monitor for three seconds and shuffles randomly. Each task was repeated six times.

6.4 Variables

In Experiment-I, subjects' eye-movements were collected through an eye-tracker device. Primarily, there were three independent variables of interest, encompassing: 1. Types of Pillars, 2. Traffic Objects and 3. Trials. These variables were used for generating a 3-way ANOVA/MANOVA analysis. On top of primary independent variables, three more independent variables were included to extend this study. Additional independent variables were: Gender, Driving Experience and Use of Glassess. Through the introduction of 3 more independent variables, a 6-way ANOVA/MANOVA study was conducted. Three dependent variables of interest in this study, includes: 1. Fixation Duration, Coordinates-X and Coordinates-Y.

Coordinates-X and Coordinates-Y data represents pixel-correspondences of each subjects' eye-movements superimposed on the monitor. Fixation Duration represents the intensity (or duration of eye-movement) fixated on a single point of observation (X,Y). Table 6.2 and Table 6.3 summarizes types of data, variables, units, and hypotheses associated with experiments conducted.

Table 6.2
Types of data, variables, units, and hypotheses associated with experiments conducted in this study

	Independent Variables	Levels	Hypotheses
Primary	Types of Pillar	Old,New	H1, H2, H3
	Traffic Objects	Pedestrian,Bicycle	H1, H2, H3
	Trials	1,...,6	H1, H2, H3
Additional	Gender	Male,Female	H1, H2, H3
	Driving Experience	Low,Medium,High	H1, H2, H3
	Use of Glasses	Glasses,No Glasses	H1, H2, H3

Table 6.3
Types of data, variables, units, and hypotheses associated with experiments conducted in this study

Dependent Variables	Units	Hypotheses
Fixation Duration	Milliseconds	H1, H2, H3
Coordinates-X	Pixels	H1, H2, H3
Coordinates-Y	Pixels	H1, H2, H3

6.5 Experimental Design

There were two different ANOVA/MANOVA studies performed in this study. First study was a 3-way ANOVA/MANOVA model, which was composed of three (primary) independent variables (Types of Pillars, Traffic Objects and Trials). An additional 6-way ANOVA/MANOVA study was conducted to further expand the primary 3-way model. Each model used same dependent variables summarized in Table 6.3. Besides these studies, several statistical studies were performed to analyze eye-tracking data. Statistical techniques used in this study are covered in Section 6.7.

6.5.1 Hypotheses and linear model for a three-way factorial analysis

The primary interest in ANOVA/MANOVA study was to explore whether pillar types, traffic objects or trials have effect on the eye-tracking data. Hypotheses to setting up factorial analysis and mathematical equation with associated factors are summarized below.

- $H0$: $\mu_{OLD} = \mu_{NEW}$ *(no effect of pillar models)*
  $H1$: $H0$ is rejected
- $H0$: $\mu_{Pedestrian} = \mu_{Bicycle}$ *(no effect of traffic objects)*
  $H1$: $H0$ is rejected
- $H0$: $\mu_{T1} = \mu_{T2}$ ... μ_{T6} *(no effect of trials)*
  $H1$: $H0$ is rejected

The basic mathematical model can be expressed in terms of the parameters of a linear model as:

$$Y_{ijkt} = \mu + \alpha_i + \beta_j + \gamma_k + \overbrace{(\alpha\beta)_{ij} + (\alpha\gamma)_{ik} + (\beta\gamma)_{jk}}^{2-way} + (\alpha\beta\gamma)_{ijk} + \varepsilon_{ijkt} \tag{6.1}$$

Y_{ijkt}: dependent variable

μ: overall mean

α_i : pillar type *(i = OLD, NEW)*

β_j : traffic objects *(j = Pedestrian, Bicycle)*

γ_k : number of trials *(k = 1,...,6)*

$(\alpha\beta)_{ij}$,$(\alpha\gamma)_{ik}$,$(\beta\gamma)_{jk}$: two-way interactions

$(\alpha\beta\gamma)_{ijk}$: three-way interaction

ε_{ijkt} : error term

6.5.2 Hypotheses and linear model for a six-way factorial analysis

This study was performed on top of the 3-way model with consideration of 3 additional independent variables, encompassing: 1. Gender, 2. Driving Experience and 3. Use of Glasses. In this study interaction effects were ignored since more than 3 interactions are hard to interpret for statistical significance on a large ANOVA/MANOVA study with varying levels. The purpose of this study to gain an additional understanding on top of the 3-way ANOVA/MANOVA conducted previously, especially exploring effects of additional independent variables on Types of Pillar, Traffic Objects and Trials. The basic mathematical model can be expressed in terms of the parameters of a linear model as:

$$\begin{aligned} Y_{ijkmnpt} &= \mu + \alpha_i + \beta_j + \gamma_k + \delta_m + \varphi_n + \lambda_p + \overbrace{(\alpha....\lambda)_{ijkmnp}}^{2-way} + \overbrace{(\alpha....\lambda)_{ijkmnp}}^{3-way} \\ &+ \overbrace{(\alpha....\lambda)_{ijkmnp}}^{4-way} + \overbrace{(\alpha....\lambda)_{ijkmnp}}^{5-way} + (\alpha\beta\gamma\delta\varphi\lambda)_{ijkmnp} + \varepsilon_{ijkmnp} \end{aligned} \tag{6.2}$$

$Y_{ijkmnpt}$: dependent variable

μ: overall mean

α_i : pillar type *(i = OLD, NEW)*

β_j : traffic objects *(j = Pedestrian, Bicycle)*

γ_k : number of trials *(k = 1,...,6)*

δ_m : gender *(m = Male, Female)*

φ_n : driving experience *(n = low, medium, higih)*

λ_p : use of glasses *(p = glasses, no glasses)*

$(\alpha....\lambda)_{ijkmnp}$: two-way interactions

$(\alpha....\lambda)_{ijkmnp}$: three-way interactions

$(\alpha....\lambda)_{ijkmnp}$: four-way interactions

$(\alpha....\lambda)_{ijkmnp}$: five-way interactions

$(\alpha\beta\gamma\delta\varphi\lambda)_{ijkmnp}$: six-way interactions

$\varepsilon_{ijkmnpt}$: error term

Equation 6.2 can be expanded with including every 2, 3, 4 and 5 way interactions:

$$
\begin{aligned}
&Y_{ijkmnpt} : \mu + \alpha_i + \beta_j + \gamma_k + \delta_m + \varphi_n + \lambda_p \\
&+ \left[\begin{array}{l} (\alpha_i\beta_j) + (\alpha_i\gamma_k) + (\alpha_i\delta_m) + (\alpha_i\varphi_n) + (\alpha_i\lambda_p) \\ +(\beta_j\gamma_k) + (\beta_j\delta_m) + (\beta_j\varphi_n) + (\beta_j\lambda_p) + (\gamma_k\delta_m) \\ +(\gamma_k\varphi_n) + (\gamma_k\lambda_p) + (\delta_m\varphi_n) + (\delta_m\lambda_p) + (\varphi_n\lambda_p) \end{array} \right] \\
&+ \left[\begin{array}{l} (\alpha_i\beta_j\gamma_k) + (\alpha_i\beta_j\delta_m) + (\alpha_i\beta_j\varphi_n) + (\alpha_i\beta_j\lambda_p) \\ +(\alpha_i\gamma_k\delta_m) + (\alpha_i\gamma_k\varphi_n) + (\alpha_i\gamma_k\lambda_p) + (\alpha_i\delta_m\varphi_n) \\ +(\alpha_i\delta_m\lambda_p) + (\alpha_i\varphi_n\lambda_p) + (\beta_j\gamma_k\delta_m) + (\beta_j\gamma_k\varphi_n) \\ +(\beta_j\gamma_k\lambda_p) + (\beta_j\delta_m\varphi_n) + (\beta_j\delta_m\lambda_p) + (\beta_j\varphi_n\lambda_p) \\ +(\gamma_k\delta_m\varphi_n) + (\gamma_k\delta_m\lambda_p) + (\gamma_k\varphi_n\lambda_p) + (\delta_m\varphi_n\lambda_p) \end{array} \right] \\
&+ \left[\begin{array}{l} (\alpha_i\beta_j\gamma_k\delta_m) + (\alpha_i\beta_j\gamma_k\varphi_n) + (\alpha_i\beta_j\gamma_k\lambda_p) + (\alpha_i\beta_j\delta_m\varphi_n) \\ +(\alpha_i\beta_j\delta_m\lambda_p) + (\alpha_i\beta_j\varphi_n\lambda_p) + (\alpha_i\gamma_k\delta_m\varphi_n) + (\alpha_i\gamma_k\delta_m\lambda_p) \\ +(\alpha_i\gamma_k\varphi_n\lambda_p) + (\alpha_i\delta_m\varphi_n\lambda_p) + (\beta_j\gamma_k\delta_m\varphi_n) + (\beta_j\gamma_k\delta_m\lambda_p) \\ +(\beta_j\gamma_k\varphi_n\lambda_p) + (\beta_j\delta_m\varphi_n\lambda_p) + (\gamma_k\delta_m\varphi_n\lambda_p) \end{array} \right] \\
&+ \left[\begin{array}{l} (\alpha_i\beta_j\gamma_k\delta_m\varphi_n) + (\alpha_i\beta_j\gamma_k\delta_m\lambda_p) + (\alpha_i\beta_j\gamma_k\varphi_n\lambda_p) \\ +(\alpha_i\beta_j\delta_m\varphi_n\lambda)_p + (\alpha_i\gamma_k\delta_m\varphi_n\lambda_p) + (\beta_j\gamma_k\delta_m\varphi_n\lambda_p) \end{array} \right] \\
&+(\alpha_i\beta_j\gamma_k\delta_m\varphi_n\lambda_p) + \varepsilon_{ijkmnp}
\end{aligned} \tag{6.3}
$$

6.6 Participants

6.6.1 Population estimates

Before starting to any experimental analysis that involves human subjects, the very first statistical step to be performed is to make estimates about the population (i.e., pilot study). The main goal of the pilot study is to estimate the number of subjects required to gain a statistical power. Pilot study also provides an additional insight about the total time required for conducting experiment as well as procedures to accommodate subjects during data collection [147].

There are various methods to estimate sample size. One of the most common ways is to use a sample size estimation based on the mean and standard deviations from pilot studies. In this method, one can assume that the collected sample mean differs from the population mean (μ), where the difference between sample and population mean can be treated as an error factor. Therefore, through the differences of means, a sample size with desired margin of error is measured [148, 149].

Based on the means and standard deviation retrieved from a pilot study, the sample size can be calculated to estimate the total number of subjects required for human data collection. In this study, Equation 6.5 is used for estimating the sample size with a confidence of $1 - \alpha$, where the mean value of μ to be within $\pm$ E.

$$E = Z_{\alpha/2} \times \left[\frac{\sigma}{\sqrt{n}}\right] \tag{6.4}$$

$$n = \left[\frac{Z_{\alpha/2} \times \sigma}{E}\right]^2 \tag{6.5}$$

where,

E:	is maximum difference between the pilot and the population mean
$Z_{\alpha/2}$:	critical value, the positive Z value that is wihtin the area of $\alpha/2$ at the right tail of the standard normal distribution
σ:	population standard deviation
n:	sample size

6.6.2 Pilot study

A sample size calculation to estimate the population mean was performed through using Equation 6.5. Data collected from four different pilot studies (on Fixation Duration) resulted with average standard deviation of ≈400 and the maximum allowable difference (± E) of ≈150. From pilot study results, one can calculate the $\alpha/2$ value (0.05 - 0.025 = 0.475), which equals to Z(0.475) = 1.96.

$$n = \left[\frac{Z_{\alpha/2} \times \sigma}{E}\right]^2 = \left[\frac{1.96 \times 400}{150}\right]^2 \approx 27 \tag{6.6}$$

Above sample size calculation assumes the normality of the data and suggests that around ≈27 subjects would be sufficient to achieve a 95% confidence. However, the pilot study resulted with a slightly skewed data. Number of replications were increased to six - to gain a thorough understanding of pillar-obscuration problems and to reach a desired statistical power. Therefore, each task was replicated six times (instead of twice) to lessen the biasing effects of violations from normality and to reduce the potential measurement errors (i.e. random and systematic errors).

6.6.3 Summary of subjects

A total of 48 subjects, 28 male and 20 female, participated in this study. The overall mean of the standing height was ≈174cm and mean weight was ≈70kg. The mean standing heights and weights were 179cm and 78kg for males, and 167cm and 59kg for females. The average height and weight values are close to the 50^{th} percentile standing height of North American population - 179cm and 165cm for female and male subjects respectively (Table 6.4). The range of standing height was between 157cm and 194cm, which covers 35^{th} percentile female (160cm) to 95^{th} percentile male (194cm) according to CATIA anthropometrics data base [150].

Around 4% of the subjects rated their driving experience as 'High', which indicates a person who drives relatively longer distances than a daily driver. Majority of subjects (65%) identified themselves as daily drivers (Medium). Around 30% of the subjects rated their driving experience as 'Low', which refers to a very minimal driving or not driving at all (Table 6.5). The use of glasses (including contact lenses) was evenly distributed within the population (Table 6.6).

Table 6.4
Descriptive statistics - Weight (kg) and Height (cm)

Gender		N	Minimum	Maximum	Mean	Std. Dev.
Male	Height	28	165	194	178.61	6.91
	Weight	28	64	106	77.79	11.66
Female	Height	20	157	180	166.70	5.15
	Weight	20	48	77	59.25	8.45
Total	Height	48	157	194	173.65	8.57
	Weight	48	48	106	70.06	13.86

Table 6.5
Descriptive statistics - Driving Experience

	Frequency	Percent
High	2	4.2
Medium	31	64.6
Low	15	31.3
Total	48	100.0

Table 6.6
Descriptive statistics - Use of Glasses

	Frequency	Percent
No Glasses	24	50.0
Use Glasses	24	50.0
Total	48	100.0

6.7 Data Analysis and Statistical Techniques

In this section an in-depth analysis was provided on eye-tracking data, which is composed of Fixation Duration, Coordinates-X and Coordinates-Y. Based on the hypotheses summarized in Table 8.2, statistical analyses were performed and results were categorized. First of all, raw data was transformed into a compound data by Weighted Moving Averages technique discussed in Equation 6.7. Later, descriptive analysis was performed on independent and dependent variables. Starting by next section comparison between 'Pillar Models', 'Traffic Objects', 'Driving Experience', 'Use of Glasses' and 'Trials' were tabulated. Normality assumptions were checked. Logarithmic transformation was applied to data that showed weak normality, so that data more closely meet normality assumptions. A combination of Analysis of Variance (ANOVA) and Multivariate Analysis of Variance (MANOVA) studies were conducted to assess whether or not results are significant. Finally, areas of interest analyses were performed to interpret statistical and visual differences between Current Pillar and New Pillar design.

6.7.1 Transformation of raw data to compound data

Weighted moving average

Eye-tracker data provides information related three types dependent variables: Fixation Duration (in milliseconds), Coordinates-X (pixels) and Coordinates-Y (pixels). Fixation Duration represents a time dependent variable, which refers to how long subject's pupils get fixated to a specific point (X and Y coordinate). Fixations are associated with areas of interest, where a subject pays significant attention to a specific point (X,Y). The duration of fixations are relatively longer than eye-gazing (random eye-movements without fixation).

It was seen in raw data that each subject had an average of four major fixations per image presented on simulation display. Weighted Moving Average (MWA) method was used for creating a compound data set (Equation 6.7), which aggregated four fixations into a single fixation reading [151, 152]. Within WMA approach, Fixation Duration was considered as the weighting factor for each X and Y coordinate. Higher the Fixation Duration (intensity), more time that subjects spend on associated point (X and Y coordinates).

$$WMA = \frac{\sum_{i=1}^{n} W_i \times V_i}{\sum_{i=1}^{n} W_i} \tag{6.7}$$

where,

WMA:	Weighted Moving Average
W:	weights (Fixation Duration)
V:	actual X and Y coordinates associated with each Fixation Duration
n:	number of data points

Fixation coordinates and fixation duration

Throughout Experiment-I, moving weighted average technique was used and compound data was formed after applying equation 6.7 to raw data. The bubble graph on Figure 6.7 demonstrates distribution of X and Y coordinates, and relative size of the Fixation Duration associated with each point (X,Y). Coordinates-X and Coordinates-Y (pixel-by-pixel correspondences of eye movements) were superimposed on simulation display. At any specific point, larger the diameter of a bubble, longer the fixation duration.

6.7.2 Descriptive statistics

A total of 1152 (48 subjects x 2 pillar models x 2 traffic objects x 6 trials) data set were collected during Experiment-I. Each data set was was composed of Fixation Duration, Coordinates-X and Coordinate-Y outputs.

Starting from next page a series of tables provided to summarize compound data. Table 6.7 represents overall descriptive statistics for Fixation Duration and Fixation Coordinates (X,Y). Tables from 6.8 to 6.12 summarize distribution of the eye-tracking

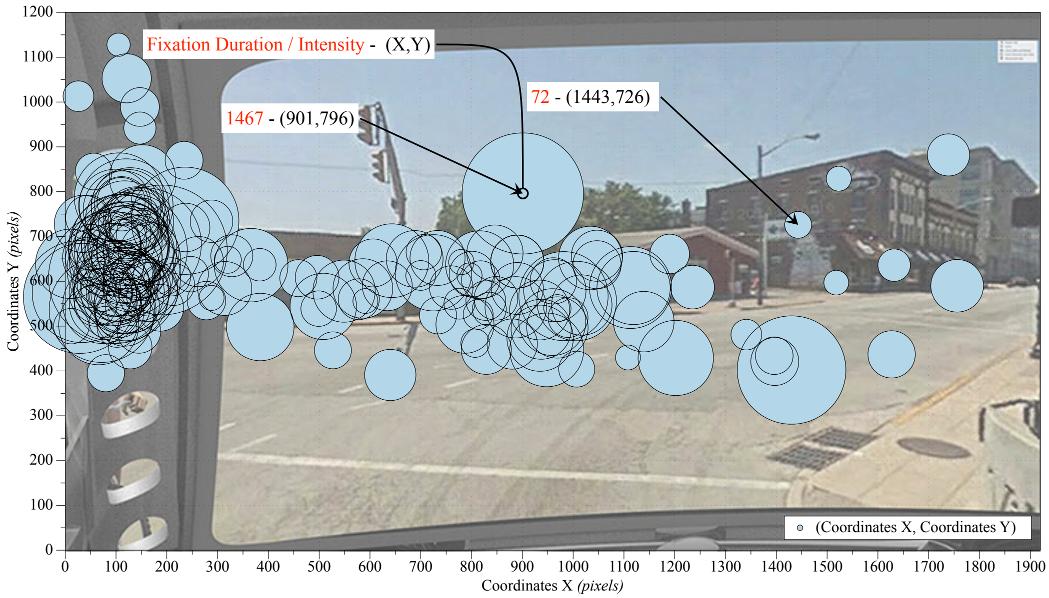

Figure 6.7. Fixation duration and coordinates data superimposed on simulation display. Area of the bubbles represent the duration of fixations.

data over independent variables of Gender (Male vs. Female), Pillar Types (Old vs. New pillar), Traffic Objects (Bicycle vs. Pedestrian), Use of Glasses (Glasses vs. No Glasses), and Driving Experience (Low, Medium and High).

Table 6.7
Summary of Fixation Duration and Coordinates (X,Y)

Variables	N	Min.	Max.	Mean	Std. Dev.
Fixation_Duration	1152	10	1988	373.50	194.34
Coordinates_X	1152	10	1686	503.67	350.15
Coordinates_Y	1152	106	880	602.16	82.88

Table 6.8: Descriptive statistics for Subjects

Gender	Dependent Var.	N	Min.	Max.	Mean	Std. Dev.
Male	Fix_Duration	672	10	1988	381.05	217.43
	Coordinates_X	672	10	1686	502.17	360.25
	Coordinates_Y	672	106	880	600.81	88.56
Female	Fix_Duration	480	104	1969	362.94	156.00
	Coordinates_X	480	28	1558	505.78	335.85
	Coordinates_Y	480	341	836	604.05	74.23

Table 6.9: Descriptive statistics for Pillar Types

Pillar Types	Dependent Var.	N	Min.	Max.	Mean	Std. Dev.
Old Pillar	Fix_Duration	576	89	1969	347.63	157.77
	Coordinates_X	576	33	1686	663.02	361.23
	Coordinates_Y	576	252	858	601.89	91.71
New Pillar	Fix_Duration	576	10	1988	399.38	222.19
	Coordinates_X	576	10	1659	344.33	253.10
	Coordinates_Y	576	106	880	602.43	73.06

Table 6.10: Descriptive statistics for Traffic Objects

Traffic Objects	Dependent Var.	N	Min.	Max.	Mean	Std. Dev.
Bicycle	Fix_Duration	576	10	1988	367.38	216.93
	Coordinates_X	576	10	1659	512.84	347.56
	Coordinates_Y	576	332	856	612.96	79.56
Pedestrian	Fix_Duration	576	89	1854	379.63	168.72
	Coordinates_X	576	16	1686	494.51	352.77

continued on next page

Table 6.10: *continued*

Traffic Objects	Dependent Var.	N	Min.	Max.	Mean	Std. Dev.
	Coordinates_Y	576	106	880	591.36	84.76

Table 6.11: Descriptive statistics for Use of Glasses

Glasses	Dependent Var.	N	Min.	Max.	Mean	Std. Dev.
No Glasses	Fix_Duration	576	103	1988	383.45	183.85
	Coordinates_X	576	58	1686	524.38	337.54
	Coordinates_Y	576	363	858	608.15	78.13
Use Glasses	Fix_Duration	576	10	1963	363.56	203.97
	Coordinates_X	576	10	1650	482.97	361.42
	Coordinates_Y	576	106	880	596.17	87.02

Table 6.12: Descriptive statistics for Driving Experience

Experience	Dependent Var.	N	Min.	Max.	Mean	Std. Dev.
Low	Fix_Duration	360	89	1988	390.85	219.03
	Coordinates_X	360	28	1686	542.01	410.86
	Coordinates_Y	360	106	858	596.72	92.41
Medium	Fix_Duration	744	10	1969	364.09	184.09
	Coordinates_X	744	10	1650	491.54	323.52
	Coordinates_Y	744	252	880	609.13	77.25
High	Fix_Duration	48	136	642	389.31	136.88
	Coordinates_X	48	135	1148	404.23	186.46
	Coordinates_Y	48	349	699	534.98	54.89

Table 6.13: Descriptive statistics for Trials

Trials	Dependent Var.	N	Min.	Max.	Mean	Std. Dev.
Trial 1	Fixation_Duration	192	10	1892	376.05	224.75
	Coordinates_X	192	10	1659	527.63	386.30
	Coordinates_Y	192	318	858	601.74	86.17
Trial 2	Fixation_Duration	192	125	1969	378.57	206.79
	Coordinates_X	192	50	1539	483.16	339.99
	Coordinates_Y	192	106	858	592.88	93.50
Trial 3	Fixation_Duration	192	113	684	357.90	115.71
	Coordinates_X	192	22	1686	491.51	339.91
	Coordinates_Y	192	351	880	609.05	80.77
Trial 4	Fixation_Duration	192	111	738	354.66	113.68
	Coordinates_X	192	33	1543	521.77	345.69
	Coordinates_Y	192	260	787	604.86	77.57
Trial 5	Fixation_Duration	192	89	1988	414.83	295.10
	Coordinates_X	192	16	1643	487.70	342.81
	Coordinates_Y	192	332	787	605.67	78.18
Trial 6	Fixation_Duration	192	90	940	359.02	135.49
	Coordinates_X	192	46	1558	510.29	345.93
	Coordinates_Y	192	367	836	598.76	80.01

6.7.3 Intra-class correlation

Background on intra-class correlation

In Experiment-I, test-retest reliability method involved subjects replicating the identical test conditions in six different trials. All subjects were required to repeat same object detection task in exact conditions for six times. Results between six trials for each task per subject were compared to assess test-retest reliability.

Literature review shows that Intra-Class Correlation (ICC) is a preferred method when there are more than two replications (test-retest) to be correlated. ICC defines the correlation of between-subject variance divided by the total variance [153, 154]. Wu [114] and Tian [113] studied the use of ICC two-way random single rater model with absolute agreement for testing-retesting reliability of human motion data. Equation 6.8 was used for ICC(2,1) analysis:

$$ICC(2,1) = \frac{BMS}{BMS + (k-1)EMS + k[(TMS - EMS)/n]} \tag{6.8}$$

where,

BMS:	Between-subject mean square
EMS:	Error mean square
TMS:	Trial mean square
k:	number of trials
n:	number of objects

Interpretation of the ICC index depends on the nature of the experiment and the domain of interest. Under different circumstances, such as application domain (e.g., applied psychology vs. engineering) and experimental conditions (e.g.,sensitivity of the data), strong and weak correlations are classified in different ranges. Most of the literature shows that magnitudes of relationship are categorized as strong, moderate and weak. Some studies show that ICC ranging from 0.7 to 1 is considered as good/high/excellent correlation between classes [155–157], while other studies [158, 159] define the perfect correlation as between 0.8 and 1.0. Substantial correlation was considered between 0.6 and 0.8, the moderate correlation between 0.4 and 0.6, and the poor correlation between 0 and 0.4. Due to the similarities of experimental setup and application domain, Wu's (2005) [114] and Tian's (2007) [113] ICC method was followed to assess the reliability of collected data. The correlation coefficient range was defined in the following table:

Table 6.14
Classification of Intra Class Correlation Index (ICC)

ICC Range	Meaning	Notes
(0.80, 1.00]	Excellent	Perfect match
(0.60, 0.80]	Good	Relative high agreement
(0.40, 0.60]	Moderate	Though reliability not high, but possible being improved
(0.00, 0.40]	Poor	No or few correlation

For 'Excellent' and 'Good' reliability, two test scores should correlate with each other very well. This level of correlation is expected for the ideal reliability test. If ICC index value reaches to score of 1.0, it is called the 'Perfect Match', which shows the highest correlation possible. For the 'Moderate' reliability, it is still possible to improve the correlation level by changing design variables. 'Poor' reliability proposes that reliability is low, which does not provide any useful information to interpret significant relations about variables. A high correlation ('Good' or 'Excellent') level is expected in this study, where ICC magnitude falls in the range of 0.6<ICC<1.0.

Results on intra-class correlation

One of the objectives of this study is to demonstrate that the correlation measurements between trials (the test-retest reliability of outcomes) should be in high correlation ('Good' or 'Excellent' correlation) range, where Intra Class Correlation (ICC) index magnitude falls in range of 0.6 <ICC index <1.0. ICC indexes for Fixation Duration, Coordinates-X and Coordinates-Y are listed in the following table:

Comparison of outcomes between six trials resulted in larger than 0.60, which demonstrate a 'good' test-retest reliability. ICC results in Table 6.15 shows that Coordinates-X provide 'excellent' test-retest reliability. Similarly, Coordinates-Y in-

Table 6.15
Intra-Class Correlation (ICC) of test-retest reliability of Trials

	ICC	95% Confidence Interval		F Test			
		Lower	Upper	Value	df1	df2	Sig.
Fixation Duration	.618	.441	.640	2.224	191	955	0.000
Coordinates X	.862	.342	.627	7.122	191	955	0.000
Coordinates Y	.794	.746	.836	4.869	191	955	0.000

dicates a very-close to ”excellent” ICC score. The lowest agreement among all responses is Fixation Duration, which resulted in ’good’ reliability.

6.7.4 Multivariable Analysis of Variance

Validity hypothesis in this study focuses on assessing the significance effects and interactions of independent variables: Gender, Pillar Type, Use of Glasses, Traffic Objects, Driving Experience, and Trials. Eye-tracking data collected in Experiment-I was also compared with user feedback on Experiment-II to check whether outcomes of Experiment-I (objective measurements - eye-tracker device) overlaps with outcomes of Experiment-II (subjective measurements - design questionnaire/review).

Background on ANOVA and MANOVA studies

Hypotheses proposed in this study targeted to detect ergonomics differences between pillar designs. In other words, one should experience a bias generated by the subjects different performance in detecting objects between Old Pillar and New Pillar. Ideally, the response generated by subjects should be overlapping even with the presence of bias. Thus, results on Objective Measurements (Experiment-I) and Subjective Measurements (Experiment-II) should reflect similar outcomes.

To measure validity, a standard criterion that can be believed as valid measurement is compared with collected data (e.g., subject feedback). Traffic Objects presented in static simulation experiment were known in advance by the experimenter. Thus, they can be defined as standard data. Collected data (both eye-tracking and object detection data) were compared with standard data to assess the validity in this study. Main effects and interaction effects were compared by multiple ANOVA and MANOVA studies. A quick overview on ANOVA/MANOVA basics are covered in this section [160–163].

A one-way ANOVA can be represented by a linear model equation:

$$y_{ij} = m + a_i + e_{ij} \tag{6.9}$$

In general, ANOVA table for the same case (one-way) can be constructed as:

Table 6.16
Descriptive Statistics of logarithmic transformed data - Skewness and Kurtosis

Source	Sum of Squares	DoF	Mean Squares	Fo
Factors	$\mathbf{SS_F = J\sum(\bar{y}_{i.} - \bar{y}_{..})^2}$	I-1	$\mathbf{MSF = \frac{SS_F}{(I-1)}}$	$\mathbf{MSF = \frac{MSF}{MSE}}$
Residual	$\mathbf{SS_E = \sum\sum(y_{i.} - \bar{y}_{i.})^2}$	I(J-1)	$\mathbf{MSE = \frac{SS_E}{I(J-1)}}$	
Corr. Total	$\mathbf{SST = \sum\sum(y_{ij} - \bar{y}_{..})^2}$	IJ-1		

MANOVA is the generalized case of ANOVA with multiple dependent variables. Therefore, there are analogous parts to the ANOVA equation. Often, number of different statistical tests are used to check the significance of MANOVA results [164]. In this study, Wilk's Lamda was used to interpret results. Pillai's Trace, Hotelling's Trace and Roy's Largest Root analysis were also provided with MANOVA tables. Underlying assumptions of MANOVA analysis are provided in details from Equation 6.10 to Equation 6.24 [162, 165].

First, the total sum-of-squares is split into sum-of-squares between sum-of-squares ($SS_{bg(y)}$) and within sum-of-squares ($SS_{wg(y)}$) groups.

$$SS_{Total(y)} = SS_{bg(y)} + SS_{wg(y)} \tag{6.10}$$

Above equation can be expressed as:

$$\sum_i \sum_j (Y_{ij} - GM_{(y)})^2 = n \sum_j \left(\bar{Y}_j - GM_{(y)}\right)^2 + \sum_i \sum_j (Y_{ij} - \bar{Y}_j)^2 \tag{6.11}$$

One can partition sum-of-squares between ($SS_{bg(y)}$) two Independent Variables. Lets assume SS_D and SS_T represent sum-of-squares of variables D and T. Accordingly, SS_{DT} represent the interaction term.

$$SS_{bg} = SS_D + SS_T + SS_{DT} \tag{6.12}$$

Then equation can be expressed as:

$$\begin{aligned} &n_{km} \sum_k \sum_m (DT_{km} - GM_{(DT)})^2 = n_k \sum_k \left(D_k - GM_{(D)}\right)^2 + \\ &n_m \sum_m \left(T_m - GM_{(T)}\right)^2 + \Bigg[n_{km} \sum_k \sum_m \left(DT_{km} - GM_{(DT)}\right)^2 - \\ &n_k \sum_k \left(D_k - GM_{(D)}\right)^2 - n_m \sum_m \left(T_m - GM_{(T)}\right)^2 \Bigg] \end{aligned} \tag{6.13}$$

Then the full-factorial design looks like this:

$$\begin{aligned} &\sum_i \sum_k \sum_m (Y_{ikm} - GM_{(ikm)})^2 = n_k \sum_k \left(D_k - GM_{(D)}\right)^2 + n_m \sum_m \left(T_m - GM_{(T)}\right)^2 + \\ &\Bigg[n_{km} \sum_k \sum_m \left(DT_{km} - GM_{(DT)}\right)^2 - n_k \sum_k \left(D_k - GM_{(D)}\right)^2 - n_m \sum_m \left(T_m - GM_{(T)}\right)^2 \Bigg] \\ &+ \sum_i \sum_k \sum_m (Y_{ikm} - DT_{km})^2 \end{aligned} \tag{6.14}$$

Because there are multiple dependent variables in MANOVA, a column matrix could be used for each dependent variable. Then, vector matrix for two dependent variables (a and b) with n samples is:

$$Y_{i \cdots n} = \begin{bmatrix} a_1 \\ b_1 \end{bmatrix} \begin{bmatrix} a_2 \\ b_2 \end{bmatrix} \begin{bmatrix} a_3 \\ b_3 \end{bmatrix} \cdots \begin{bmatrix} a_n \\ b_n \end{bmatrix} \tag{6.15}$$

Similarly, there are column matrices associated with each Independent Variable. For 'n' many dependent variable and 'm' levels of independent variables, the column matrices like:

$$DT_{i\cdots k,j\cdots m} = \begin{bmatrix} \bar{X}_1 \\ \bar{X}_2 \\ \vdots \\ \bar{X}_n \end{bmatrix} \tag{6.16}$$

$$D_1 = \begin{bmatrix} \bar{X}_1 \\ \bar{X}_2 \\ \vdots \\ \bar{X}_n \end{bmatrix}, D_2 = \begin{bmatrix} \bar{X}_1 \\ \bar{X}_2 \\ \vdots \\ \bar{X}_n \end{bmatrix} \cdots D_m = \begin{bmatrix} \bar{X}_1 \\ \bar{X}_2 \\ \vdots \\ \bar{X}_n \end{bmatrix} \tag{6.17}$$

In addition, a single matrix of grand means are calculated for each dependent variable averaged across all individuals in matrix.

$$GM = \begin{bmatrix} X_1 \\ X_2 \\ \vdots \\ X_n \end{bmatrix} \tag{6.18}$$

Differences are found by subtracting matrices. The error term is calculated by subtracting the grand mean matrix from each of dependent variable score. Then, each column matrix is multiplied by its transpose.

Finally, sum-of-total-squares can be expressed by partitioning sum-of-squares for independent variables, interactions and within-group error. A study with two independent variables and two dependent variables can be expressed as:

$$\begin{aligned} &\text{Step1} \rightarrow (Y_{ikm} - GM) \\ &\text{Step2} \rightarrow (Y_{ikm} - GM)(Y_{ikm} - GM)' \end{aligned} \tag{6.19}$$

$$\begin{aligned}
&\sum_i \sum_k \sum_m (Y_{ikm} - GM)(Y_{ikm} - GM)' = n_k \sum_k (D_k - GM)(D_k - GM)' \\
&+n_m \sum_m (T_m - GM)(T_m - GM)' + [n_{km} \sum_{km} (DT_{km} - GM)(DT_{km} - GM)' \\
&-n_k \sum_k (D_k - GM)(D_k - GM)' - n_m \sum_m (T_m - GM)(T_m - GM)'] \\
&+ \sum_i \sum_k \sum_m (Y_{ikm} - DT_{km})(Y_{ikm} - DT_{km})'
\end{aligned} \tag{6.20}$$

One can see that final results yield four different S matrices for a study with two dependent and two independent variables. Determinant of each matrix represents generalized variance of the associated terms (Equation 5.12).

$$SS_{Total} = SS_{\text{IndependentVariables}} + SS_{\text{Interaction}} + SS_{\text{Within-GroupError}} \tag{6.21}$$

One of the most popular methods of analyzing significance of MANOVA results is Wilk's Lambda test. Using the determinants of each matrix (5.12), we can assess the significance of MANOVA results through ratios of determinants used for Wilk's Labmda (λ) calculation.

$$\lambda = \frac{|S_{error}|}{|S_{effect} + S_{error}|} \tag{6.22}$$

An estimate for F for Wilk's Lambda test can be calculated from below equation:

$$F(df_1, df_2) = \left(\frac{1-y}{y}\right)\left(\frac{df_2}{df_1}\right) \tag{6.23}$$

where,

$$\begin{aligned}
&y = \lambda^{1/s} \\
&s = \sqrt{\tfrac{p^2(df_{effect})^2 - 4}{p^2 + (df_{effect})^2 - 5}}, \\
&\text{p = number of Dependent Variables} \\
&df_1 = p(df_{effect}) \\
&df_2 = s\left[(df_{error}) - \tfrac{p - df_{effect} + 1}{2}\right] - \left[\tfrac{p(df_{effect}) - 2}{2}\right]
\end{aligned} \tag{6.24}$$

Normality assumption

One of the prerequisites of any parametric study is to check normality of the data. In this section, Skewness and Kurtosis investigations were performed on eye-tracker data to assess normality assumptions. One can see at Table 6.17 that Fixation Duration and Coordinates-X data resulted in a highly positive skewness. In contrast, Coordinates-Y data resulted with a slight negative skewness (-0.33) and moderate kurtosis (2.14).

Table 6.17
Descriptive statistics of raw data - Skewness and Kurtosis

	Fixation Duration	Coordinates_X	Coordinates_Y
N	1152	1152	1152
Mean	373.50	503.67	602.16
Median	344.00	390.00	600.00
Std. Deviation	194.34	350.15	82.88
Skewness	4.29	.97	-.33
Std. Error of Skewness	.07	.07	.07
Kurtosis	29.12	.25	2.14
Std. Error of Kurtosis	.14	.14	.14

Some may argue that these values are relatively acceptable to satisfy normality assumptions [166], however, on a different normality evaluation approach, Kolmogorov-Smirnov and Shapiro-Wilk tests showed that all dependent variables violated normality assumptions. Each test had 'p' value smaller than zero, which indicated that the data is not normally distributed (Table 6.18).

Since Fixation Duration, Coordinates-X and Coordinates-Y violated normality assumption, each data set was normalized by applying logarithmic transformation. There are two major assumptions for logarithmic transformation; 1) positive skewness and 2) Non-negative values. Each dependent variable satisfied these assumptions. Table 6.13 shows variables with smaller skewness after logarithmic transformation was performed. A similar observation can be gathered from the 'Logarithmic Transformed' column on Figure 6.3, which also illustrates a close association to normality assumption with improved skewness and kurtosis.

Table 6.18
Kolmogorov-Smirnov and Shapiro-Wilk normality tests

	Kolmogorov-Smirnov			Shapiro-Wilk		
	Statistic	df	Sig.	Statistic	df	Sig.
Fix_Duration	.16	1152	.000	.68	1152	.000
Coordinates_X	.13	1152	.000	.91	1152	.000
Coordinates_Y	.04	1152	.000	.98	1152	.000

Table 6.19
Descriptive Statistics of logarithmic transformed data - Skewness and Kurtosis

	Fixation Duration	Coordinates X	Coorrdinates Y
N	1152	1152	1152
Mean	2.53	2.59	602.16
Median	2.54	2.59	600.00
Std. Deviation	.18	.33	82.88
Skewness	-.15	-.47	-.33
Std. Error of Skewness	.07	.072	.07
Kurtosis	6.55	.30	2.14
Std. Error of Kurtosis	.14	.14	.14

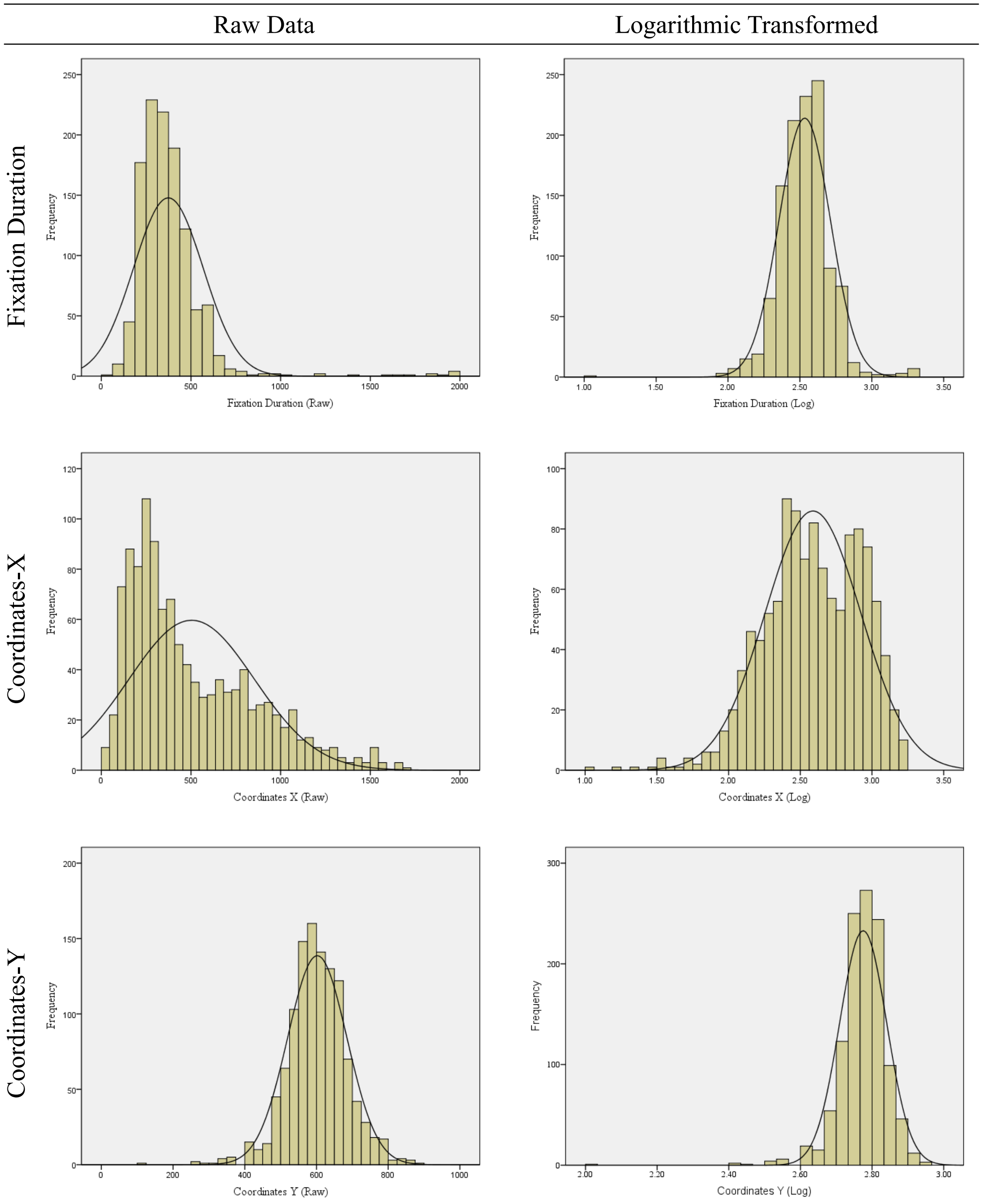

Figure 6.8. Histogram plots show differences in skewness and kurtosis associated with Raw Data and Logarithmic Transformed data. One can see that Logarithmic Transformed plots appear to meet normal distribution better than Raw Data plots.

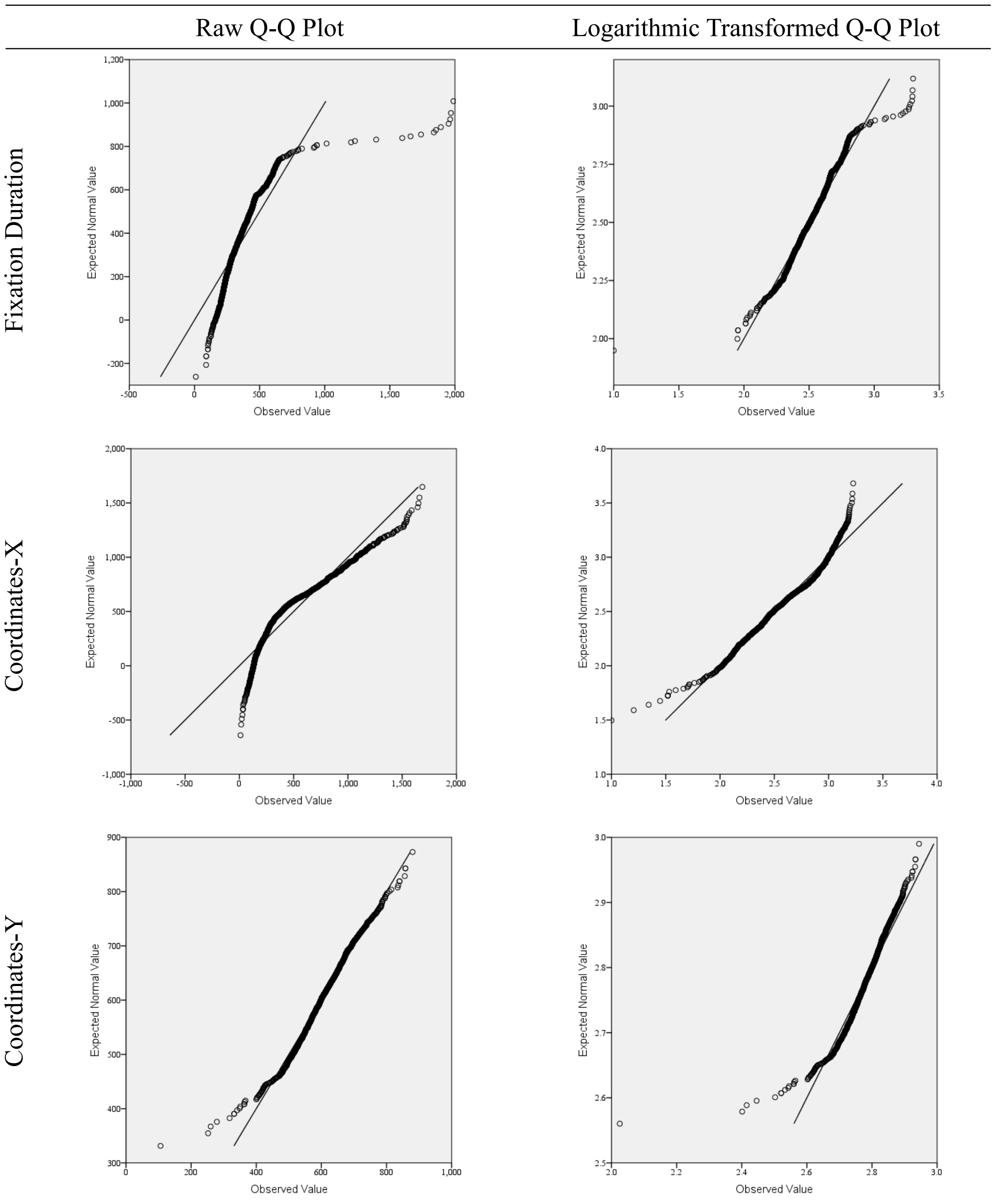

Figure 6.9. Quantile-Quantile plot shows distribution of Raw and Logarithmic Transformed data. One can see that Logarithmic Transformed data has better linear fit compared to Raw Data.

6.7.5 Three-way ANOVA/MANOVA - main effects and interaction

Even though logarithmic transformation performed previously smoothed out some of the outliers and scattered points in raw data, the normalization process caused a slight loss of fidelity. A blend of Analysis of Variance (ANOVA) and Multivariate Analysis of Variance (MANOVA) were conducted on three independent variables (Type of Pillars, Traffic Objects and Trials) and three dependent variables (Fixation Duration, Coordinates-X and Coordinates-Y). Each analysis covered raw and compound (logarithmic transformed) data in combinations to explore whether or not independent variables are significantly affect experimental results. In addition, interaction effects were also explored. A total of twelve analysis of variance studies (six ANOVAs and six MANOVAs) were conducted.

Prior to conducting MANOVA investigations, a series of Pearson correlation analysis were performed between all dependent variables to check whether dependent variables correlated to each other in small or moderate range [167]. Although correlation values were small in some cases, a meaningful pattern of correlations were observed for most of the dependent values, suggesting appropriateness of a MANOVA (Table 6.20).

Table 6.20
Pearson correlations of raw and logarithmic transformed dependent variables

Dependent Variables	Fixation Duration	Coordinates-X	Coordinates-Y
	(Raw/Log)	(Raw/Log)	(Raw/Log)
Fixation Dur. (Raw/Log)	1 / 1	-.119 / -.126	.020 / .008
Coordinates-X (Raw/Log)	-.119 / -.0.126	1 / 1	-.209 / -.165
Coordinates-Y (Raw/Log)	.020 / .008	.-209 / -.165	1 / 1

Analysis of variance - I (ANOVA-I)

ANOVA-I study sought to determine whether Fixation Duration differed across the factors of: Pillar Models, Traffic Objects, and Trials. A 2 x 2 x 6 (24) mixed design ANOVA was performed on multi-levels. Pillar Models are within two levels (New and Old), Traffic Objects are within two (Bicycle and Pedestrian) and Trials are within six levels (T1 to T6).

Table 6.21: Three-way ANOVA-I results on Fixation Duration

Source	Sum of Squares	df	Mean Square	F	Sig.
Corrected Model	1930775.041a	23	83946.741	2.280	.001
Intercept	160710327.022	1	160710327.022	4363.952	.000
Pillar_Types	771023.272	1	771023.272	20.936	.000
Traffic_Objects	43230.251	1	43230.251	1.174	.279
Trials	489345.265	5	97869.053	2.658	.021
Pillar_Types * Traffic_Objects	51133.355	1	51133.355	1.388	.239
Pillar_Types * Trials	137348.661	5	27469.732	.746	.589
Traffic_Objects * Trials	157031.098	5	31406.220	.853	.512
Pillar_Types * Traffic_Objects * Trials	281663.140	5	56332.628	1.530	.178
Error	41540616.938	1128	36826.788		
Total	204181719.000	1152			
Corrected Total	43471391.978	1151			

a R Squared = .044 (Adjusted R Squared = .025)

The ANOVA-I analysis revealed that there is a significant main effect of Pillar Types ($F = 20.396$, $p < .000$) and Trials ($F = 2.658$, $p = .021$) on Fixation Duration. Traffic Objects ($F = 1.174$, $p = .279$) has no significant effect on Fixation Duration, suggesting that Pillar Types and Trials effect the eye-fixation intensity during the simulation. There is no significant interaction found between independent variables.

Analysis of variance - II (ANOVA-II)

ANOVA-II study sought to determine whether Coordinates-X differed across the factors of: Pillar Models, Traffic Objects, and Trials. A 2 x 2 x 6 (24) mixed design ANOVA was performed on multi-levels. Pillar Models are within two levels (New and Old), Traffic Objects are within two (Bicycle and Pedestrian) and Trials are within six levels (T1 to T6).

Table 6.22: Three-way ANOVA-II results on Coordinates-X

Source	Sum of Squares	df	Mean Square	F	Sig.
Corrected Model	30523655.492a	23	1327115.456	13.536	.000
Intercept	292248554.070	1	292248554.070	2980.765	.000
Pillar_Types	29251369.584	1	29251369.584	298.347	.000
Traffic_Objects	96671.709	1	96671.709	.986	.321
Trials	339650.018	5	67930.004	.693	.629
Pillar_Types * Traffic_Objects	13495.876	1	13495.876	.138	.711
Pillar_Types * Trials	297302.734	5	59460.547	.606	.695
Traffic_Objects * Trials	175259.879	5	35051.976	.358	.878
Pillar_Types * Traffic_Objects * Trials	349905.692	5	69981.138	.714	.613

continued on next page

Table 6.22: *continued*

Source	Sum of Squares	df	Mean Square	F	Sig.
Error	110594533.437	1128	98044.799		
Total	433366743.000	1152			
Corrected Total	141118188.930	1151			

a R Squared = .216 (Adjusted R Squared = .200)

The ANOVA-II analysis revealed that there is a significant main effect of Pillar Types ($F = 298.347$, $p < .000$) on Coordinates-X. Traffic Objects ($F = .986$, $p = .321$) and Trials ($F = .693$, $p = .629$) has no significant effect on Coordinates-X, suggesting that only Pillar Types effect the pixel correspondence of eye movements on X axis. No significant interaction was found between independent variables.

Analysis of variance - III (ANOVA-III)

ANOVA-III study sought to determine whether Coordinates-Y differed across the factors of: Pillar Models, Traffic Objects, and Trials. A 2 x 2 x 6 (24) mixed design ANOVA was performed on multi-levels. Pillar Models are within two levels (New and Old), Traffic Objects are within two (Bicycle and Pedestrian) and Trials are within six levels (T1 to T6).

Table 6.23: Three-way ANOVA-II results on Coordinates-Y

Source	Sum of Squares	df	Mean Square	F	Sig.
Corrected Model	359169.770a	23	15616.077	2.334	.000
Intercept	417712177.709	1	417712177.709	62436.079	.000

continued on next page

Table 6.23: *continued*

Source	Sum of Squares	df	Mean Square	F	Sig.
Pillar_Types	83.959	1	83.959	.013	.911
Traffic_Objects	134269.938	1	134269.938	20.070	.000
Trials	31671.671	5	6334.334	.947	.450
Pillar_Types * Traffic_Objects	130454.063	1	130454.063	19.499	.000
Pillar_Types * Trials	22117.525	5	4423.505	.661	.653
Traffic_Objects * Trials	20999.671	5	4199.934	.628	.679
Pillar_Types * Traffic_Objects * Trials	19572.942	5	3914.588	.585	.711
Error	7546587.521	1128	6690.237		
Total	425617935.000	1152			
Corrected Total	7905757.291	1151			

a R Squared = .45 (Adjusted R Squared = .26)

The ANOVA-III analysis revealed that there is a significant main effect of Traffic Objects ($F = 20.070$, $p < .000$) on Coordinates-Y. Pillar Types ($F = .013$, $p = .911$) and Trials ($F = .947$, $p = .450$) found to generate no significant effect on Coordinates-Y. A two-way interaction effect between Pillar Types * Traffic Objects was found on Coordinates-Y outcomes.

Analysis of variance - IV (ANOVA-IV)

ANOVA-IV study sought to determine whether log-transformed Fixation Duration differed across the factors of: Pillar Models, Traffic Objects, and Trials. A 2 x 2 x 6 (24) mixed design ANOVA was performed on multi-levels. Pillar Models are within two levels (New and Old), Traffic Objects are within two (Bicycle and Pedestrian) and Trials are within six levels (T1 to T6).

Table 6.24: Three-way ANOVA-IV results on Log-Transformed Fixation Duration

Source	Sum of Squares	df	Mean Square	F	Sig.
Corrected Model	1.710a	23	.074	2.386	.000
Intercept	7394.396	1	7394.396	237288.457	.000
Pillar_Types	.461	1	.461	14.805	.000
Traffic_Objects	.310	1	.310	9.933	.002
Trials	.244	5	.049	1.567	.166
Pillar_Types * Traffic_Objects	.222	1	.222	7.130	.008
Pillar_Types * Trials	.157	5	.031	1.005	.413
Traffic_Objects * Trials	.186	5	.037	1.192	.311
Pillar_Types * Traffic_Objects * Trials	.131	5	.026	.838	.522
Error	35.151	1128	.031		
Total	7431.257	1152			
Corrected Total	36.861	1151			

a R Squared = .046 (Adjusted R Squared = .027)

The ANOVA-IV analysis revealed that there is a significant main effect of Pillar Types ($F = 14.805$, $p < .000$) and Traffic Objects ($F = 9.933$, $p = .002$) on log-transformed Fixation Duration. Trials ($F = 1.567$, $p = .166$) has no significant effect on log-transformed Fixation Duration, suggesting that Pillar Types and Traffic Objects effect the eye-fixation intensity during the simulation. A two-way interaction effect between Pillar Types * Traffic Objects was found on log-transformed fixation outcomes.

Analysis of variance - V (ANOVA-V)

ANOVA-V study sought to determine whether log-transformed Coordinates-X data differed across the factors of: Pillar Models, Traffic Objects, and Trials. A 2 x 2 x 6 (24) mixed design ANOVA was performed on multi-levels. Pillar Models are within two levels (New and Old), Traffic Objects are within two (Bicycle and Pedestrian) and Trials are within six levels (T1 to T6).

Table 6.25: Three-way ANOVA-V results on Log-Transformed Coordinates-X

Source	Sum of Squares	df	Mean Square	F	Sig.
Corrected Model	27.178a	23	1.182	13.147	.000
Intercept	7717.701	1	7717.701	85867.011	.000
Pillar_Types	26.041	1	26.041	289.734	.000
Traffic_Objects	.170	1	.170	1.889	.170
Trials	.296	5	.059	.660	.654
Pillar_Types * Traffic_Objects	.034	1	.034	.376	.540
Pillar_Types * Trials	.142	5	.028	.316	.904
Traffic_Objects * Trials	.074	5	.015	.164	.976
Pillar_Types * Traffic_Objects * Trials	.421	5	.084	.937	.456
Error	101.384	1128	.090		
Total	7846.264	1152			
Corrected Total	128.562	1151			

continued on next page

Table 6.25: *continued*

Source	Sum of Squares	df	Mean Square	F	Sig.
a R Squared = .211 (Adjusted R Squared = .195)					

The ANOVA-V analysis revealed that there is a significant main effect of Pillar Types (F = 289.734, p <.000) on log-transformed Coordinates-X. Traffic Objects (F = 1.889, p = .170) and Trials (F = .660, p = .654) have no significant effect on log-transformed Coordinates-X, suggesting that only Pillar Types effect pixel correspondence of eye movements on X axis. A two-way interaction effect between Pillar Types * Traffic Objects was found on log-transformed Coordinates-X outcomes.

Analysis of variance - VI (ANOVA-VI)

ANOVA-VI study sought to determine whether log-transformed Coordinates-Y data differed across the factors of: Pillar Models, Traffic Objects, and Trials. A 2 x 2 x 6 (24) mixed design ANOVA was performed on multi-levels. Pillar Models are within two levels (New and Old), Traffic Objects are within two (Bicycle and Pedestrian) and Trials are within six levels (T1 to T6).

Table 6.26: Three-way ANOVA-VI results on Log-Transformed Coordinates-Y

Source	Sum of Squares	df	Mean Square	F	Sig.
Corrected Model	.210a	23	.009	2.155	.001
Intercept	8872.016	1	8872.016	2098020.359	.000
Pillar_Types	.002	1	.002	.365	.546
Traffic_Objects	.081	1	.081	19.198	.000

continued on next page

Table 6.26: *continued*

Source	Sum of Squares	df	Mean Square	F	Sig.
Trials	.026	5	.005	1.246	.285
Pillar_Types * Traffic_Objects	.065	1	.065	15.324	.000
Pillar_Types * Trials	.012	5	.002	.550	.738
Traffic_Objects * Trials	.016	5	.003	.778	.565
Pillar_Types * Traffic_Objects * Trials	.008	5	.002	.361	.875
Error	4.770	1128	.004		
Total	8876.996	1152			
Corrected Total	4.980	1151			

a R Squared = .042 (Adjusted R Squared = .023)

The ANOVA-VI analysis revealed that there is a significant main effect of Traffic Objects (F = 19.198, p <.546) on log-transformed Coordinates-Y. Pillar Types (F = .365, p = .546) and Trials (F = 1.246, p = .285) have no significant effect on log-transformed Coordinates-Y, suggesting that only Traffic Objects effect pixel correspondence of eye movements on Y axis. A two-way interaction effect between Pillar Types * Traffic Objects was found on log-transformed Coordinates-Y outcomes.

Multivariable analysis of variance - I (MANOVA-I)

MANOVA-I analysis was performed to identify whether each independent variable has significant effect on three dependent variables accordingly; Fixation Duration, Coordinates-X and Coordinates-Y. A 2 x 2 x 6 (24) mixed design MANOVA analysis was conducted. Pillar Type is the within subjects variable with two levels (Old and New), Traffic Objects within two levels (Bicycle and Pedestrian) and Trials are with six levels (T1 to T6).

Table 6.27: Multivariable Analysis of Variance on Fixation Duration, Coordinates X and Coordinates Y

Effect	Test	Value	F	Sig.
Intercept	Pillai's Trace	.986	27021.910b	.000
	Wilks' Lambda	.014	27021.910b	.000
	Hotelling's Trace	71.994	27021.910b	.000
	Roy's Largest Root	71.994	27021.910b	.000
Pillar_Types	Pillai's Trace	.226	109.565b	.000
	Wilks' Lambda	.774	109.565b	.000
	Hotelling's Trace	.292	109.565b	.000
	Roy's Largest Root	.292	109.565b	.000
Traffic_Objects	Pillai's Trace	.023	8.651b	.000
	Wilks' Lambda	.977	8.651b	.000
	Hotelling's Trace	.023	8.651b	.000
	Roy's Largest Root	.023	8.651b	.000
Trials	Pillai's Trace	.019	1.462	.110
	Wilks' Lambda	.981	1.462	.110
	Hotelling's Trace	.019	1.462	.110
	Roy's Largest Root	.012	2.793c	.016
Pillar_Types * Traffic_Objects	Pillai's Trace	.020	7.756b	.000
	Wilks' Lambda	.980	7.756b	.000
	Hotelling's Trace	.021	7.756b	.000
	Roy's Largest Root	.021	7.756b	.000
Pillar_Types * Trials	Pillai's Trace	.010	.765	.718
	Wilks' Lambda	.990	.765	.718
	Hotelling's Trace	.010	.764	.719

continued on next page

Table 6.27: *continued*

Effect	Test	Value	F	Sig.
	Roy's Largest Root	.006	1.325c	.251
Traffic_Objects * Trials	Pillai's Trace	.008	.639	.845
	Wilks' Lambda	.992	.638	.845
	Hotelling's Trace	.009	.638	.845
	Roy's Largest Root	.006	1.427c	.212
Pillar_Types * Traffic_Objects * Trials	Pillai's Trace	.014	1.028	.422
	Wilks' Lambda	.986	1.027	.423
	Hotelling's Trace	.014	1.026	.424
	Roy's Largest Root	.008	1.799c	.110

MANOVA-I results showed that Pillar Types (F = 109.565, p <.000) and Traffic Objects (F = 8.651, p <.000) do have significant effect on Fixation Duration, Coordinates-X and Coordinates-Y. Trials (F = 1.462, p = .110) has no effect on collected data, which suggests that Pillar Types and Traffic Objects effect the pixel correspondence of eye movements on Fixation Duration, Coordinates-X and Coordinates-Y during the simulation. A two-way interaction was found between Pillar Types * Traffic Objects (F = 7.756, p <.000).

Multivariable analysis of variance - II (MANOVA-II)

MANOVA-II analysis was performed to identify whether each independent variable has significant effect on three dependent variables accordingly; logarithmic transformed Fixation Duration, Coordinates-X and Coordinates-Y. A 2 x 2 x 6 (24) mixed design MANOVA analysis was conducted. Pillar Type is the within subjects variable with two levels (Old and New), Traffic Objects within two levels (Bicycle and Pedestrian) and Trials are with six levels (T1 to T6).

Table 6.28: Multivariable Analysis of Variance on logarithmic transformed Fixation Duration, Coordinates-X and Coordinates-Y

Effect	Test	Value	F	Sig.
Intercept	Pillai's Trace	.996	104292.423b	.000
	Wilks' Lambda	.004	104292.423b	.000
	Hotelling's Trace	277.866	104292.423b	.000
	Roy's Largest Root	277.866	104292.423b	.000
Pillar_Types	Pillai's Trace	.223	107.718b	.000
	Wilks' Lambda	.777	107.718b	.000
	Hotelling's Trace	.287	107.718b	.000
	Roy's Largest Root	.287	107.718b	.000
Traffic_Objects	Pillai's Trace	.030	11.668b	.000
	Wilks' Lambda	.970	11.668b	.000
	Hotelling's Trace	.031	11.668b	.000
	Roy's Largest Root	.031	11.668b	.000
Trials	Pillai's Trace	.014	1.085	.364
	Wilks' Lambda	.986	1.085	.365
	Hotelling's Trace	.014	1.084	.365
	Roy's Largest Root	.009	1.987c	.078
Pillar_Types * Traffic_Objects	Pillai's Trace	.025	9.797b	.000
	Wilks' Lambda	.975	9.797b	.000
	Hotelling's Trace	.026	9.797b	.000
	Roy's Largest Root	.026	9.797b	.000
Pillar_Types * Trials	Pillai's Trace	.011	.845	.627
	Wilks' Lambda	.989	.844	.628

continued on next page

Table 6.28: *continued*

Effect	Test	Value	F	Sig.
	Hotelling's Trace	.011	.844	.629
	Roy's Largest Root	.006	1.255c	.281
Traffic_Objects * Trials	Pillai's Trace	.010	.759	.725
	Wilks' Lambda	.990	.759	.725
	Hotelling's Trace	.010	.759	.725
	Roy's Largest Root	.008	1.722c	.127
Pillar_Types * Traffic_Objects * Trials	Pillai's Trace	.010	.789	.691
	Wilks' Lambda	.990	.788	.692
	Hotelling's Trace	.011	.788	.693
	Roy's Largest Root	.006	1.318c	.254

MANOVA-II results showed that Pillar Types (F = 107.781, p <.000) and Traffic Objects (F = 11.668, p <.000) do have significant effect on logarithmic transformed Fixation Duration, Coordinates-X and Coordinates-Y. Trials (F = 1.085, p = .364) has no effect on collected data, suggesting that Pillar Types and Traffic Objects effect the pixel correspondence of eye movements on logarithmic transformed Fixation Duration, Coordinates-X and Coordinates-Y during the simulation. A two-way interaction was found between Pillar Types * Traffic Objects (F = 9.797, p <.000).

Multivariable analysis of variance - III (MANOVA-III)

MANOVA-III analysis was performed to identify whether each independent variable has significant effect on three dependent variables accordingly; logarithmic transformed Fixation Duration, logarithmic transformed Coordinates-X and Coordinates-Y. A 2 x 2 x 6 (24) mixed design MANOVA analysis was conducted. Pillar Type is the within subjects variable with two levels (Old and New), Traffic Objects within two levels (Bicycle and Pedestrian) and Trials are with six levels (T1 to T6).

Table 6.29: Multivariable Analysis of Variance on logarithmic transformed Fixation Duration, logarithmic transformed Coordinates-X and Coordinates-Y

Effect	Test	Value	F	Sig.
Intercept	Pillai's Trace	.997	146768.323b	.000
	Wilks' Lambda	.003	146768.323b	.000
	Hotelling's Trace	391.035	146768.323b	.000
	Roy's Largest Root	391.035	146768.323b	.000
Pillar_Types	Pillai's Trace	.215	103.020b	.000
	Wilks' Lambda	.785	103.020b	.000
	Hotelling's Trace	.274	103.020b	.000
	Roy's Largest Root	.274	103.020b	.000
Traffic_Objects	Pillai's Trace	.031	11.956b	.000
	Wilks' Lambda	.969	11.956b	.000
	Hotelling's Trace	.032	11.956b	.000
	Roy's Largest Root	.032	11.956b	.000
Trials	Pillai's Trace	.014	1.038	.411
	Wilks' Lambda	.986	1.038	.412
	Hotelling's Trace	.014	1.038	.412
	Roy's Largest Root	.009	1.977c	.079
Pillar_Types * Traffic_Objects	Pillai's Trace	.026	9.865b	.000
	Wilks' Lambda	.974	9.865b	.000
	Hotelling's Trace	.026	9.865b	.000
	Roy's Largest Root	.026	9.865b	.000
Pillar_Types * Trials	Pillai's Trace	.009	.712	.775

continued on next page

Table 6.29: *continued*

Effect	Test	Value	F	Sig.
	Wilks' Lambda	.991	.711	.776
	Hotelling's Trace	.009	.710	.776
	Roy's Largest Root	.005	1.100c	.359
Traffic_Objects * Trials	Pillai's Trace	.009	.684	.803
	Wilks' Lambda	.991	.684	.803
	Hotelling's Trace	.009	.684	.803
	Roy's Largest Root	.007	1.657c	.142
Pillar_Types * Traffic_Objects * Trials	Pillai's Trace	.011	.833	.642
	Wilks' Lambda	.989	.832	.643
	Hotelling's Trace	.011	.831	.644
	Roy's Largest Root	.006	1.273c	.273

MANOVA-III results showed that Pillar Types ($F = 103.020$, $p < .000$) and Traffic Objects ($F = 11.956$, $p < .000$) do have significant effect on logarithmic transformed Fixation Duration, logarithmic transformed Coordinates-X and Coordinates-Y. Trials ($F = 1.038$, $p = .412$) has no effect on collected data, suggesting that Pillar Types and Traffic Objects effect the pixel correspondence of eye movements on logarithmic transformed Fixation Duration, logarithmic transformed Coordinates-X and Coordinates-Y during the simulation. A two-way interaction was found between Pillar Types * Traffic Objects ($F = 9.865$, $p < .000$).

Multivariable analysis of variance - IV (MANOVA-IV)

MANOVA-IV analysis was performed to identify whether each independent variable has significant effect on three dependent variables accordingly; logarithmic transformed Fixation Duration, Coordinates-X and logarithmic transformed Coordinates-

Y. A 2 x 2 x 6 (24) mixed design MANOVA analysis was conducted. Pillar Type is the within subjects variable with two levels (Old and New), Traffic Objects within two levels (Bicycle and Pedestrian) and Trials are with six levels (T1 to T6).

Table 6.30: Multivariable Analysis of Variance on logarithmic transformed Fixation Duration, Coordinates-X and logarithmic transformed Coordinates-Y

Effect	Test	Value	F	Sig.
Intercept	Pillai's Trace	1.000	826851.860b	.000
	Wilks' Lambda	.000	826851.860b	.000
	Hotelling's Trace	2202.980	826851.860b	.000
	Roy's Largest Root	2202.980	826851.860b	.000
Pillar_Types	Pillai's Trace	.219	105.511b	.000
	Wilks' Lambda	.781	105.511b	.000
	Hotelling's Trace	.281	105.511b	.000
	Roy's Largest Root	.281	105.511b	.000
Traffic_Objects	Pillai's Trace	.029	11.094b	.000
	Wilks' Lambda	.971	11.094b	.000
	Hotelling's Trace	.030	11.094b	.000
	Roy's Largest Root	.030	11.094b	.000
Trials	Pillai's Trace	.016	1.195	.267
	Wilks' Lambda	.984	1.195	.267
	Hotelling's Trace	.016	1.194	.268
	Roy's Largest Root	.009	2.044c	.070
Pillar_Types * Traffic_Objects	Pillai's Trace	.021	8.101b	.000
	Wilks' Lambda	.979	8.101b	.000
	Hotelling's Trace	.022	8.101b	.000

continued on next page

Table 6.30: *continued*

Effect	Test	Value	F	Sig.
	Roy's Largest Root	.022	8.101b	.000
Pillar_Types * Trials	Pillai's Trace	.010	.785	.696
	Wilks' Lambda	.990	.784	.697
	Hotelling's Trace	.010	.783	.698
	Roy's Largest Root	.005	1.079c	.370
Traffic_Objects * Trials	Pillai's Trace	.011	.816	.660
	Wilks' Lambda	.989	.816	.661
	Hotelling's Trace	.011	.816	.661
	Roy's Largest Root	.007	1.619c	.152
Pillar_Types * Traffic_Objects * Trials	Pillai's Trace	.009	.693	.794
	Wilks' Lambda	.991	.692	.795
	Hotelling's Trace	.009	.692	.795
	Roy's Largest Root	.005	1.070c	.375

MANOVA-IV results showed that Pillar Types ($F = 105.511$, $p < .000$) and Traffic Objects ($F = 11.094$, $p < .000$) do have significant effect on logarithmic transformed Fixation Duration, Coordinates-X and logarithmic transformed Coordinates-Y. Trials ($F = 1.195$, $p = .267$) has no effect on collected data, suggesting that Pillar Types and Traffic Objects effect the pixel correspondence of eye movements on logarithmic transformed Fixation Duration, Coordinates-X and logarithmic transformed Coordinates-Y during the simulation. A two-way interaction was found between Pillar Types * Traffic Objects ($F = 8.101$, $p < .000$).

Multivariable analysis of variance - V (MANOVA-V)

MANOVA-V analysis was performed to identify whether each independent variable has significant effect on three dependent variables accordingly; Fixation Duration, logarithmic transformed Coordinates-X and logarithmic transformed Coordinates-Y. A 2 x 2 x 6 (24) mixed design MANOVA analysis was conducted. Pillar Type is the within subjects variable with two levels (Old and New), Traffic Objects within two levels (Bicycle and Pedestrian) and Trials are with six levels (T1 to T6).

Table 6.31: Multivariable Analysis of Variance on Fixation Duration, logarithmic transformed Coordinates-X and logarithmic transformed Coordinates-Y

Effect	Test	Value	F	Sig.
Intercept	Pillai's Trace	1.000	813920.826b	.000
	Wilks' Lambda	.000	813920.826b	.000
	Hotelling's Trace	2168.528	813920.826b	.000
	Roy's Largest Root	2168.528	813920.826b	.000
Pillar_Types	Pillai's Trace	.213	101.460b	.000
	Wilks' Lambda	.787	101.460b	.000
	Hotelling's Trace	.270	101.460b	.000
	Roy's Largest Root	.270	101.460b	.000
Traffic_Objects	Pillai's Trace	.022	8.320b	.000
	Wilks' Lambda	.978	8.320b	.000
	Hotelling's Trace	.022	8.320b	.000
	Roy's Largest Root	.022	8.320b	.000
Trials	Pillai's Trace	.020	1.494	.098
	Wilks' Lambda	.980	1.494	.098
	Hotelling's Trace	.020	1.494	.098

continued on next page

Table 6.31: *continued*

Effect	Test	Value	F	Sig.
	Roy's Largest Root	.013	2.854c	.014
Pillar_Types * Traffic_Objects	Pillai's Trace	.016	6.104b	.000
	Wilks' Lambda	.984	6.104b	.000
	Hotelling's Trace	.016	6.104b	.000
	Roy's Largest Root	.016	6.104b	.000
Pillar_Types * Trials	Pillai's Trace	.008	.576	.896
	Wilks' Lambda	.992	.575	.896
	Hotelling's Trace	.008	.575	.896
	Roy's Largest Root	.005	1.099c	.359
Traffic_Objects * Trials	Pillai's Trace	.008	.601	.877
	Wilks' Lambda	.992	.600	.877
	Hotelling's Trace	.008	.600	.877
	Roy's Largest Root	.006	1.325c	.251
Pillar_Types * Traffic_Objects * Trials	Pillai's Trace	.013	.994	.458
	Wilks' Lambda	.987	.993	.459
	Hotelling's Trace	.013	.992	.460
	Roy's Largest Root	.008	1.737c	.123

MANOVA-V results showed that Pillar Types ($F = 101.460$, $p < .000$) and Traffic Objects ($F = 8.320$, $p < .000$) do have significant effect on Fixation Duration, logarithmic transformed Coordinates-X and logarithmic transformed Coordinates-Y. Trials ($F = 1.494$, $p = .098$) has no effect on collected data, suggesting that Pillar Types and Traffic Objects effect the pixel correspondence of eye movements on Fixation Duration, logarithmic transformed Coordinates-X and logarithmic transformed

Coordinates-Y during the simulation. A two-way interaction was found between Pillar Types * Traffic Objects (F = 6.104, p <.000).

Multivariable analysis of variance - VI (MANOVA-V)

MANOVA-VI analysis was performed to identify whether each independent variable has significant effect on three dependent variables accordingly; logarithmic transformed Fixation Duration, logarithmic transformed Coordinates-X and logarithmic transformed Coordinates-Y. A 2 x 2 x 6 (24) mixed design MANOVA analysis was conducted. Pillar Type is the within subjects variable with two levels (Old and New), Traffic Objects within two levels (Bicycle and Pedestrian) and Trials are with six levels (T1 to T6).

Table 6.32: Multivariable analysis of variance on logarithmic transformed Fixation Duration, logarithmic transformed Coordinates-X and logarithmic transformed Coordinates-Y

Effect	Test	Value	F	Sig.
Intercept	Pillai's Trace	1.000	888289.180b	.000
	Wilks' Lambda	.000	888289.180b	.000
	Hotelling's Trace	2366.667	888289.180b	.000
	Roy's Largest Root	2366.667	888289.180b	.000
Pillar_Types	Pillai's Trace	.212	100.966b	.000
	Wilks' Lambda	.788	100.966b	.000
	Hotelling's Trace	.269	100.966b	.000
	Roy's Largest Root	.269	100.966b	.000
Traffic_Objects	Pillai's Trace	.029	11.319b	.000
	Wilks' Lambda	.971	11.319b	.000
	Hotelling's Trace	.030	11.319b	.000

continued on next page

Table 6.32: *continued*

Effect	Test	Value	F	Sig.
	Roy's Largest Root	.030	11.319b	.000
Trials	Pillai's Trace	.015	1.144	.310
	Wilks' Lambda	.985	1.144	.310
	Hotelling's Trace	.015	1.143	.311
	Roy's Largest Root	.009	1.994c	.077
Pillar_Types * Traffic_Objects	Pillai's Trace	.021	8.148b	.000
	Wilks' Lambda	.979	8.148b	.000
	Hotelling's Trace	.022	8.148b	.000
	Roy's Largest Root	.022	8.148b	.000
Pillar_Types * Trials	Pillai's Trace	.009	.659	.827
	Wilks' Lambda	.991	.658	.827
	Hotelling's Trace	.009	.658	.828
	Roy's Largest Root	.005	1.103c	.357
Traffic_Objects * Trials	Pillai's Trace	.010	.724	.762
	Wilks' Lambda	.990	.724	.762
	Hotelling's Trace	.010	.724	.762
	Roy's Largest Root	.007	1.557c	.169
Pillar_Types * Traffic_Objects * Trials	Pillai's Trace	.010	.743	.742
	Wilks' Lambda	.990	.742	.743
	Hotelling's Trace	.010	.741	.744
	Roy's Largest Root	.005	1.112c	.352

MANOVA-VI results showed that Pillar Types ($F = 100.966$, $p < .000$) and Traffic Objects ($F = 11.319$, $p < .000$) do have significant effect on logarithmic transformed

Fixation Duration, logarithmic transformed Coordinates-X and logarithmic transformed Coordinates-Y. Trials (F = 1.144, p = .310) has no effect on collected data, suggesting that Pillar Types and Traffic Objects effect the pixel correspondence of eye movements on logarithmic transformed Fixation Duration, logarithmic transformed Coordinates-X and logarithmic transformed Coordinates-Y during the simulation. A two-way interaction was found between Pillar Types * Traffic Objects (F = 8.148, p <.000).

Summary of analysis of variance tests

Table 6.46 summarizes results of all analysis of variance tests conducted on eye-tracker data. Independent variables with stars on Table 6.46 refers to 'p' values smaller than zero (p <0.000), which indicates a significance at the alpha level of 0.05. One can see that significant factors have overlapping results throughout the study. The very last row on Table 6.46 summarizes percentage accumulations of variables that have a significant MANOVA effect.

Table 6.33: Summary of significance (p-values) of ANOVA and MANOVA analyses

Tests	Dependent Variables	Pillar Types	Traffic Objects	Trials
ANOVA-I	Fix.Dur.	.000*	.279	.021*
ANOVA-II	Coord.X	.000*	.321	.679
ANOVA-III	Coord.Y	.911	.000*	.450
ANOVA-IV	Fix.Dur.LOG	.000*	.002*	.166
ANOVA-V	Coord.XLOG	.000*	.170	.654
ANOVA-VI	Coord.YLOG	.546	.000*	.285
MANOVA-I	Fix.Dur. Coord.X	.000*	.000*	.110

continued on next page

Table 6.33: *continued*

Tests	Dependent Variables	Pillar Types	Traffic Objects	Trials
	Coord.Y			
	Fix.Dur.LOG			
MANOVA-II	Coord.X	.000*	.000*	.365
	Coord.Y			
	Fix.Dur.LOG			
MANOVA-III	Coord.XLOG	.000*	.000*	.411
	Coord.Y			
	Fix.Dur.LOG			
MANOVA-IV	Coord.X	.000*	.000*	.267
	Coord.YLOG			
	Fix.Dur.			
MANOVA-V	Coord.XLOG	.000*	.000*	.098
	Coord.YLOG			
	Fix.Dur.LOG			
MANOVA-VI	Coord.XLOG	.000*	.000*	.310
	Coord.YLOG			
Percentages		83%	75%	8%

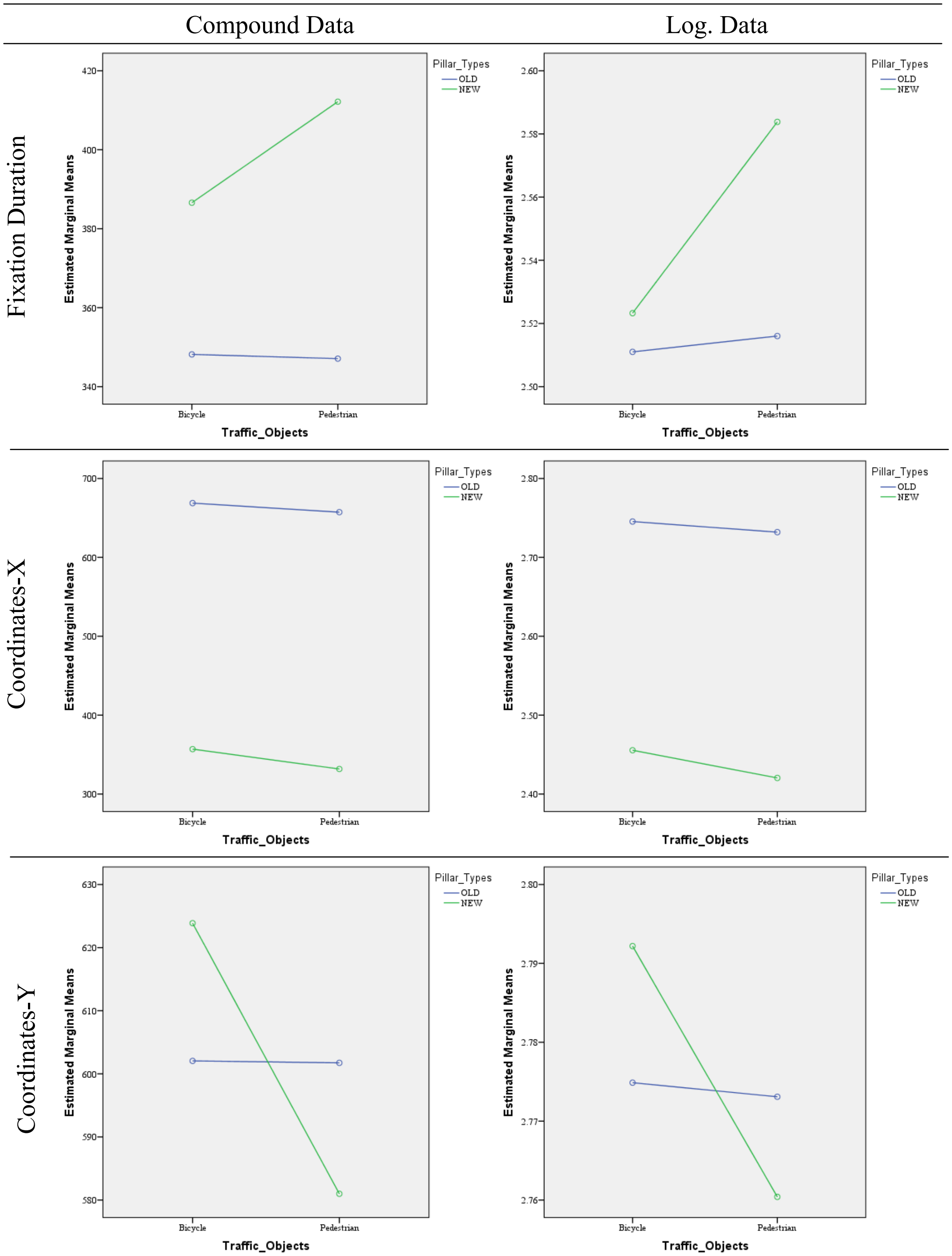

Figure 6.10. ANOVA 2-way Pillar Type * Traffic Objects interactions for eye-tracking data: Fixation Duration, Coordinates-X and Coordinates-Y

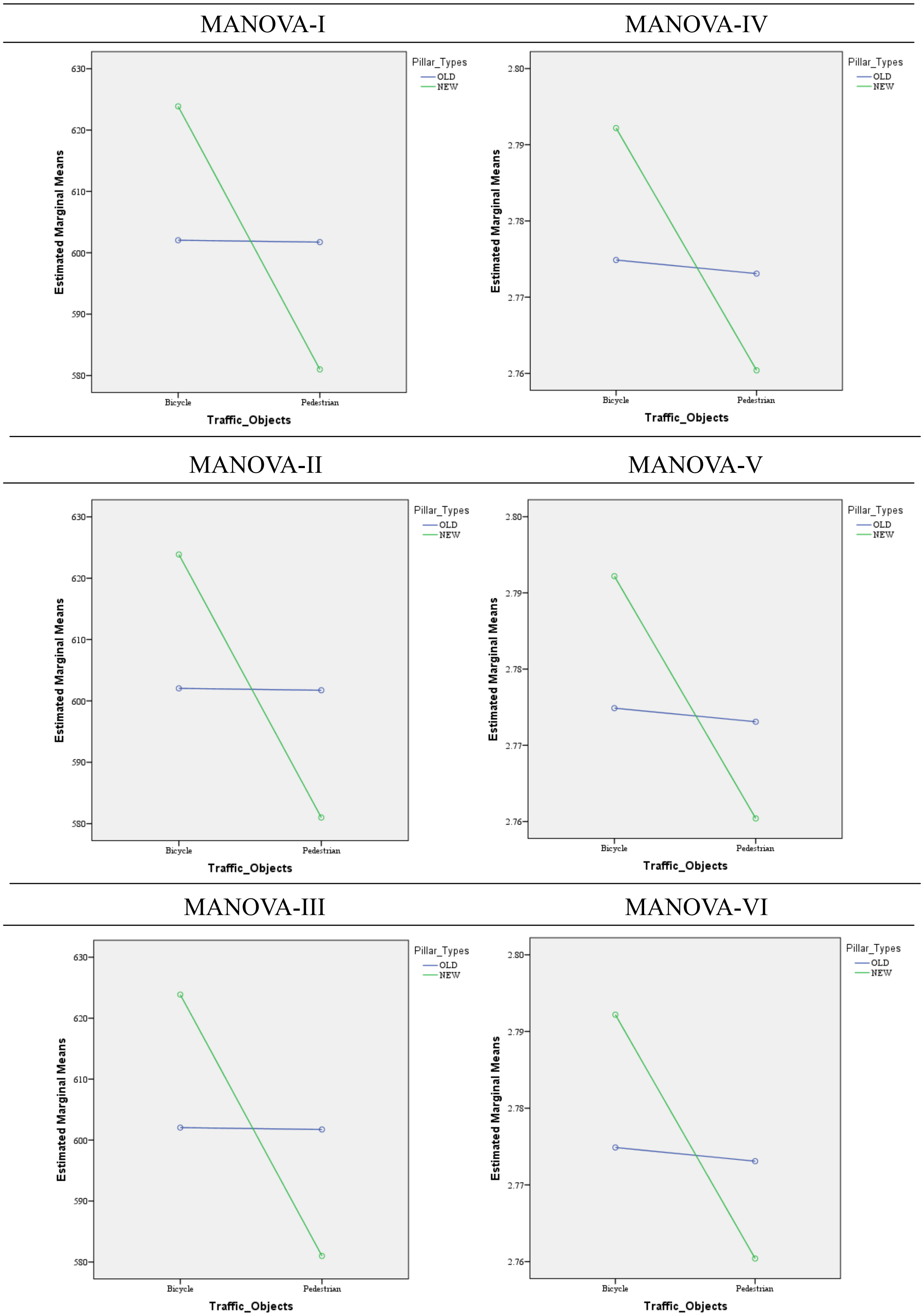

Figure 6.11. MANOVA 2-way interactions for six different MANOVA analysis with varying raw and log.transformed data

6.7.6 Six-way ANOVA/MANOVA - main effects

This section provides an extended overview of the two-way ANOVA/MANOVA analysis performed previously. Main goals and hypotheses covered in this study focus on the effect of Type of Pillars and Trials on eye-tracking data. However, a more detailed study were performed to explore the effects of Gender, Traffic Object, Use of Glasses and Driving Experience on top of Types of Pillars and Trials.

Even though logarithmic transformation performed previously smoothed out some of the outliers and scattered points in raw data, the normalization process caused a slight loss of fidelity. A blend of Analysis of Variance (ANOVA) and Multivariate Analysis of Variance (MANOVA) were conducted on six independent variables and three dependent variables. Each analysis covered raw and logarithmic transformed data in combinations to explore whether or not independent variables are significantly affect experimental results. A total of twelve analysis of variance studies (six ANOVAs and six MANOVAs) conducted.

Analysis of variance - I (ANOVA-I)

ANOVA-I study sought to determine whether Fixation Duration differed across the factors of: Gender, Pillar Models, Traffic Objects, Use of Glasses, Driving Experience, and Trials. A 2 x 2 x 2 x 2 x 3 x 6 (288) mixed design ANOVA was performed on multi-levels. Subject's Gender was within subjects variable with two levels (Male and Female); Pillar Models (New and Old), Traffic Objects (Bicycle and Pedestrian), Use of Glasses (Glasses and No Glasses). Driving Experience is within subjects variable with three levels (Low, Medium and High), and Trials are with six levels (T1 to T6).

Table 6.34: ANOVA-I results on Fixation Duration

Source	Sum of Squares	df	Mean Square	F	Sig.
Corrected Model	10056352.939	239	42076.791	1.148	.083
Intercept	58064029.321	1	58064029.321	1584.747	.000
Pillar_Types	309397.361	1	309397.361	8.444	.004
Traffic_Objects	20850.225	1	20850.225	.569	.451
Trials	160756.337	5	32151.267	.878	.496
Gender	94241.282	1	94241.282	2.572	.109
Driving_Experience	127315.854	2	63657.927	1.737	.177
Glasses	146175.051	1	146175.051	3.990	.046
Pillar_Types * Traffic_Objects	9059.459	1	9059.459	.247	.619
Pillar_Types * Trials	20740.518	5	4148.104	.113	.989
Pillar_Types * Gender	46498.968	1	46498.968	1.269	.260
Pillar_Types * Driving_Experience	244585.742	2	122292.871	3.338	.036
Pillar_Types * Glasses	42079.807	1	42079.807	1.148	.284
Traffic_Objects * Trials	80522.647	5	16104.529	.440	.821
Traffic_Objects * Gender	1263.130	1	1263.130	.034	.853
Traffic_Objects * Driving_Experience	63477.930	2	31738.965	.866	.421
Traffic_Objects * Glasses	18379.533	1	18379.533	.502	.479
Trials * Gender	372733.869	5	74546.774	2.035	.072

continued on next page

Table 6.34: *continued*

Source	Sum of Squares	df	Mean Square	F	Sig.
Trials * Driving_Experience	157504.022	10	15750.402	.430	.932
Trials * Glasses	57909.093	5	11581.819	.316	.903
Gender * Driving_Experience	286982.189	1	286982.189	7.833	.005
Gender * Glasses	42769.837	1	42769.837	1.167	.280
Driving_Experience * Glasses	356330.311	1	356330.311	9.725	.002

The ANOVA-I analysis revealed that there is a significant main effect of Pillar Types (F = 8.444, p = .004) and Glasses (F = 3.990, p = .046) on Fixation Duration. Traffic Objects (F = .569, p = .451), Trials (F = .8786, p = .496), Gender (F = 2.572, p = .109) and Driving Experience (F = 1.737, p = .177) have no significant effect on Fixation Duration, suggesting that Pillar Types and Use of Glasses effect the eye-fixation intensity during the simulation. There is a significant interaction found between Driving Experience and use of Glasses (F = 9.725, p = .002).

Analysis of variance - II (ANOVA-II)

ANOVA-II study sought to determine whether Coordinates-X differed according the factors of: Gender, Pillar Models, Traffic Objects, Use of Glasses, Driving Experience, and Trials. A 2 x 2 x 2 x 2 x 3 x 6 (288) mixed design ANOVA analysis was conducted. Subject's Gender is the within subjects variable with two levels (Male and Female); Pillar Models (New and Old), Traffic Objects (Bicycle and Pedestrian); Use of Glasses (Glasses and No Glasses). Driving Experience is the within subjects variable with three levels (Low, Medium and High), and Trials are with six levels (T1 to T6).

Table 6.35: ANOVA-II results on Coordinates-X

Source	Sum of Squares	df	Mean Square	F	Sig.
Corrected Model	50569062.071	239	211586.034	2.131	.000
Intercept	88280889.355	1	88280889.355	889.155	.000
Pillar_Types	7417062.758	1	7417062.758	74.704	.000
Traffic_Objects	142807.815	1	142807.815	1.438	.231
Trials	210305.328	5	42061.066	.424	.832
Gender	17719.861	1	17719.861	.178	.673
Driving_Experience	1464268.104	2	732134.052	7.374	.001
Glasses	62250.021	1	62250.021	.627	.429
Pillar_Types * Traffic_Objects	2494.076	1	2494.076	.025	.874
Pillar_Types * Trials	388763.356	5	77752.671	.783	.562
Pillar_Types * Gender	158301.898	1	158301.898	1.594	.207
Pillar_Types * Driving_Experience	1639265.841	2	819632.921	8.255	.000
Pillar_Types * Glasses	318859.184	1	318859.184	3.212	.073
Traffic_Objects * Trials	204766.646	5	40953.329	.412	.840
Traffic_Objects * Gender	91016.599	1	91016.599	.917	.339
Traffic_Objects * Driving_Experience	78156.151	2	39078.075	.394	.675
Traffic_Objects * Glasses	28617.026	1	28617.026	.288	.591

continued on next page

Table 6.35: *continued*

Source	Sum of Squares	df	Mean Square	F	Sig.
Trials * Gender	306643.331	5	61328.666	.618	.686
Trials * Driving_Experience	383172.376	10	38317.238	.386	.953
Trials * Glasses	161241.029	5	32248.206	.325	.898
Gender * Driving_Experience	96272.285	1	96272.285	.970	.325
Gender * Glasses	2869510.846	1	2869510.846	28.901	.000
Driving_Experience * Glasses	288190.364	1	288190.364	2.903	.089

The ANOVA-II analysis revealed that there is a significant main effect of Pillar Types ($F = 74.704$, $<.000$) and Driving Experience ($F = 7.373$, $p = .001$) on Coordinates-X. Traffic Objects ($F = 1.438$, $p = .231$), Trials ($F = .424$, $p = .832$), Gender ($F = .178$, $p = .673$) and Glasses ($F = 0.627$, $p = .429$) have no significant effect on Coordinates X, suggesting that Pillar Types and Driving Experience effect the pixel correspondence of eye movements on X axis. There is a significant interaction found between Gender and use of Glasses ($F = 28.901$, $p < .002$).

Analysis of variance - III (ANOVA-III)

ANOVA-III study sought to determine whether Coordinates-Y differed according the factors of: subject's Gender, Pillar Models, Traffic Objects, Use of Glasses, Driving Experience, and Trials. A 2 x 2 x 2 x 2 x 3 x 6 (288) mixed design ANOVA analysis was conducted. Subject's Gender is the within subjects variable with two levels (Male and Female); Pillar Models (New and Old), Traffic Objects (Bicycle and Pedestrian); Use of Glasses (Glasses and No Glasses). Driving Experience is the within subjects variable with three levels (Low, Medium and High), and Trials are with six levels (T1 to T6).

Table 6.36: ANOVA-III results on Coordinates-Y

Source	Sum of Squares	df	Mean Square	F	Sig.
Corrected Model	2072401.48a	239.00	8671.14	1.36	.001
Intercept	138531026.81	1.00	138531026.81	21658.25	.000
Pillar_Types	2029.44	1.00	2029.44	.32	.573
Traffic_Objects	25214.87	1.00	25214.87	3.94	.047
Trials	11272.72	5.00	2254.54	.35	.881
Gender	13963.12	1.00	13963.12	2.18	.140
Driving_Experience	182720.56	2.00	91360.28	14.28	.000
Glasses	108450.35	1.00	108450.35	16.96	.000
Pillar_Types * Traffic_Objects	23394.97	1.00	23394.97	3.66	.056
Pillar_Types * Trials	18746.70	5.00	3749.34	.59	.711
Pillar_Types * Gender	7659.17	1.00	7659.17	1.20	.274
Pillar_Types * Driving_Experience	27611.87	2.00	13805.94	2.16	.116
Pillar_Types * Glasses	24659.59	1.00	24659.59	3.86	.050
Traffic_Objects * Trials	38935.67	5.00	7787.13	1.22	.299
Traffic_Objects * Gender	55.76	1.00	55.76	.01	.926
Traffic_Objects * Driving_Experience	4503.16	2.00	2251.58	.35	.703

continued on next page

Table 6.36: *continued*

Source	Sum of Squares	df	Mean Square	F	Sig.
Traffic_Objects * Glasses	4897.08	1.00	4897.08	.77	.382
Trials * Gender	17517.05	5.00	3503.41	.55	.740
Trials * Driving_Experience	31618.21	10.00	3161.82	.49	.894
Trials * Glasses	30300.57	5.00	6060.11	.95	.449
Gender * Driving_Experience	81395.25	1.00	81395.25	12.73	.000
Gender * Glasses	95367.59	1.00	95367.59	14.91	.000
Driving_Experience * Glasses	23510.83	1.00	23510.83	3.68	.056

The ANOVA-III analysis revealed that there is a significant main effect of Traffic Objects ($F = 3.94$, $p = .047$), Driving Experience ($F = 14.28$, $p < .000$) and Glasses ($F = 16.96$, $p < .000$) on Coordinates-Y. Pillar Types ($F = .32$, $p = .573$), Trials ($F = .35$, $p = .881$) and Gender ($F = 2.18$, $p = .140$) have no significant effect on Coordinates Y, suggesting that Traffic Objects, Driving Experience and Glasses effect the pixel correspondence of eye movements on Y axis during the simulation. There is a significant interaction found between Gender and Driving Experience ($F = 12.73$, $p < .000$), and Gender and Glasses ($F = 14.91$, $p < .000$).

Analysis of variance - IV - (ANOVA-IV)

ANOVA-IV study sought to determine whether logarithmic transformed Fixation Duration differed according the factors of: subject's Gender, Pillar Models, Traffic Objects, Use of Glasses, Driving Experience, and Trials. A 2 x 2 x 2 x 2 x 3 x 6

(288) mixed design ANOVA analysis was conducted. Subject's Gender is the within subjects variable with two levels (Male and Female); Pillar Models (New and Old), Traffic Objects (Bicycle and Pedestrian), Use of Glasses (Glasses and No Glasses). Driving Experience is the within subjects variable with three levels (Low, Medium and High), and Trials are with six levels (T1 to T6).

Table 6.37: ANOVA-IV results on Fixation Duration, Logarithmic transformed

Source	Sum of Squares	df	Mean Square	F	Sig.
Corrected Model	8.62a	239.00	.04	1.17	.063
Intercept	2610.66	1.00	2610.66	84315.01	.000
Pillar_Types	.22	1.00	.22	7.00	.008
Traffic_Objects	.10	1.00	.10	3.32	.069
Trials	.12	5.00	.02	.76	.577
Gender	.00	1.00	.00	.02	.892
Driving_Experience	.15	2.00	.07	2.35	.096
Glasses	.31	1.00	.31	10.14	.002
Pillar_Types * Traffic_Objects	.04	1.00	.04	1.28	.259
Pillar_Types * Trials	.06	5.00	.01	.41	.841
Pillar_Types * Gender	.00	1.00	.00	.00	.981
Pillar_Types * Driving_Experience	.14	2.00	.07	2.30	.101
Pillar_Types * Glasses	.04	1.00	.04	1.43	.232
Traffic_Objects * Trials	.07	5.00	.01	.44	.820
Traffic_Objects * Gender	.00	1.00	.00	.10	.754

continued on next page

Table 6.37: *continued*

Source	Sum of Squares	df	Mean Square	F	Sig.
Traffic_Objects * Driving_Experience	.05	2.00	.02	.76	.467
Traffic_Objects * Glasses	.00	1.00	.00	.07	.799
Trials * Gender	.15	5.00	.03	.98	.431
Trials * Driving_Experience	.20	10.00	.02	.66	.761
Trials * Glasses	.06	5.00	.01	.37	.871
Gender * Driving_Experience	.21	1.00	.21	6.69	.010
Gender * Glasses	.02	1.00	.02	.52	.472
Driving_Experience * Glasses	.49	1.00	.49	15.95	.000

The ANOVA-IV analysis revealed that there is a significant main effect of Pillar Types (F = 7.00, p = .008) and Glasses (F = 10.14, p = .002) on logarithmic transformed Fixation Duration. Traffic Objects (F = 3.32, p = .069), Trials (F = .76, p = .577), Gender (F = .02, p = .892) and Driving Experience (F = 2.35, p = .096) have no significant effect on logarithmic transformed Fixation Duration data, suggesting that Pillar Types and Glasses effect the eye-fixation intensity during the simulation. There is a significant interaction found between Gender and Driving Experience (F = 6.69, p = .010), and Driving Experience and Glasses (F = 15.95, p <.000).

Analysis of variance - V (ANOVA-V)

ANOVA-V study sought to determine whether logarithmic transformed Coordinates-X data differed according the factors of: subject's Gender, Pillar Models, Traffic

Objects, Use of Glasses, Driving Experience, and Trials. A 2 x 2 x 2 x 2 x 3 x 6 (288) mixed design ANOVA analysis was conducted. Subject's Gender is the within subjects variable with two levels (Male and Female); Pillar Models (New and Old), Traffic Objects (Bicycle and Pedestrian); Use of Glasses (Glasses and No Glasses). Driving Experience is the within subjects variable with three levels (Low, Medium and High), and Trials are with six levels (T1 to T6).

Table 6.38: ANOVA-V results on logarithmic transformed Coordinates-X

Source	Sum of Squares	df	Mean Square	F	Sig.
Corrected Model	44.20a	239.00	.18	2.00	.000
Intercept	2667.46	1.00	2667.46	28837.59	.000
Pillar_Types	7.01	1.00	7.01	75.79	.000
Traffic_Objects	.21	1.00	.21	2.32	.128
Trials	.20	5.00	.04	.42	.833
Gender	.01	1.00	.01	.06	.806
Driving_Experience	.33	2.00	.16	1.78	.169
Glasses	.42	1.00	.42	4.53	.034
Pillar_Types * Traffic_Objects	.00	1.00	.00	.03	.869
Pillar_Types * Trials	.29	5.00	.06	.62	.683
Pillar_Types * Gender	.20	1.00	.20	2.14	.144
Pillar_Types * Driving_Experience	1.26	2.00	.63	6.79	.001
Pillar_Types * Glasses	.07	1.00	.07	.74	.391
Traffic_Objects * Trials	.20	5.00	.04	.43	.829
Traffic_Objects * Gender	.05	1.00	.05	.55	.457

continued on next page

Table 6.38: *continued*

Source	Sum of Squares	df	Mean Square	F	Sig.
Traffic_Objects * Driving_Experience	.08	2.00	.04	.46	.633
Traffic_Objects * Glasses	.04	1.00	.04	.46	.499
Trials * Gender	.20	5.00	.04	.43	.830
Trials * Driving_Experience	.33	10.00	.03	.36	.964
Trials * Glasses	.26	5.00	.05	.55	.736
Gender * Driving_Experience	.03	1.00	.03	.38	.539
Gender * Glasses	3.27	1.00	3.27	35.37	.000
Driving_Experience * Glasses	.43	1.00	.43	4.67	.031

The ANOVA-V analysis revealed that there is a significant main effect of Pillar Types ($F = 75.79$, $p < .000$) and Glasses ($F = 4.53$, $p = .034$) on logarithmic transformed Coordinates-X. Traffic Objects ($F = 2.32$, $p = .128$), Trials ($F = .42$, $p = .833$), Gender ($F = .06$, $p = .806$) and Driving Experience ($F = 1.78$, $p = .169$) have no significant effect on Coordinates-X, suggesting that Pillar Types and Glasses effect the pixel correspondence of eye movements on X axis during the simulation. There is a significant interaction found between Pillar Types and Driving Experience ($F = 6.79$, $p < .000$), Gender and Glasses ($F = 35.57$, $< .000$), and Driving Experience and Glasses ($F = 4.67$, $p = .031$).

Analysis of variance - VI (ANOVA-VI)

ANOVA-VI study sought to determine whether logarithmic transformed Coordinates-Y data differed according the factors of: subject's Gender, Pillar Models, Traffic Objects, Use of Glasses, Driving Experience, and Trials. A 2 x 2 x 2 x 2 x 3 x 6 (288) mixed design ANOVA analysis was conducted. Subject's Gender is the within subjects variable with two levels (Male and Female); Pillar Models (New and Old), Traffic Objects (Bicycle and Pedestrian), Use of Glasses (Glasses and No Glasses). Driving Experience is the withing subjects variable with three levels (Low, Medium and High), and Trials are with six levels (T1 to T6).

Table 6.39: ANOVA-VI results on logarithmic transformed Coordinates-Y

Source	Sum of Squares	df	Mean Square	F	Sig.
Corrected Model	1.281a	239	.005	1.322	.002
Intercept	3081.397	1	3081.397	759887.267	.000
Pillar_Types	.003	1	.003	.854	.356
Traffic_Objects	.015	1	.015	3.718	.054
Trials	.008	5	.002	.419	.836
Gender	.014	1	.014	3.545	.060
Driving_Experience	.110	2	.055	13.609	.000
Glasses	.072	1	.072	17.761	.000
Pillar_Types * Traffic_Objects	.013	1	.013	3.207	.074
Pillar_Types * Trials	.013	5	.003	.618	.686
Pillar_Types * Gender	.004	1	.004	1.050	.306
Pillar_Types * Driving_Experience	.019	2	.010	2.353	.096

continued on next page

Table 6.39: *continued*

Source	Sum of Squares	df	Mean Square	F	Sig.
Pillar_Types * Glasses	.012	1	.012	3.051	.081
Traffic_Objects * Trials	.026	5	.005	1.290	.266
Traffic_Objects * Gender	.001	1	.001	.183	.669
Traffic_Objects * Driving_Experience	.003	2	.002	.424	.654
Traffic_Objects * Glasses	.006	1	.006	1.469	.226
Trials * Gender	.008	5	.002	.418	.836
Trials * Driving_Experience	.023	10	.002	.567	.842
Trials * Glasses	.024	5	.005	1.204	.305
Gender * Driving_Experience	.047	1	.047	11.561	.001
Gender * Glasses	.041	1	.041	10.216	.001
Driving_Experience * Glasses	.016	1	.016	4.000	.046

The ANOVA-VI analysis revealed that there is a significant main effect of Driving Experience ($F = 13.609$, $p < .000$) and Glasses ($F = 17.761$, $p < .000$) on logarithmic transformed Coordinates-Y. Pillar Types ($F = .854$, $p = .356$), Traffic Objects ($F = 3.718$, $p = .054$), Trials ($F = .419$, $p = .836$) and Gender ($F = 3.545$, $p = .060$) have no significant effect on Coordinates-Y, suggesting that Driving Experience and Glasses effect the pixel correspondence of eye movements on Y axis during the simulation.

There is a significant interaction found between Gender and Driving Experience (F = 11.561, p = .001), and Gender and Glasses (F = 10.216, p = .001).

Multivariable analysis of variance - I (MANOVA-I)

MANOVA-I analysis was performed to identify whether each independent variable has significant effect on three dependent variables accordingly; Fixation Duration, Coordinates-X and Coordinates-Y. A 2 x 2 x 2 x 2 x 3 x 6 (288) mixed design MANOVA analysis was conducted. Subject's Gender is the within subjects variable with two levels (Male and Female); Pillar Models (New and Old), Traffic Objects (Bicycle and Pedestrian), Use of Glasses (Glasses and No Glasses). Driving Experience is the within subjects variable with three levels (Low, Medium and High), and Trials are with six levels (T1 to T6).

Table 6.40: Multivariable Analysis of Variance on Fixation Duration, Coordinates-X and Coordinates-Y

Effect	Test	Value	F	Sig.
Intercept	Pillai's Trace	.968	9245.577b	.000
	Wilks' Lambda	.032	9245.577b	.000
	Hotelling's Trace	30.480	9245.577b	.000
	Roy's Largest Root	30.480	9245.577b	.000
Pillar_Types	Pillai's Trace	.083	27.308b	.000
	Wilks' Lambda	.917	27.308b	.000
	Hotelling's Trace	.090	27.308b	.000
	Roy's Largest Root	.090	27.308b	.000
Traffic_Objects	Pillai's Trace	.008	2.500b	.058
	Wilks' Lambda	.992	2.500b	.058
	Hotelling's Trace	.008	2.500b	.058

continued on next page

Table 6.40: *continued*

Effect	Test	Value	F	Sig.
	Roy's Largest Root	.008	2.500b	.058
Trials	Pillai's Trace	.010	.586	.888
	Wilks' Lambda	.990	.585	.888
	Hotelling's Trace	.010	.585	.889
	Roy's Largest Root	.006	1.118c	.349
Gender	Pillai's Trace	.006	1.681b	.169
	Wilks' Lambda	.994	1.681b	.169
	Hotelling's Trace	.006	1.681b	.169
	Roy's Largest Root	.006	1.681b	.169
Driving_Experience	Pillai's Trace	.060	9.383	.000
	Wilks' Lambda	.941	9.441b	.000
	Hotelling's Trace	.063	9.499	.000
	Roy's Largest Root	.053	16.065c	.000
Glasses	Pillai's Trace	.026	8.066b	.000
	Wilks' Lambda	.974	8.066b	.000
	Hotelling's Trace	.027	8.066b	.000
	Roy's Largest Root	.027	8.066b	.000
Pillar_Types * Traffic_Objects	Pillai's Trace	.004	1.361b	.253
	Wilks' Lambda	.996	1.361b	.253
	Hotelling's Trace	.004	1.361b	.253
	Roy's Largest Root	.004	1.361b	.253
Pillar_Types * Trials	Pillai's Trace	.010	.596	.880
	Wilks' Lambda	.990	.596	.880
	Hotelling's Trace	.010	.596	.880

continued on next page

Table 6.40: *continued*

Effect	Test	Value	F	Sig.
	Roy's Largest Root	.008	1.462c	.200
Pillar_Types * Gender	Pillai's Trace	.006	1.716b	.162
	Wilks' Lambda	.994	1.716b	.162
	Hotelling's Trace	.006	1.716b	.162
	Roy's Largest Root	.006	1.716b	.162
Pillar_Types * Driving_Experience	Pillai's Trace	.035	5.330	.000
	Wilks' Lambda	.966	5.357b	.000
	Hotelling's Trace	.036	5.384	.000
	Roy's Largest Root	.033	9.898c	.000
Pillar_Types * Glasses	Pillai's Trace	.008	2.438b	.063
	Wilks' Lambda	.992	2.438b	.063
	Hotelling's Trace	.008	2.438b	.063
	Roy's Largest Root	.008	2.438b	.063
Traffic_Objects * Trials	Pillai's Trace	.012	.758	.725
	Wilks' Lambda	.988	.758	.726
	Hotelling's Trace	.013	.758	.726
	Roy's Largest Root	.009	1.641c	.146
Traffic_Objects * Gender	Pillai's Trace	.001	.367b	.777
	Wilks' Lambda	.999	.367b	.777
	Hotelling's Trace	.001	.367b	.777

continued on next page

Table 6.40: *continued*

Effect	Test	Value	F	Sig.
	Roy's Largest Root	.001	.367b	.777
Traffic_Objects * Driving_Experience	Pillai's Trace	.003	.474	.828
	Wilks' Lambda	.997	.474b	.828
	Hotelling's Trace	.003	.473	.829
	Roy's Largest Root	.002	.640c	.589
Traffic_Objects * Glasses	Pillai's Trace	.002	.495b	.686
	Wilks' Lambda	.998	.495b	.686
	Hotelling's Trace	.002	.495b	.686
	Roy's Largest Root	.002	.495b	.686
Trials * Gender	Pillai's Trace	.018	1.097	.353
	Wilks' Lambda	.982	1.098	.352
	Hotelling's Trace	.018	1.098	.352
	Roy's Largest Root	.013	2.429c	.034
Trials * Driving_Experience	Pillai's Trace	.016	.482	.992
	Wilks' Lambda	.984	.481	.992
	Hotelling's Trace	.016	.481	.992
	Roy's Largest Root	.009	.815c	.614
Trials * Glasses	Pillai's Trace	.009	.523	.930
	Wilks' Lambda	.991	.522	.930
	Hotelling's Trace	.009	.521	.930
	Roy's Largest Root	.006	1.029c	.399

continued on next page

Table 6.40: *continued*

Effect	Test	Value	F	Sig.
Gender * Driving_Experience	Pillai's Trace	.023	7.243b	.000
	Wilks' Lambda	.977	7.243b	.000
	Hotelling's Trace	.024	7.243b	.000
	Roy's Largest Root	.024	7.243b	.000
Gender * Glasses	Pillai's Trace	.038	11.958b	.000
	Wilks' Lambda	.962	11.958b	.000
	Hotelling's Trace	.039	11.958b	.000
	Roy's Largest Root	.039	11.958b	.000
Driving_Experience * Glasses	Pillai's Trace	.015	4.610b	.003
	Wilks' Lambda	.985	4.610b	.003
	Hotelling's Trace	.015	4.610b	.003
	Roy's Largest Root	.002	.316c	.003

MANOVA-I results showed that Pillar Types ($F = 27.308$, $p < 0.000$), Driving Experience ($F = 9.441$, $p < 0.001$) and Glasses ($F = 8.066$, $p < 0.001$) do have significant effect on Fixation Duration, Coordinates X and Coordinates Y. Traffic Objects ($F = 2.500$, $p = .058$), Trails ($F = .585$, $p = .888$) and Gender ($F = 1.1681$, $p = .169$) have no effect on Coordinates-Y, suggesting that Pillar Types, Driving Experience and Glasses effect the pixel correspondence of eye movements on Fixation Duration, Coordinates-X and Coordinates-Y during the simulation.

Multivariable Analysis of Variance - II (MANOVA-II)

MANOVA-II analysis was performed to identify whether each independent variable has significant effect on three dependent variables accordingly; logarithmic transformed Fixation Duration, Coordinates-X and Coordinates-Y. A 2 x 2 x 2 x 2 x 3 x 6 (288) mixed design MANOVA analysis was conducted. Subject's Gender is the within subjects variable with two levels (Male and Female); Pillar Models (New and Old), Traffic Objects (Bicycle and Pedestrian), Use of Glasses (Glasses and No Glasses). Driving Experience is the within subjects variable with three levels (Low, Medium and High), and Trials are with six levels (T1 to T6).

Table 6.41: Multivariable Analysis of Variance on logarithmic transformed Fixation Duration, Coordinates-X and Coordinates-Y

Effect	Test	Value	F	Sig.
Intercept	Pillai's Trace	.992	36421.988	.000
	Wilks' Lambda	.008	36421.988	.000
	Hotelling's Trace	120.072	36421.988	.000
	Roy's Largest Root	120.072	36421.988	.000
Pillar_Types	Pillai's Trace	.081	26.822	.000
	Wilks' Lambda	.919	26.822	.000
	Hotelling's Trace	.088	26.822	.000
	Roy's Largest Root	.088	26.822	.000
Traffic_Objects	Pillai's Trace	.011	3.418	.017
	Wilks' Lambda	.989	3.418	.017
	Hotelling's Trace	.011	3.418	.017
	Roy's Largest Root	.011	3.418	.017
Trials	Pillai's Trace	.009	.543	.917
	Wilks' Lambda	.991	.543	.918
	Hotelling's Trace	.009	.542	.918
	Roy's Largest Root	.005	.871	.500
Gender	Pillai's Trace	.002	.747	.524

continued on next page

Table 6.41: *continued*

Effect	Test	Value	F	Sig.
	Wilks' Lambda	.998	.747	.524
	Hotelling's Trace	.002	.747	.524
	Roy's Largest Root	.002	.747	.524
Driving_Experience	Pillai's Trace	.061	9.630	.000
	Wilks' Lambda	.939	9.689	.000
	Hotelling's Trace	.064	9.749	.000
	Roy's Largest Root	.054	16.406	.000
Glasses	Pillai's Trace	.032	9.984	.000
	Wilks' Lambda	.968	9.984	.000
	Hotelling's Trace	.033	9.984	.000
	Roy's Largest Root	.033	9.984	.000
Pillar_Types * Traffic_Objects	Pillai's Trace	.006	1.766	.152
	Wilks' Lambda	.994	1.766	.152
	Hotelling's Trace	.006	1.766	.152
	Roy's Largest Root	.006	1.766	.152
Pillar_Types * Trials	Pillai's Trace	.011	.695	.792
	Wilks' Lambda	.989	.694	.793
	Hotelling's Trace	.011	.694	.793
	Roy's Largest Root	.009	1.554	.170
Pillar_Types * Gender	Pillai's Trace	.004	1.234	.296
	Wilks' Lambda	.996	1.234	.296
	Hotelling's Trace	.004	1.234	.296
	Roy's Largest Root	.004	1.234	.296

continued on next page

Table 6.41: *continued*

Effect	Test	Value	F	Sig.
Pillar_Types * Driving_Experience	Pillai's Trace	.033	5.023	.000
	Wilks' Lambda	.968	5.048	.000
	Hotelling's Trace	.033	5.073	.000
	Roy's Largest Root	.031	9.412	.000
Pillar_Types * Glasses	Pillai's Trace	.009	2.603	.051
	Wilks' Lambda	.991	2.603	.051
	Hotelling's Trace	.009	2.603	.051
	Roy's Largest Root	.009	2.603	.051
Traffic_Objects * Trials	Pillai's Trace	.012	.756	.728
	Wilks' Lambda	.988	.756	.728
	Hotelling's Trace	.012	.755	.728
	Roy's Largest Root	.009	1.626	.150
Traffic_Objects * Gender	Pillai's Trace	.001	.361	.781
	Wilks' Lambda	.999	.361	.781
	Hotelling's Trace	.001	.361	.781
	Roy's Largest Root	.001	.361	.781
Traffic_Objects * Driving_Experience	Pillai's Trace	.003	.447	.848
	Wilks' Lambda	.997	.446	.848
	Hotelling's Trace	.003	.446	.848
	Roy's Largest Root	.002	.524	.666
Traffic_Objects * Glasses	Pillai's Trace	.001	.331	.803
	Wilks' Lambda	.999	.331	.803

continued on next page

Table 6.41: *continued*

Effect	Test	Value	F	Sig.
	Hotelling's Trace	.001	.331	.803
	Roy's Largest Root	.001	.331	.803
Trials * Gender	Pillai's Trace	.012	.745	.740
	Wilks' Lambda	.988	.745	.740
	Hotelling's Trace	.012	.744	.741
	Roy's Largest Root	.008	1.494	.189
Trials * Driving_Experience	Pillai's Trace	.018	.562	.974
	Wilks' Lambda	.982	.561	.974
	Hotelling's Trace	.019	.561	.974
	Roy's Largest Root	.011	.964	.473
Trials * Glasses	Pillai's Trace	.009	.534	.923
	Wilks' Lambda	.991	.534	.923
	Hotelling's Trace	.009	.533	.924
	Roy's Largest Root	.006	1.011	.410
Gender * Driving_Experience	Pillai's Trace	.022	6.966	.000
	Wilks' Lambda	.978	6.966	.000
	Hotelling's Trace	.023	6.966	.000
	Roy's Largest Root	.023	6.966	.000
Gender * Glasses	Pillai's Trace	.038	11.872	.000
	Wilks' Lambda	.962	11.872	.000
	Hotelling's Trace	.039	11.872	.000
	Roy's Largest Root	.039	11.872	.000

continued on next page

Table 6.41: *continued*

Effect	Test	Value	F	Sig.
Driving_Experience * Glasses	Pillai's Trace	.021	6.477	.000
	Wilks' Lambda	.979	6.477	.000
	Hotelling's Trace	.021	6.477	.000
	Roy's Largest Root	.021	6.477	.000

MANOVA-II results showed that Pillar Types (F = 26.822, p <0.000), Traffic Objects (F = 3.418, p <0.017), Driving Experience (F = 9.689, p <0.000), and Glasses (F= 9.984, p <0.001) do have significant effect on logarithmic transformed Fixation Duration, Coordinates-X and Coordinates-Y. Trials (F = .543, p = .917) and Gender (F = .747, p = .524) have no effect, suggesting that Pillar Types, Traffic Objects, Driving Experience and Glasses effect the pixel correspondence of eye movements on logarithmic transformed Fixation Duration, Coordinates-X and Coordinates-Y during the simulation.

Multivariable analysis of variance - III (MANOVA-III)

MANOVA-III analysis was performed to identify whether each independent variable has significant effect on three dependent variables accordingly; logarithmic transformed Fixation Duration, logarithmic transformed Coordinates-X and Coordinates-Y. A 2 x 2 x 2 x 2 x 3 x 6 (288) mixed design MANOVA analysis was conducted. Subject's Gender is the within subjects variable with two levels (Male and Female); Pillar Models (New and Old), Traffic Objects (Bicycle and Pedestrian); Use of Glasses (Glasses and No Glasses). Driving Experience is the within subjects variable with three levels (Low, Medium and High), and Trials are with six levels (T1 to T6).

Table 6.42: Multivariable Analysis of Variance on logarithmic transformed Fixation Duration, logarithmic transformed Coordinates-X and Coordinates-Y

Effect	Test	Value	F	Sig.
Intercept	Pillai's Trace	.994	51153.191	.000
	Wilks' Lambda	.006	51153.191	.000
	Hotelling's Trace	168.637	51153.191	.000
	Roy's Largest Root	168.637	51153.191	.000
Pillar_Types	Pillai's Trace	.082	27.021	.000
	Wilks' Lambda	.918	27.021	.000
	Hotelling's Trace	.089	27.021	.000
	Roy's Largest Root	.089	27.021	.000
Traffic_Objects	Pillai's Trace	.012	3.734	.011
	Wilks' Lambda	.988	3.734	.011
	Hotelling's Trace	.012	3.734	.011
	Roy's Largest Root	.012	3.734	.011
Trials	Pillai's Trace	.008	.513	.935
	Wilks' Lambda	.992	.512	.936
	Hotelling's Trace	.008	.512	.936
	Roy's Largest Root	.005	.957	.443
Gender	Pillai's Trace	.003	.851	.466
	Wilks' Lambda	.997	.851	.466
	Hotelling's Trace	.003	.851	.466
	Roy's Largest Root	.003	.851	.466
Driving_Experience	Pillai's Trace	.046	7.107	.000
	Wilks' Lambda	.954	7.171	.000
	Hotelling's Trace	.048	7.235	.000

continued on next page

Table 6.42: *continued*

Effect	Test	Value	F	Sig.
	Roy's Largest Root	.046	13.933	.000
Glasses	Pillai's Trace	.039	12.180	.000
	Wilks' Lambda	.961	12.180	.000
	Hotelling's Trace	.040	12.180	.000
	Roy's Largest Root	.040	12.180	.000
Pillar_Types * Traffic_Objects	Pillai's Trace	.006	1.832	.140
	Wilks' Lambda	.994	1.832	.140
	Hotelling's Trace	.006	1.832	.140
	Roy's Largest Root	.006	1.832	.140
Pillar_Types * Trials	Pillai's Trace	.010	.618	.863
	Wilks' Lambda	.990	.617	.863
	Hotelling's Trace	.010	.617	.863
	Roy's Largest Root	.007	1.356	.239
Pillar_Types * Gender	Pillai's Trace	.005	1.410	.239
	Wilks' Lambda	.995	1.410	.239
	Hotelling's Trace	.005	1.410	.239
	Roy's Largest Root	.005	1.410	.239
Pillar_Types * Driving_Experience	Pillai's Trace	.028	4.340	.000
	Wilks' Lambda	.972	4.358	.000
	Hotelling's Trace	.029	4.375	.000
	Roy's Largest Root	.027	8.087	.000
Pillar_Types * Glasses	Pillai's Trace	.006	1.980	.115
	Wilks' Lambda	.994	1.980	.115

continued on next page

Table 6.42: *continued*

Effect	Test	Value	F	Sig.
	Hotelling's Trace	.007	1.980	.115
	Roy's Largest Root	.007	1.980	.115
Traffic_Objects * Trials	Pillai's Trace	.012	.748	.736
	Wilks' Lambda	.988	.748	.737
	Hotelling's Trace	.012	.748	.737
	Roy's Largest Root	.009	1.615	.153
Traffic_Objects * Gender	Pillai's Trace	.001	.229	.876
	Wilks' Lambda	.999	.229	.876
	Hotelling's Trace	.001	.229	.876
	Roy's Largest Root	.001	.229	.876
Traffic_Objects * Driving_Experience	Pillai's Trace	.003	.485	.820
	Wilks' Lambda	.997	.485	.820
	Hotelling's Trace	.003	.484	.821
	Roy's Largest Root	.002	.552	.647
Traffic_Objects * Glasses	Pillai's Trace	.001	.380	.767
	Wilks' Lambda	.999	.380	.767
	Hotelling's Trace	.001	.380	.767
	Roy's Largest Root	.001	.380	.767
Trials * Gender	Pillai's Trace	.011	.675	.811
	Wilks' Lambda	.989	.675	.811
	Hotelling's Trace	.011	.675	.812
	Roy's Largest Root	.008	1.531	.178
Trials * Driving_Experience	Pillai's Trace	.017	.527	.984
	Wilks' Lambda	.983	.527	.984

continued on next page

Table 6.42: *continued*

Effect	Test	Value	F	Sig.
	Hotelling's Trace	.017	.526	.984
	Roy's Largest Root	.010	.895	.538
Trials * Glasses	Pillai's Trace	.010	.611	.868
	Wilks' Lambda	.990	.610	.869
	Hotelling's Trace	.010	.610	.869
	Roy's Largest Root	.006	1.039	.393
Gender * Driving_Experience	Pillai's Trace	.022	6.923	.000
	Wilks' Lambda	.978	6.923	.000
	Hotelling's Trace	.023	6.923	.000
	Roy's Largest Root	.023	6.923	.000
Gender * Glasses	Pillai's Trace	.044	14.057	.000
	Wilks' Lambda	.956	14.057	.000
	Hotelling's Trace	.046	14.057	.000
	Roy's Largest Root	.046	14.057	.000
Driving_Experience * Glasses	Pillai's Trace	.022	6.919	.000
	Wilks' Lambda	.978	6.919	.000
	Hotelling's Trace	.023	6.919	.000
	Roy's Largest Root	.023	6.919	.000

MANOVA-III results showed that Pillar Types ($F = 27.021$, $p < 0.000$), Traffic Objects ($F = 3.734$, $p < 0.011$), Driving Experience ($F = 7.171$, $p < 0.000$), and Glasses ($F = 12.180$, $p < 0.001$) do have significant effect on logarithmic transformed Fixation Duration, logarithmic transformed Coordinates-X and Coordinates-Y. Trials ($F = .512$, $p = .936$) and Gender ($F = .851$, $p = .466$) have no effect, suggesting that Pillar Types, Traffic Objects, Driving Experience and Glasses effect the pixel correspondence of eye movements on logarithmic transformed Fixation Duration, logarithmic transformed Coordinates X and Coordinates Y during the simulation.

Multivariable analysis of variance - IV (MANOVA-IV)

MANOVA-IV analysis was performed to identify whether each independent variable has significant effect on three dependent variables accordingly; logarithmic transformed Fixation Duration, Coordinates-X and logarithmic transformed Coordinates-Y. A 2 x 2 x 2 x 2 x 3 x 6 (288) mixed design MANOVA analysis was conducted. Subject's Gender is the within subjects variable with two levels (Male and Female); Pillar Models (New and Old), Traffic Objects (Bicycle and Pedestrian), Use of Glasses (Glasses and No Glasses). Driving Experience is the within subjects variable with three levels (Low, Medium and High), and Trials are with six levels (T1 to T6).

Table 6.43: Multivariable Analysis of Variance on logarithmic transformed Fixation Duration, Coordinates-X and logarithmic transformed Coordinates-Y

Effect	Test	Value	F	Sig.
Intercept	Pillai's Trace	.999	295905.312	.000
	Wilks' Lambda	.001	295905.312	.000
	Hotelling's Trace	975.512	295905.312	.000
	Roy's Largest Root	975.512	295905.312	.000
Pillar_Types	Pillai's Trace	.080	26.325	.000
	Wilks' Lambda	.920	26.325	.000
	Hotelling's Trace	.087	26.325	.000
	Roy's Largest Root	.087	26.325	.000
Traffic_Objects	Pillai's Trace	.011	3.252	.021
	Wilks' Lambda	.989	3.252	.021

continued on next page

Table 6.43: *continued*

Effect	Test	Value	F	Sig.
	Hotelling's Trace	.011	3.252	.021
	Roy's Largest Root	.011	3.252	.021
Trials	Pillai's Trace	.009	.574	.897
	Wilks' Lambda	.991	.573	.897
	Hotelling's Trace	.009	.573	.898
	Roy's Largest Root	.005	.927	.462
Gender	Pillai's Trace	.004	1.199	.309
	Wilks' Lambda	.996	1.199	.309
	Hotelling's Trace	.004	1.199	.309
	Roy's Largest Root	.004	1.199	.309
Driving_Experience	Pillai's Trace	.058	9.110	.000
	Wilks' Lambda	.942	9.154	.000
	Hotelling's Trace	.061	9.198	.000
	Roy's Largest Root	.049	15.018	.000
Glasses	Pillai's Trace	.033	10.320	.000
	Wilks' Lambda	.967	10.320	.000
	Hotelling's Trace	.034	10.320	.000
	Roy's Largest Root	.034	10.320	.000
Pillar_Types * Traffic_Objects	Pillai's Trace	.005	1.581	.192
	Wilks' Lambda	.995	1.581	.192
	Hotelling's Trace	.005	1.581	.192
	Roy's Largest Root	.005	1.581	.192
Pillar_Types * Trials	Pillai's Trace	.011	.689	.798
	Wilks' Lambda	.989	.688	.799

continued on next page

Table 6.43: *continued*

Effect	Test	Value	F	Sig.
	Hotelling's Trace	.011	.688	.799
	Roy's Largest Root	.008	1.503	.186
Pillar_Types * Gender	Pillai's Trace	.004	1.149	.328
	Wilks' Lambda	.996	1.149	.328
	Hotelling's Trace	.004	1.149	.328
	Roy's Largest Root	.004	1.149	.328
Pillar_Types * Driving_Experience	Pillai's Trace	.033	5.040	.000
	Wilks' Lambda	.967	5.065	.000
	Hotelling's Trace	.034	5.090	.000
	Roy's Largest Root	.031	9.440	.000
Pillar_Types * Glasses	Pillai's Trace	.008	2.377	.069
	Wilks' Lambda	.992	2.377	.069
	Hotelling's Trace	.008	2.377	.069
	Roy's Largest Root	.008	2.377	.069
Traffic_Objects * Trials	Pillai's Trace	.012	.762	.721
	Wilks' Lambda	.988	.761	.722
	Hotelling's Trace	.013	.761	.722
	Roy's Largest Root	.009	1.590	.160
Traffic_Objects * Gender	Pillai's Trace	.002	.474	.701
	Wilks' Lambda	.998	.474	.701
	Hotelling's Trace	.002	.474	.701
	Roy's Largest Root	.002	.474	.701
Traffic_Objects * Driving_Experience	Pillai's Trace	.003	.467	.833

continued on next page

Table 6.43: *continued*

Effect	Test	Value	F	Sig.
	Wilks' Lambda	.997	.467	.833
	Hotelling's Trace	.003	.466	.834
	Roy's Largest Root	.002	.625	.599
Traffic_Objects * Glasses	Pillai's Trace	.002	.552	.647
	Wilks' Lambda	.998	.552	.647
	Hotelling's Trace	.002	.552	.647
	Roy's Largest Root	.002	.552	.647
Trials * Gender	Pillai's Trace	.011	.693	.794
	Wilks' Lambda	.989	.692	.794
	Hotelling's Trace	.011	.692	.795
	Roy's Largest Root	.007	1.298	.263
Trials * Driving_Experience	Pillai's Trace	.020	.600	.958
	Wilks' Lambda	.980	.600	.958
	Hotelling's Trace	.020	.600	.958
	Roy's Largest Root	.012	1.116	.347
Trials * Glasses	Pillai's Trace	.010	.634	.849
	Wilks' Lambda	.990	.633	.850
	Hotelling's Trace	.010	.633	.850
	Roy's Largest Root	.007	1.329	.250
Gender * Driving_Experience	Pillai's Trace	.021	6.490	.000
	Wilks' Lambda	.979	6.490	.000
	Hotelling's Trace	.021	6.490	.000
	Roy's Largest Root	.021	6.490	.000
Gender * Glasses	Pillai's Trace	.035	10.921	.000

continued on next page

Table 6.43: *continued*

Effect	Test	Value	F	Sig.
	Wilks' Lambda	.965	10.921	.000
	Hotelling's Trace	.036	10.921	.000
	Roy's Largest Root	.036	10.921	.000
Driving_Experience * Glasses	Pillai's Trace	.021	6.622	.000
	Wilks' Lambda	.979	6.622	.000
	Hotelling's Trace	.022	6.622	.000
	Roy's Largest Root	.022	6.622	.000

MANOVA-IV results showed that Pillar Types ($F = 26.325$, $p < 0.000$), Traffic Objects ($F = 3.252$, $p = 0.021$), Driving Experience ($F = 9.110$, $p < 0.000$), and Glasses ($F = 10.320$, $p < 0.001$) do have significant effect on logarithmic transformed Fixation Duration, Coordinates-X and logarithmic transformed Coordinates-Y. Trials ($F = .573$, $p = .897$) and Gender ($F = 1.199$, $p = .309$) have no effect, suggesting that Pillar Types, Traffic Objects, Driving Experience and Glasses effect the pixel correspondence of eye movements on logarithmic transformed Fixation Duration, Coordinates-X and logarithmic transformed Coordinates-Y during the simulation.

Multivariable analysis of variance - V (MANOVA-V)

MANOVA-V analysis was performed to identify whether each independent variable has significant effect on three dependent variables accordingly; Fixation Duration, logarithmic transformed Coordinates-X and logarithmic transformed Coordinates-Y. A 2 x 2 x 2 x 2 x 3 x 6 (288) mixed design MANOVA analysis was conducted. Subject's Gender is the within subjects variable with two levels (Male and Female); Pillar Models (New and Old), Traffic Objects (Bicycle and Pedestrian), Use of Glasses

(Glasses and No Glasses). Driving Experience is the within subjects variable with three levels (Low, Medium and High), and Trials are with six levels (T1 to T6).

Table 6.44: Multivariable Analysis of Variance on Fixation Duration, logarithmic transformed Coordinates-X and logarithmic transformed Coordinates-Y

Effect	Test	Value	F	Sig.
Intercept	Pillai's Trace	.999	294459.636	.000
	Wilks' Lambda	.001	294459.636	.000
	Hotelling's Trace	970.746	294459.636	.000
	Roy's Largest Root	970.746	294459.636	.000
Pillar_Types	Pillai's Trace	.081	26.656	.000
	Wilks' Lambda	.919	26.656	.000
	Hotelling's Trace	.088	26.656	.000
	Roy's Largest Root	.088	26.656	.000
Traffic_Objects	Pillai's Trace	.009	2.608	.050
	Wilks' Lambda	.991	2.608	.050
	Hotelling's Trace	.009	2.608	.050
	Roy's Largest Root	.009	2.608	.050
Trials	Pillai's Trace	.009	.577	.894
	Wilks' Lambda	.991	.577	.895
	Hotelling's Trace	.010	.576	.895
	Roy's Largest Root	.006	1.142	.336
Gender	Pillai's Trace	.007	2.151	.092
	Wilks' Lambda	.993	2.151	.092
	Hotelling's Trace	.007	2.151	.092
	Roy's Largest Root	.007	2.151	.092
Driving_Experience	Pillai's Trace	.041	6.381	.000

continued on next page

Table 6.44: *continued*

Effect	Test	Value	F	Sig.
	Wilks' Lambda	.959	6.430	.000
	Hotelling's Trace	.043	6.480	.000
	Roy's Largest Root	.041	12.423	.000
Glasses	Pillai's Trace	.034	10.628	.000
	Wilks' Lambda	.966	10.628	.000
	Hotelling's Trace	.035	10.628	.000
	Roy's Largest Root	.035	10.628	.000
Pillar_Types * Traffic_Objects	Pillai's Trace	.004	1.238	.295
	Wilks' Lambda	.996	1.238	.295
	Hotelling's Trace	.004	1.238	.295
	Roy's Largest Root	.004	1.238	.295
Pillar_Types * Trials	Pillai's Trace	.008	.511	.936
	Wilks' Lambda	.992	.511	.936
	Hotelling's Trace	.008	.511	.936
	Roy's Largest Root	.007	1.186	.314
Pillar_Types * Gender	Pillai's Trace	.006	1.872	.133
	Wilks' Lambda	.994	1.872	.133
	Hotelling's Trace	.006	1.872	.133
	Roy's Largest Root	.006	1.872	.133
Pillar_Types * Driving_Experience	Pillai's Trace	.029	4.543	.000
	Wilks' Lambda	.971	4.561	.000
	Hotelling's Trace	.030	4.579	.000
	Roy's Largest Root	.027	8.347	.000

continued on next page

Table 6.44: *continued*

Effect	Test	Value	F	Sig.
Pillar_Types * Glasses	Pillai's Trace	.005	1.569	.195
	Wilks' Lambda	.995	1.569	.195
	Hotelling's Trace	.005	1.569	.195
	Roy's Largest Root	.005	1.569	.195
Traffic_Objects * Trials	Pillai's Trace	.012	.744	.741
	Wilks' Lambda	.988	.744	.741
	Hotelling's Trace	.012	.743	.742
	Roy's Largest Root	.009	1.556	.170
Traffic_Objects * Gender	Pillai's Trace	.001	.323	.809
	Wilks' Lambda	.999	.323	.809
	Hotelling's Trace	.001	.323	.809
	Roy's Largest Root	.001	.323	.809
Traffic_Objects * Driving_Experience	Pillai's Trace	.004	.553	.768
	Wilks' Lambda	.996	.552	.768
	Hotelling's Trace	.004	.552	.769
	Roy's Largest Root	.002	.732	.533
Traffic_Objects * Glasses	Pillai's Trace	.003	.764	.515
	Wilks' Lambda	.997	.764	.515
	Hotelling's Trace	.003	.764	.515
	Roy's Largest Root	.003	.764	.515
Trials * Gender	Pillai's Trace	.016	.983	.470
	Wilks' Lambda	.984	.985	.469
	Hotelling's Trace	.016	.986	.467
	Roy's Largest Root	.013	2.446	.033

continued on next page

Table 6.44: *continued*

Effect	Test	Value	F	Sig.
Trials * Driving_Experience	Pillai's Trace	.016	.485	.992
	Wilks' Lambda	.984	.484	.992
	Hotelling's Trace	.016	.484	.992
	Roy's Largest Root	.009	.811	.618
Trials * Glasses	Pillai's Trace	.011	.688	.799
	Wilks' Lambda	.989	.688	.799
	Hotelling's Trace	.011	.687	.800
	Roy's Largest Root	.007	1.330	.249
Gender * Driving_Experience	Pillai's Trace	.021	6.630	.000
	Wilks' Lambda	.979	6.630	.000
	Hotelling's Trace	.022	6.630	.000
	Roy's Largest Root	.022	6.630	.000
Gender * Glasses	Pillai's Trace	.042	13.227	.000
	Wilks' Lambda	.958	13.227	.000
	Hotelling's Trace	.044	13.227	.000
	Roy's Largest Root	.044	13.227	.000
Driving_Experience * Glasses	Pillai's Trace	.017	5.181	.001
	Wilks' Lambda	.983	5.181	.001
	Hotelling's Trace	.017	5.181	.001
	Roy's Largest Root	.017	5.181	.001

MANOVA-V results showed that Pillar Types ($F = 26.656$, $p < 0.000$), Driving Experience ($F = 6.383$, $p < 0.000$) and Glasses ($F = 10.628$, $p < 0.001$) do have significant effect on Fixation Duration, logarithmic transformed Coordinates-X and logarithmic transformed Coordinates-Y. Traffic Objects (F = 2.608, p = .050), Trials (F = .577, p = .895) and Gender (F = 2.141, p = .092) have no effect, suggesting that Pillar Types, Traffic Objects, Driving Experience and Glasses effect the pixel correspondence of eye movements on Fixation Duration, logarithmic transformed Coordinates-X and logarithmic transformed Coordinates-Y during the simulation.

Multivariable analysis of variance - VI (MANOVA-VI)

MANOVA-VI analysis was performed to identify whether each independent variable has significant effect on three dependent variables accordingly; logarithmic transformed Fixation Duration, logarithmic transformed Coordinates-X and logarithmic transformed Coordinates-Y. A 2 x 2 x 2 x 2 x 3 x 6 (288) mixed design MANOVA analysis was conducted. Subject's Gender is the within subjects variable with two levels (Male and Female); Pillar Models (New and Old), Traffic Objects (Bicycle and Pedestrian), Use of Glasses (Glasses and No Glasses). Driving Experience is the within subjects variable with three levels (Low, Medium and High), and Trials are with six levels (T1 to T6).

Table 6.45: Multivariable Analysis of Variance on logarithmic transformed Fixation Duration, logarithmic transformed Coordinates-X and logarithmic transformed Coordinates-Y

Effect	Test	Value	F	Sig.
Intercept	Pillai's Trace	.999	318050.905	.000
	Wilks' Lambda	.001	318050.905	.000
	Hotelling's Trace	1048.519	318050.905	.000
	Roy's Largest Root	1048.519	318050.905	.000
Pillar_Types	Pillai's Trace	.081	26.569	.000

continued on next page

Table 6.45: *continued*

Effect	Test	Value	F	Sig.
	Wilks' Lambda	.919	26.569	.000
	Hotelling's Trace	.088	26.569	.000
	Roy's Largest Root	.088	26.569	.000
Traffic_Objects	Pillai's Trace	.012	3.538	.014
	Wilks' Lambda	.988	3.538	.014
	Hotelling's Trace	.012	3.538	.014
	Roy's Largest Root	.012	3.538	.014
Trials	Pillai's Trace	.009	.542	.918
	Wilks' Lambda	.991	.541	.919
	Hotelling's Trace	.009	.541	.919
	Roy's Largest Root	.005	.978	.430
Gender	Pillai's Trace	.004	1.323	.266
	Wilks' Lambda	.996	1.323	.266
	Hotelling's Trace	.004	1.323	.266
	Roy's Largest Root	.004	1.323	.266
Driving_Experience	Pillai's Trace	.043	6.687	.000
	Wilks' Lambda	.957	6.744	.000
	Hotelling's Trace	.045	6.800	.000
	Roy's Largest Root	.043	13.125	.000
Glasses	Pillai's Trace	.039	12.402	.000
	Wilks' Lambda	.961	12.402	.000
	Hotelling's Trace	.041	12.402	.000
	Roy's Largest Root	.041	12.402	.000
Pillar_Types * Traffic_Objects	Pillai's Trace	.005	1.633	.180

continued on next page

Table 6.45: *continued*

Effect	Test	Value	F	Sig.
	Wilks' Lambda	.995	1.633	.180
	Hotelling's Trace	.005	1.633	.180
	Roy's Largest Root	.005	1.633	.180
Pillar_Types * Trials	Pillai's Trace	.010	.614	.866
	Wilks' Lambda	.990	.613	.866
	Hotelling's Trace	.010	.613	.867
	Roy's Largest Root	.007	1.330	.249
Pillar_Types * Gender	Pillai's Trace	.004	1.311	.270
	Wilks' Lambda	.996	1.311	.270
	Hotelling's Trace	.004	1.311	.270
	Roy's Largest Root	.004	1.311	.270
Pillar_Types * Driving_Experience	Pillai's Trace	.028	4.328	.000
	Wilks' Lambda	.972	4.345	.000
	Hotelling's Trace	.029	4.362	.000
	Roy's Largest Root	.027	8.050	.000
Pillar_Types * Glasses	Pillai's Trace	.006	1.711	.163
	Wilks' Lambda	.994	1.711	.163
	Hotelling's Trace	.006	1.711	.163
	Roy's Largest Root	.006	1.711	.163
Traffic_Objects * Trials	Pillai's Trace	.012	.748	.736
	Wilks' Lambda	.988	.748	.737
	Hotelling's Trace	.012	.747	.738
	Roy's Largest Root	.008	1.549	.172
Traffic_Objects * Gender	Pillai's Trace	.001	.322	.810

continued on next page

Table 6.45: *continued*

Effect	Test	Value	F	Sig.
	Wilks' Lambda	.999	.322	.810
	Hotelling's Trace	.001	.322	.810
	Roy's Largest Root	.001	.322	.810
Traffic_Objects * Driving_Experience	Pillai's Trace	.003	.515	.797
	Wilks' Lambda	.997	.515	.798
	Hotelling's Trace	.003	.514	.798
	Roy's Largest Root	.002	.618	.604
Traffic_Objects * Glasses	Pillai's Trace	.002	.599	.616
	Wilks' Lambda	.998	.599	.616
	Hotelling's Trace	.002	.599	.616
	Roy's Largest Root	.002	.599	.616
Trials * Gender	Pillai's Trace	.010	.619	.862
	Wilks' Lambda	.990	.619	.862
	Hotelling's Trace	.010	.618	.862
	Roy's Largest Root	.007	1.328	.250
Trials * Driving_Experience	Pillai's Trace	.018	.562	.974
	Wilks' Lambda	.982	.562	.974
	Hotelling's Trace	.019	.561	.974
	Roy's Largest Root	.011	.997	.444
Trials * Glasses	Pillai's Trace	.012	.708	.779
	Wilks' Lambda	.988	.708	.779
	Hotelling's Trace	.012	.707	.780
	Roy's Largest Root	.007	1.361	.237

continued on next page

Table 6.45: *continued*

Effect	Test	Value	F	Sig.
Gender * Driving_Experience	Pillai's Trace	.021	6.432	.000
	Wilks' Lambda	.979	6.432	.000
	Hotelling's Trace	.021	6.432	.000
	Roy's Largest Root	.021	6.432	.000
Gender * Glasses	Pillai's Trace	.042	13.176	.000
	Wilks' Lambda	.958	13.176	.000
	Hotelling's Trace	.043	13.176	.000
	Roy's Largest Root	.043	13.176	.000
Driving_Experience * Glasses	Pillai's Trace	.023	7.073	.000
	Wilks' Lambda	.977	7.073	.000
	Hotelling's Trace	.023	7.073	.000
	Roy's Largest Root	.023	7.073	.000

MANOVA-VI results show that Pillar Types ($F = 26.569$, $p < 0.000$), Traffic Objects ($F = 3.538$, $p = 0.014$), Driving Experience ($F = 6.744$, $p < 0.000$), and Glasses ($F = 12.402$, $p < 0.000$) do have significant effect on logarithmic transformed Fixation Duration, logarithmic transformed Coordinates-X and logarithmic transformed Coordinates-Y, suggesting that Pillar Types, Traffic Objects, Driving Experience and Glasses effect the pixel correspondence of eye movements on Fixation Duration, Coordinates-X and Coordinates-Y during the simulation. Trails ($F = .541$, $p = .919$) and Gender ($F = 1.323$, $p = .266$) have no effect on logarithmic transformed Fixation Duration, logarithmic transformed Coordinates-X and logarithmic transformed Coordinates-Y.

Summary of analysis of variance tests

Table 6.46 summarizes results of all analysis of variance tests conducted on eye-tracker data. Independent variables with stars on Table 6.46 refers to 'p' values smaller than zero (p <0.000), which indicates a significance at the alpha level of 0.05. One can see that significant factors have overlapping results throughout the study. The very last row on Table 6.46 summarizes percentage accumulations of variables that have a significant MANOVA effect.

Table 6.46: Summary of significance (p-values) of ANOVA and MANOVA analyses

Tests	Dependent Variables	Pillar Types	Traff. Obj.	Trials	Gender	Driv. Exper.	Use Glass
ANOVA-I	Dur.	.004*	.451	.496	.109	.177	.046*
ANOVA-II	Coor.X	.000*	.231	.832	.673	.001*	.429
ANOVA-III	Coor.Y	.573	.047*	.881	.140	.000*	.000*
ANOVA-IV	Dur.LOG	.008*	.069	.577	.892	.096	.002*
ANOVA-V	Coor.XLOG	.000*	.128	.833	.806	.169	.034*
ANOVA-VI	Coor.YLOG	.573	.047*	.881	.140	.000*	.000*
MANOVA-I	Fix.Dur. Coor.X Coor.Y	.000*	.058	.888	.169	.000*	.000*
MANOVA-II	Dur.LOG Coor.X Coor.Y	.000*	.017*	.917	.524	.000*	.000*
MANOVA-III	Dur.LOG Coor.XLOG Coor.Y	.000*	.011*	.936	.466	.000*	.000*

continued on next page

Table 6.46: *continued*

Tests	Dependent Variables	Pillar Types	Traff. Obj.	Trials	Gender	Driv. Exper.	Use Glass
MANOVA-IV	Dur.LOG Coor.X Coor.YLOG	.000*	.021*	.897	.309	.000*	.000*
MANOVA-V	Dur. Coor.XLOG Coor.YLOG	.000*	.050	.894	.092	.000*	.000*
MANOVA-VI	Dur.LOG Coor.XLOG Coor.YLOG	.000*	.014*	.919	.266	.000*	.000*
Percentages		83%	50%	0%	0%	75%	92%

6.7.7 Area of interest observations

One of the main hypotheses proposed in this study is that New Pillar (Proposed Pillar) and Current Pillar (Old pillar) are significantly different in terms of providing ergonomics improvements (e.g., success of detecting traffic objects). Summary of ANOVA and MANOVA analyses in Table 6.46 demonstrated that Pillar Types contributes significantly on visual detection of traffic object. In this section, eye-tracker data was analyzed to find what portion of the simulation display received significant fixation and eye movements during simulation.

First of all, simulation screen was split into five evenly distributed areas of interest, each being fixed to 380 by 1200 (380×1200) pixels in width (X-axis) and height (Y-axis). The X-axis spans from (0,0) at the origin to (1920,0), which equals to five even split areas of interest (380×5). Throughout this section total Fixation Duration and Coordinates (X,Y) of eye-tracker data were superimposed on each corresponding areas of interest.

In this study, A-pillar section of the windshield area represented as Area-1, which covers the very first 380×1200 portion of the simulation display. Figure 6.12 shows the split simulation window with evenly distributed (380×1200) areas of interest.

Figure 6.12. Simulation screen split in five evenly distributed areas of interest. Area-1 represents the A-pillar zone of New Pillar design with circular see-through gaps.

Projection of compound coordinates

In this section eye-tracker data was plotted on simulation screen that was divided into five split areas of interest. One can see that Old Pillar model has a wider (a more homogeneous) distribution of points across the X-axis. In contrast, eye-movements of subjects on the New Pillar is more concentrated towards the A-pillar zone (Figure 6.13).

A total of 1152 (576×2) data points were evenly distributed between Current Pillar (576 points) and New Pillar (576 points) on Figure 6.13. For Area-1, a total of 157 hits were counted for Current Pillar design, whereas, New Pillar received a total of 405 hits. Histogram plots also show that there is an accumulation of eye-movements data towards Area-1 on New Pillar plot when compared to Old Pillar. In parallel to these findings, bar chart on Figure 6.14 also demonstrates that projection of subjects' eye-movements on Area-1 for Old Pillar is only 27%, while New Pillar model receives a 43% more total number of hits for the same area.

Total fixation duration

Another variable that provides insightful information about subjects' traffic object detection performance is the Fixation Duration. In this section Fixation Duration data was plotted onto five different areas of interests. First, intensity (duration) of fixations were superimposed on compound coordinates data (Figure 6.15). The size of each bubble demonstrates the relative duration of the associated fixation. Per each point on the plot (X and Y coordinates), the larger the bubble diameter gets, longer the fixation duration becomes. One can see that New Pillar design has higher concentration of overlapping bubble points when compared to Old Pillar design. This observation is especially significant on Area-1, where New Pillar plot has distinctively condensed area of fixation. A parallel observation can be captured when compared total fixation duration (in milliseconds) between Old Pillar and New Pillar model. Bar plot on Figure 6.16 shows a 16% increase in total fixation duration at Area-1.

Review of heat-maps and burnout images

Compound coordinates and fixation data provided an in-depth information about distribution of subjects' eye-movements and where fixation concentrations occur on the simulation display. In this section, coordinates data and fixation intensities were

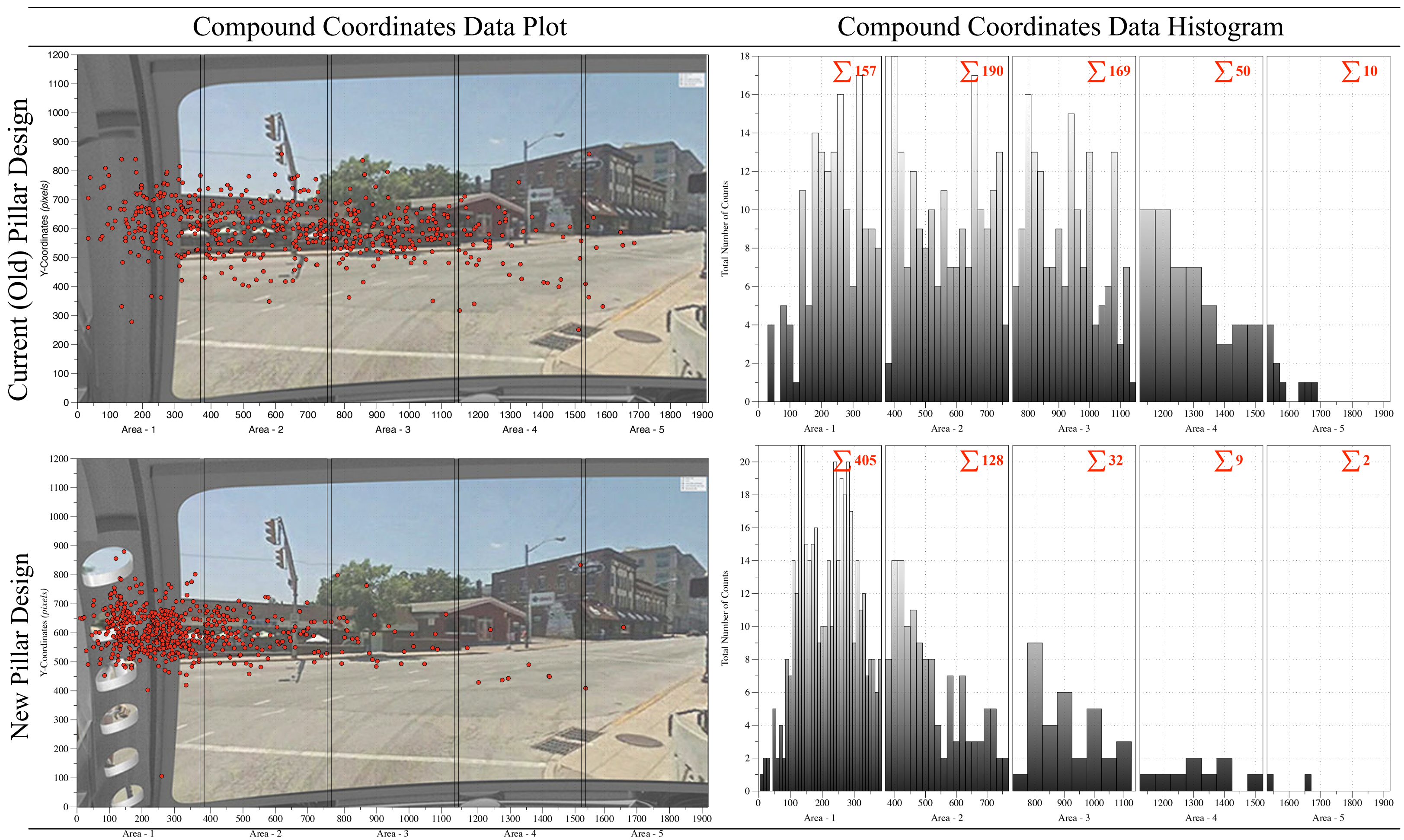

Figure 6.13. Distribution of compound coordinates data with histograms on areas of interest for Old and New Pillar design. An increased concentration of eye-movements seen at Area-1 for New Pillar design.

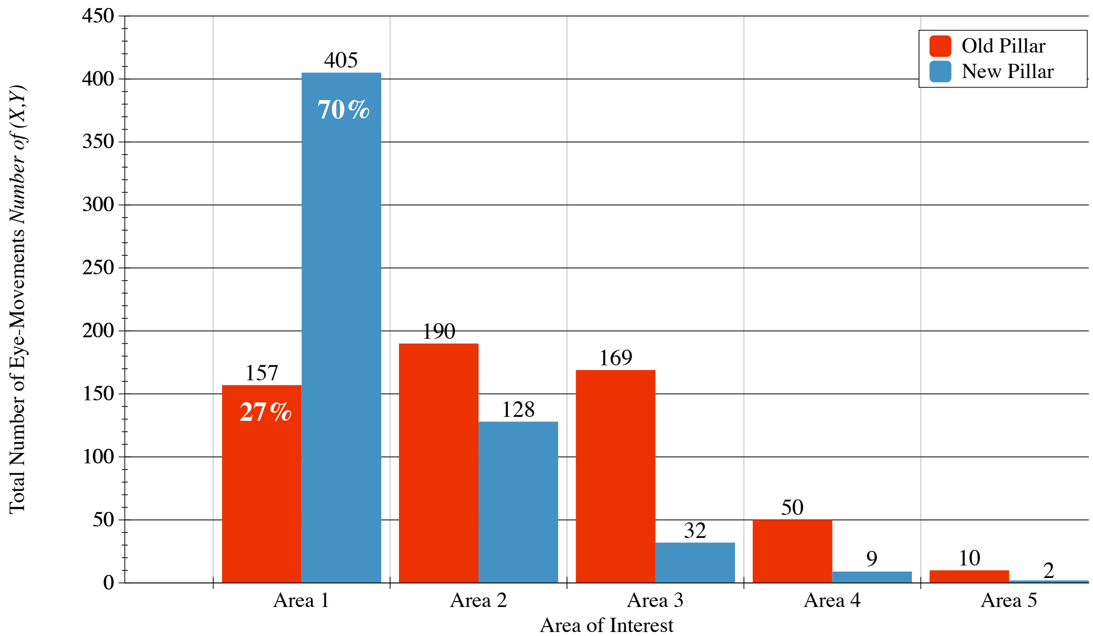

Figure 6.14. Comparison of total number of hits (X,Y) between Old and New Pillar. There is a 43% increase in the total number of eye-movements at Area-1 when subjects use New Pillar design.

superimposed to generate heat-maps and burnout images, which provide additional information about areas of interest.

Heat-maps are one of the versatile visual communication techniques used in image processing, which provide color-coded representation of eye-movements in relation to the concentration of looks that each area of interest receives [168]. Heat-maps provided in Figure 6.17 and 6.18 were generated through superimposing fixation data over compound coordinates data. Red (hot) areas show high levels of concentration, whereas, blue (cold) areas represent low levels of concentration. Once can see that there is a distinctive concentration (hot zone) found at Area-1 on New Pillar design.

Burnout images also provides similar information, where only concentrated (areas subject to high fixation duration) areas were presented, and the rest of the image was blackened. One can see from Figures 6.17 and 6.18 that differences in burnout images visibility associated between Old Pillar and New Pillar design. Subjects on

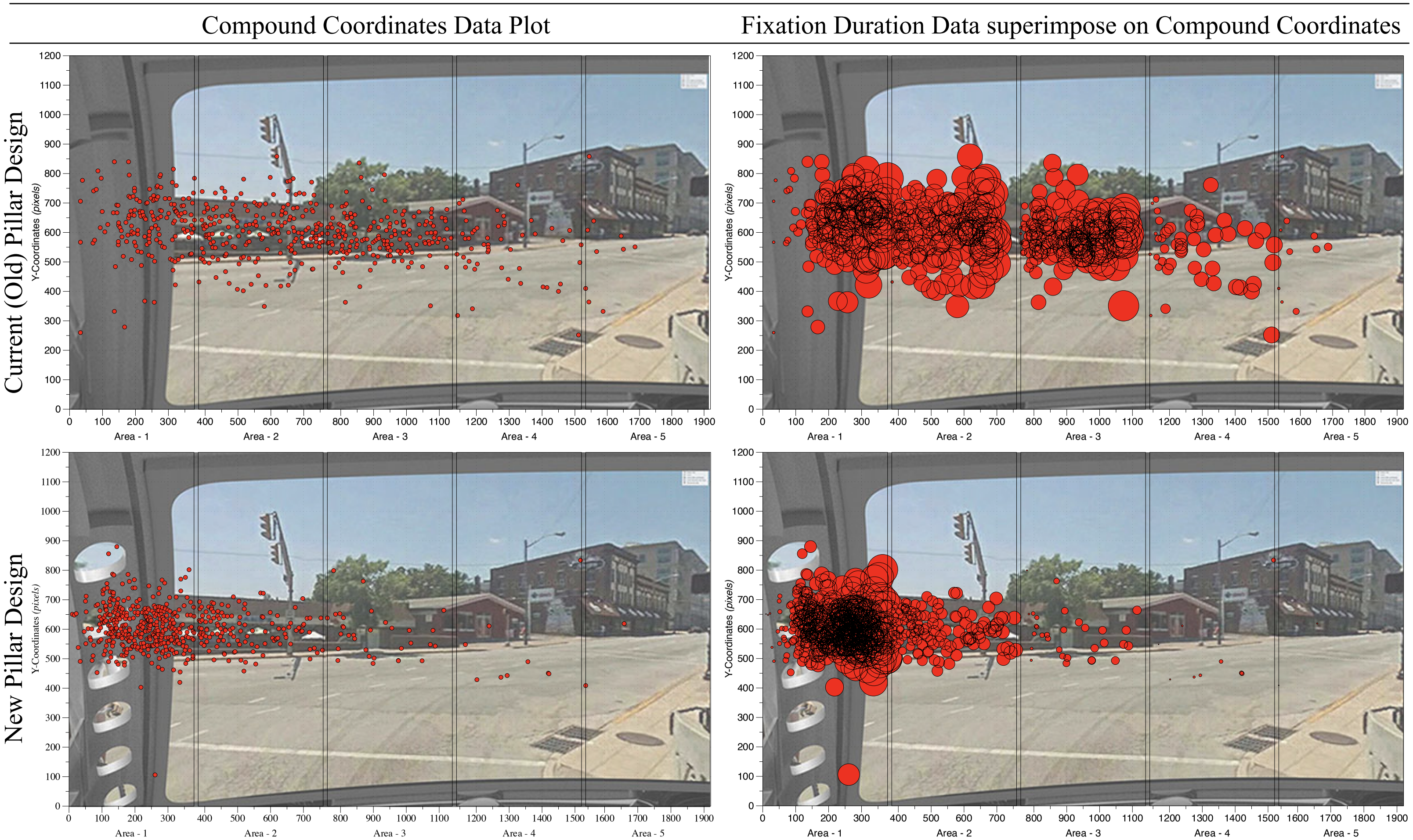

Figure 6.15. Distribution of compound coordinates with fixation duration on areas of interest. An increased concentration (overlapping bubbles) of eye fixations is seen on New Pillar design at Area-1.

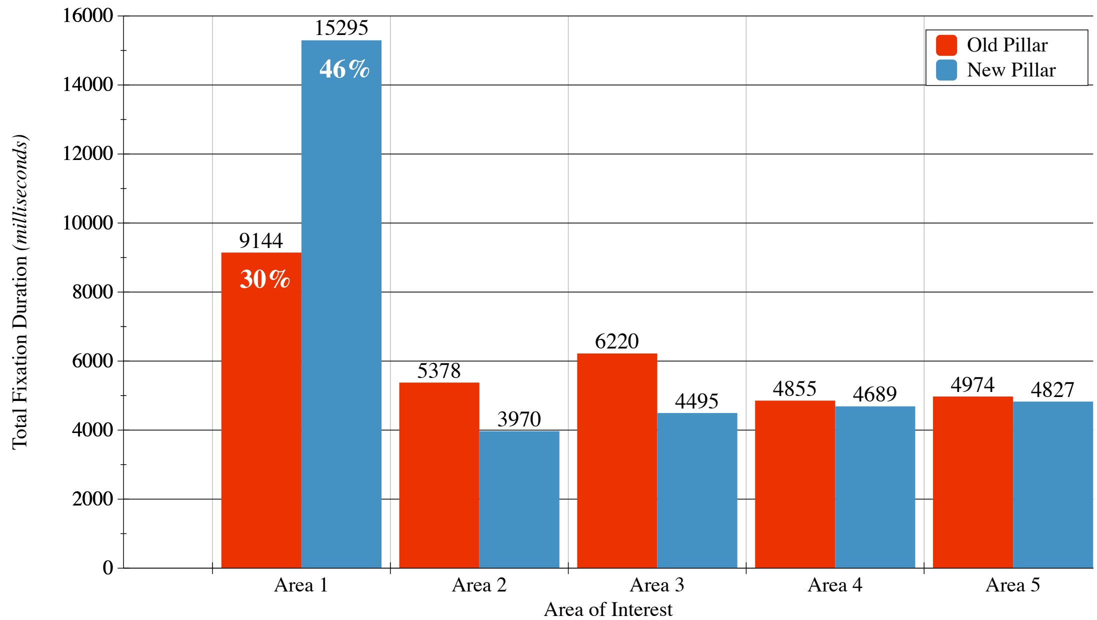

Figure 6.16. Comparison of total fixation duration data between Old and New Pillar.

New Pillar performed very concentrated visual search. In contrast, a dispersed visual search was performed by subjects on Old Pillar design.

Heat-maps and burnout images provided another group of supporting evidence that there is a significant difference found between Old Pillar and New Pillar design in terms of eye-movement concentrations and fixation duration. Old Pillar was associated with dispersed eye-movements on X-axis. In contrast eye-movements and fixations on New Pillar design were heavily concentrated on the A-pillar zone.

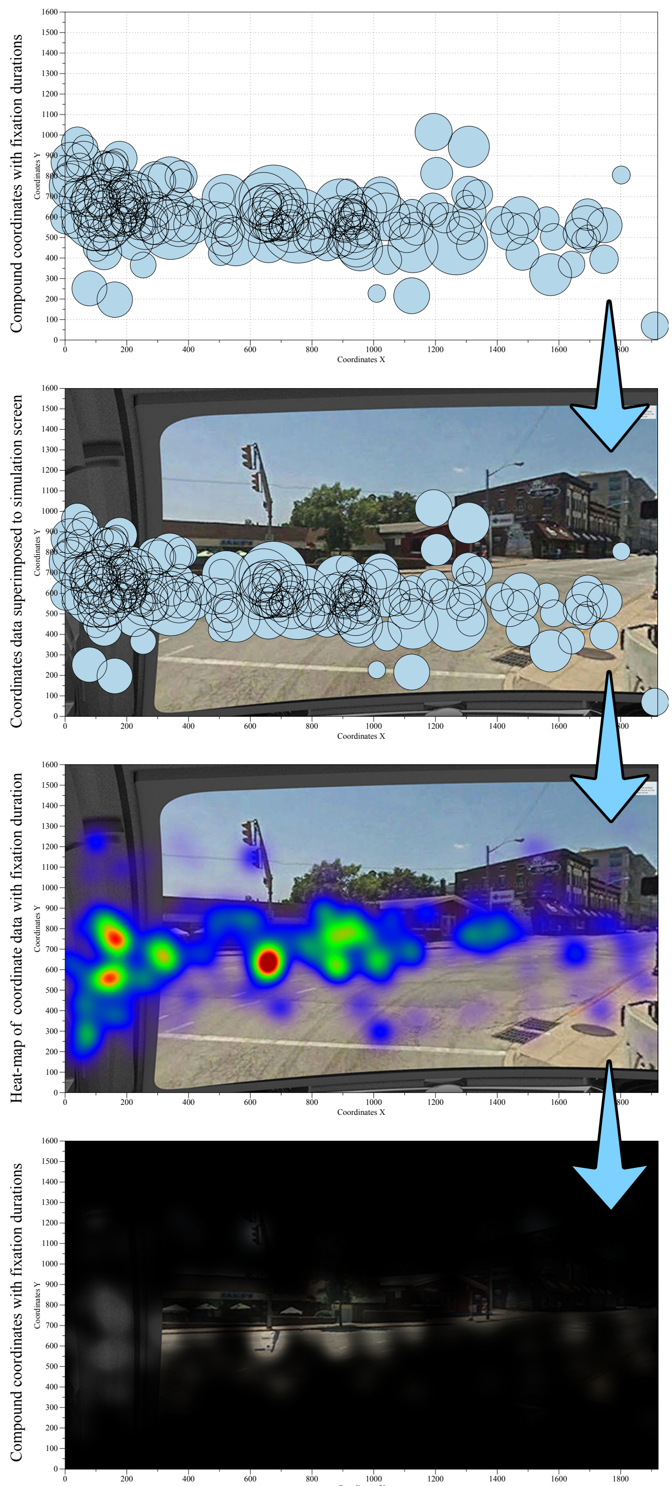

Figure 6.17. Old Pillar design demonstrates a dispersed data along X-axis. Heat-maps and burnout data are relatively homegenous and spread with weak concentration at Area-1.

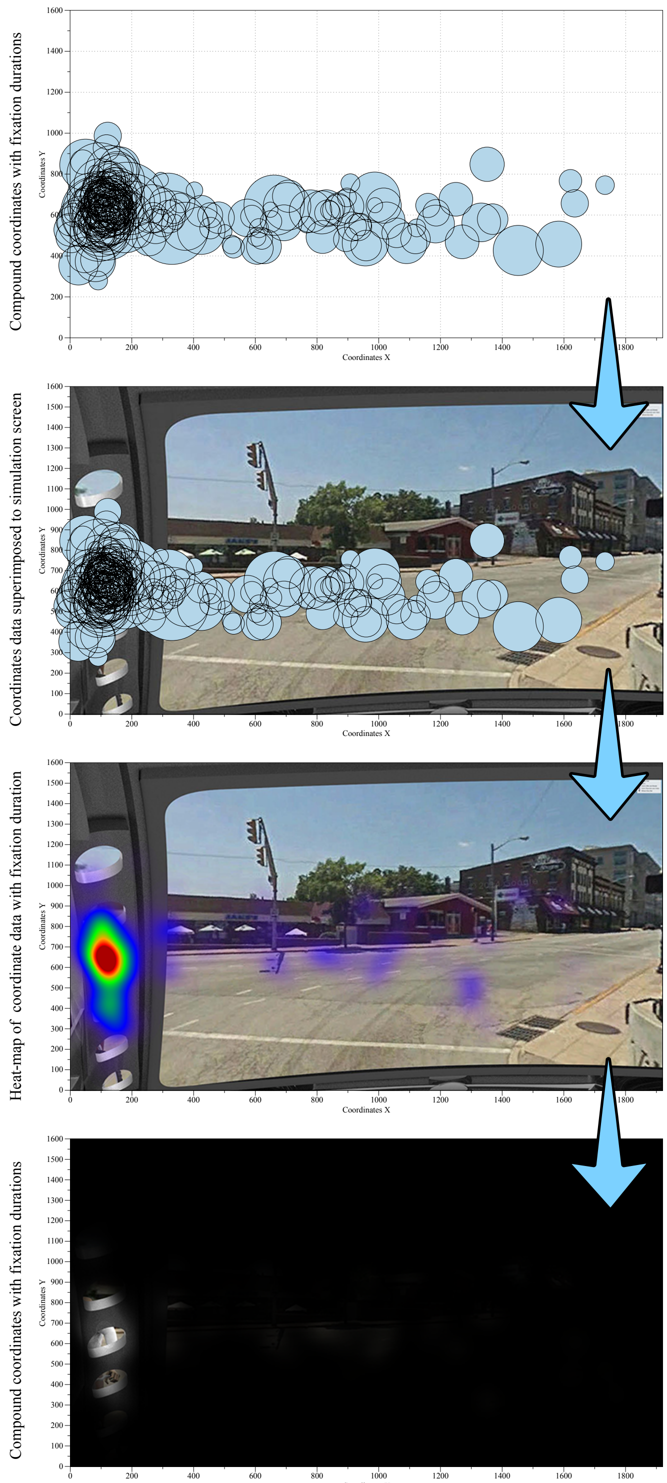

Figure 6.18. Heat-maps and burnout images on New Pillar demonstrates higher concentration of eye-movements and fixation on A-pillar zone.

6.8 Results and Discussions

A good test-retest reliability on Trials was observed throughout this study (Table 6.20). Outcomes of six trials demonstrated a 'good' ICC scores of .618, .862 and .794 for Fixation Duration, Coordinates-X and Coordinates-Y data accordingly.

One can see from Table 6.47 that there was no statistically significant difference in mean outcomes in Fixation Duration, Coordinates-X and Coordinates-Y between Trials, but there were statistically significant differences between Pillar Types and Traffic Objects. Across all MANOVA studies, New Pillar found to be significantly different than Old Pillar model both for Fixation Duration, Coordinates-X and Coordinates-Y outcomes. Only at Coordinates-Y Pillar Type did not generate a significant effect. Similar to MANOVA studies, ANOVA results showed a strong agreement that a different between New Pillar and Old Pillar model was observed in terms of generating different outcomes on detecting traffic objects. Pedestrians found to be significantly different than Bicycle bot for Fixation Duration, Coordinates-X and Coordinates-Y outcomes. This difference was detected across all MANOVA studies except 6-way MANOVA-V study. MANOVA studies showed that Trials found not to be generating different outcomes. Cells shaded in yellow in Table 6.47 shows mutual findings on ANOVA/MANOVA studies between 3-way and 6-way models for main effects. In contrast, cells highlighted in red shows where an agreement does not hold.

Six-way ANOVA/MANOVA study was conducted to explore further information about subjects' eye-tracking attributes. Results revealed valuable information in regarding effects of Gender, Driving Experience and Use of Glasses on eye-tracking outcomes. One can see from Table 6.46 that there was no statistically significant difference in mean outcomes in Fixation Duration, Coordinates-X and Coordinates-Y on Gender, but there were statistically significant differences between Driving Experience and Use of Glasses.

Summary of interactions effects at Figure 7.9 and Figure 7.10 demonstrate that 2-way interactions found between Pillar Types and Traffic Objects. One can see that non-parallel intersecting lines overlaps with significance found on ANOVA/MANOVA studies.

In addition to ANOVA/MANOVA studies conducted, Areas of Interest observations revealed that subjects generated higher number of eye-movements and fixations at Area-1 section of the simulator window. Figure 6.13 and Figure 6.15 show that a dense eye-movements and fixations were associated with Area-1 section of the simulator monitor. Eye-movements and Fixation Duration related data on New Pillar were resulted higher (43% and 16%) more than Old Pillar model.

Heat-maps and burnout images also demonstrated supporting visual evidence that subjects eye-movements were concentrated on Area-1 section, which represents the A-pillar zone of the vehicle windshield. Comparison between Figure 6.17 and Figure 6.18 shows that subjects did a lateral eye-gazing across x-axis when using Old Pillar model, whereas, a highly concentrated search on Area-1 (A-pillar zone) was generated by subjects when New Pillar model was projected on simulator monitor.

Table 6.47: Summary of significance (p-values) of ANOVA and MANOVA analyses on main effects

Tests	Dependent Variables	Pillar Types		Traffic Objects		Trials	
		3-way	6-way	3-way	6-way	3-way	6-way
ANOVA-I	Fix.Dur.	.000*	.004*	.279	.451	.021*	.469
ANOVA-II	Coord.X	.000*	.000*	.321	.231	.679	.832
ANOVA-III	Coord.Y	.911	.573	.000*	.047*	.450	.881
ANOVA-IV	Fix.Dur.LOG	.000*	.008*	.002*	.069	.166	.577
ANOVA-V	Coord.XLOG	.000*	.000*	.170	.128	.654	.833
ANOVA-VI	Coord.YLOG	.546	.573	.000*	.047*	.285	.881
MANOVA-I	Fix.Dur. Coord.X	.000*	.000*	.000*	.058	.110	.888

continued on next page

Table 6.47: *continued*

Tests	Dependent Variables	Pillar Types		Traffic Objects		Trials	
		3-way	6-way	3-way	6-way	3-way	6-way
	Coord.Y						
	Fix.Dur.LOG						
MANOVA-II	Coord.X	.000*	.000*	.000*	.017*	.365	.917
	Coord.Y						
	Fix.Dur.LOG						
MANOVA-III	Coord.XLOG	.000*	.000*	.000*	.011*	.411	.936
	Coord.Y						
	Fix.Dur.LOG						
MANOVA-IV	Coord.X	.000*	.000*	.000*	.021*	.267	.897
	Coord.YLOG						
	Fix.Dur.						
MANOVA-V	Coord.XLOG	.000*	.000*	.000*	.050	.098	.894
	Coord.YLOG						
	Fix.Dur.LOG						
MANOVA-VI	Coord.XLOG	.000*	.000*	.000*	.014*	.310	.919
	Coord.YLOG						
Percentages		83%	83%	75%	50%	8%	0%

7. EXPERIMENT - II

7.1 Introduction

7.1.1 Overview

Experiment-I provided information about the accumulation of eye-movements on specific areas (areas-of-interest) of the LCD monitor. However, this approach does not reveal important information whether subjects did actually identify a traffic object or not. Goal of the Experiment-II is to provide whether subjects did actually detect traffic objects projected on LCD monitor or not. Furthermore, Experiment-II also reveals information about the effectiveness/success of pillar models in terms of assisting users in detecting traffic objects.

Experiment-II was split into three sub-experiments: Traffic Object Detection Experiment, Cooper-Harper Test and User Questionnaire/Review. Each experiment represents different levels of performance related data (Figure 8.1).

7.1.2 Connections to human-in-the-loop design framework

Experiment-II demonstrates how an additional human related data could be connected into human-in-the-loop design framework. In this specific design study three sub-experiments was used as means of collecting human subject data. Shaded area in Figure 7.2 shows how data collected through Traffic Object Detection experiment. Similarly, Figure 7.3 demonstrates a visual synopsis of how Experiment-II was integrated to DHM within human-in-the-loop framework.

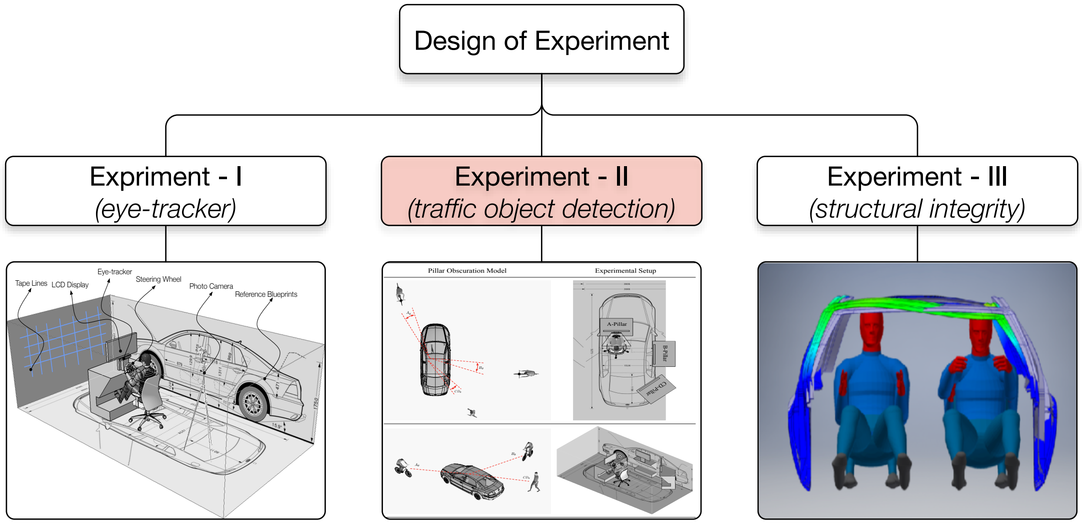

Figure 7.1. Experiment-II is a human subject data collection experiment through three sub-experiments: Traffic Object Detection Experiment, Cooper-Harper Test and User Questionnaire/Review.

7.2 Experimental Setup

7.2.1 Pillar obscuration simulation

A modified version of the static simulator used in Experiment-I was utilized in Experiment-II. The modified setup was composed of three LCD monitors that represents corresponding pillar sections of the referenced vehicle. Still images that were gathered from Google Maps projected on each corresponding LCD monitor. These images represents actual road environment for constructing a virtual traffic scene (Figure 7.7). Similar to Experiment-I, a steering wheel, an adjustable seat and pedals were provided as simple physical probes. Dimensions of the experimental setup, locations of the driver's seat and orientation of each pillar were based on the reference vehicle blueprints. Figure 7.4 shows experimental components that are placed in experiment room according to blueprints of the reference vehicle.

In Experiment-II, three LCD displays were used without an eye-tracker device. Each LCD display was located on paired pillar zones, where static images associated

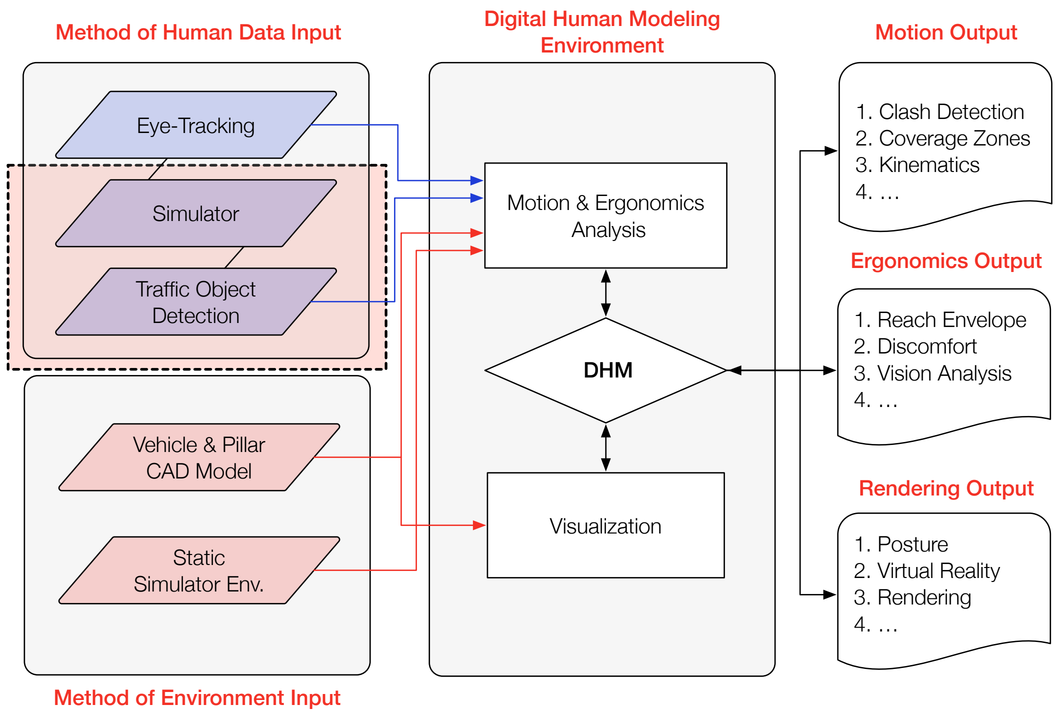

Figure 7.2. Shaded area in red (inside dashed lines) represents how Experiment-II was integrated to data flow process within human-in-the-loop framework. Experiment-II gathered human subject related data through three sub-experiments.

to driver's point-of-view were projected. Figures 7.5 and 7.6 show a generic view of the experimental setup, and how traffic simulation scenario was transferred to physical experiment setup.

7.2.2 Traffic objects

A realistic traffic scenario was created by using still images from Google Maps. Bikers, pedestrians, motorcyclists were used as traffic objects. Each object was placed within associated pillar obscuration angle. Traffic environment was based on a three-way road junction located in the heart of the Purdue University campus at West Lafayette, Indiana (Latitude - 40^{o}25'26.64"N and Longitude - 86^{o}54'28.46"W). The junction is known for its accumulated local traffic - heavily composed of pedestrians,

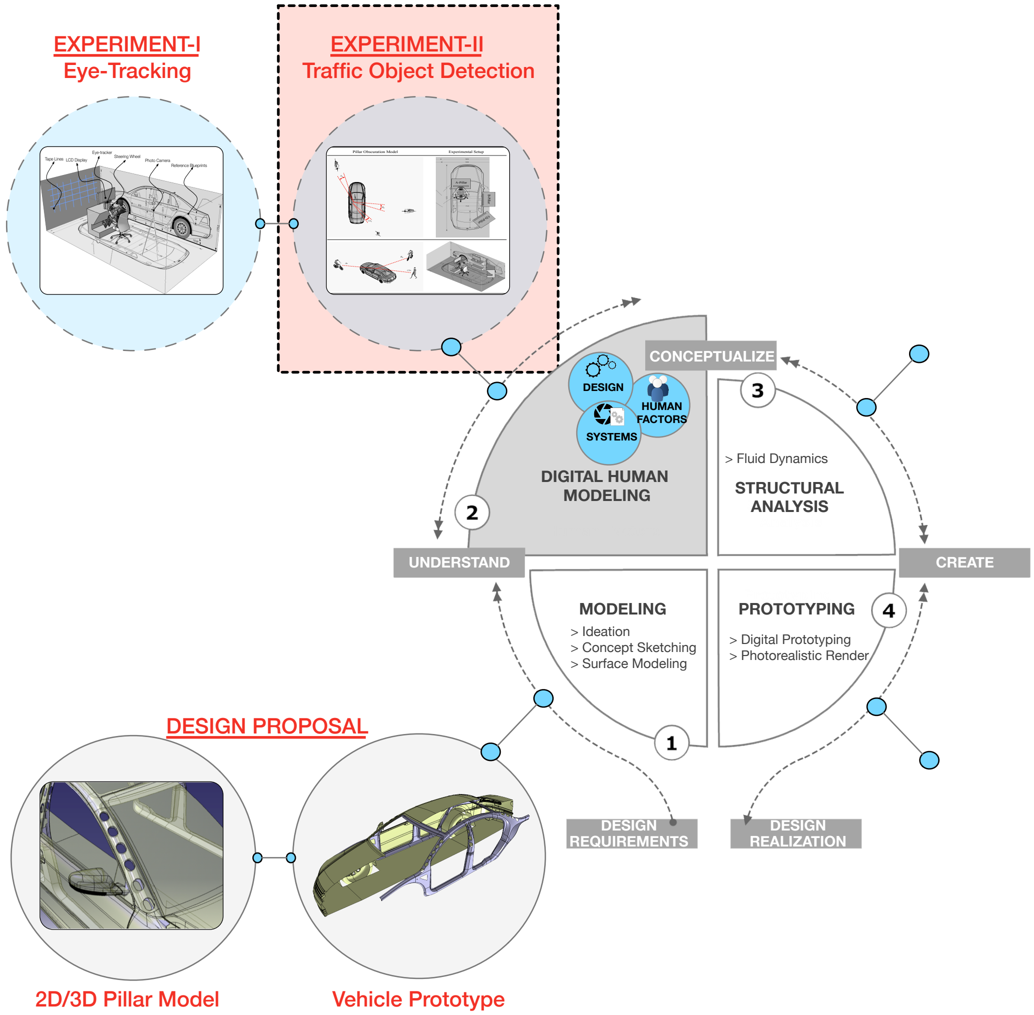

Figure 7.3. Shaded area in red (inside dashed lines) represents which portion of the human-in-the-loop design framework was used to integrate human aspects of data during design process.

bikers and family cars. Three dimensional images of the road junction were taken from Google Maps. Based on the reference vehicle and associated with A, B and CD pillar obscuration zones, three traffic objects were situated on the Google Maps image. Each object was situated within obscuration angle. Later, still images were taken from driver's point-of-view. These images represent three different driving scenarios corresponding A, B and CD pillars (Figure 7.7).

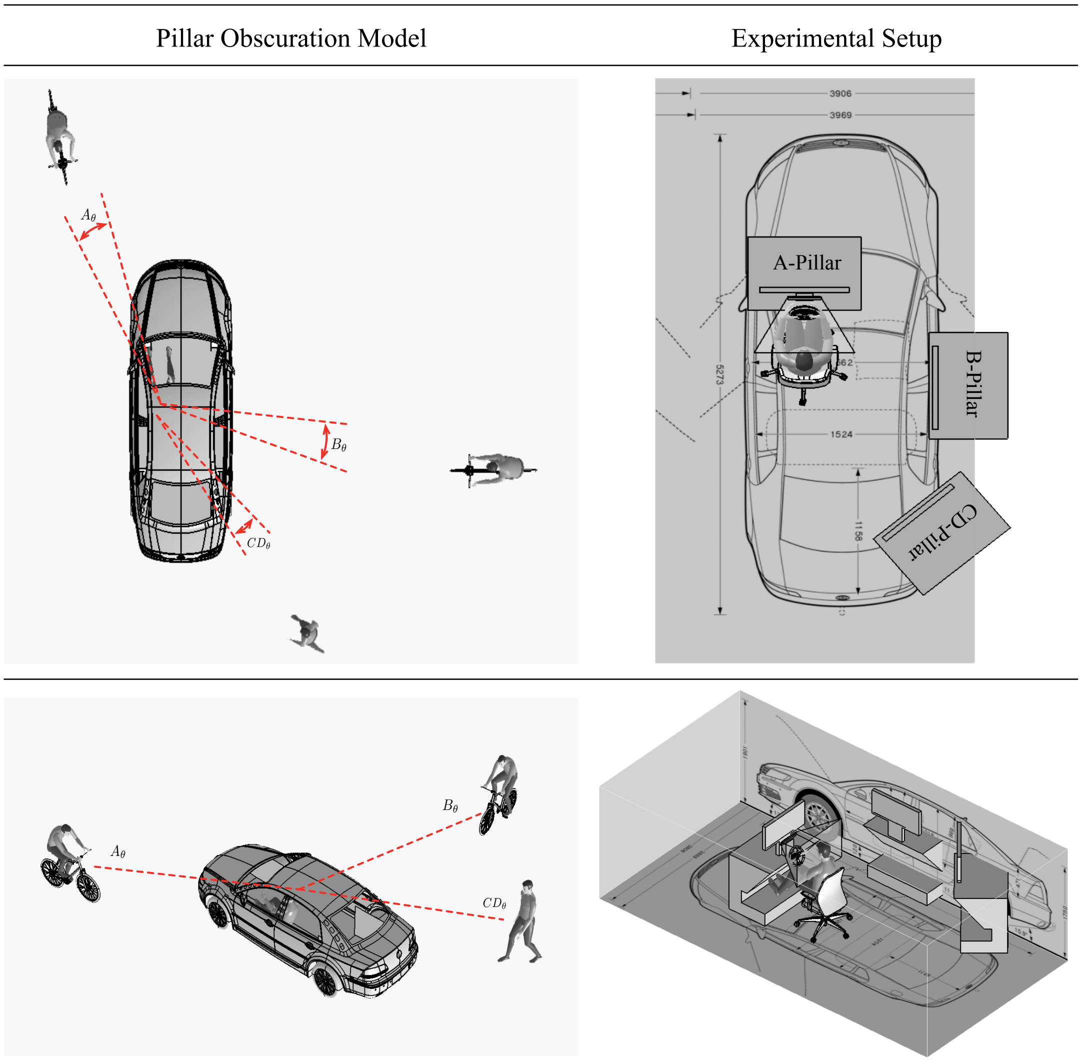

Figure 7.4. Orientation of traffic objects that are within pillar obscuration zones were projected to LCD displays. Static images on the LCD display represented the depth field of the driver's point-of-view.

In A-pillar obscuration scenario, reference vehicle was located on the very right lane as it is attempting to make a right turn. Traffic objects were located within the left side of the A-pillar obscuration angle. This scenario represents a very typical A-pillar obscuration happen at a pedestrian lane crossing.

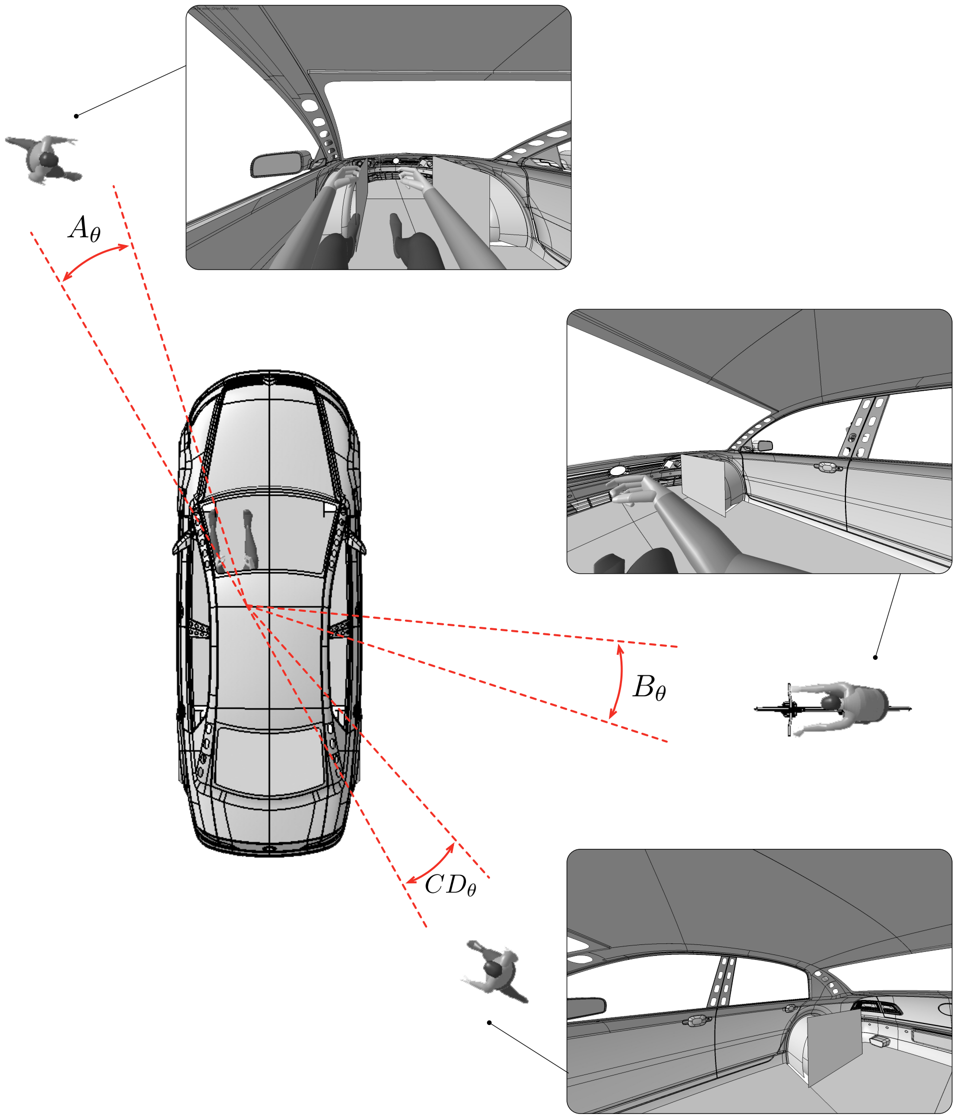

Figure 7.5. First group of traffic objects placed within obscuration zones (A_θ, B_θ, CD_θ) associated with each pillar (A, B, CD). Images show drivers point-of-view when looked at associated pillar and traffic element.

Similarly, for B-pillar obscuration scenario, traffic objects were located on the right side of the vehicle. In this setup, reference car was driving straight on its course and traffic objects were merging to the main road.

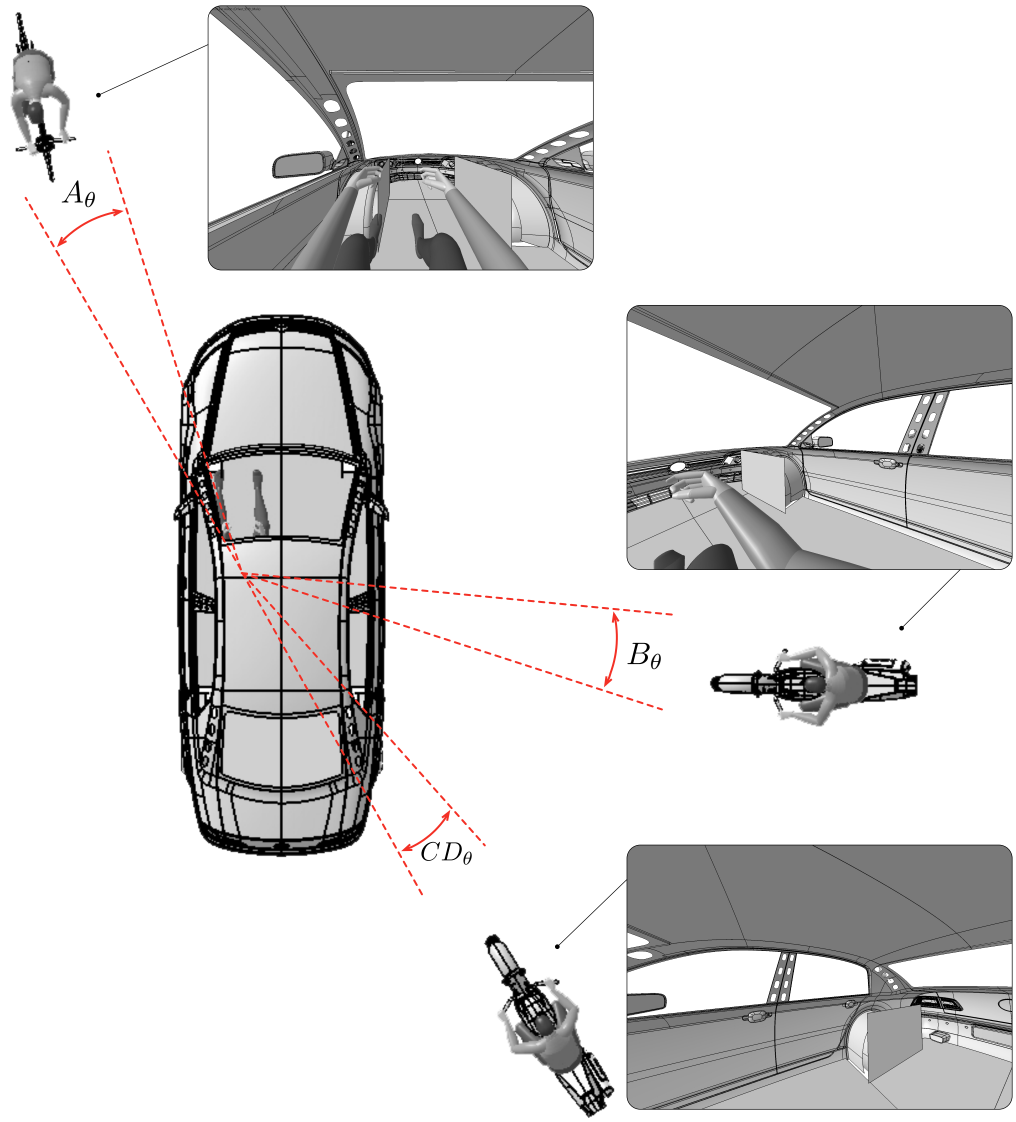

Figure 7.6. Second group of traffic objects placed within obscuration zones (A_θ, B_θ, CD_θ) associated with each pillar (A, B, CD). Images show drivers point-of-view when looked at associated pillar and traffic element.

Finally, for CD pillar obscuration, traffic elements were oriented rear right-end of the vehicle. This scenario represented a situation where the reference vehicle was attempting a back-up maneuver for parallel parking.

In each obscuration case, traffic scenarios represented a combination of visual tasks that include checking the crosswalk, monitoring merging traffic and watching other traffic objects. In each scenario, much the same to regular driving conditions, driver must check right and left side of the vehicle as he/she continues on the course. If traffic objects are not present in the scene, no action is required. If traffic objects are within vicinity of the vehicle, driver must make multiple maneuvers to avoid them. Although static simulator did not propose any medium of controlling simulation environment, subjects were advised to look for traffic objects on the monitor as if they were in a real driving condition.

7.2.3 Pillar obscuration scenario

Throughout this experiment two traffic objects were assigned to each pillar (A, B and CD) and placed within obscuration angle zone of each pillar. A block-design approach was taken by grouping pillar types with traffic objects under each pillar model (Old and New Pillar). Traffic objects and pillar types were randomized during data collection. Each traffic object was located within associated pillar obscuration angle as represented in Figure 7.4 and Figure 7.7. Table 7.1 shows assignment of traffic objects per pillar type within each block (Pillar model).

Table 7.1: Traffic object assignment per pillar model and pillar type

Pillar Model	Pillar Type	Traffic Objects	Trials
	A	Pedestrian	6
		Bicycle	6
Current Pillar	B	Motorcycle	6
		Bicycle	6
	CD	Pedestrian	6
		Motorcycle	6
	A	Pedestrian	6
		Bicycle	6

continued on next page

Table 7.1: *continued*

Pillar Model	Pillar Type	Traffic Objects	Trials
New Pillar	B	Motorcycle	6
		Bicycle	6
	CD	Pedestrian	6
		Motorcycle	6

7.3 Procedure

Experiment-II was conducted for A, B and CD pillar for Old Pillar and New Pillar model. Subjects filled-up Traffic Object Detection form after each static image displayed on the screen. Therefore, a total of 72 (3 x 24) Traffic Object Detection forms were used throughout the Experiment-II. For each pillar type, 2 Cooper-Harper test were conducted to detect visual performance of drivers when used Old Pillar model and New Pillar model. Thus, a total of 6 Cooper-Harper tests were used. Finally, 3 questionnaires were given to subjects to evaluate pillar models in categories of visibility, aesthetics and safety. Figure 7.8 summarizes overall data flow.

Specific procedures followed during Experiment-II were:

1. After Experiment-I completed, subjects were asked to start Experiment-II with Traffic Object Detection tasks. Subject went through Traffic Object Detection forms, which were static shuffling randomly with three seconds between each other.

2. For each pillar model (Old and New), subjects were asked to fill up a modified Cooper-Harper test after completing each A, B and CD pillar Object Detection Form experiment, sequentially.

3. After simulator tasks, subjects were asked to fill up three short questionnaires.

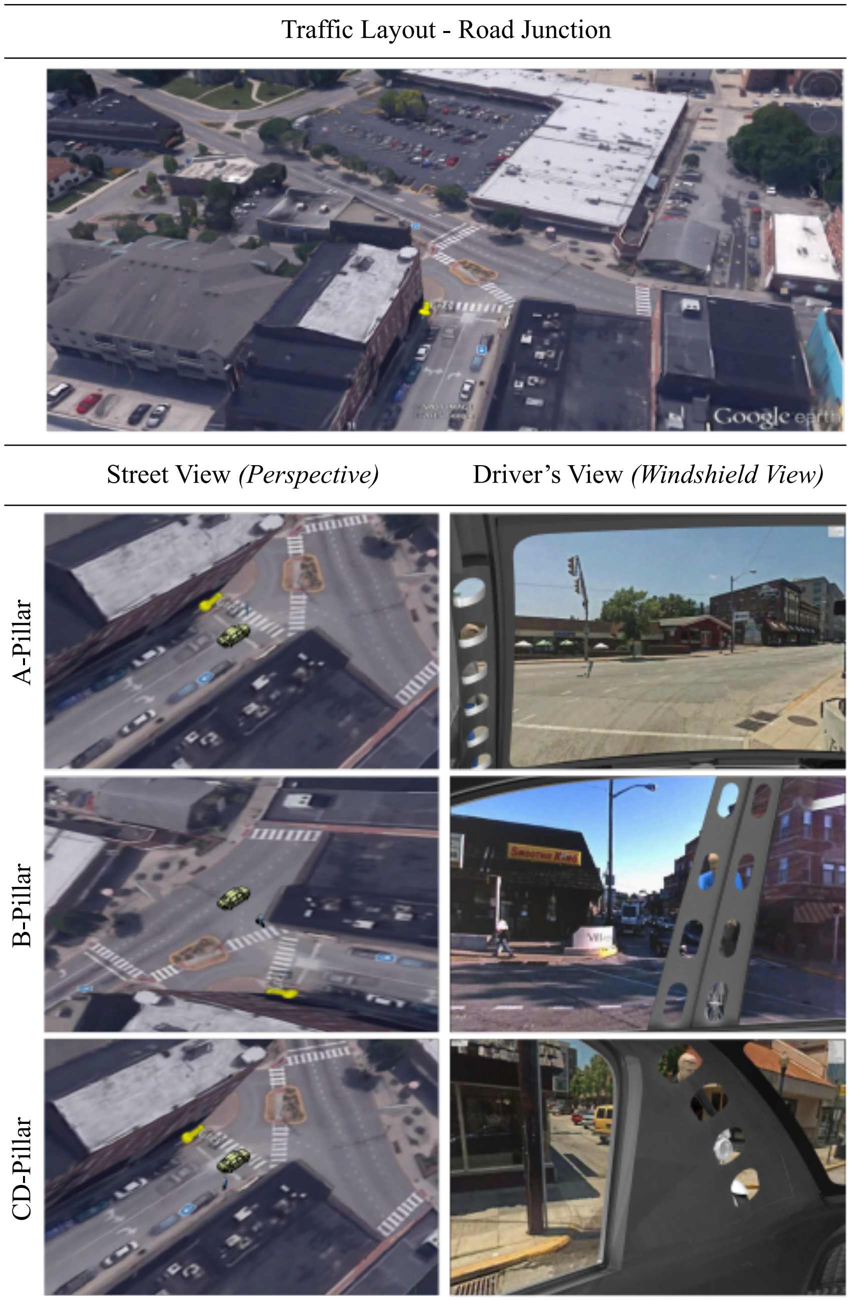

Figure 7.7. Reference vehicle and traffic objects were inserted into corresponding traffic scenario. Images represent perceptive layout of the traffic environment and driver's point-of-view are shown in groups. Each traffic object was located within pillar obscuration angle (A_θ, B_θ, CD_θ) associated with each A, B and CD pillars.

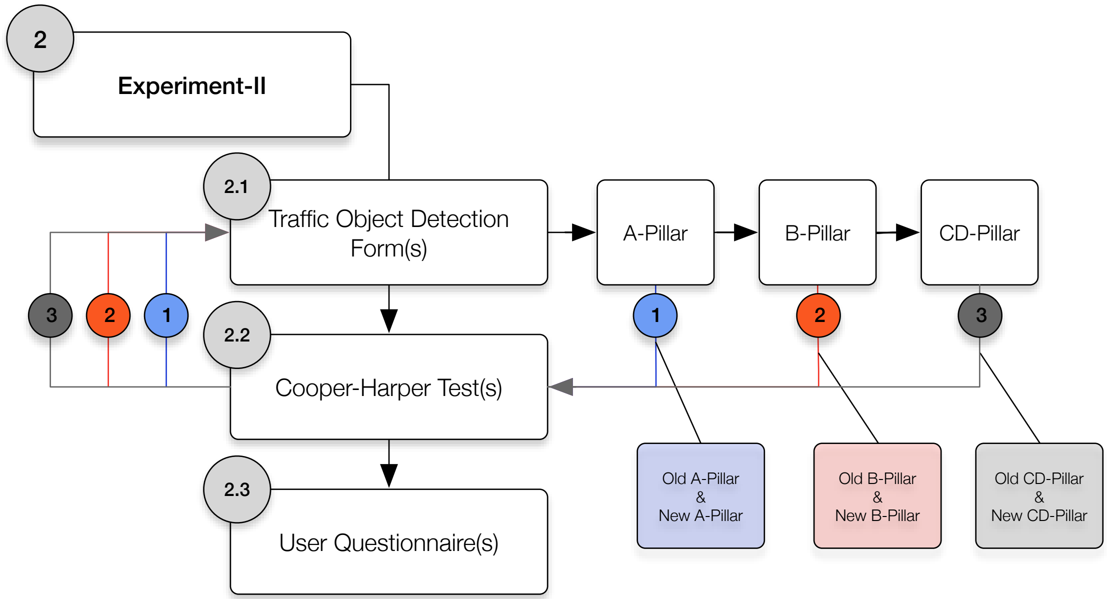

Figure 7.8. Traffic Object Detection form is composed of three levels of questions that needs to be answered sequentially.

4. After all simulator tasks and questionnaires were completed, subjects were required to sign off human subject log, and exited the experiment.

7.4 Variables

In Experiment-II, subjects' response was collected through three sub-experiments. There were four dependent variables, encompassing: 1. Object Detection, 2. Performance, 3. Ease of Detection, and 4. Design Review.

Object Detection data represents binary variable whether subjects detect a traffic object on monitor or not. Similarly, Traffic Object Detection Performance was a binary selection. Subjects choose one correct traffic object among four choices. Ease of Detection data and Design Review were Rating/Score data. Table 7.2 summarizes types of data, variables, units, and hypotheses associated with experiments conducted.

Table 7.2
Types of data, variables, units, and hypotheses associated with experiments conducted in this study

Dependent Variables	Type	Hypotheses
Traffic Object Detection	Binary	H1, H2, H3
Object Detection Performance	Binary	H1, H2, H3
Ease of Detection	Rating/Score	H1, H2, H3
Design Review	Rating/Score	H1, H2, H3

7.5 Experimental Design

Each sub-experiment in Experiment-II was analyzed to provide further understanding on whether pillar designs provide improvements in detecting traffic objects or not. Table 7.3 summarizes details on measurements, goals and statistical methods used in Experiment-II.

Table 7.3: Summary of methods of measurement, goal of measurement, statistical methods in Experiment-II

Method of Measurement	Goal of Measurement	Statistical, Numerical and Visual Methods
Detection Form	Detection Performance	Descriptive Statistics
		Bar Graphs
Cooper-Harper	Design Improvement	Descriptive Statistics
		Line Graphs
Questionnaire	User Preference	Descriptive Statistics
		Bar Graphs
	Internal Consistency	Cronbach's Alpha

7.6 Participants

Participant pool was exactly the same. All participants who attended to Experiment-I were also participated Experiment-II. A detailed information regarding participants were previously provided in Chapter 6. You can find summary of subjects and descriptive statics in tables provided in Section 6.6.3.

7.7 Data Analysis and Statistical Techniques

7.7.1 Traffic object detection experiment

Experiment-II started with Traffic Object Detection experiment. Subjects' input was collected through a Traffic Object Detection Form. Each simulation image representing A, B and CD pillars were displayed on a large monitor. Instead of using an eye-tracker device, subjects' data was collected through filling up Traffic Object Detection forms. This form was automatically initated right after a traffic object scenario was displayed on LCD monitor. Similar to Experiment-I, each image shuffled randomly in every 3 seconds. Between each image Traffic Detection Form was automatically displayed to subjects. There were three levels of question sets associated Traffic Object Detection Form.

In the first level of the question set, subjects were asked whether they detect a traffic object or not. Those who say 'yes' proceeded to second level and were asked about the type of a traffic object they saw. Finally, subjects were asked about how easy/hard it was to detect traffic objects. This section was split into three different subsections to explain each level of the Traffic Object Detection form.

Level - 1, success of detecting traffic objects

In this section subjects were asked whether they see a traffic object on simulation display or not. If their answer is 'yes', the they jumped to Level-2. Answering 'no' automatically canceled out subjects participation to second and third levels of the Traffic Object Detection form.

Figure 7.9 summarizes the data of successfully identifying traffic objects for Old and New pillar design for A, B and CD pillars. One can see that in every pillar type (A, B and CD), New Pillar design generates higher traffic object detection rate when compared to Old Pillar design. Summary plot (D) at Figure 7.9 shows that at least around 95% improvement is achieved when New Pillar design is used.

Level - 2, success of correct detection of traffic objects

In this level of the Traffic Object Detection Form subjects' were asked to select what type of traffic objects they saw during the simulation. Depending on the pillar type, different traffic objects were projected on the simulation display. There were four choices available (Pedestrian, traffic sign, motorcycle, and bicycle), and one being the correct answer.

In A-pillar simulation, correct traffic objects were Bicycle and Pedestrian. In B-pillar simulation Bicycle and Motorcycle were correct choices. In CD pillar simulation Motorcycle and Pedestrian were correct choices.

Figure 7.10 shows that percentage of correct traffic object detection rate is around 94% for A, B and CD pillar. This result indicates that subjects who answered first questions "yes" had success of 94% in detecting correct traffic objects. In contrast, subjects had a very poor correct traffic object detection performance. Figure 7.11 shows that only close to 1% of subjects were able to correctly detect traffic objects with Old Pillar design.

Level - 3, ease of detecting traffic objects

In this section subject's perception on ease of traffic object detection was analyzed. There were six categories ranked in Likert Scale from Very "Very Hard to See" to "Very Easy to see" for detecting traffic object.

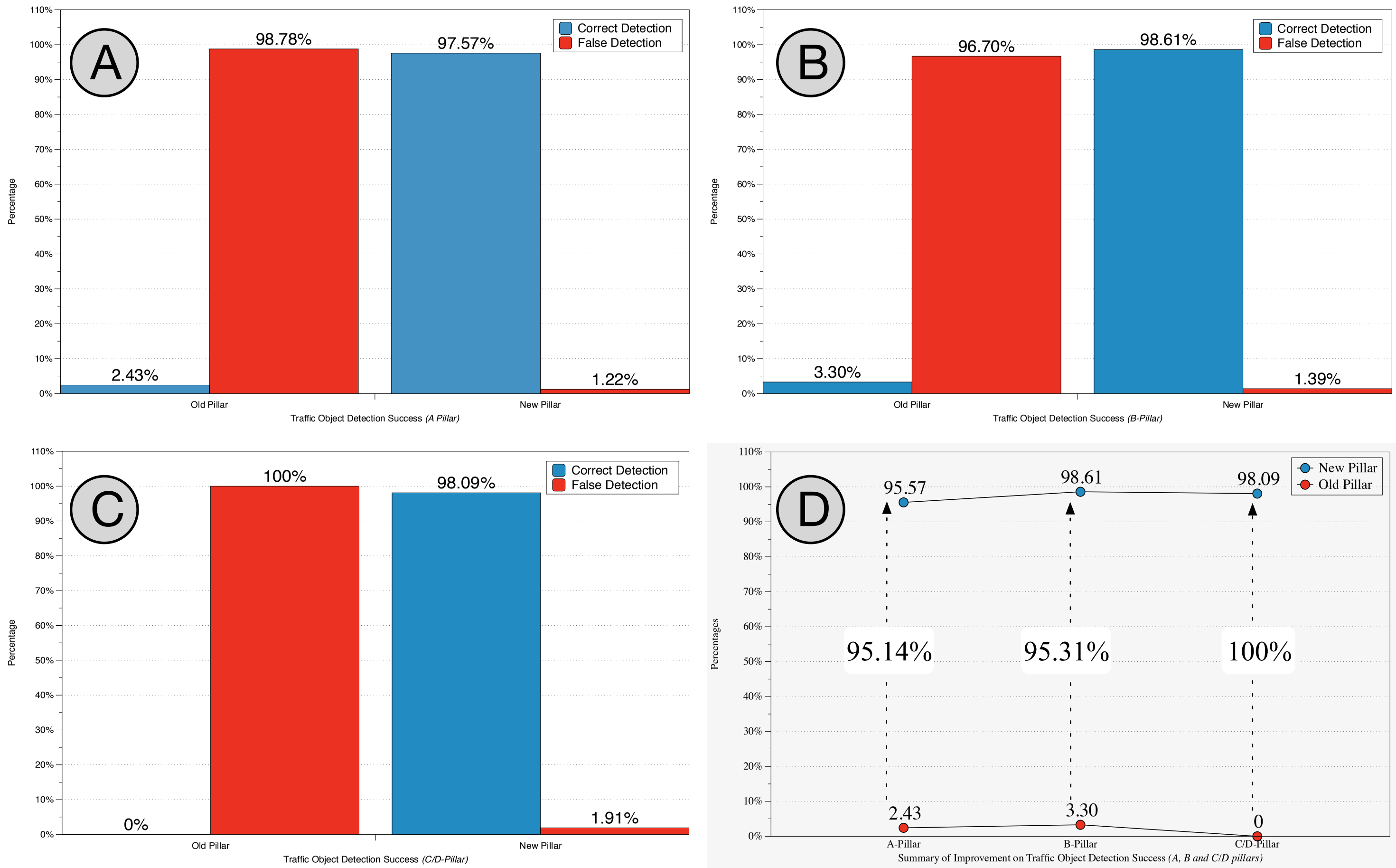

Figure 7.9. A), B) and C) represents improvements on traffic object detection between Old and New Pillar design for A, B and CD pillar respectively. D) represents summary of percentage improvement on traffic object detection between Old and New Pillar designs.

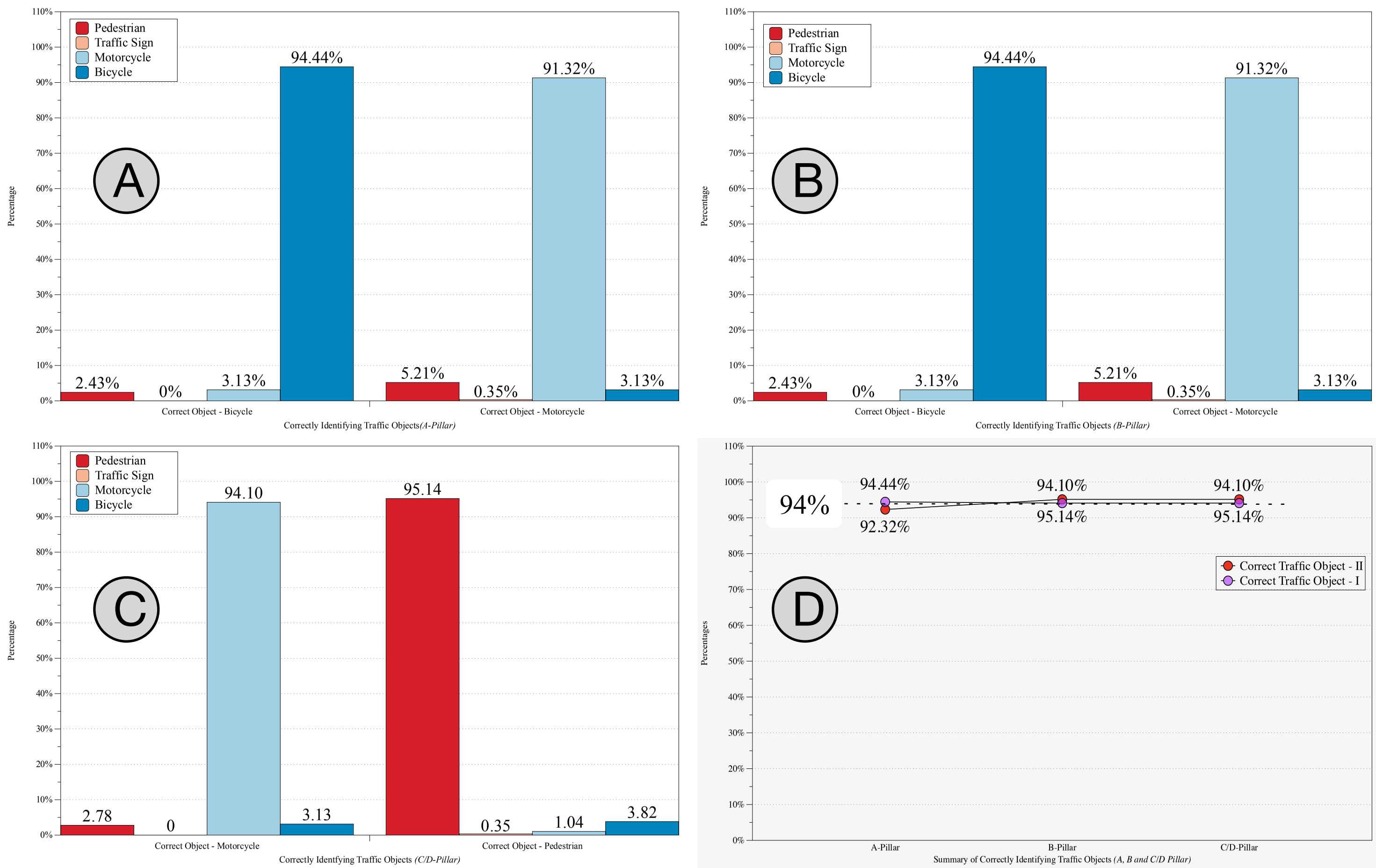

Figure 7.10. A), B) and C) represents improvements on correctly identifying traffic objects between Old and New Pillar design for A, B and CD pillar respectively. D) represents summary of traffic object detection between A, B and CD pillars for New Pillar design.

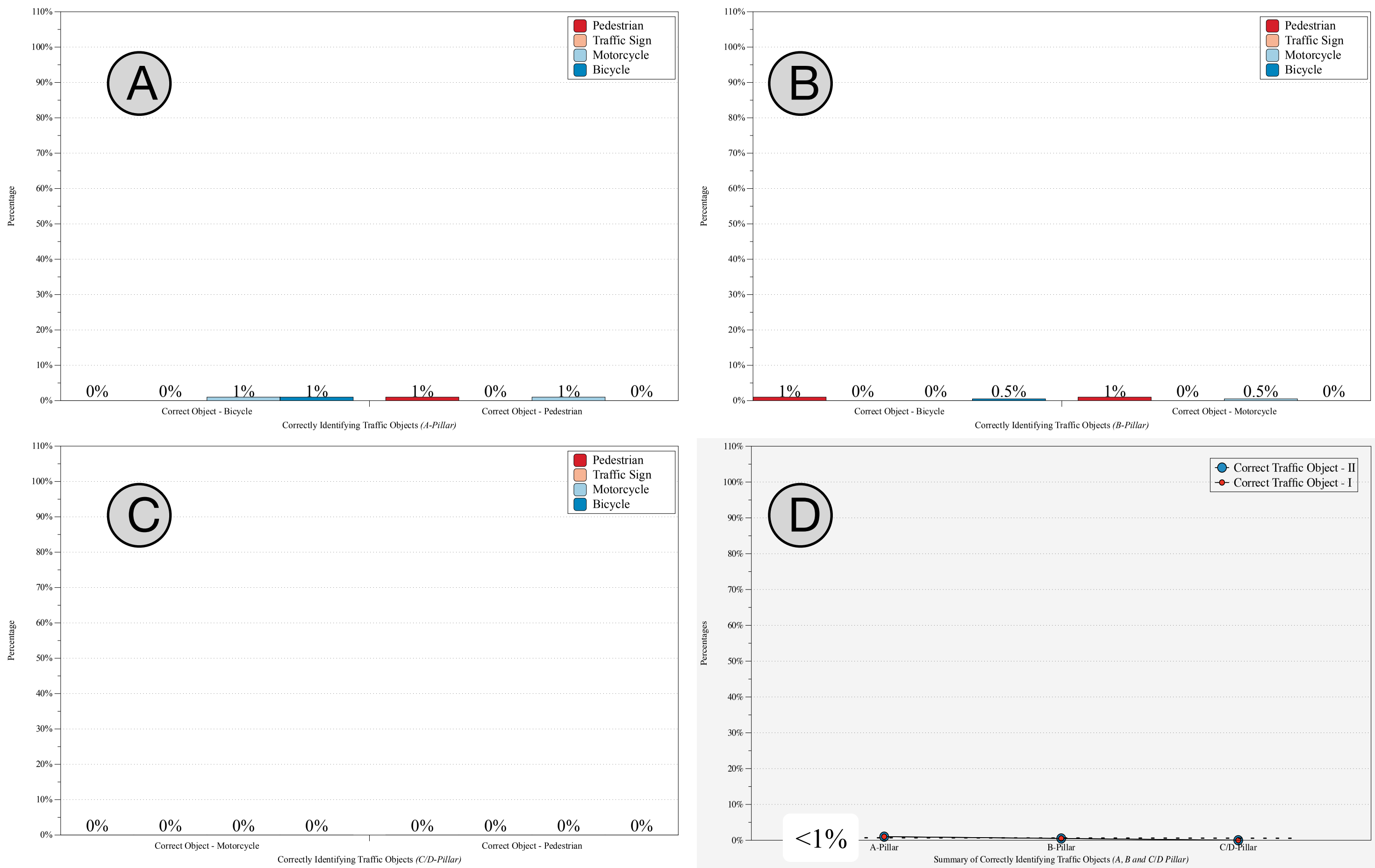

Figure 7.11. A), B) and C) represents improvements on correctly identifying traffic objects between Old and Old Pillar design for A, B and CD pillar respectively. D) represents summary of traffic object detection between A, B and C pillars for Old Pillar design.

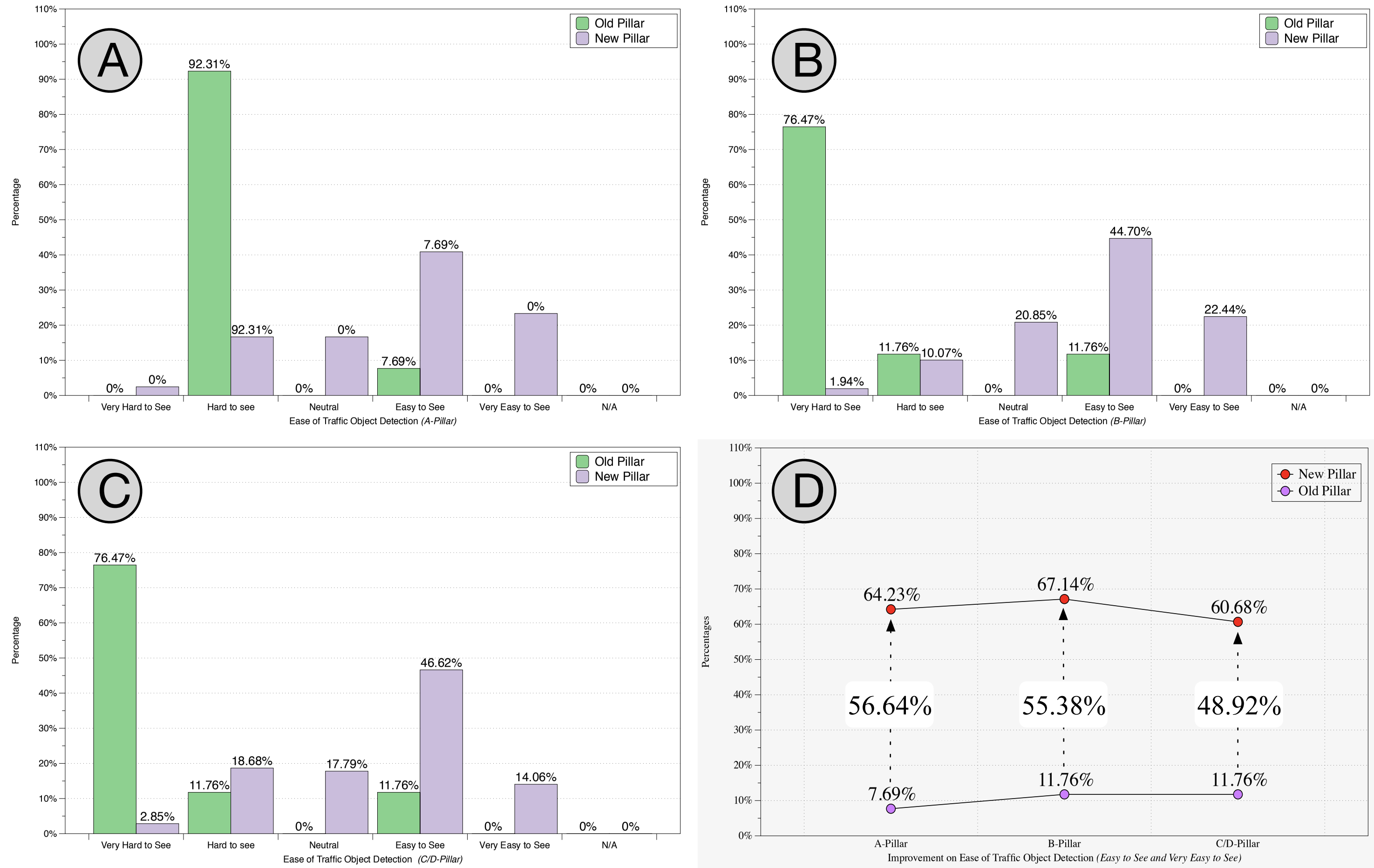

Figure 7.12. A), B) and C) represents differences in ease of detecting traffic objects between Old and New Pillar design. D) summarizes combined (Easy to See and Very Easy to See) percent improvement on ease of detecting between Old and New Pillar design.

Results show that New Pillar design generates higher ease of detection across A, B and CD pillars. One can see that subjects have consistent agreement on detecting traffic objects on Old Pillar is harder than detecting traffic objects on New Pillar. Figure 7.12 shows distribution of scores on A, B and CD pillars for Old and New Pillar at A), B) and C) respectively. Summary of combined results for 'Easy to See' and 'Very Easy to See' in plot D) presents 50% improvement on ease of detecting traffic objects between Old and New Pillar design.

7.7.2 Cooper Harper test

Background on Cooper-Harper test

Cooper-Harper test is originally used in aviation industry to evaluate how pilot-aircraft interactions affect handling qualities of aircraft [169]. A modified version of Cooper-Harper test was used in this experiment to assess whether pillar designs affect driver's visual performance in detecting traffic objects. In modified Cooper-Harper test pillars were considered as a cockpit design attribute. Subjects were asked to rate design changes between different pillar models. Each subject completed two Cooper-Harper test for A, B and CD pillars associated with Old and New Pillar model.

This test also assesses whether pillar design provides desirable design feature to assist drivers in detecting traffic objects. If a pillar design provides ease of detecting traffic objects, thus, it is associated with lower visual workload. Within the Cooper Harper flowchart, high scores indicate design deficiencies, thus, pillar design does not effectively assist drivers. Lower scores are associated with good pillar design, which provides some degree of visual assistance to drivers. The degree of design success is determined by the Cooper-Harper rating. Higher Cooper Harper rating suggests that a design change is required. Figure 7.13 shows a modified Cooper-Harper flowchart distributed for A-pillar, for Old and New Pillar model. Similarly, same flowchart was used for B and CD pillars with associated images representing traffic environment and pillar model.

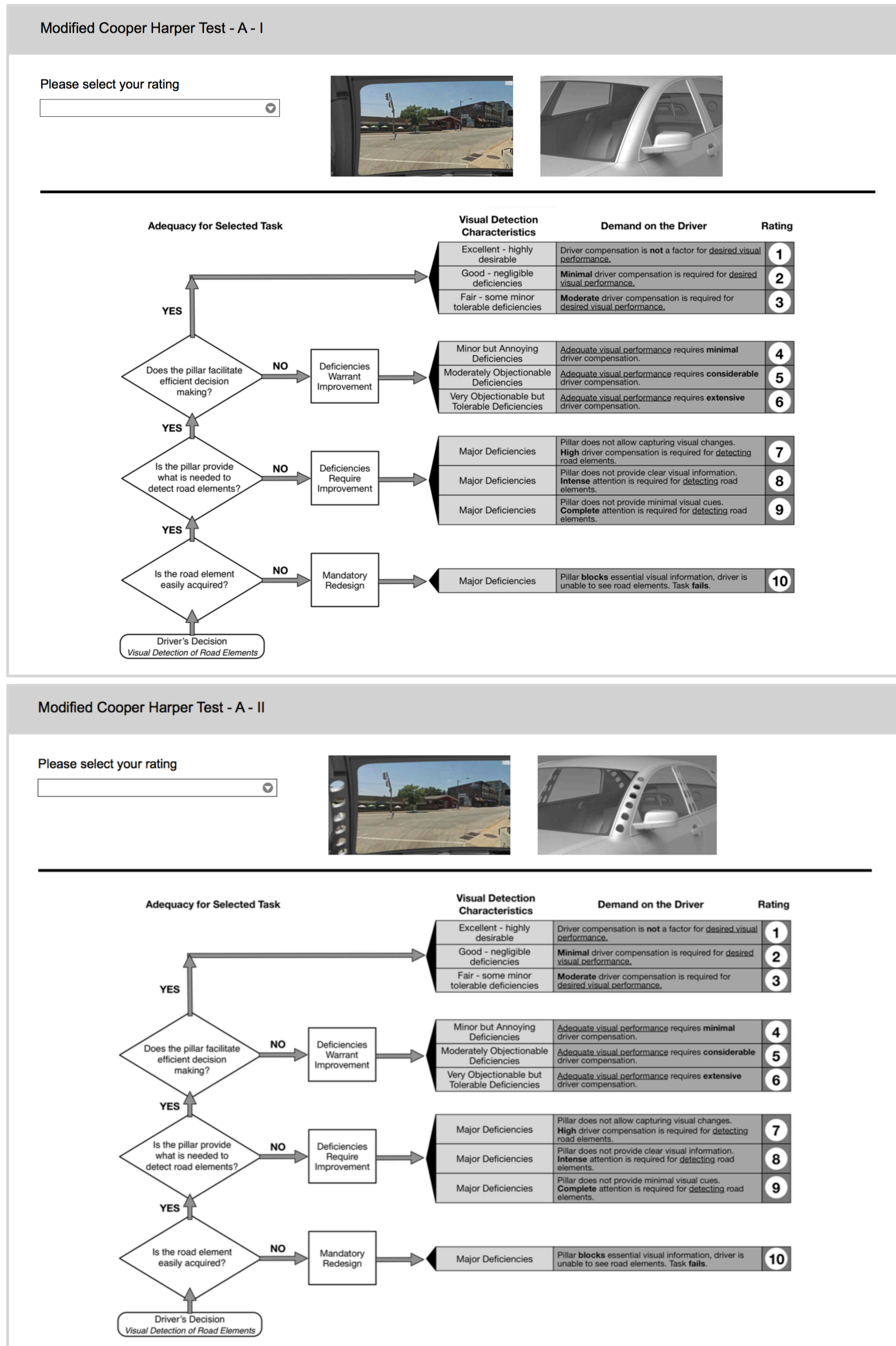

Figure 7.13. Cooper-Harper flowchart was used for evaluating how design changes were perceived by subjects between Old Pillar and New Pillar model for A-pillar. Same flowchart combinations were used for B and CD pillar.

Results on Cooper-Harper test

Cooper Harper test builds on top of the knowledge gained from Experiment-I data. It provides additional information about subjects' opinion on whether each pillar design (Old and New pillar) offers sufficient adequacy to drivers (subjects) in detecting traffic objects. It measures whether pillar design has deficiencies or desirable design features in terms of providing visual assistance to drivers. Subjects used Cooper Harper flowchart and ranked each pillar model in terms of visual demands on the driver. If a pillar design provides ease of detecting traffic objects, it reduces the mental workload required for detecting traffic objects in the simulation. Within the Cooper Harper flowchart, higher scores indicate design deficiencies. Lower scores are associated with good pillar design, which provides visual assistance to drivers. Thus, high Cooper Harper rating scores suggest that a design change is required.

Table 7.4
Distribution of Cooper Harper scores

Pillar Type	Pillar Design	N	Min.	Max.	Mean	Std. Dev.
A	Old Pillar	48	2	10	8.23	2.53
	New Pillar	48	1	8	3.38	1.69
B	Old Pillar	48	2	10	8.54	2.05
	New Pillar	48	1	8	3.23	1.55
CD	Old Pillar	48	3	10	8.98	1.82
	New Pillar	48	1	10	4.29	2.15

Table 7.4 shows that on average Old Pillar received a higher Cooper Harper score when compared to New Pillar scores. Higher Cooper Harper scores indicate a design change is required, which refer to a high mental workload is required to correctly identify traffic objects. New Pillar design yielded around 40% improvement across A, B and CD Pillar (Figure 7.14).

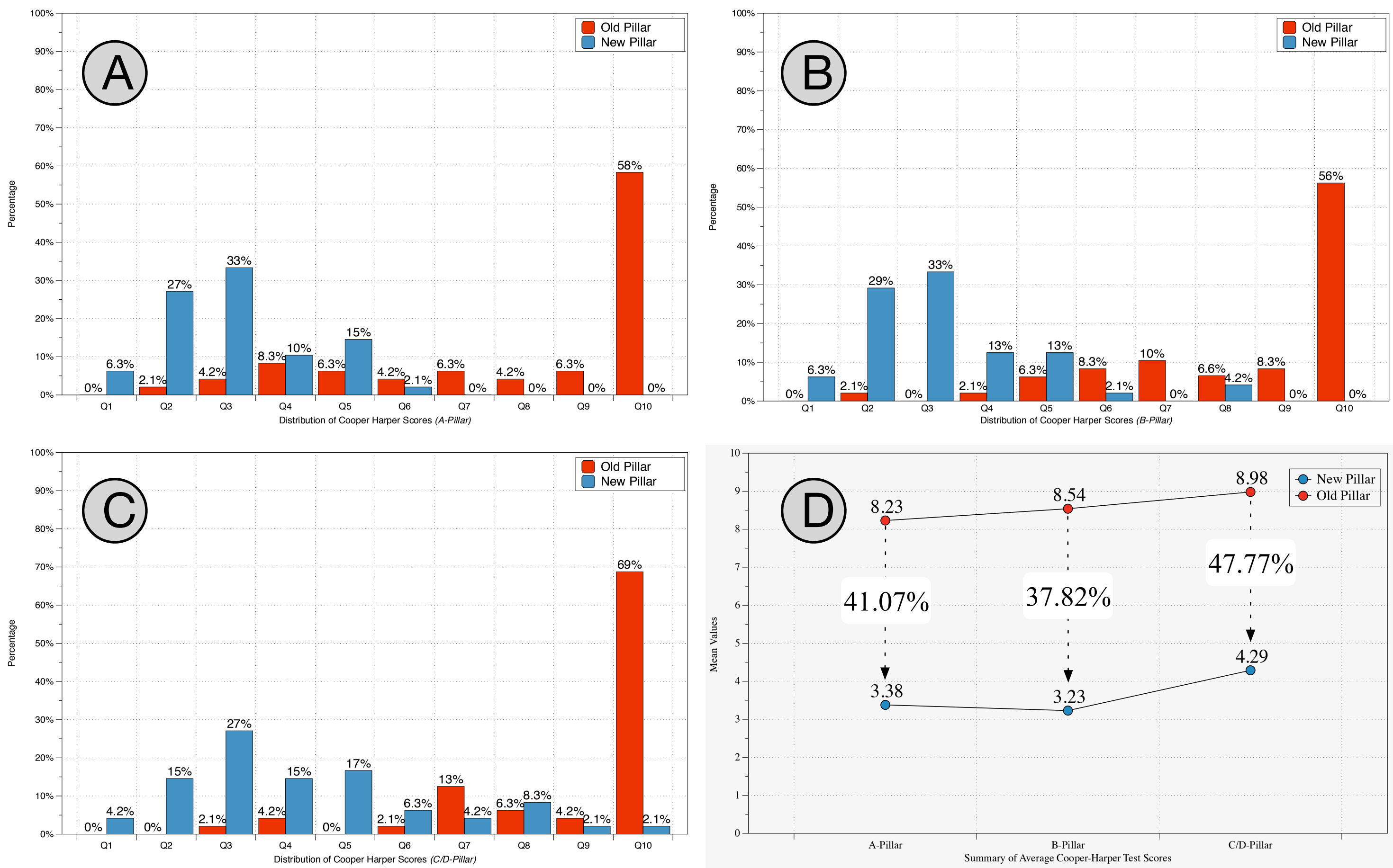

Figure 7.14. A), B) and C) show distribution of Cooper Harper scores for A, B and CD pillars. D) summarizes improvement of design deficiencies and lower mental workload between Old and New Pillar design.

7.7.3 Pillar design review

Background on pillar design review

Pillar models used in this experiment were evaluated via set of questionnaire. The goal of this questionnaire was to capture user preference related data regarding visibility, safety and aesthetics of the pillar models. There were two types of pillar design review/questionnaire that represent: 1. Old Pillar and 2. New Pillar design (Figure 7.15).

These questionnaires were distributed at the end of the subject data collection. After subjects completed Experiment-I and first two sub-experiments of Experiment-II, they were asked to start pillar design review (last sub-experiment of Experiment-II). Each questionnaire was designed in a Likert scale from zero to seven - ranging from 'Strongly Agree' to 'Strongly Disagree' respectively. Also, 'Not Applicable' option was provided to subjects in case the question is not applicable.

Although subjects don't have any daily driving experience with New Pillar design, they were asked to use their discretion and experienced gained throughout this study while reviewing visibility, safety and aesthetics related attributes of New Pillar design. During questionnaire session, subjects were encouraged to look at pillar designs on CAD environment and to ask questions to obtain a better understanding of the characteristics of each pillar.

An additional usability related form was distributed after pillar design review/questionnaire was completed. This form was composed of a two-page long general questionnaire, which was conducted to collect subjects overall feedback about their daily driving experiences regarding pillar obscuration problems (Figure 7.16). This portion of the questionnaire was not used in statistical analysis. It was distributed capturing subjects' opinion on pillars related driving obscuration experiences and feedback on about overall experimental procedures.

PILLAR MODEL - I

VISIBILITY AND DETECTION OF A & B PILLAR

	Strongly Agree	Agree	Slightly Agree	Neutral	Slightly Disagree	Disagree	Strongly Disagree	N/A
1. In this simulation experiment it was easy to detect/see traffic objects.	O	O	O	O	O	O	O	O

VISIBILITY AND DETECTION OF C/D PILLAR

	Strongly Agree	Agree	Slightly Agree	Neutral	Slightly Disagree	Disagree	Strongly Disagree	N/A
2. In this simulation experiment it was easy to detect/see traffic objects when parallel and/or backing up.	O	O	O	O	O	O	O	O

SAFETY AND AESTHETICS

	Strongly Agree	Agree	Slightly Agree	Neutral	Slightly Disagree	Disagree	Strongly Disagree	N/A
3. This pillar design provides a safe driving environment.	O	O	O	O	O	O	O	O
4. This pillar design provides comfortable driving experience.	O	O	O	O	O	O	O	O
5. This pillar design is aesthetically pleasing.	O	O	O	O	O	O	O	O

PILLAR MODEL - II

VISIBILITY AND DETECTION OF A & B PILLAR

	Strongly Agree	Agree	Slightly Agree	Neutral	Slightly Disagree	Disagree	Strongly Disagree	N/A
1. In this simulation experiment it was easy to detect/see traffic objects.	O	O	O	O	O	O	O	O

VISIBILITY AND DETECTION OF C/D PILLAR

	Strongly Agree	Agree	Slightly Agree	Neutral	Slightly Disagree	Disagree	Strongly Disagree	N/A
2. In this simulation experiment it was easy to detect/see traffic objects when parallel and/or backing up.	O	O	O	O	O	O	O	O

SAFETY AND AESTHETICS

	Strongly Agree	Agree	Slightly Agree	Neutral	Slightly Disagree	Disagree	Strongly Disagree	N/A
3. This pillar design provides a safe driving environment.	O	O	O	O	O	O	O	O
4. This pillar design provides comfortable driving experience.	O	O	O	O	O	O	O	O
5. This pillar design is aesthetically pleasing.	O	O	O	O	O	O	O	O

Figure 7.15. Pillar Design Review form was distributed to subjects to evaluate Old Pillar and New Pillar model in terms of visibility, aesthetics and safety. Photorealistic rendering of the reference vehicle, both representing Old Pillar and New Pillar model, were provided at the top of the form. Each image clearly demonstrates differences between solid and see-through pillars models for A, B and CD pillar.

USER EXPERIENCE QUESTIONNAIRE

VISIBILITY AND DETECTION OF A/B PILLAR

	Strongly Agree	Agree	Slightly Agree	Neutral	Slightly Disagree	Disagree	Strongly Disagree	N/A
1. In the car I drive it is easy to detect/see traffic objects.	○	○	○	○	○	○	○	○
2. In the car I drive A/B pillars reduces my visibility of detecting/seeing traffic objects.	○	○	○	○	○	○	○	○
3. In the car I drive A/B pillars propose near misses or accidents because objects being obscured.	○	○	○	○	○	○	○	○
4. This simulation created similar visual effects/perception for detecting/seeing traffic objects.	○	○	○	○	○	○	○	○

VISIBILITY AND DETECTION OF C/D PILLAR

	Strongly Agree	Agree	Slightly Agree	Neutral	Slightly Disagree	Disagree	Strongly Disagree	N/A
5. In the car I drive it is easy to detect/see when parallel and/or backing up.	○	○	○	○	○	○	○	○
6. In the car I drive C/D pillars reduces my visibility of detecting/seeing traffic objects when backing up.	○	○	○	○	○	○	○	○
7. In the car I drive C/D pillars propose near misses or accidents because objects being obscured.	○	○	○	○	○	○	○	○
8. This simulation created similar visual effects/perception for detecting/seeing traffic objects.	○	○	○	○	○	○	○	○

SAFETY AND AESTHETICS

	Strongly Agree	Agree	Slightly Agree	Neutral	Slightly Disagree	Disagree	Strongly Disagree	N/A
9. In the car I drive it pillars propose safe driving environment.	○	○	○	○	○	○	○	○
10. In the car I drive pillars provide comfortable driving experience.	○	○	○	○	○	○	○	○
11. In the car I drive pillar designs are aesthetically pleasing.	○	○	○	○	○	○	○	○

PRODUCT FEEDBACK

	Strongly Agree	Agree	Slightly Agree	Neutral	Slightly Disagree	Disagree	Strongly Disagree	N/A
12. New pillar design is effective in detecting traffic objects.	○	○	○	○	○	○	○	○
13. New pillar design is effective in increasing my visibility.	○	○	○	○	○	○	○	○
14. New pillar design is effective in improving obscuration problem.	○	○	○	○	○	○	○	○

CONCENTRATION LEVEL

	Significantly Higher than Normal	Higher than Normal	Slightly Higher than Normal	Neutral	Slightly Lower than Normal	Lower than Normal	Significantly Lower than Normal	N/A
15. In the car I drive my concentration level is...	○	○	○	○	○	○	○	○
16. In this simulation my concentration level was...	○	○	○	○	○	○	○	○

Figure 7.16. A two page User Experience Questionnaire was distributed to subjects' at the very end of Experiment-II. Subjects were asked to provide a feedback about their daily driving experiences. This includes a general understanding or perception about pillar obscuration problem and their perception about visibility, aesthetics and safety aspects of pillars. This questionnaire is used as a method of collecting users daily experiences about pillar obscuration problem.

Background on Cronbach's alpha test

Cronbach's Alpha test determines the average correlation found in data. It is often used in a survey or rating type data to check how reliability associated with the variation is accounted [170]. Especially, it is used in cases where same set of questions/tasks are re-administered in a mixed manner to the same respondent [171]. The underlying goal of this study was to assess whether the same set of items presented to subjects generate similar responses. Equation 7.1 was used for conducting Cronbach's Alpha test.

$$\alpha = \frac{n}{n-1} \times \left(1 - \frac{\sum_{i=1}^{n} {\sigma_{y}}_{i}^{2}}{\sigma_X^2} \right) \tag{7.1}$$

where,

n:	sum of components or test items
σ_X^2:	variance of the observed scores
$\sigma_{y_i}^2$:	variance of the item i

Table 7.5
Classification of Cronbach's Alpha range

ICC Range	Meaning	Notes
(0.80, 1.00]	Good	High inter-rater reliability
(0.50, 0.80]	Acceptable	Modest inter-reliability
(0.30, 0.50]	Poor	A reliability is present, but not high enough
(0.00, 0.30]	Unacceptable	No or few correlation

Correlation values of Cronbach's Alpha test can range from 0 to 1, with values close to 1 represent a high inter-rater reliability. Although there is no universally agreed range, a correlation value larger than 0.8 is generally considered a good indication of internal consistency [172]. In this dissertation scores on Table 7.5 were used.

Results on Cronbach's alpha

Cronbach's alpha results show that there is an acceptable consistency on subject's responds to questions provided on design questionnaire/review. One can see from Table 7.6 that design reviews have correlations (Cronbach's Alpha and Inter-Class) between 0.46 and 0.74, which demonstrates a moderate internal consistency.

Table 7.6
Cronbach's Alpha and Inter-Class Correlation scores

	Cronbach's Alpha	Inter-Class Correlation
Old Pillar Review (Q1 to Q5)	.74	0.68
New Pillar Review (Q1 to Q5)	.55	0.46

Results on pillar design review

Results showed that subjects rate New Pillar design higher than Old Pillar design in every category (Table 7.17). Across all pillar types (A, B and CD), New Pillar received higher average ratings when compared to Old Pillar design.

Table 7.7
Descriptive statistics for Old Pillar design review

	N	Minimum	Maximum	Mean	Std. Deviation
Q1	48	2	6	2.83	.808
Q2	48	2	7	2.90	1.242
Q3	48	2	6	2.88	.866
Q4	48	2	6	3.08	1.088
Q5	48	0	7	4.31	1.504
Total	240	0	7	3.20	1.255

Table 7.8
Descriptive statistics for New Pillar design review

	N	Minimum	Maximum	Mean	Std. Deviation
Q1	48	3	7	6.42	.871
Q2	48	2	7	6.02	1.041
Q3	48	6	7	6.46	.504
Q4	48	2	7	5.88	1.196
Q5	48	2	7	4.50	1.786
Total	240	2.00	7.00	5.8542	1.35359

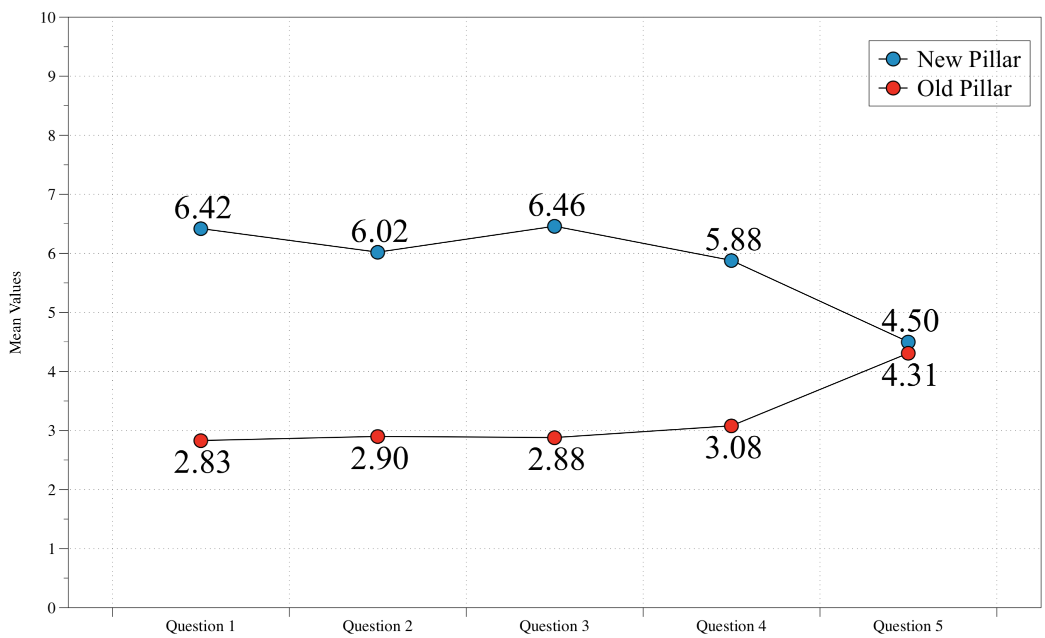

Figure 7.17. Comparison of mean ratings showed that New Pillar design scored higher than Old Pillar design in each category.

7.8 Results and Discussions

Subjects data gathered through three sub-experiments showed that New Pillar model with see-through gaps provided a means of detecting traffic objects better than Old Pillar model with solid pillar design. Traffic Object Detection experiment results showed that there was on average more than 95% improvement in detecting traffic objects when New Pillar design model was used. Amongst those who detected traffic objects with New Pillar design, roughly 94% of these subjects made a correct detection. In contrast to New Pillar design, traffic object detection rate was less than 1% when subjects Old Pillar model was used. Results also showed that subject who correctly detected traffic objects found that it was easier to detect traffic objects when New Pillar was projected on LCD screen. New Pillar model generated around 50% higher in ease-of-detection results when compared to Old Pillar design (Figure 7.18).

Cooper-Harper tests results showed that subjects rated New Pillar design model better than Old Pillar design in terms of providing visual assistance to drivers when detecting traffic objects. Across all pillar types (A, B and CD pillars), New Pillar design received on average 45% lower subject ratings (Figure 7.14). (In this Cooper-Harper test, lower the ratings better the design changes.)

Similar results were also obtained at pillar design questionnaire/review experiment. Across all design questions provided in design questionnaire/review, subjects rated New Pillar design higher than Old Pillar design. Across all pillar types (A,B and CD pillars), average scores were consistently higher for visibility, detecting traffic objects and safety related design attributes. Only aesthetics received a slightly higher score (Figure 7.17).

Percentage Averages Results for Traffic Object Detection Experiment

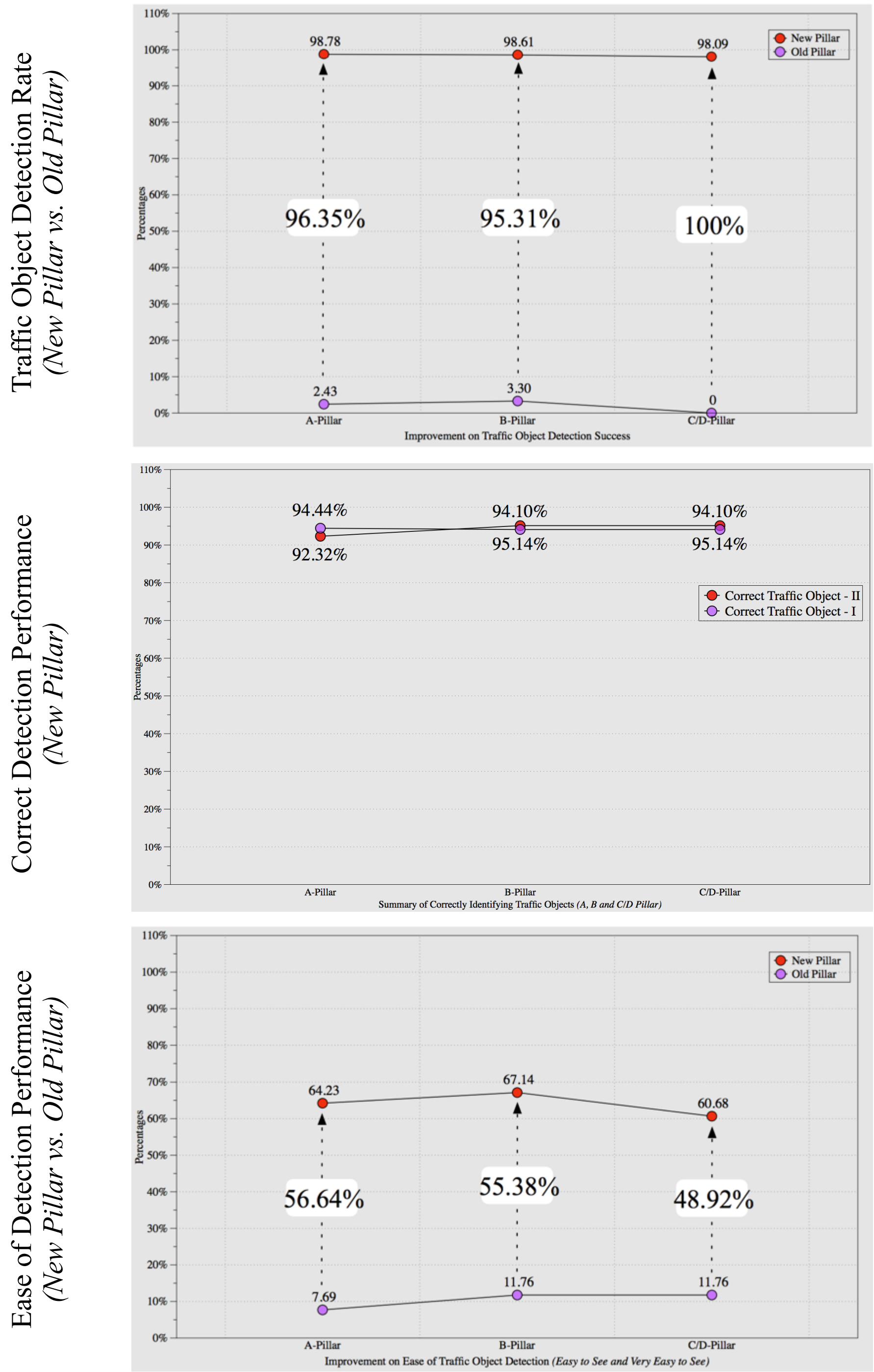

Figure 7.18. Comparison of averages (in percentages) of traffic detection success, correct detection performance and ease of detection success in Experiment-II.

8. EXPERIMENT - III

8.1 Introduction

8.1.1 Overview

One of the objectives of this study is to determine whether proposed pillar design cause any changes in the structural integrity of the referenced vehicle. New Pillar design uses cut-out sections to provide a see-through experience in contrast to solid pillars. A major concern is whether vehicle frame resist forces generated during a collision. To validate changes occur in structural integrity, a FEA study was conducted on solid and see-through pillar frames associated with Old Pillar model and New Pillar model.

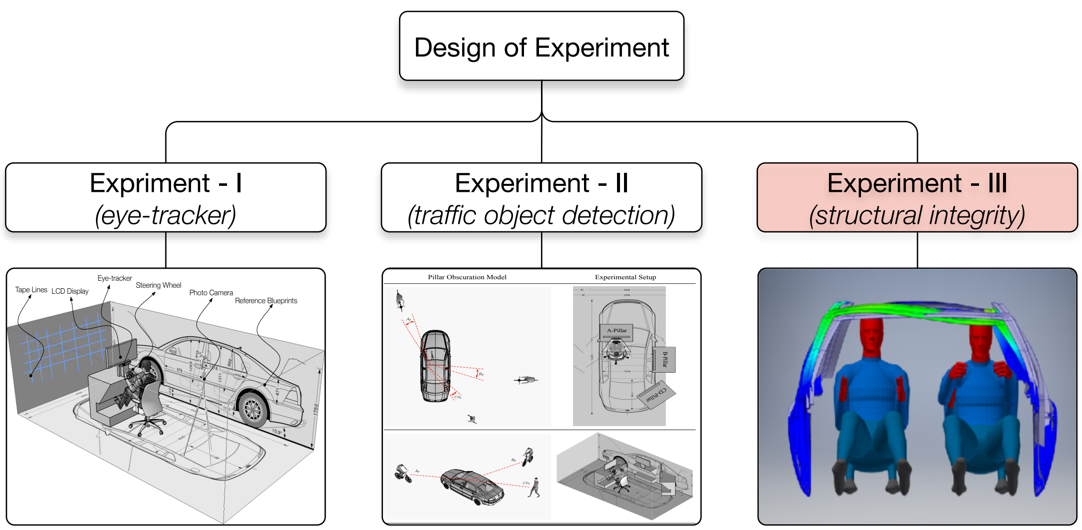

Figure 8.1. Experiment-III is a roof-crush simulation experiment. No subject data collection was involved in this experiment.

8.1.2 Connections to human-in-the-loop design framework

Experiment-II demonstrates how an structural integrity related analysis could be connected into human-in-the-loop design framework. In this simulation experiment reference vehicle went through a roof-crush test. Shaded area in Figure 8.2 shows how data collected through structural integrity test was linked to the design process. Similarly, Figure 8.3 demonstrates a visual synopsis of how Experiment-III was integrated to DHM within human-in-the-loop framework.

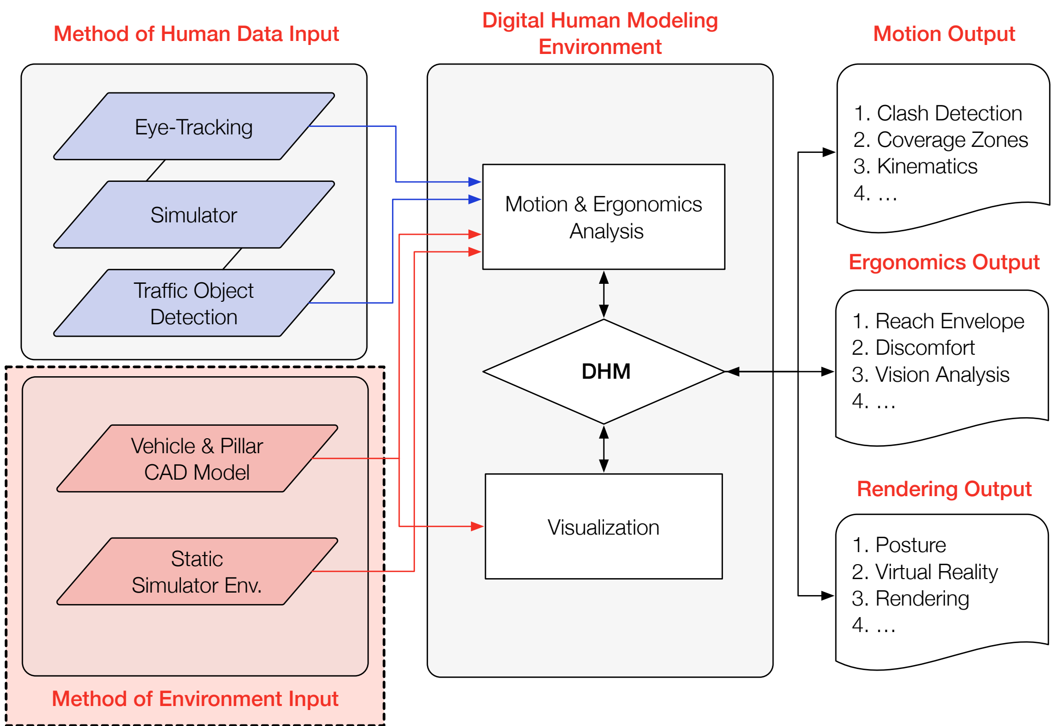

Figure 8.2. Shaded area in red (inside dashed lines) represents how Experiment-III was integrated to data flow process within human-in-the-loop framework. Experiment-III captured structural integrity related data through Finite Element Analysis (FEA) study.

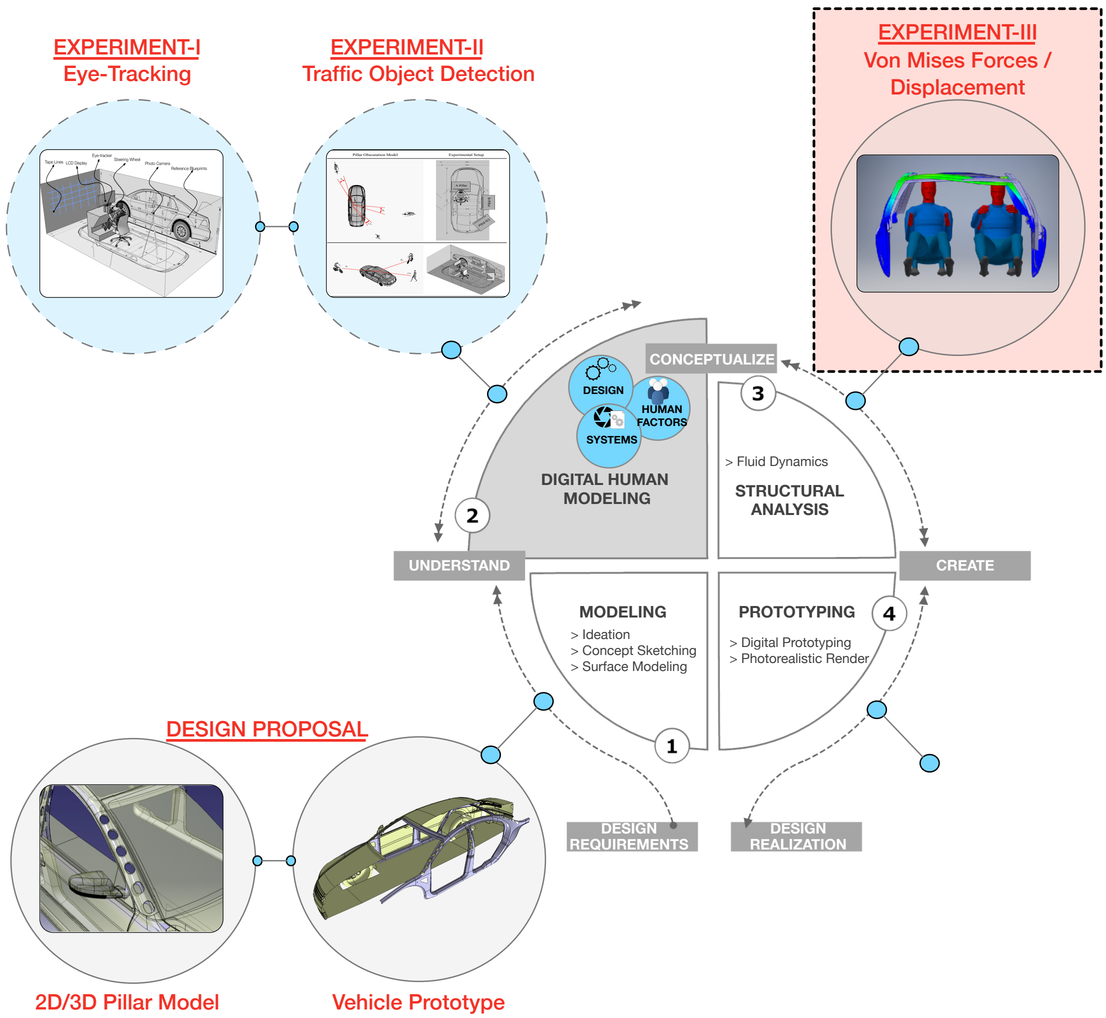

Figure 8.3. Shaded area in red (inside dashed lines) represents which portion of the human-in-the-loop design framework was used to integrate structural integrity related data to overall design process.

8.2 Experimental Setup

8.2.1 Roof-crush simulation

In Experiment-III, structural integrity of pillar designs (Old vs. New Pillar) were compared in terms of reaction forces and displacements due to applied static loads. The main goal of this analysis is to demonstrate whether New Pillar design with see-through-gaps compromises structural integrity based on roof-crush criteria. A series of Finite Element Analysis (FEA) test were conducted to determine how Von Mises stresses and displacements vary between Old Pillar and New Pillar design.

The FEA test was based on Federal Motor Vehicle Safety Standards (FMVSS) of roof-crush resistance test (article No-216), which is a quasi-static compression test conducted on a vehicle roof. This experiment did not involve any human-subject data collection. Instead, DHM manikins representing subjects' height and weight were used with CAD vehicle frame models. A DHM manikin representing 95^{th} percentile male subject from CATIA anthropometric library. This manikin was constructed based on largest percentile of subject's participated this study.

8.2.2 Roof-crash test criteria

According to the Federal Motor Vehicle Safety Standard (FMVSS), the roof-crush resistance test (article No.216) mandates that a passenger car requires to withstand a load of 1.5 times the vehicle's unloaded weight multiplied by 9.8 (or maximum 22,240Newtons) in kg with no more than 125mm of maximum displacement at roof-crush area. The maximum displacement is the resultant vector of displacements in X, Y and Z axes associated at roof section.

In this study, static loads were applied in increasing order. The maximum applied static load on the FEA model value was converted to a vector force through multiplying curb weight of the car model (≈1500kg) by FMVSS safety ratio of 1.5 and by 9.8 (gravity constant), which equals to 22,000N. The resultant vector has 3 dimensional axial components, which are oriented with the angle between the horizontal force vector and vertical force vector of 65 degrees. Similarly, the force vector makes a longitudinal angle of 5 degrees with the roof-base. Figure 8.4 shows vector force applied on roof top of the CAD model, which represents a virtual resultant force similar to a resultant force generated through a hydraulic crush test device used during the actual FMVSS roof-crush test.

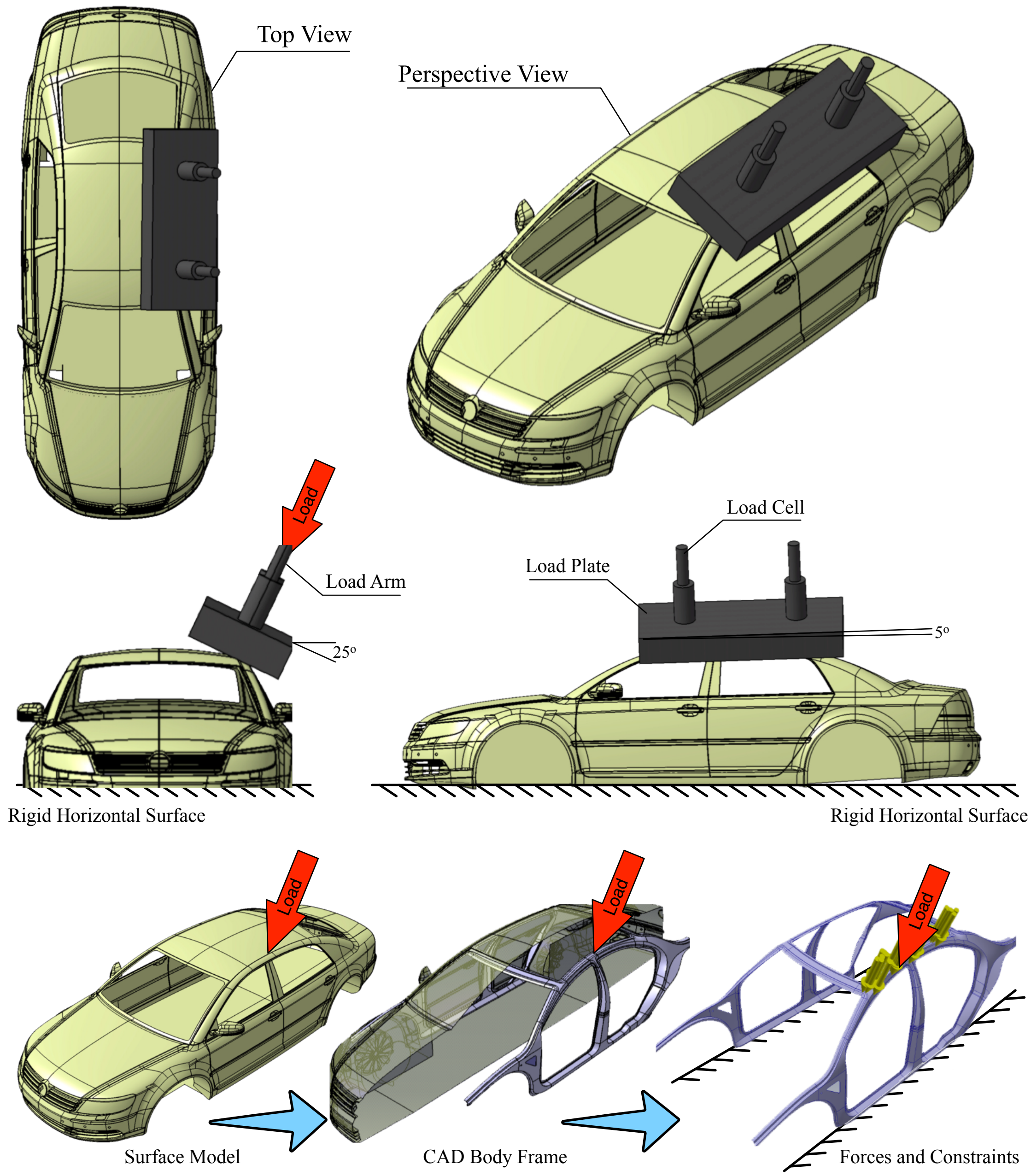

Figure 8.4. Test device location and application to the body frame represented with associated angles. 3D solid body frame was loaded with incremental static loads. Virtual load cell and load plate with associated angles are located on roof-top based on FMVSS resistance test requirements.

8.3 Procedure

A generic body frame that overlaps with surface model used in this study. The body frame represents current pillar design (Old Pillar) found in family cars, and used for benchmarking the New Pillar design. For New Pillar design, each see-through-gap that overlaps with the surface model were drilled (cut-out) from the body frame (Figure 8.5). Throughout this study High Strength Low Alloy (HSLA) steel was used as applied material with yield strength of 420MPa. HSLA steel is commonly used in pillars and various body frame components that require high crash-worthiness and/or rigidity. Von Mises stress distributions (in MPa) and displacements (in mm) were measured to analyze the effects of static loads applied on body frame.

The body frame was composed of multiple sub-assembly models (CAD models) that were bonded together (rigidly constrained) (Figure 8.6). Surfaces located underneath the body frame were anchored to the simulation environment with fixed constraints, which prevented body frame from translating and/or rotating. Fixed constraints act as a rigid support between the body frame and the virtual ground. Static loads were applied to adjacent surfaces that made up A, B and CD pillars. Each static load was distributed homogeneously on adjacent surfaces. Throughout this study, linear structural FEA method was conducted, which assumes linear material properties, small deformations of parts compared to overall dimensions of the model, static loading (no dynamic loads), no affects of temperature, and no buckling.

CAD body frame associated to Old and New Pillar designs were loaded with static loads from 1650kg to 2250kg with increments of ≈200kg. Figure 8.6 shows constraints and vector forces applied on body frame. During FEA analysis material properties, boundary conditions and applied loads were kept identical. The only difference between two FEA analysis between Old Pillar and New Pillar was see-through-holes found on New Pillar design.

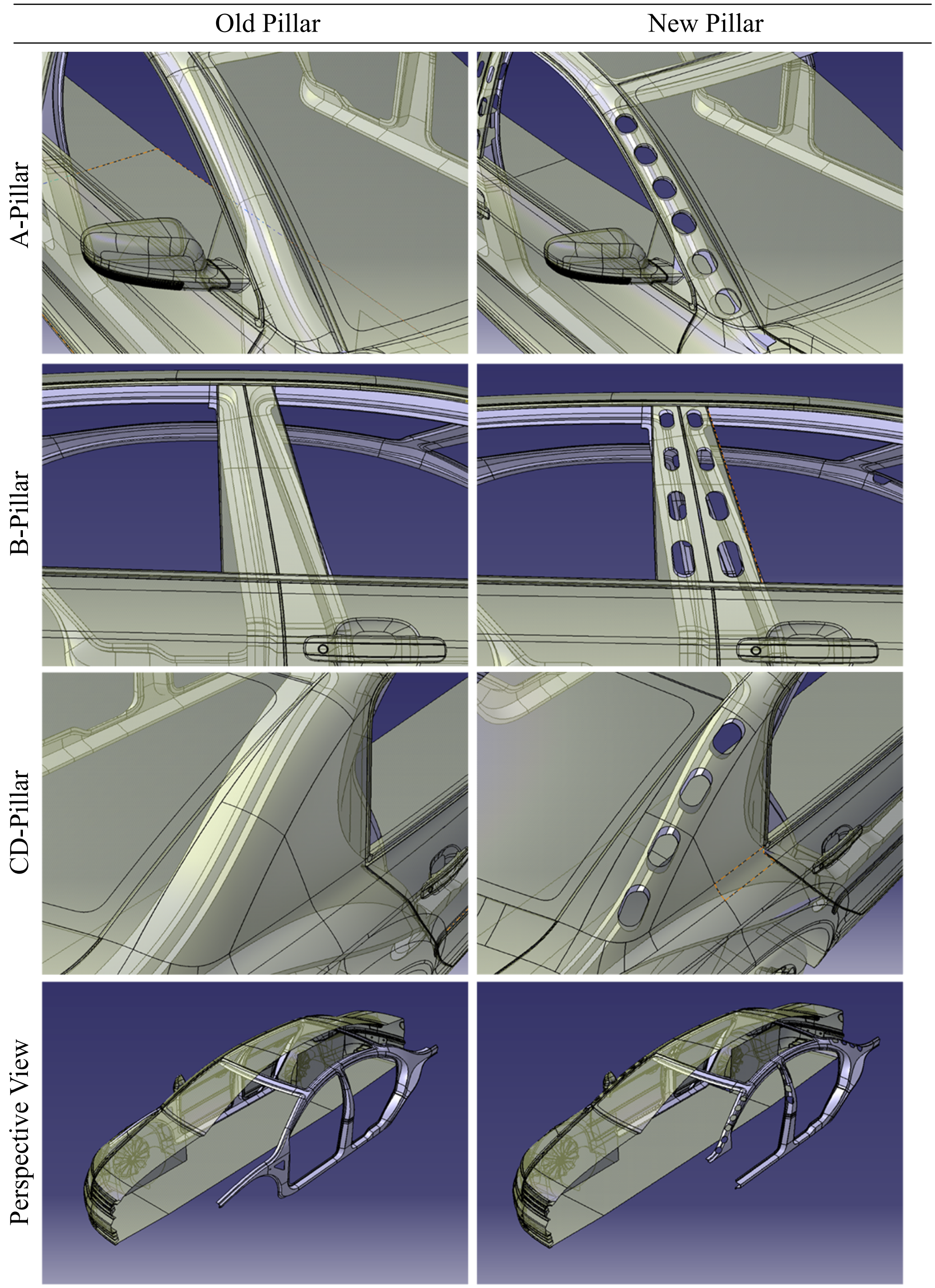

Figure 8.5. CAD body frame represents the structural frame (chassis) of the vehicle based on the surface model. See-through-gaps are drilled out to create the body frame associated to New Pillar model.

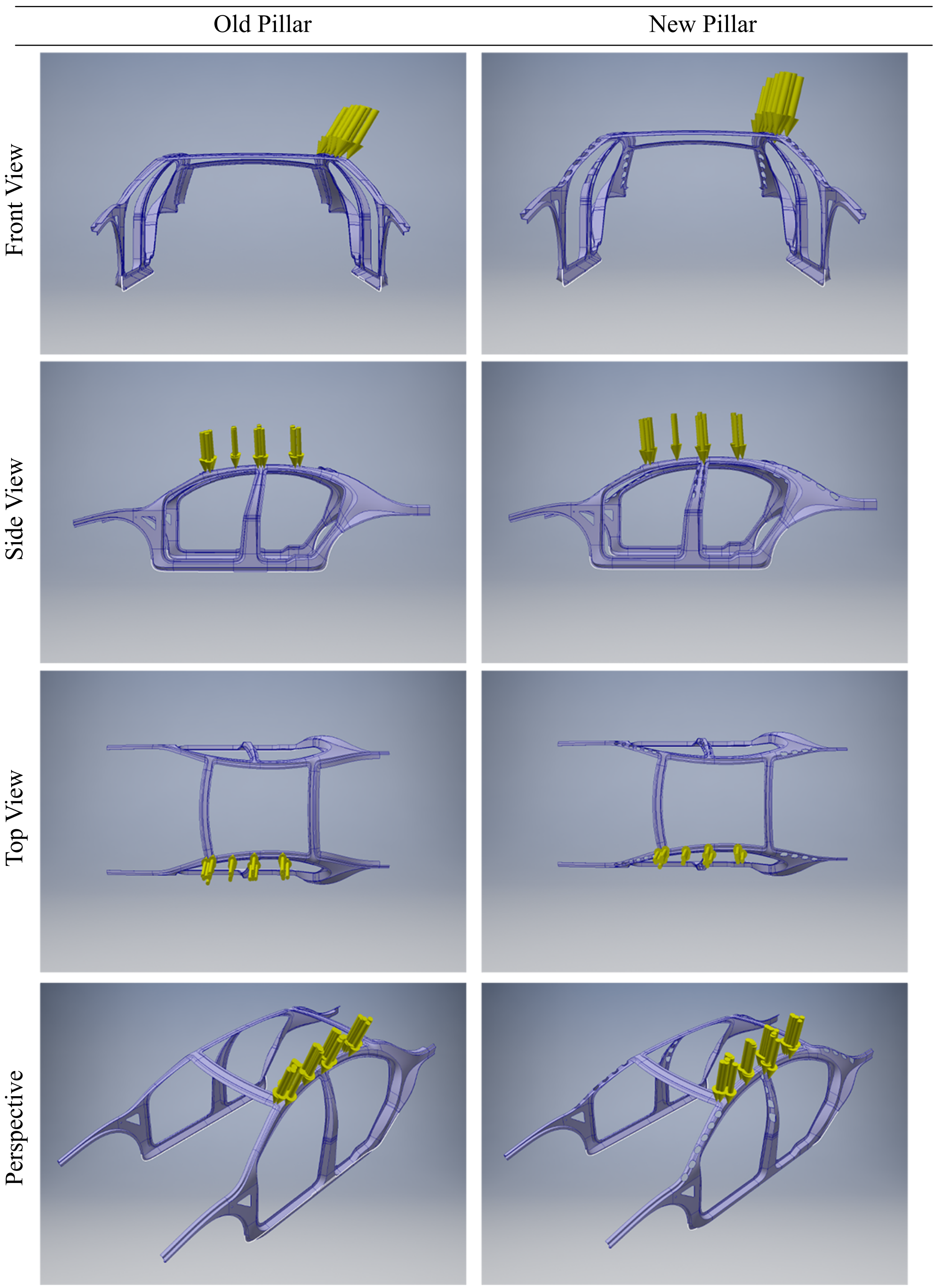

Figure 8.6. Static loads were applied on roof top with angular values based on FMVSS resistance test requirements.

8.4 Variables

During Experiment-III, roof-crush test simulation results were grouped into two variables: 1. Von Misses Forces and 2. Displacement. Von Mises Force data represents mean values of reaction forces generated during roof-crush test. These force vales are measured in MPa. Similarly, displacement data provides information about deformation occur on vehicle structure as a result of roof-crush loading. Displacement data is measured in millimeters.

Table 8.1 summarizes variables, units, and hypotheses associated with Finite Element Analysis (FEA) conducted in Experiment-III.

Table 8.1
Types of data, variables, units, and hypotheses associated with experiments conducted in this study

Dependent Variables	Type	Hypotheses
Displacement	Millimeters	H4
Stresses	MPa	H4

8.5 Experimental Design

Experiment-III was composed of a FEA study that represents a roof-crust scenario based on FMVSS article 216. Reaction forces and displacements associated with applied load were analyzed to monitor whether vehicle structure meet roof-crush test requirements or not. Structural integrity related data was plotted and compared with required roof-crush test limits under varying loading conditions.

Table 8.2: Summary of methods of measurement, goal of measurement, statistical, numerical methods

Method of Measurement	Goal of Measurement	Statistical, Numerical and Visual Methods
FEA	Structural Integrity	Descriptive Statistics
		Stress & Displacement
		Bar Graphs
	Correlation	ICC & Pearson

8.6 Participants

No subjects were involved to this experiment. Experiment-III was a simulation experiment and did not require any subjects for data collection. A digital manikin dummy model was used as a figurative representation of a 95% male subject. This manikin was used throughout simulation process.

8.7 Data Analysis and Statistical Techniques

8.7.1 Background on finite element analysis

Finite Element Analysis (FEA) is a computerized method of predicting forces acting on solid bodies or meshed-surfaces. FEA analysis is based on partial differential equations technique for approximating the boundary value problems. It is an ideal tool for analyzing complex geometries, detailed material properties and complicated applied forces [25, 173, 174]. FEA methods use a complex system of surface topology (mesh) that is composed of nodes. Nodes are assigned with certain size (density) throughout the mesh, depending on the anticipated stress levels associated with particular topology. Depending on the generated stresses, nodes can have coarse or very fine character (Figure 8.7). In general, finer the mesh, higher the precision of predictions. There are also various numerical approximation techniques and solvers (mesh-free methods, stretch grid method, smoothed finite elements,etc.) associated with different FEA methods.

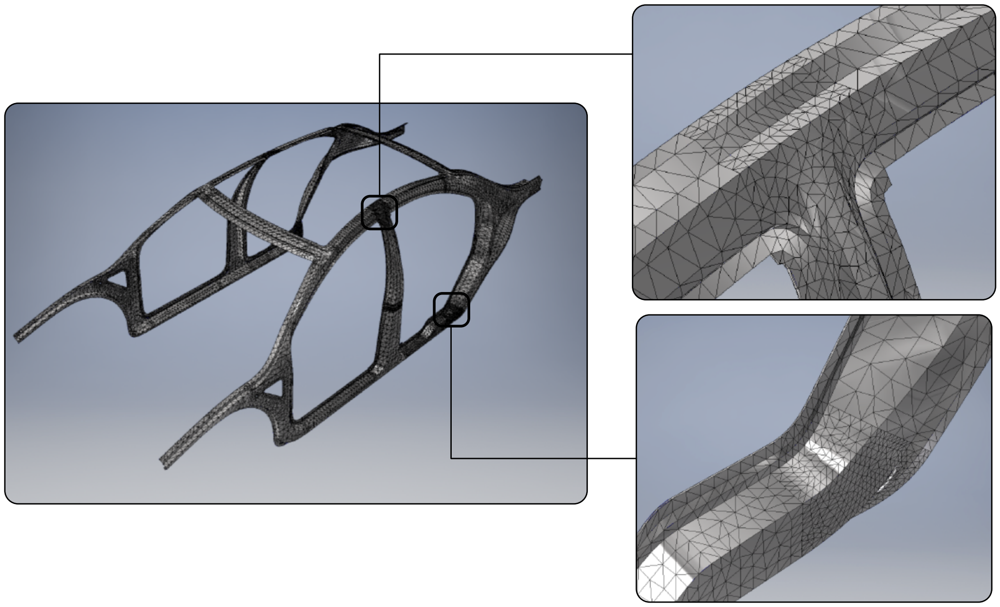

Figure 8.7. Areas of fine and coarse mesh associated to FEA analysis. One can see the transition from coarse to finer mesh on joints where pillars are connected to the body frame.

In the case of a complex loading scenario with 3-dimensional components, three different stresses on normal directions (X, Y and Z), as well as up to three different shear stresses on shear directions (X on Y, Y on Z and X on Z) are observed. Thus, up to six stress values can be represented on a 3D body (Figure 8.8).

8.7.2 Von Mises stress analysis

In theory, each stress value associated with a 3D solid body can be solved individually by using strength of materials equations. However, as the surface topology and variables of interest get more complex, traditional strength calculations become time consuming. In addition, general strength of materials equations are cumbersome in

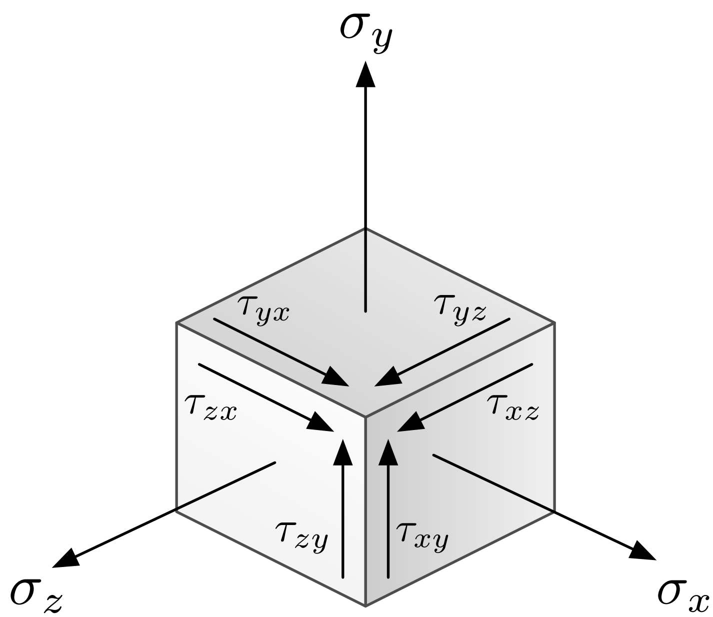

Figure 8.8. Principal and shear stresses presented on X, Y, and Z axes.

providing compound affects of individual stresses. Von Mises stress method combines six individual stresses (principal and shear) into a single resolved stress value that includes both magnitude and directions of the stress vectors. This approach provides a yield criterion through combining resolved stress values [175, 176].

The yield strength of the assigned material is taken as the reference point, which provides information about the first step in part failure. If the single resolved stress value is greater than the yield strength of the material, then once can conclude the part is starting to fail according to Von Mises method. Figure 8.9 shows the yield strength assumption for Von Mises method used in this study [177, 178].

Equation 8.1 shows Von Mises stress calculation that combines principal stresses and shear stresses into a single resolved value.

$$\sigma_{VM} = \sqrt{0.5\left[(\sigma_{xx}-\sigma_{yy})^2+(\sigma_{yy}-\sigma_{zz})^2+(\sigma_{zz}-\sigma_{xx})^2\right]+6({\tau_{xy}}^2+{\tau_{yz}}^2+{\tau_{zx}}^2)} \tag{8.1}$$

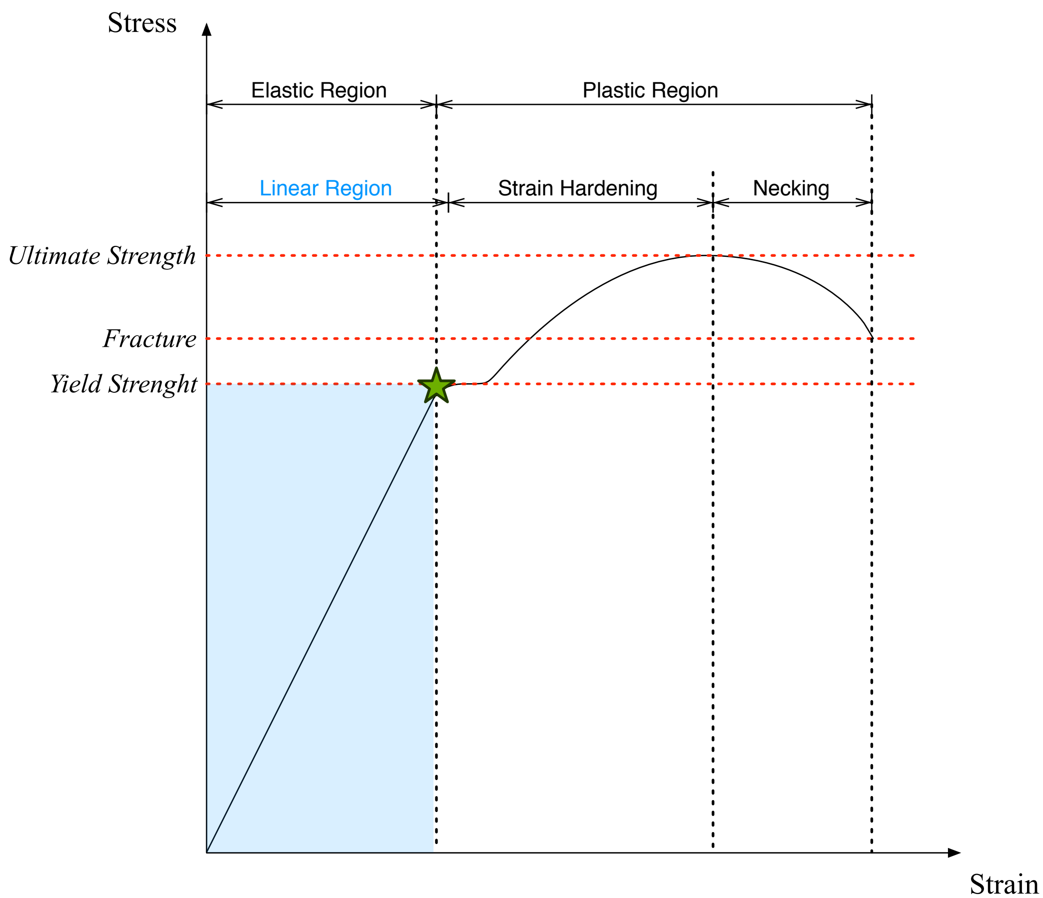

Figure 8.9. Stress-strain graph demonstrates linear assumptions used for part failure at yield strength. Shaded area represents linear assumption on part failure. FEA model discussed in this study assumes linear material properties with no effects of dynamic loading, temperature, buckling and crack propagation.

FEA approach used in this study is not universally applicable to all cases. It is best used for concept product evaluation with moderate fidelity. The fidelity of the analysis depends on various factors: material properties, affect of temperature, surface topology, application type (dynamic vs. static), etc. [179]. Static stress assumptions used in this study are:

- Deflection and stresses are linearly proportioned to the applied load.
- Material properties are linear. The stress-strain curve is a linear straight line.

- Loading is static and applied very slowly. No dynamic loading, vibration and impact is considered.
- Temperature has no effects on the part.
- Deformation of the part is small comparing to the overall size of the geometry.
- Sudden failures, crack propagation or buckling are not a concern.

8.7.3 Finite element analysis

In this section Von Mises stress distributions and displacements associated with applied static loads on A, B and CD pillars were summarized. Differences between outcomes for each pillar design (Old vs. New Pillar) were also displayed to check whether see-through type cut-outs generate any difference on FEA results.

The FMVSS roof-crush resistance test (Article.216) setup described on Section 4.9 was used throughout this study (Figure 4.18). The FEA CAD model body frame model was a derivative of the surface model used in Experiment-I and Experiment-II. After boundary conditions and loads were assigned to the FEA model based on FMVSS roof-crush criteria, a mesh with linear tetrahedrons was generated. The mesh defaults has average element size of 0.100, grading factor of 1.5 and maximum turn angle of 60.0 degrees. Average element size describes the fraction of the longest axis between CAD surface. Grading factor specifies the ratio of maximum adjacent mesh edges for transitioning between coarse to fine tetrahedrons. Maximum turn angle indicates the maximum angle of arcs (from 1 to 90 degrees) of tetrahedrons. In each mesh model, lower the ratios, finer (smaller) the mesh elements. A finer mesh leads to a higher fidelity, which also increases the time and computation required to solve the FEA model. Figure 8.10 shows the FEA workflow with mesh model created based on topology, applied loads and boundary conditions.

A strong (excellent) correlation found on Von Mises stresses and displacement results between Old Pillar and New Pillar design. Table 8.3 shows a strong liner

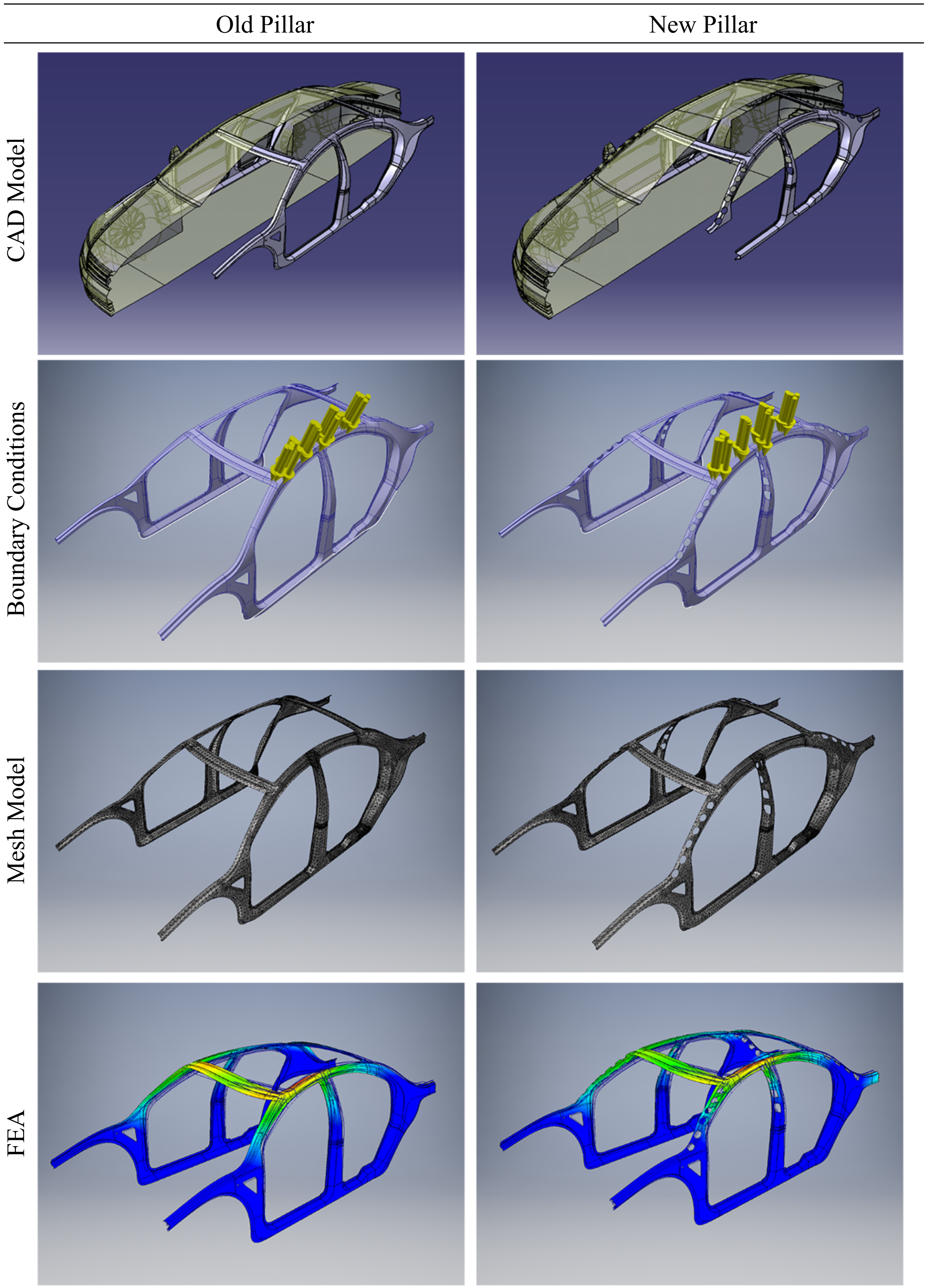

Figure 8.10. FEA work-flow starts from CAD model. Loads are applied and boundary conditions are defined. Mesh model is generated and Von Mises analysis is conducted.

relation between FEA results for Old Pillar and New Pillar design. Correlation results indicate that a liner relation is still present even with see-through gaps drilled on CAD frame body. Pearson Correlation and Intra-Class Correlation (ICC) results summarized on Table 8.3 show that FEA outcomes did not differ significantly.

Table 8.3
Pearson and Intra-Class Correlation correlation of FEA results

	Pearson Correlation	Intra-Class Correlation
Displacement	0.97	0.88
Stress	0.99	0.98

One of the major findings of the FEA is that New Pillar design generates a slightly larger stress values (9.8% on average) and higher displacement values (20.3% on average) (Table 8.4). Von Mises stresses and displacements across all pillar types (A, B or CD) increase as the applied static loads becomes larger.

Table 8.4
Descriptive statistics of Von Mises stress and displacement values (in cm)

		Minimum	Maximum	Mean	Std. Deviation
Displacement	Old Pillar	20.27	63.17	43.8167	15.66
	New Pillar	28.77	84.20	54.9475	17.84
Stress	Old Pillar	129.00	438.00	293.33	103.23
	New Pillar	129.00	502.00	318.08	121.46

Most of the Von Mises stresses across pillar types were lower than the yield strength of 420MPa (yield strength of assigned HSLA material (420MPa HSLA steel) [180–182]. However, B and CD pillars at 20,000N and 22,000N were resulted with a yield strength of higher than 420MPa (421MPa, 438MPa, 447MPa and 502MPa for Old and New Pillar respectively), which indicates a potential failure (Figure 8.11).

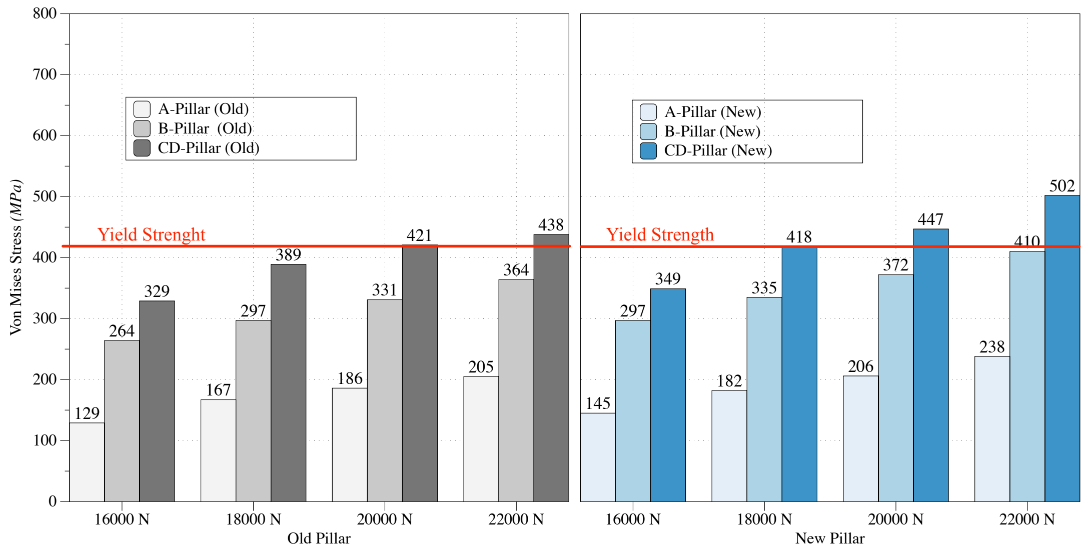

Figure 8.11. Comparison of Von Mises stress values associated with static loads and pillar types between Old Pillar and New Pillar. CD-pillar results on Old and New Pillar design at 20000N and 22000N resulted higher than maximum yield strength.

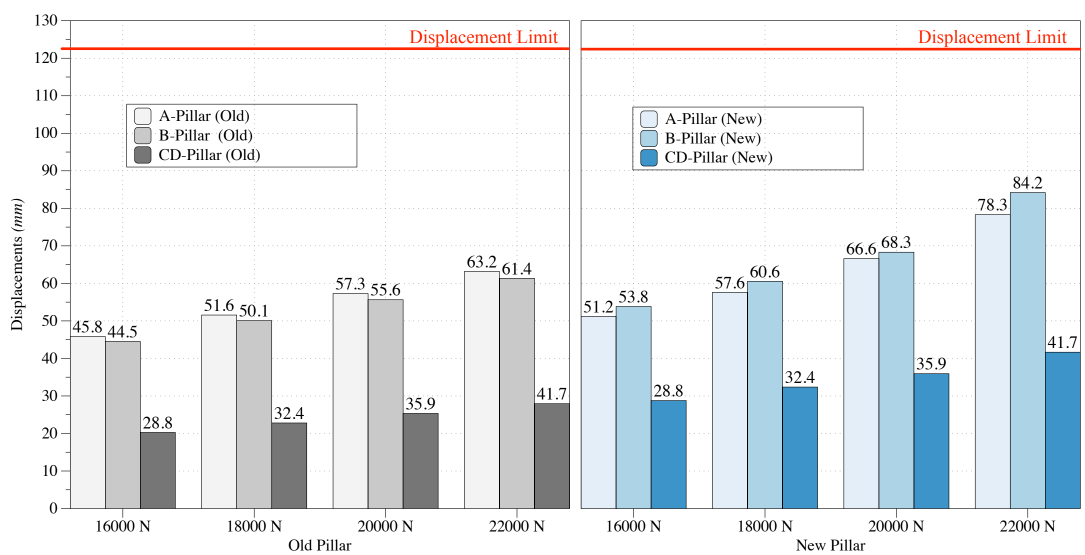

Figure 8.12. Comparison of displacement values associated with static loads and pillar types between Old Pillar and New Pillar. All displacement values are within maximum crush limit of 125mm.

Displacement values for all pillar designs were less than the maximum roof-crush threshold value of 125mm. Maximum displacement at 22,000N on Old Pillar yielded 22mm, whereas under same loading condition Old Pillar design yielded 84.2mm (Figure 8.12).

8.8 Results and Discussions

Structural integrity simulation conducted in Experiment-III revealed that New Pillar model with see-through-gaps comply with FMVSS standards. Maximum displacement at 22,000N was measured as 84.2mm for B-pillar, which is below the recommended upper limit of 125mm noted in FMVSS standards. Von Mises measurements shows that a slightly higher stress value (502MPA) was measured for B-pillar at maximum loading of 22,000N. Although the measured maximum stress value was slightly higher than the FMVSS requirements, the maximum deformation was within 125mm window. FEA stress simulation showed that a deformation occurs at 22,000N, but the maximum value complied with roof-crush requirements. Figure 8.13 shows that at maximum loading scenario of 22,000N, measured maximum deformation provided sufficient head room for a 95% male manikin inserted into vehicle.

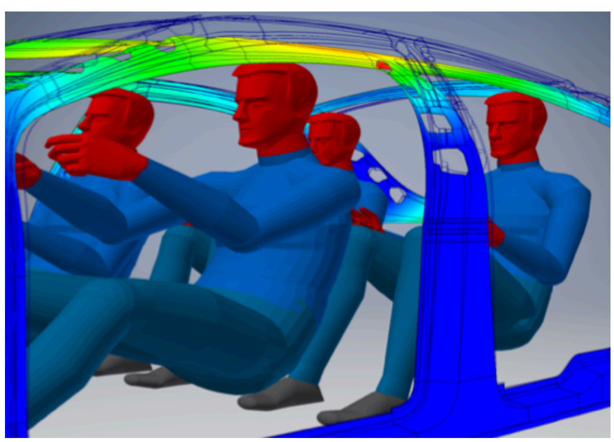

Figure 8.13. Comparison of displacement values associated with static loads and pillar types between Old Pillar and New Pillar. All displacement values are within maximum crush limit of 125mm.

9. DISCUSSIONS

This chapter is split in two subsections: Hypothesis and Limitations. In Hypotheses section, summary of findings supporting each hypothesis are covered in four separate sections. Finally, limitations associated with experimental setup, data collection methodologies and simulation assumptions are summarized.

9.1 Hypotheses

9.1.1 Hypothesis #1

Hypothesis #1 *(H1)* = *For visual field analysis, correlation of visual field results (within subjects) between six trials should be at least in high correlation ('Good' or 'Excellent'), where Intra-Class Correlation (ICC) index falls in range of 0.6 <ICC <1.0.*

Comparison of Fixation Duration (in milliseconds), Coordinates-X (in pixels) and Coordinates-Y (in pixels) data between six trials resulted in ICC scores bigger than 0.6. Results in Table 6.15 shows that eye-tracker data provides 'excellent' test-retest reliability on capturing eye movements (X and Y coordinates) and 'good' reliability in detecting duration of pupil fixations associated with X,Y coordinates.

In addition to the ICC scores, similar observations are captured in ANOVA and MANOVA analyses. One can see from Table 6.46 that, in each ANOVA and MANOVA analysis Trials did not show any significant effect on Fixation Duration, Coordinates-X and Coordinates-Y. A strong test-retest reliability is also summarized in Figure 9.1, where Trials data for each dependent variable shows an analogous pattern with relatively approximate values.

From above results, one can conclude that in each trial eye-tracker simulation data provides sufficient test-retest reliability for Fixation Duration, Coordinates-X and Coordinates-Y outcomes.

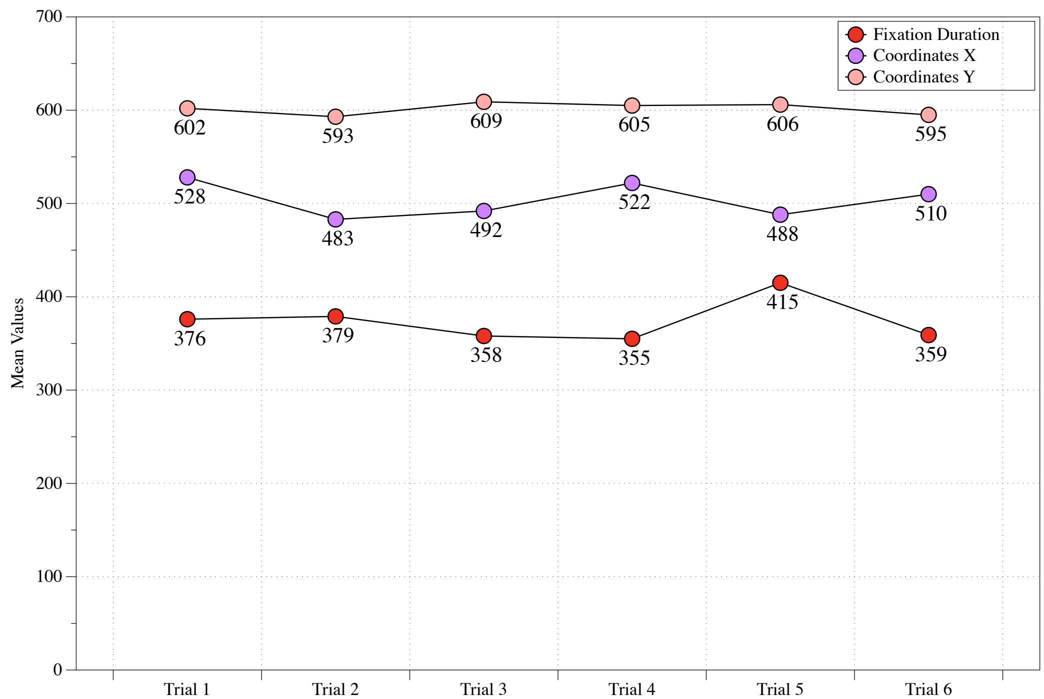

Figure 9.1. Mean average values of Fixation Duration, Coordinates-X and Coordinates-Y associated with each Trial. An analogous pattern is visible between dependent variables at each trial.

9.1.2 Hypothesis #2

Hypothesis #2 *(H2)* = *For each subject, visual detection of road elements with Proposed Pillar (New Pillar) design and with Current Pillar (Old Pillar) design are significantly different.*

One can see from summary of ANOVA and MANOVA results in Table 6.46 that Pillar Type has significant effect on Fixation Duration, Coordinates-X and Coordinates-Y readings around 83% of a time. In addition, Area of Interest study in Figure 6.7 and 6.8 shows an intense accumulation of data (fixation duration and eye-movements) at Area-1 in New Pillar design. In contrast, Old Pillar model shows a significantly weaker concentration at Area-1. New Pillar model receives a 43% higher total number of hits on Area-1 when compared to Old Pillar model.

On top of these results observed in Objective Experiment (Experiment-I), Subjective Experiment (Experiment-II) also shows around 95% improvement on Traffic Object Detection. Subjects who were able to detect traffic objects with New Pillar design also had 94% performance improvement in correctly identifying traffic objects. Data shows that detecting traffic objects on Old Pillar is harder than detecting traffic objects with New Pillar design. Results of Cooper Harper test also reflects that subjects had an agreement that a high driver mental workload is required when using Old Pillar model (Figure 7.14). In addition, subjects rated New Pillar design higher than Old Pillar design in every evaluation category (visibility, safety and aesthetics).

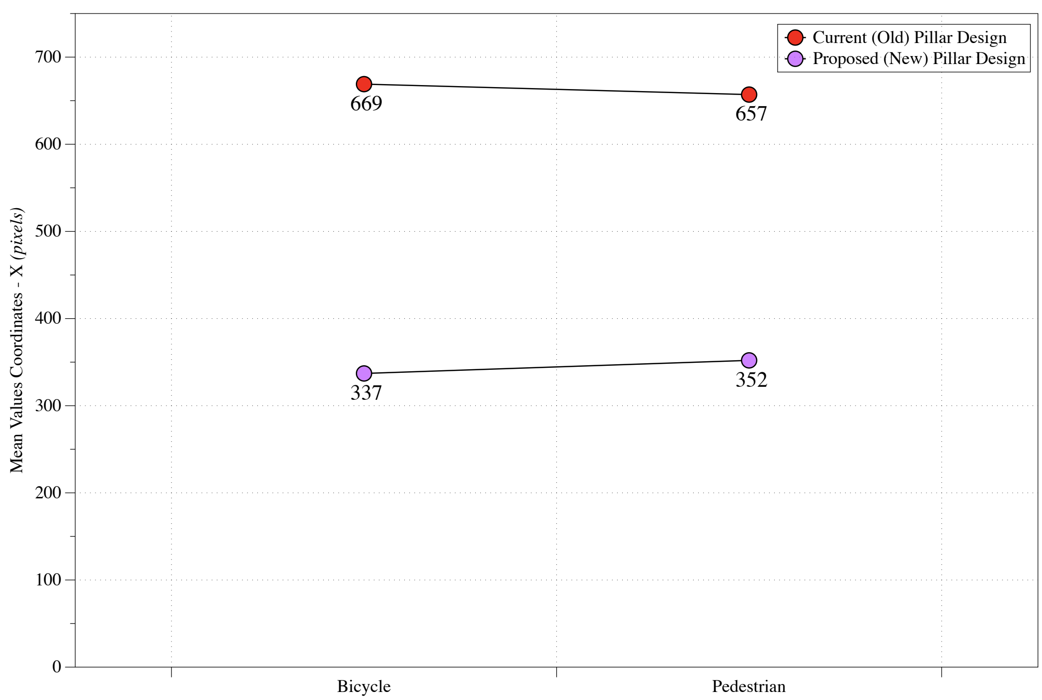

Figure 9.2. Comparison of mean values of Coordinates-X data between Old and New Pillar. New Pillar design generated significantly lower values on X-axis, which indicates that subjects make less eye-movements to detect a traffic object.

Similar results can be also observed in Figure 9.2, where mean outcomes of Coordinates-X differ significantly between Old Pillar and New Pillar. New Pillar design generates around 350 pixels less than Older Pillar design, which indicates subjects detected traffic objects on New Pillar easier and stopped making more eye-gazes. Lower average values of Coordinates-X data overlaps with subjective results found in Experiment-II.

From above results, one can conclude that, for each subject, visual detection of road elements with New Pillar design is significantly different that Old Pillar design.

9.1.3 Hypothesis #3

Hypothesis #3 *(H3)* = *Proposed Pillar (New) design is significantly better than Current Pillar (Old) design in terms of concept design criteria; forward (A-pillar), side (B-pillar) and rear field (CD-pillar) visibility.*

Experiment-I provided an extensive data about subjects forward visibility (A-pillar). Differences generated on traffic object detection between New Pillar and Old Pillar were demonstrated on Figure 6.17 and 6.17. In New Pillar design, subjects eye-movements were mostly concentrated on the Area-1, whereas in Old Pillar most of the eye-movements were scattered across the simulation display. Heat-maps and burnout images show significant differences generated by pillar designs.

Improvements in forward (A-pillar), side (B-pillar) and rear field (CD-pillar) visibility, ease of detection and Cooper-Harper tests were plotted in Figure 9.3. Once can see that New Pillar design offers around 95% of traffic object improvement when compared to Old Pillar design. Subjects also found that New Pillar design provides a lower demand on drivers (subjects) when compared to detecting traffic objects with Old Pillar design.

Summary of results in Section 6.6.3 also provides an additional insight about subjects' opinion on pillar visibility. Figure 7.17 shows that subjects rated New

Pillar design better than Old Pillar design in terms of overall visibility and visual safety (success of detecting traffic objects).

From above results, one can conclude that forward (A-pillar), side (B-pillar) and rear field (CD-pillar) visibility during detection of traffic objects with New Pillar design is significantly different than Old Pillar design.

9.1.4 Hypothesis #4

Hypothesis #4 *(H4)* = *Mean values of maximum forces and displacement values for front, side and rear loading on Proposed Pillar (New) design are not significantly different than Current Pillar (Old) design.*

Finite Element Analysis (FEA) conducted on Experiment-III (based on FMVSS roof-crush test requirements) demonstrated that New Pillar design with see-through gaps did not significantly differ than Old Pillar design in terms of structural integrity. Table 8.4 shows that mean values of stress and displacement results between Old Pillar and New Pillar design follow an increasing trend when applied force values increased from 16,000N to 22,000N. Only B-pillar and CD-pillar at 20,000N and 22,000N received higher stress values than yield strength of HSLA material, which indicates a possible part failure. All displacement values were found within the acceptable crush region of 125mm specified on FMVSS requirements.

Figure 9.4 shows the affects of maximum displacement measured during FEA experiment on occupants. The maximum displacement measured for Old Pillar and New Pillar design was 63.17cm and 84.20cm respectively. In each case, maximum displacement occurred at the maximum static loading (22,000N). One can see at Figure 9.4 that New Pillar design provides sufficient head room for 95^{th} percentile occupants when maximum loading was applied to the pillars. Visual representation of displacement with manikins overlaps with FEA results, where no clash or contact between upper torso of manikins and vehicle frame were detected.

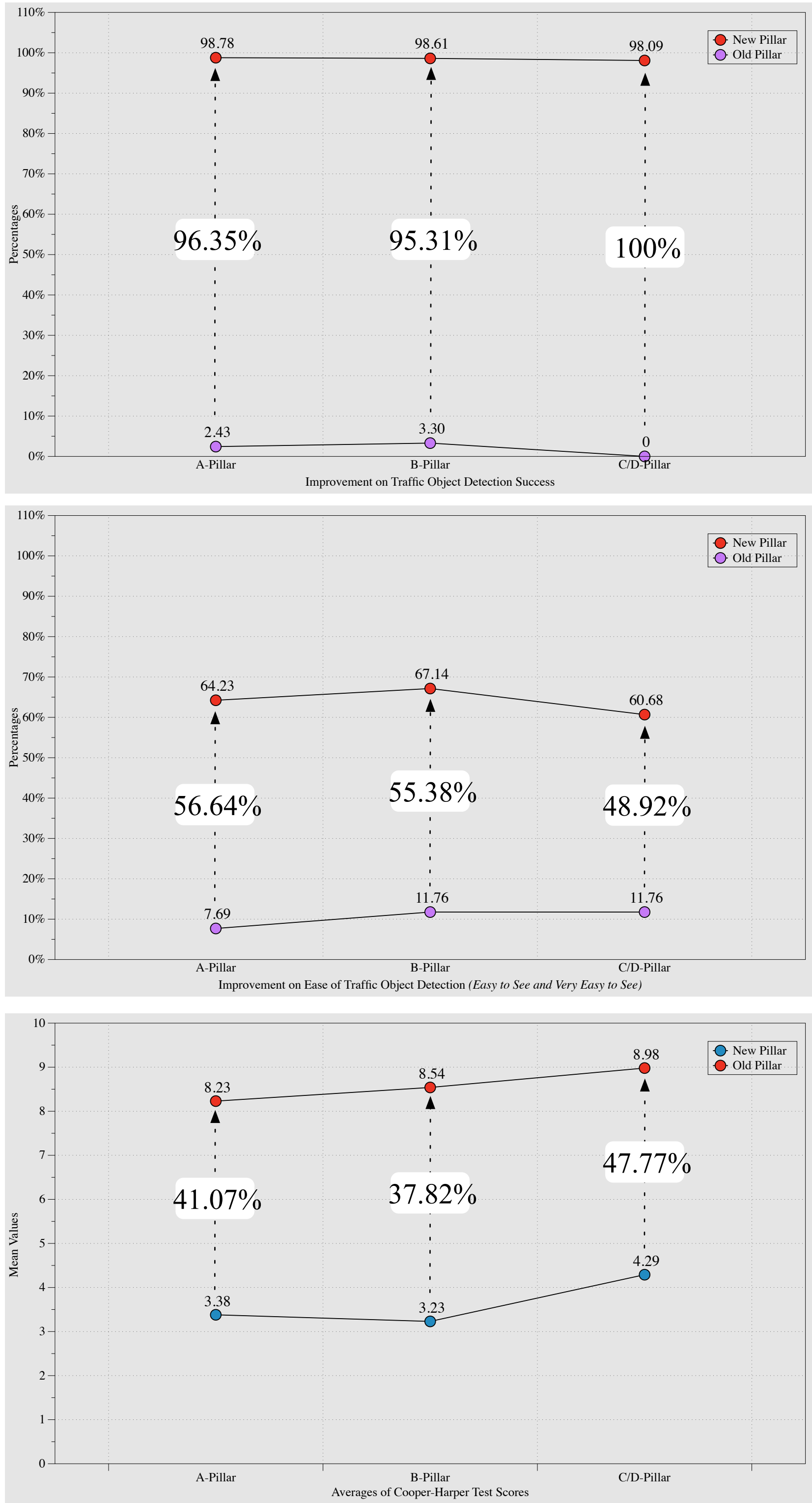

Figure 9.3. Summary of forward (A-pillar), side (B-pillar) and rear field (CD-pillar) visibility improvements. Across each category New Pillar design provides improved results compared to Old Pillar design.

Old Pillar	New Pillar

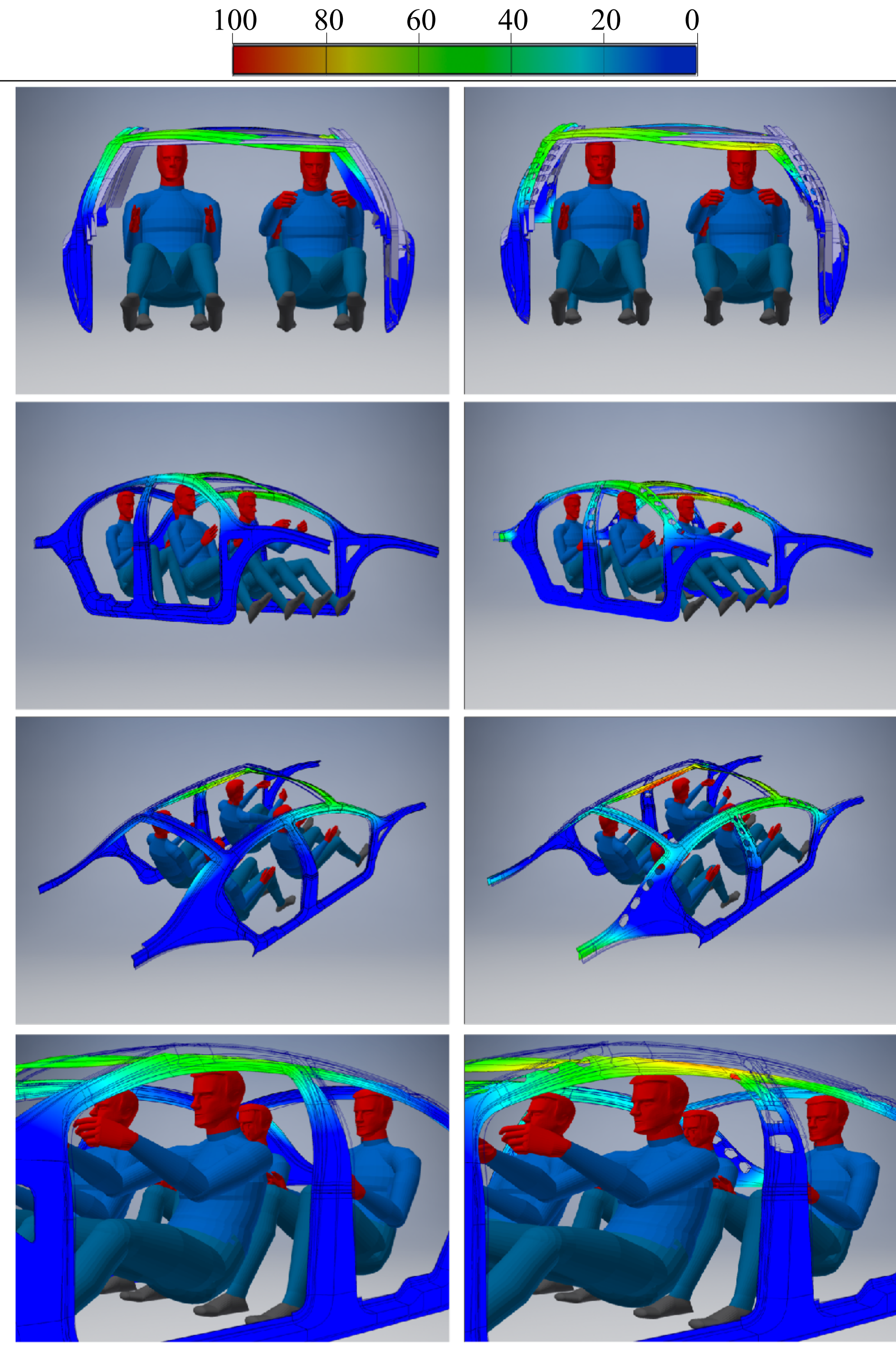

Figure 9.4. Available head room at peak crush loading (22,000N). Deformed area does not provide any clash/contact with occupants

9.2 Limitations

9.2.1 Human data collection

One of the motivations during the development of this dissertation is to provide a high-fidelity human data collection method with balanced financial investments. Most of the human factors studies in design domain require high capital investments and use of advance digital data collection tools. Although high-end data collection tools may provide an additional insight, there are many alternative methods and devices that provide sufficient fidelity within acceptable cost margins. In past decade, devices such as motion capture, eye-tracker and 3D scanners went through significant changes, especially in terms of precision and connectivity. Now, various low-end devices provide sufficient fidelity and flexibility in importing and exporting raw data within different operating systems. However, a seamless integration is still limited. Building a custom design framework requires connectivity with multiple stand-alone devices, which depend on hands-on experience and technical expertise.

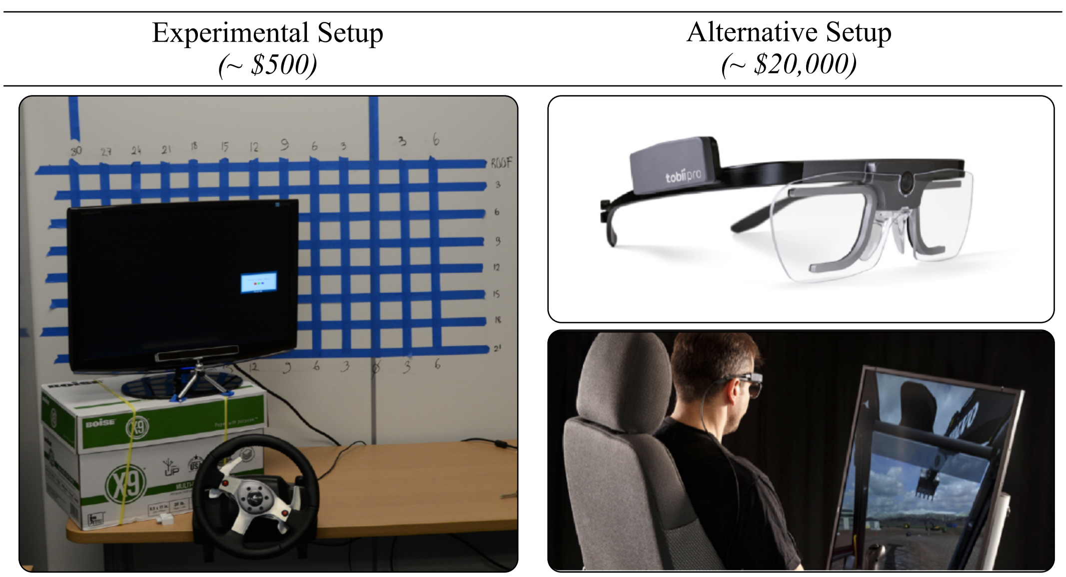

Figure 9.5. Comparison between eye-tracker setup used in this dissertation and a commercial alternative [183]. Current setup provides a relatively similar fidelity within conservative financial approach.

In this study a cost effective eye-tracker system was used with simple physical probes (steering wheel, pedals, monitor). There are various packages (eye-tracker, analysis software) available, which could render this experiment with increased fidelity, however cost would be significantly higher (Figure 9.5). An expensive experimental setup not always lead to a more precise data collection. Although using a low-end system increased time and post-processing required for initial setup, skills and expertise developed become invaluable assets. Depending on the nature of the experiment, a high-end setup would be more suitable. In this experiment, desired fidelity was achieved within a financially conservative approach.

9.2.2 Driving experiment

One of the limitations of this study is that a static driving simulator was used instead of a full-dynamic driving simulator. The static driving simulator was composed of a large scale monitor, steering wheel, pedals and an adjustable seat. Static simulator was stationary and did not provide any dynamic interaction with the traffic environment. During the simulation, static images that represent the driver's point of view for A, B and CD-pillar were projected on the monitor. Meanwhile, subjects' dynamic motion of eye-movements were recorded through an eye-tracker device.

In theory, the same experiment could be conducted in a simulator that has dynamic range of motions (in X, Y and Z axes) with real-time control of the vehicle. This approach could provide a higher fidelity of simulating traffic objects and collecting eye-tracking data that is closer to a real driving experience. One of the major limitations of this approach is the cost associated with a full-scale simulator. Another major limitation is the lack of ability to modify cockpit environment for the purpose of this experiment, which requires modification of pillar with see-through gaps (cut-outs). This modification would be hard to achieve in a full-scale physical simulator. Instead, an interactive simulator setup, which can map subject's inputs (steering, acceleration,.etc.) with a dynamic driving simulation was used (Figure 9.6).

Experimental Setup *(~ $3000)*	Alternative Setup *(~ $65,000)*
	

Figure 9.6. Comparison of static and dynamic simulators [184]. Static simulator used in this experiment lacks of interactivity and dynamic control. However, it generated a desired fidelity with significant savings comparing to dynamic simulators.

9.2.3 Structural analysis

There are various strategies to solve a FEA problem, which heavily depend on the complexity of the problem and the desired precision. In this study, FEA analysis was conducted with assumptions of: static structural test with linear deformations, no effects of heat and no presence of buckling. The main goal was to develop a proof-of-concept study that would demonstrate the affect of forces acting on a see-through pillar. This assumptions holds validity since FMVSS requirements rely only on static loading. In addition, material used in this study (HSLA) shows linear deformation character in elastic region. In an ideal case, FEA test should cover not only static but also dynamic loading scenarios (i.e. fatigue), full-body vehicle dynamics (i.e. vibrations) and impact tests (i.e. crash-test) (Figure 9.7). These tests look into loads acting on body frame in more details, which goes beyond the scope of this study.

Experimental Setup *(Static Linear FEA)*	Alternative Setup *(Non-Linear FEA)*
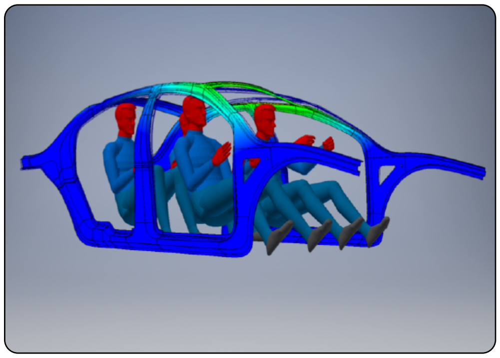	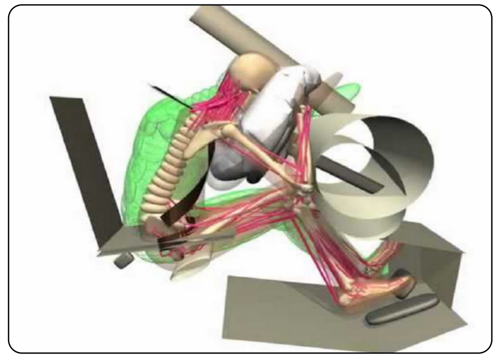

Figure 9.7. Static FEA simulation and non-linear FEA simulation [185]. A higher fidelity could be achieved by using a holistic simulation approach, which considers dynamic loading, vehicle dynamics and impact tests.

9.2.4 Shape of the see-through-gaps

In this study, oval shaped see-through-gaps were cut out from the body frame of opaque pillars found in regular automobiles. The shape of the cut-out area could effect the performance of traffic object detection, as well as the structural integrity of the vehicle. There could be various shapes applied depending on the type of the vehicle (family car vs. truck), structural integrity requirements (larger gaps reduce crash worthiness, etc.), aesthetics preferences (sharp, flowing, smooth, etc.) and manufacturing techniques (laser cut, molding,etc.) employed. A further study that focus on shape optimization could generate a better understanding about which shape would be best to increase driver's detection performance while satisfying other design variables (type of a vehicle, structural integrity, cost, etc.) (Figure 9.8). In this study an oval shape was created by combining two intersecting circles that were joined at their sides with parallel lines. Oval shapes are known for their fatigue resistance and are commonly used in aerospace industry (e.g., windows). In contrast to square shape cut outs, where stresses are concentrated at the sharp edges, oval shapes distribute stresses evenly.

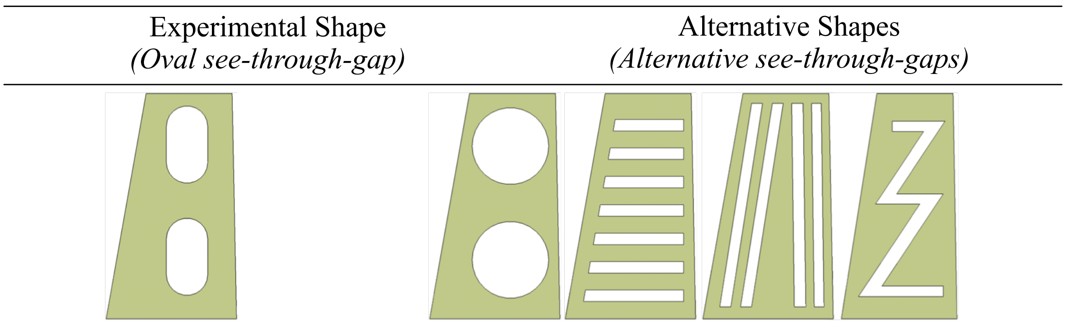

Figure 9.8. Alternative see-through gaps. Only oval see-through gaps provided in this study. There are various alternatives can be selected to optimize visibility and structural integrity.

9.2.5 Assistive and augmented technologies

Advancements in automotive electronics are in an ever increasing trend. Augmented technologies such as blind spot monitoring, lane departure warnings, autonomous parking and rear-view cameras are becoming part of safety packages in mid-to-high priced vehicles. Although many companies provide packages that assist drivers, their performance in-real-time events require thorough research (Figure A.3). In case of detecting road objects, especially while driving in downtown areas with confined spaces and hard-to-see spots, any secondary demand on driver would reduce the reaction time. Most of the cameras provided in high-end automobiles require synchronous visual attention between camera screen and the windshield (road). The additional visual task (checking camera and road back and forth) could be analogues as text-and-driving where more than 1.5 seconds of visual loss would be catastrophic. In addition camera systems have provide cues that are hard to represent high fidelity of human vision. Tracking the perimeter of vehicle in continuously changing terrain, speed, weather, and traffic conditions over a small low resolution display that is located on the main console require significant motor-skills and psycho-physical adjustments.

Experimental Setup *(A-Pillar Traffic Object Detection)*	Concept Technology *(Proposed Video Overlay on A-Pillar)*
	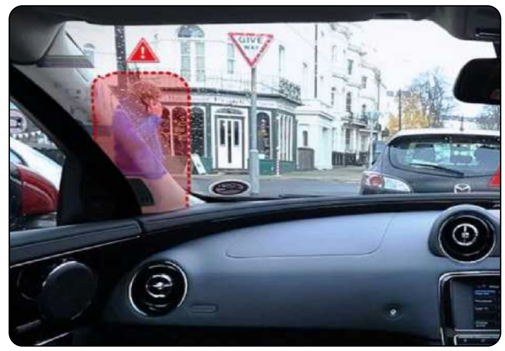

Figure 9.9. A conceptual video display mechanism provides a real-time vision to pillar obscuration [186].

10. CONCLUSIONS

In this dissertation, we introduced *'human-in-the-loop design framework'*, which utilizes Digital Human Modeling (DHM) to incorporate Human Factors Engineering (HFE) design principles early in design process. This framework embodies scientific methods (e.g., mathematics) and artistic approaches (e.g., visualization) to assess human well-being and overall system performance.

The fidelity of the design framework was evaluated through an automotive pillar design study. A concept pillar design that provides a see-through visual experience was proposed as a design alternative to increase safety and visual comfort. It is targeted to enhance driving experience with a balanced blend of functionality, aesthetics and cost effectiveness.

Results show that human-in-the-loop design framework was able to detect ergonomics differences (visual improvements) between pillar designs (Old Pillar vs. New Pillar design), and replicate physical test conditions in virtual environment with high test-retest reliability. Eye-tracker data (Fixation Duration, Coordinates-X and Coordinates-Y) shows that proposed pillar model (New Pillar) with see-through gaps provide a higher traffic object detection performance when compared to Old Pillar model. Data captured through eye-tracking experiment was also supported by subject feedback and questionnaires, where subjects found New Pillar design requires lower mental workload when detecting traffic objects. Subjects also rated New Pillar design higher than Old Pillar design in terms of overall visibility and visual safety.

In addition to eye-tracker data and subject questionnaires, New Pillar design showed a sufficient structural integrity based on Federal Motor Vehicle Safety Standard (FMVSS) tests. Finite Element Analysis (FEA) data revealed that majority of Von Mises stress values associated with New Pillar design were below the yield strength of the High Strength Low Alloy (HSLA) material used in pillar design. Displacement values were also within the roof-crush limits (125mm) defined by FMVSS. The maximum deformation (84mm) occurred during static roof-crush test resulted with minimal or acceptable risk of injury to occupants. At the maximum loading (22,000N) scenario, 95^{th} percentile occupants had sufficient head room and no clash was detected between occupants and the deformed body frame.

This study demonstrated that most of the limitations related to fidelity and exchangebility of DHM design studies could be resolved through the human-in-the-loop design framework. In this dissertation, a sketch-to-analysis type design framework was demonstrated through integrating various multi-disciplinary design methods such as: surface modeling, CAD, HFE, human-subject data collection and FEA (Figure 10.1). This approach has important advantages over most of the engineering design platforms that do not consider human aspects early in design process. Some of the advantages of human-in-the-loop design framework are:

- Human-in-the-loop design framework demonstrated that DHM tools can reduce cost and time associated with design process without compromising fidelity (Figure 8.1).
- Human-in-the-loop design process can be applied to small to large scale design studies, from conception to creation (Figure 8.1).
- This framework embodies scientific and visual aspects of human element in design process, which is rarely represented in HFE research (Figure 8.1).
- Asides traditional human factors interventions (questionnaires, ergonomics checklists, etc.), human-in-the-loop design framework allows integration of traditional techniques with digital design (FEA, CFD, etc.) tools/methods (Figure 8.1).
- It's ease of integration with various digital design tools makes human-in-the-loop framework a cost effective design approach for human-subject data collection studies (Figure 8.1).

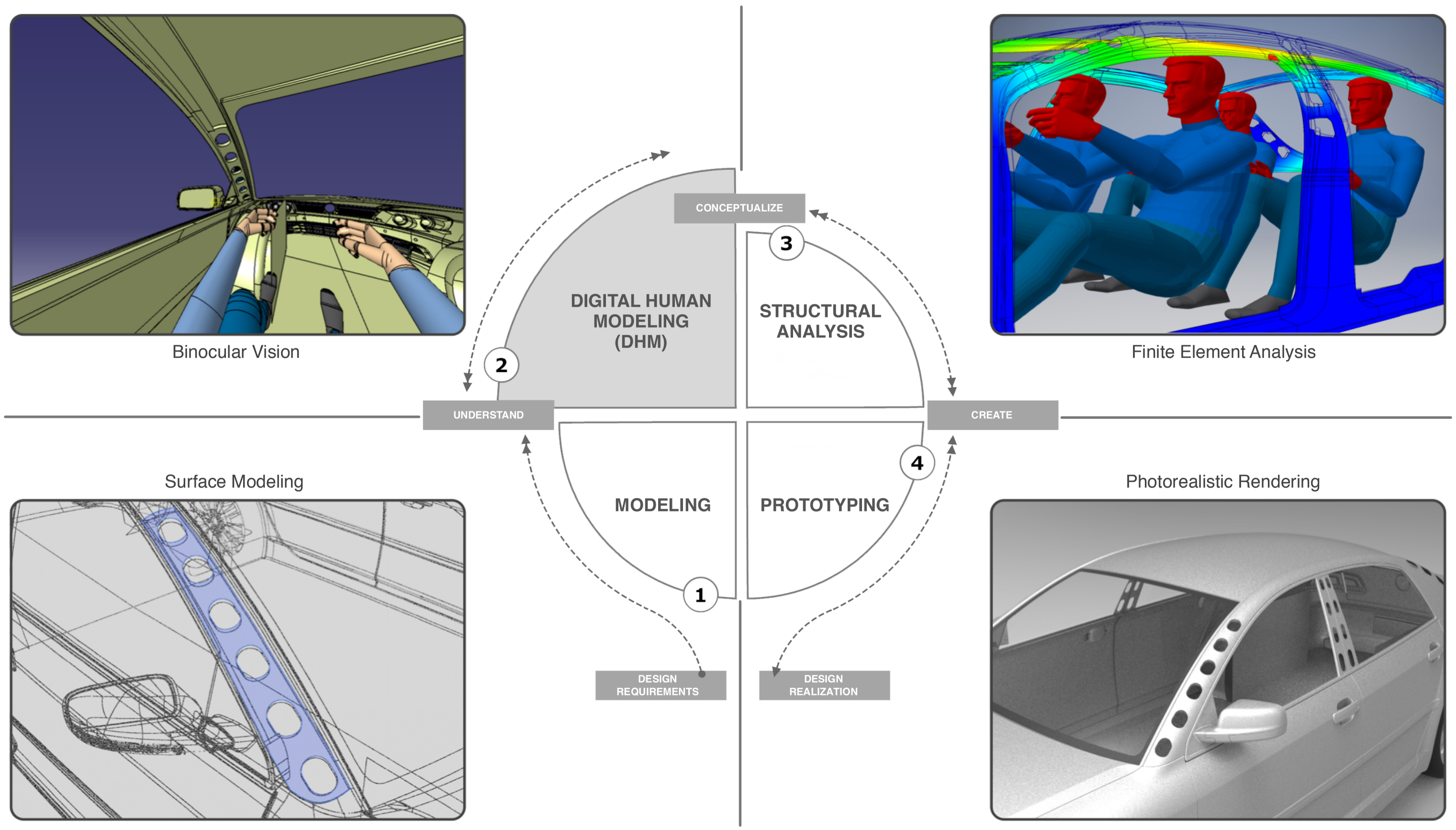

Figure 10.1. Human-in-the-loop design framework embodies scientific and visualization aspects of human element early in design process, from conception to creation of products.

11. FUTURE WORK

Besides all the successful results demonstrated in this study, integrating human factors principles into design process through DHM has limitations. Amongst the most, fidelity and exchangeability of design models between HFE and multi-physics simulation tools require the most attention. Human-in-the-loop framework offers a method for integrating HFE design principles with Engineering Design and Industrial Design methods, however a seamless integration is still missing between DHM and multi-physics simulation packages (e.g., CAE, CFD, FEA).

In most of the design applications significant post processing and data exchange are still required. There are fidelity related limitations when evaluating human physiology and cognition, as well as representing actual environmental conditions. On top, research regarding cognitive capabilities of humans is not well reflected in DHM packages. There are also adaptation related challenges in front of DHM community. Industrial and educational transformation is crucial to expand the coverage of DHM tools, which require domain specific attention. A summary of critical work needed is presented under two topics: 'Fidelity' and 'Adaptation'.

11.1 Fidelity Concern in DHM Domain

Working with virtual/digital tools instead of physical objects has both advantages and disadvantages [92]. A leading PLM consultancy, CIMdata, concluded: on average, organizations using digital manufacturing (high technology investment products) technologies can reduce lead time to market by 30%, the number of design changes by 65% and time spent in the manufacturing planning process by 40%. Production throughput can be increased by 15% and overall production costs can be cut by 13% [187]. However, virtual/digital applications require relatively high capital investments, training and user expertise. For mass production and/or Research and Development (R&D) environment digital tools (e.g., DHM) have significant economical potential. In contrast, when the lot size is very small and innovation is not a concern, high technology investments become less attractive [188, 189]. Once a sufficient budget, the cost of building a digital human model and executing DHM analyses will be less than the cost associated with building a physical prototype [74, 190].

DHM tools share similar advantages and disadvantages. Most of the inexperienced DHM software users consider the tools are difficult to use. On the other hand, more experienced users, mostly in aerospace and automotive industries, feel functions are inadequate and needs customization [77, 92]. Besides software-related problems mentioned above, one of the biggest limitations in DHM is the fidelity of the analysis tools or in other words 'to which extend does DHM represent/replicate the reality?'. Variation in DHM platforms, differences between mathematical and visual models used and coverage of different analysis models are some of the few variables affect the fidelity of the DHM [77].

A digital human model has many components ranging from skin, muscles to cognition. All of these components should work together and function in a similar way to a real human. Therefore, all the aspects of the DHM components must be checked and validated for visual and functional realism [77, 191].

As the applications of DHM and CEA tools are advancing and expanding, increasing fidelity becomes critical. Its no longer sufficient to work with cartoon appearance virtual human models with very simple analysis and functions. Realism is paramount, and the success of engineering design research through DHM highly depends on visual and functional realism [191]. Below sub-sections show some of the most important topics related to factors influencing fidelity.

11.1.1 Realistic visualization

Visual appearance of the manikin is critical for both engineering analysis and communication purposes. The ongoing collaboration between industrial design and engineering departments in various companies highlight the need of human-like manikins [92]. Lamkull (2005) investigated the effects of the body posture assessment between manufacturing engineering managers, simulation engineers and ergonomists [192]. This study showed that the ergonomic judgment is affected by different appearance modes. A more realistic looking manikin was rated higher. In current DHM packages, simulation of skin deformation, visual effects of vibration on body and realistic body motions are simulated with limitations [77]. This problem has computing performance considerations in terms of price and cost. However, there are various studies in recent years showing a promising photo-realistic digital human simulations that represents real human physics and visualization with high-fidelity [77, 193].

11.1.2 Anthropometry

Anthropometric information forms the backbone of human models in digital environment. Anthropometric data should provide up-to-date information about type, gender, age, physical measurements of the workers inserted into digital environments [77]. Anthropometric data should also cover wide range of population depending on the application domain. As an example, DHM integrated vehicle crash test software should consider not only adults, but also small children and even occupants with disabilities. A study carried out by Oudenhuijzen and Zehner (2000), assessed the anthropometrics of DHM software in terms of accuracy. In this study live subjects are compared with CAD manikins. Results showed that accuracy not only differed between human subjects and manikins, but also between manikins [194].

11.1.3 Predictive capabilities

Recent advancements in CAE tools expanded the traditional application area of DHM. Current applications provide solutions in product development, vehicle analysis and design. A fundamental component of the integrated (CAE and DHM) DHM is posture prediction and analysis.

In predictive DHM applications, postures and motions are not based on Mo-Cap data. Instead, optimization-based approach generates realistic postures retrieved from a database. Motions, joint angles and segments, with multi-degrees of freedom, are optimized and determined through performance measures such as discomfort, joint displacement, vision and energy. The same optimization-base approach takes into account the anthropometrics limitations and constraints.

The predictive capabilities increase the fidelity of human models by minimizing the use of pre-coded postures/motions [93]. One example shows that if you throw a ball to the manikin in digital environment, manikins predictive behavior should react on the coming ball without the need of any pre-coding or user manipulation. Within the predictive capabilities platform, the software user should assign specific body posture and pick up to required motion to execute the task realistically [191].

11.1.4 Cognitive aspects

Integration of human sensation channels significantly contribute to fidelity of DHM. Besides visual channels, other sensation channels are not well modeled. Human emotion, decision making and mental workload have not adequately represented in current models [195]. A high-fidelity cognitive model that incorporate decision making and human reliability could be incorporated to DHM research [196].

A realistic (high fidelity) manikin should be consisted of both cognitive and physical aspects of DHM. Representing only physical aspects of humans is not sufficient to replicate the real word scenarios. Cognitive and performance aspects such as facial representation, stress, mental workload should be included in digital manikins [77,92].

11.1.5 Posture and motion

Computer manikins used in DHM packages differ from how real humans move and position their body parts. Its hard to replicate a realistic human posture/motion due to the complexity of human shapes, behaviors and limitations of degrees-of-freedom in body segments/joints [197]. The biomechanical modeling does not permit addition of large number of degrees-of-freedom (DOF) associated with various joints. Therefore there are posture and motion related limitations that contribute of realistic motion/behavior [92, 93].

11.1.6 Segmentation / Degrees-of-Freedom (DOF)

Digital computer models consist of multiple numbers of segments and joints, which are linked through mathematical constraints. These constraints provide range of motion restrictions similar to real human body. In order to obtain high accuracy of motion, large numbers of segments are needed. In contrast, low numbers of segments provide ease of handling. Fidelity of motions (also fidelity of manikin model) can increase with multi-joints and segments, which can replicate similar motion and posture restrictions as real humans.

Traditional DHM models use single-degree-of-freedom (SDF) approach, which is often associated with a rigid body mass. Studies showed that a lumped parameter model with multi-degrees-of-freedom (MDF) models is an improved approach over SDF used in low-fidelity human models [93, 198].

11.1.7 Inner and exterior body

Most of human manikins only consist of the exterior body elements. Inner body components are also essential to create a realistic human motion and behavior in digital environment. A complete DHM platform requires inner and outer body elements for realism [191]. As an example, dynamic human-object simulations (crash testing) require both outer and inner components of the manikin, which, together, play important role in visual and mathematical analysis of injuries [199].

11.1.8 Micro and macro motions

Type of motions has a strong impact on fidelity of DHM models. Various human tasks (e.g., gripping, picking) require very precise and detailed motions. DHM domain is in search of models that can be used effectively to perform ergonomic assessments of different types of reaching and materials handling tasks. Most of the macro motions can be simulated with high fidelity, however simulating micro motions need improved prediction and analysis capabilities. Some aspects of working environments, such as vibration, also affect the fidelity of both macro and micro motions. Vibration comfort is also a central concern in transportation design industry. Future DHM tools should contain improved analysis tools that incorporate micro and macro motions with affects of vibration [92].

11.1.9 Analysis models

Analysis models should include improved visual and scientific (mathematical) outputs within a user-friendly software interface. An ideal DHM platform should be capable of guiding users during simulation setup and analysis. One of the problems in analysis models is the inadequate representation of mathematical models used for performance analysis such as Metabolic Energy Expenditure, NIOSH Lifting Guidelines, etc. Although available DHM packages use very similar mathematical equations to manual methods, they are still differ in their assumptions or in calculation methodology. Many of those analyses have been taken from a paper version and incorporated into DHM software [77]. Even though most of these models are theoretically sound, but directly transferring these models without fidelity studies is not the optimal way of achieving fidelity. This approach may lead some of inexperienced users to have problems about not knowing the limitations and background of the analysis models [92].

11.2 Adaptation and Expandability Concerns in HFE and DHM

The future of any scientific branch, especially HFE and DHM, depends on how well the domain incorporates issues of emerging areas, and disseminate scientific theory into practice [32]. One of the critical challenges of HFE and DHM is to translate scientific findings and professional experiences about human needs, abilities and limitations into design guidance [65].

Today, our grand challenges are dynamic, fast evolving and cross-disciplinary. Economic, socio-political and ecological considerations will impact human prosperity [1] [2, 3]. Thus, design process require a holistic approach, where a diverse pool of parameters (multiple stakeholders, resources, constraints, etc.) should be taken into the account. Human-in-the-loop design framework can offer solutions to some of these challenges. There are various domains that DHM can bring human-centered design principles early in the design process. Following section summarizes some of the emerging areas where human-in-the-loop framework can extend current theory and application of HFE and DHM.

11.2.1 Sustainability

Sustainability is one of the grand challenges that affect every facet of life [12, 200]. Researchers agree that methods of conservation and recycling is solely not sufficient to resolve sustainability concerns [201]. With increased population and expanding economies, resources become more scarce than ever. Creating resilient societies depend on how design actions are taken today. One should think short and long-term projection as well as consequences associated with decision-making.

Sustainability has direct connections to safeguarding ecology and maintaining the quality of life. Thus, it is inevitable that theory and good practice in HFE must be introduced early in the design process [202]. Although some of the researcher imply the importance of HFE, sustainability and HFE connections is only partially explored. Theory and practice of HFE in meeting sustainability objectives are limited [12, 94].

DHM is one of the most robust design tools that can potentially integrate human-centered design theory and methods into sustainability area. Human-in-the-loop framework can be utilized to evaluate human safety, comfort and performance.

One of the application areas that require DHM involvement is Air Quality management. Air pollution is a critical environmental issue, which limits sustainable development and causes health risks [94, 203–205]. A Metabolic Energy Expenditure tool based on HFE theory could help engineers to assess the adverse affects of poor indoors air quality on human health and performance. Compared to conventional methods, DHM has the advantage of simulating, analyzing and presenting humans inside areas with poor air quality with advance visualization and performance analyses [94]. Simulations in the context of accepted engineering analysis can influence design decisions as well as safety and health. DHM in this context also reduces the need for in-situ human data collection and extensive prototyping, especially in confined areas with hazardous and toxic material handling [94].

11.2.2 Safety, reliability and quality

Safety and reliability are one of the most important characteristics of a successful product, which often a good indicator of market share. They are also essential components of total quality assurance, however do not solely ensure quality [206]. Ignoring or omitting safety and reliability aspects often result in market loss [207, 208]. It could also lead to injury and catastrophic failure. However, many industries suffer from poor safety and reliability. Most of the quality assurance practices evolve around the idea of evaluating products at the late stage of design process (e.g., beta prototyping). This leads to accumulation of unforeseen problems, which do not get detected until the a product is in use [207].

Human-in-the-loop design framework has potential to detect problems related to quality, which has direct connections to safety and reliability concerns early in the design stage. This approach can increase the probability of designing products with building quality into products earlier.

11.2.3 Multi-Physics simulations

Human Factors theory and methods focus on assessing human-well being and overall performance of the system. Thus, domain coverage is extensive. Anything that has connection and/or interactions with human element makes connections to HFE. This extensive approach requires understanding and synthesis of coupled natural, artificial and human systems. Thus, next generation human-centered design tools should recognize complex coupled systems at multiple scales. Within HFE domain a framework that provides methods and tools for simulating humans in a complex coupled systems is limited [94]. This approach requires development of domain specific tools (simulation packages) depending on the design and problem of interest [94]. One of the potential benefits of human-in-the-loop design framework is to integrate simulation tools with HFE theory and methods. However, the coverage of these simulations packages are limited (e.g. comfort angles, binocular vision, lifting analysis, etc.) [14, 65, 209].

LIST OF REFERENCES

LIST OF REFERENCES

[1] C. L. Dym. *Engineering design: a synthesis of views*. Cambridge University Press, 1994.

[2] C. L. Dym, P. Little, E. J. Orwin, and R. E. Spjut. *Engineering design: a project-based introduction*. Wiley New York, 2004.

[3] C. L. Dym and D. C. Brown. *Engineering design: representation and reasoning*. Cambridge University Press, 2012.

[4] N. Cross. *Engineering design methods: strategies for product design*. John Wiley & Sons, 2008.

[5] J. Liu and Z. Sun. Representing design intents for design thinking process modelling. In *Global Design to Gain a Competitive Edge*, pages 187–197. Springer, 2008.

[6] B. E. Bürdek. *Design history, theory and practice of product design*. Springer Science & Business Media, 2005.

[7] I. Van de Poel and D. E. Goldberg. *Philosophy and engineering: An emerging agenda*, volume 2. Springer Science & Business Media, 2010.

[8] N. King and A. Majchrzak. Concurrent engineering tools: are the human issues being ignored? *Engineering Management, IEEE Transactions on*, 43(2):189–201, 1996.

[9] A. M. Lund and J. E. Tschirgi. Designing for people: integrating human factors into the product realization process. *Selected Areas in Communications, IEEE Journal on*, 9(4):496–500, 1991.

[10] H. O. Demirel and V. G. Duffy. Applications of digital human modeling in industry. In *Digital Human Modeling*, pages 824–832. Springer, 2007.

[11] H. O. Demirel and V. G. Duffy. Digital human modeling for product lifecycle management. In *Digital Human Modeling*, pages 372–381. Springer, 2007.

[12] H. O. Demirel and V. G. Duffy. A sustainable human centered design framework based on human factors. In *Digital Human Modeling and Applications in Health, Safety, Ergonomics, and Risk Management. Healthcare and Safety of the Environment and Transport*, pages 307–315. Springer, 2013.

[13] J. C. Manganelli. *Designing complex, interactive, architectural systems with CIAS-DM: A model-based, human-centered, design & analysis methodology*. PhD thesis, Clemson University, 2013.

[14] R. Haslam and P. Waterson. Ergonomics and sustainability. *Ergonomics*, 56(3):343–347, 2013.

[15] V. Hubka and W. E. Eder. *Design science: introduction to the needs, scope and organization of engineering design knowledge*. Springer Science & Business Media, 2012.

[16] W. E. Eder. Viewpoint engineering designart, science and relationships. *Design Studies*, 16(1):117–127, 1995.

[17] A. H. Maslow. A theory of human motivation. *Psychological Review*, 50(4):370, 1943.

[18] A. A. Harms, B. W. Baetz, and R. Volti. *Engineering in time: The systematics of engineering history and its contemporary context*. Imperial College Press, 2004.

[19] J. R. Lindbeck. *Design textbook*. McKnight & McKnight Publishing Company, 1963.

[20] P. J. Grillo. *Form, function, and design*. Courier Corporation, 1975.

[21] National Academy of Engineering. *Educating the Engineer of 2020:: Adapting Engineering Education to the New Century*. National Academies Press, 2005.

[22] P. H. Bloch. Product design and marketing: reflections after fifteen years. *Journal of Product Innovation Management*, 28(3):378–380, 2011.

[23] K. C. Kapur and M. Pecht. *Reliability engineering*. John Wiley & Sons, 2014.

[24] M. Clark and K. Friedman. *Proposal for a School of Design at the University of California, Irvine*. University of California, 2002.

[25] T. Chandrupatla. *Finite element analysis for engineering & Tech*. Universities Press, 2004.

[26] D. Grasso and M. Burkins. *Holistic engineering education: Beyond technology*. Springer Science & Business Media, 2010.

[27] X. X. Liu, H. P. Zhao, and L. Gan. The importance of reasonable application of materials in the industrial product design. In *Advanced Materials Research*, volume 830, pages 68–71. Trans Tech Publ, 2014.

[28] R. Eggert. *Engineering design*. Pearson/Prentice Hall, 2005.

[29] D. F. X. Mathaisel, J. M. Manary, and N. H. Criscimagna. *Engineering for sustainability*. CRC Press, 2012.

[30] S. Cox. *Reliability, Safety, and Risk Management*. Wiley Online Library, 1991.

[31] R. Frank. *Understanding smart sensors*. Artech House, 2013.

[32] D. Caple. Emerging challenges to the ergonomics domain. *Ergonomics*, 51(1):49–54, 2008.

[33] S. B. Niku. *Creative design of products and systems*. Wiley New York, 2009.

[34] N. Roozenburg and J. Eekels. *Product design: fundamentals and methods*, volume 2. Wiley Chichester, 1995.

[35] W. Lidwell, K. Holden, and J. Butler. *Universal principles of design, revised and updated: 125 ways to enhance usability, influence perception, increase appeal, make better design decisions, and teach through design*. Rockport Pub, 2010.

[36] J. P. Protzen and D. J. Harris. *The universe of design: Horst Rittel's theories of design and planning*. Routledge, 2010.

[37] D. P. Raymer. *Aircraft Design: A Conceptual Approach and Rds-student, Software for Aircraft Design, Sizing, and Performance Set (AIAA Education)*. AIAA (American Institute of Aeronautics & Ast, 2006.

[38] N. Cross, J. Naughton, and D. Walker. Design method and scientific method. *Design Studies*, 2(4):195–201, 1981.

[39] S. Pugh. *Total design: integrated methods for successful product engineering*. Addison-Wesley, 1991.

[40] L. L. Bucciarelli. An ethnographic perspective on engineering design. *Design Studies*, 9(3):159–168, 1988.

[41] D. P. Raymer. *Aircraft design: a conceptual approach*. 1989.

[42] K. Otto and K. Wood. *Product design: techniques in reverse engineering and new product development*. , 2003.

[43] D. G. Ullman. *The mechanical design process*, volume 2. McGraw-Hill New York, 1992.

[44] S. J. Czaja and S. N. Nair. Human factors engineering and systems design. *Handbook of Human Factors and Ergonomics, Third Edition*, pages 32–49, 2006.

[45] A. A. Hopgood. *Intelligent systems for engineers and scientists*. CRC press, 2011.

[46] L. Zhiliang. The epistemological basis of industrial designing. *Design Studies*, 12(2):109–113, 1991.

[47] S. Moody. The role of industrial design in technological innovation. *Design Studies*, 1(6):329–339, 1980.

[48] M. Alexander. Creative marketing and innovative consumer product designsome case studies. *Design Studies*, 6(1):41–50, 1985.

[49] M. Berkowitz. Product shape as a design innovation strategy. *Journal of Product Innovation Management*, 4(4):274–283, 1987.

[50] M. Yamamoto and D. R. Lambert. The impact of product aesthetics on the evaluation of industrial products. *Journal of Product Innovation Management*, 11(4):309–324, 1994.

[51] N. Crilly, J. Moultrie, and P. J. Clarkson. Seeing things: consumer response to the visual domain in product design. *Design studies*, 25(6):547–577, 2004.

[52] W. P. Holmes, M. A. Azam, and P. C. Hills. A preliminary study of the relationship between industrial design and engineering design. In *Proceedings of the 1st Conference on Designing Interactive Systems: Processes, Practices, Methods, & Techniques*, pages 105–114. ACM, 1995.

[53] M. Evans. Applying ergonomics methods during the industrial design of consumer products. *Human Factors in Consumer Products*, pages 193–202, 1998.

[54] K. T. Ulrich. *Product design and development*. Tata McGraw-Hill Education, 2003.

[55] M. Tovey. Styling and design: intuition and analysis in industrial design. *Design Studies*, 18(1):5–31, 1997.

[56] S. Hsiao, F. Y. Chiu, and C. S. Chen. Applying aesthetics measurement to product design. *International Journal of Industrial Ergonomics*, 38(11):910–920, 2008.

[57] G. Gemser and M. A. A. M. Leenders. How integrating industrial design in the product development process impacts on company performance. *Journal of Product Innovation Management*, 18(1):28–38, 2001.

[58] P. Hekkert. Design aesthetics: principles of pleasure in design. *Psychology Science*, 48(2):157, 2006.

[59] D. R. Wallace and M. J. Jakiela. Automated product concept design: Unifying aesthetics and engineering. *Computer Graphics and Applications, IEEE*, 13(4):66–75, 1993.

[60] G. Kariuki and K. Löwe. Incorporation of human factors in the design process.

[61] E. Hollnagel. Human factors/ergonomics as a systems discipline? 'the human use of human beings' revisited. *Applied Ergonomics*, 45(1):40–44, 2014.

[62] J. Schaffrina. Interrelations of industrial design, ergonomics, and the user. *Selected Areas in Communications, IEEE Journal on*, 9(4):501–505, 1991.

[63] W. Karwowski, M. M. Soares, and N. A. Stanton. *Human Factors and Ergonomics in Consumer Product Design: Uses and Applications*. CRC Press, 2011.

[64] W. Karwowski. Ergonomics and human factors: the paradigms for science, engineering, design, technology and management of human-compatible systems. *Ergonomics*, 48(5):436–463, 2005.

[65] S. Dekker and J. Nyce. How can ergonomics influence design? moving from research findings to future systems. *Ergonomics*, 47(15):1624–1639, 2004.

[66] A. Chapanis. Ergonomics in product development: a personal view. *Ergonomics*, 38(8):1625–1638, 1995.

[67] W. Karwowski. The discipline of ergonomics and human factors. *Handbook of Human Factors and Ergonomics*, 3, 2006.

[68] J. Dul, R. Bruder, P. Buckle, P. Carayon, P. Falzon, W. S. Marras, J. R. Wilson, and B. Van der Doelen. A strategy for human factors/ergonomics: developing the discipline and profession. *Ergonomics*, 55(4):377–395, 2012.

[69] K. McSweeney, J. Pray, and B Craig. Integration of human factors engineering into designan applied approach. In *Royal Institution of Naval Architects (RINA) Human Factors Conference Proceedings*, 2009.

[70] J. R. Wilson. Fundamentals of ergonomics in theory and practice. *Applied Ergonomics*, 31(6):557–567, 2000.

[71] C. J. Vincent, Y. Li, and A. Blandford. Integration of human factors and ergonomics during medical device design and development: It's all about communication. *Applied Ergonomics*, 45(3):413–419, 2014.

[72] A. B. Proaps and R. A. Kennedy. Enhancing hf/e outreach goals through multidisciplinary collaboration. *Ergonomics in Design: The Quarterly of Human Factors Applications*, 22(3):23–25, 2014.

[73] R. Ahasan and D. Imbeau. Who belongs to ergonomics? an examination of the human factors community. *Work Study*, 52(3):123–128, 2003.

[74] D. B. Chaffin and C. Nelson. *Digital human modeling for vehicle and workplace design.* Society of Automotive Engineers Warrendale, PA, 2001.

[75] B. J. Daams. *Force exertion in user product interaction.* CRC Press, 2003.

[76] J. Noyes. *Designing for humans.* Psychology Press, 2002.

[77] H. O. Demirel. Sensory feedback mechanism for virtual build methodology. Master's thesis, Purdue University, 2009.

[78] N. A. Stanton. *Human factors in consumer products.* CRC Press, 1997.

[79] A. Naumann and M. Rötting. Digital human modeling for design and evaluation of human-machine systems. *MMI-Interaktiv*, 12:27–35, 2007.

[80] A. Mital, A. Desai, A. Subramanian, and A. Mital. *Product development: a structured approach to consumer product development, design, and manufacture.* Elsevier, 2014.

[81] E. B. Magrab, S. K. Gupta, F. P. McCluskey, and P. Sandborn. *Integrated product and process design and development: the product realization process.* CRC Press, 2009.

[82] M. D. Shuster. The arts and engineering [focus on education]. *Control Systems, IEEE*, 28(4):96–98, 2008.

[83] Y. Liu. The aesthetic and the ethic dimensions of human factors and design. *Ergonomics*, 46(13-14):1293–1305, 2003.

[84] J. H. Burgess. *Designing for humans: the human factor in engineering.* McGraw-Hill, 1986.

[85] J. Ward and J. Clarkson. Human factors engineering and the design of medical devices. *Handbook of Human Factors and Ergonomics in Health Care and Patient Safety. New Jersey: Lawrence Earlbaum*, pages 367–382, 2007.

[86] B. S. Blanchard and W. J. Fabrycky. *Systems engineering and analysis*, volume 4. Prentice Hall Englewood Cliffs, New Jersey, 1990.

[87] INCOSE. *Systems Engineering Handbook: A Guide for System Life Cycle Processes and Activities*. John Wiley & Sons, 2015.

[88] J. Village, C. Searcy, F. Salustri, and P. W. Neumann. Design for human factors (dfhf): a grounded theory for integrating human factors into production design processes. *Ergonomics*, (ahead-of-print):1–18, 2015.

[89] P. R. Wiese and P. John. *Engineering design in the multi-discipline era: a systems approach*. Wiley, 2003.

[90] V. Hubka and W. E. Eder. A scientific approach to engineering design. *Design Studies*, 8(3):123–137, 1987.

[91] W. Karwowski. The discipline of human factors and ergonomics. *Handbook of Human Factors and Ergonomics*, 4:3–37, 2012.

[92] A. Sundin and R. Örtengren. Digital human modeling for cae applications. *Handbook of Human Factors and Ergonomics, Third Edition*, pages 1053–1078, 2006.

[93] J. Yang, K. Abdel-Malek, K. Farrell, and K. Nebel. The iowa interactive digital-human virtual environment. In *ASME 2004 International Mechanical Engineering Congress and Exposition*, pages 1059–1067. American Society of Mechanical Engineers, 2004.

[94] H. O. Demirel, L. Zhang, and V. G. Duffy. Opportunities for meeting sustainability objectives. *International Journal of Industrial Ergonomics*, 2014.

[95] D. Lämkull, L. Hanson, and R. Örtengren. A comparative study of digital human modelling simulation results and their outcomes in reality: A case study within manual assembly of automobiles. *International Journal of Industrial Ergonomics*, 39(2):428–441, 2009.

[96] J. M. Porter, K. Case, R. Marshall, D. Gyi, and R. S. neé Oliver. beyond jack and jill: designing for individuals using hadrian. *International Journal of Industrial Ergonomics*, 33(3):249–264, 2004.

[97] K. Abdel-Malek. Human modeling and applications special issue. *Computer-Aided Design*, 39(7):539, 2007.

[98] P. Brown. Cad: Do computers aid the design process after all? *Intersect: The Stanford Journal of Science, Technology and Society*, 2(1):52–66, 2009.

[99] T. M. Cappelli and V. G. Duffy. Motion capture for job risk classifications incorporating dynamic aspects of work. Technical report, SAE Technical Paper, 2006.

[100] K. Landau. *Ergonomic software tools in product and workplace design: a review of recent developments in human modeling and other design aids*. Ergon, 2000.

[101] D. B. Chaffin. Human motion simulation for vehicle and workplace design. *Human Factors and Ergonomics in Manufacturing & Service Industries*, 2007.

[102] A. Freivalds. *Biomechanics of the upper limbs: mechanics, modeling and musculoskeletal injuries*. CRC Press, 2011.

[103] S. Konz and S. Johnson. *Work design: occupational ergonomics*. Holcomb Hathaway, Publishers, 2004.

[104] N. Özkaya, M. Nordin, D. Goldsheyder, and D. Leger. *Fundamentals of biomechanics: equilibrium, motion, and deformation*. Springer Science & Business Media, 2012.

[105] M. G. Helander. The human factors profession. *Handbook of Human Factors and Ergonomics*, pages 3–16, 1997.

[106] S. K. Chandrasegaran, K. Ramani, R. D. Sriram, I. Horváth, A. Bernard, R. F. Harik, and W. Gao. The evolution, challenges, and future of knowledge representation in product design systems. *Computer-aided esign*, 45(2):204–228, 2013.

[107] W. Hsu and I. Woon. Current research in the conceptual design of mechanical products. *Computer-Aided Design*, 30(5):377–389, 1998.

[108] V. G. Duffy and G. Salvendy. Concurrent engineering and virtual reality for human resource planning. *Computers in Industry*, 42(2):109–125, 2000.

[109] C. Wickman and R. Söderberg. Increased concurrency between industrial and engineering design using cat technology combined with virtual reality. *Concurrent Engineering*, 11(1):7–15, 2003.

[110] H. O. Demirel and V. G. Duffy. Impact of force feedback on computer aided ergonomic analyses. In *Digital Human Modeling*, pages 608–613. Springer, 2009.

[111] V. G. Duffy. Modified virtual build methodology for computer-aided ergonomics and safety. *Human Factors and Ergonomics in Manufacturing & Service Industries*, 17(5):413–422, 2007.

[112] J. Brazier. The car that jill built: A case study of the 2005 mustang. In *6th Applied Ergonomics Conference, Dallas, TX, March*, 2003.

[113] R. Tian. *Validity and Reliability of Dynamic Virtual Interactive Design Methodology*. ProQuest, 2007.

[114] T. Wu. *Reliability and Validity of Virtual Build Methodology for Ergonomics Analyses*. PhD thesis, Mississippi State University, 2005.

[115] C. P. Nemeth. *Human factors methods for design: Making systems human-centered*. CRC press, 2004.

[116] A. N. Brezing and M. Lower. Engineering and industrial design: an integrated interdisciplinary design theory. In *ASME 2008 International Design Engineering Technical Conferences and Computers and Information in Engineering Conference*, pages 351–357. American Society of Mechanical Engineers, 2008.

[117] S. Y. Baek and K. Lee. Parametric human body shape modeling framework for human-centered product design. *Computer-Aided Design*, 44(1):56–67, 2012.

[118] R. Feyen, Y. Liu, D. Chaffin, G. Jimmerson, and B. Joseph. Computer-aided ergonomics: a case study of incorporating ergonomics analyses into workplace design. *Applied Ergonomics*, 31(3):291–300, 2000.

[119] D. B. Chaffin. Improving digital human modelling for proactive ergonomics in design. *Ergonomics*, 48(5):478–491, 2005.

[120] C. M. Burns and K. J. Vicente. A participant-observer study of ergonomics in engineering design:: how constraints drive design process. *Applied Ergonomics*, 31(1):73–82, 2000.

[121] D. G. Jansson and S. M. Smith. Design fixation. *Design Studies*, 12(1):3–11, 1991.

[122] J. R. Hauser and D. Clausing. The house of quality. *Handbook of Human Factors and Ergonomics*, 66(3):63–73, 1988.

[123] Y. H. Cho and B. K. Han. Application of slim a-pillar to improve drivers field of vision. *International Journal of Automotive Technology*, 11(4):517–524, 2010.

[124] R. L. Moore and H. P. R. Smith. Paper 6: Visibility from the driver's seat: The conspicuousness of vehicles, lights and signals. In *Proceedings of the Institution of Mechanical Engineers, Conference Proceedings*, volume 181, pages 56–70. SAGE Publications, 1966.

[125] M. Sivak, B. Schoettle, M. P. Reed, and M. J. Flannagan. Body-pillar vision obstructions and lane-change crashes. *Journal of safety research*, 38(5):557–561, 2007.

[126] C. Quigley, S. Cook, and R. Tait. Field of vision (a-pillar geometry)-a review of the needs of drivers: final report. 2001.

[127] F. Vargas-Martin and M. A. Garcia-Perez. Visual fields at the wheel. *Optometry & Vision Science*, 82(8):675–681, 2005.

[128] C. M. Haslegrave. Visual aspects in vehicle design. *Automotive Ergonomics*, pages 79–98, 1993.

[129] J. P. Szlyk, K. Severing, and G. A. Fishman. Peripheral visual field loss and driving performance. 1991.

[130] M. G. Wade and C. Hammond. Forward looking blindspots: A report of a-pillar induced field-of-view obstruction and driver performance in a simulated rural environment. 2002.

[131] H. T. Zwahlen. Conspicuity of suprathreshold reflective targets in a driver's peripheral visual field at night. *Transportation Research Record*, (1213), 1989.

[132] M. P. Reed. Intersection kinematics: a pilot study of driver turning behavior with application to pedestrian obscuration by a-pillars. 2008.

[133] United Nations Economics Commission for Europe. The draft regulation on driver's field of vision. Technical report, United Nations Economics Commission for Europe, 2001.

[134] M. Sivak, B. Schoettle, M. P. Reed, and M. J. Flannagan. Influence of visibility out of the vehicle cabin on lane-change crashes. *Accident Analysis & Prevention*, 38(5):969–972, 2006.

[135] Bike Magazine. *Killer Pillars, are safer cars actually causing more accidents?*, 2015 (accessed July 28, 2015). `http://www.safespeed.org.uk/pr134.html`.

[136] Society of Automotive Engineers. *SAE J941*, 2015 (accessed July 29, 2015). `http://standards.sae.org/j941_201003/`.

[137] European Economic Community. *EEC 77/649*, 2015 (accessed July 29, 2015). `http://http://www.automotive-accessories.co.uk/docs/ForwardViewinfo.pdf`.

[138] U.S. Government Publishing Office. *Roof crush resistance; applicable unless a vehicle is certified to 571.216A*, 2015 (accessed July 29, 2015). `http://http://www.gpo.gov/fdsys/pkg/CFR-2011-title49-vol6/pdf/CFR-2011-title49-vol6-sec571-216.pdf`.

[139] drawingdatabase.com. *Volkswagen Phaeton 2011*, 2015 (accessed May 25, 2015). `http://drawingdatabase.com/volkswagen-phaeton-2011/`.

[140] Caomengxing at GrabCad. *Volkswagen Phaeton 2011 model*, 2015 (accessed May 25, 2015). `https://grabcad.com/library/phaeton`.

[141] A. Gupta and Bhardwaj S. *Body-in-white model 1*, 2015 (accessed May 25, 2015). `https://grabcad.com/library/body-in-white`.

[142] A. Gupta and Bhardwaj S. *Body-in-white model 2*. `https://grabcad.com/library/car-frame-4`, year =.

[143] S. G. Rabinovich. *Measurement errors and uncertainties: theory and practice*. Springer Science & Business Media, 2006.

[144] M. Viswanathan. *Measurement error and research design*. Sage, 2005.

[145] E. G. Carmines and R. A. Zeller. *Reliability and validity assessment*, volume 17. Sage publications, 1979.

[146] Eye Tribe. *The Eye Tribe - Eye Tracker*, 2015 (accessed May 25, 2015). `https://theeyetribe.com/products/`.

[147] J. Krauth. *Experimental design: a handbook and dictionary for medical and behavioral research*, volume 14. Elsevier, 2000.

[148] R. A. Johnson. *Statistics: principles and methods*. John Wiley & Sons, 2009.

[149] K. Black. *Business statistics: for contemporary decision making*. John Wiley & Sons, 2011.

[150] Dessault Systemes. *Virtual Ergonomics Solution*, 2015 (accessed July 31, 2015). `http://www.3ds.com/fileadmin/PRODUCTS/DELMIA/OFFERS/Virtual-Ergonomics-Solutions/PDF/DELMIA-Virtual-Ergonomics-brochure.pdf`.

[151] M. Kutz. *Mechanical Engineers' Handbook, Materials and Engineering Mechanics*, volume 1. John Wiley & Sons, 2015.

[152] M. Ben-Daya, D. Ait-Kadi, S. O. Duffuaa, J. Knezevic, and A. Raouf. *Handbook of maintenance management and engineering*, volume 7. Springer, 2009.

[153] C. R. Denegar and D. W. Ball. Research reviews, assessing reliability and precision of measurement: An introduction to lntraclass correlation and standard error of measurement. *Journal of Sport Rehabilitation*, 2:35–42, 1993.

[154] Kimberley S. Van S., S. M. Rispens, M. Pijnappels, A. Daffertshofer, and J. H. van Dieen. Assessing gait stability: the influence of state space reconstruction on inter-and intra-day reliability of local dynamic stability during over-ground walking. *Journal of biomechanics*, 46(1):137–141, 2013.

[155] W. Dankaerts, P. B. OSullivan, A. F. Burnett, L. M. Straker, and L. A. Danneels. Reliability of emg measurements for trunk muscles during maximal and sub-maximal voluntary isometric contractions in healthy controls and clbp patients. *Journal of Electromyography and Kinesiology*, 14(3):333–342, 2004.

[156] E. H. Wertheim, S. J. Paxton, and L. Tilgner. Test–retest reliability and construct validity of contour drawing rating scale scores in a sample of early adolescent girls. *Body Image*, 1(2):199–205, 2004.

[157] M. Henriksen, H. Lund, R. Moe-Nilssen, H. Bliddal, and B. Danneskiod-Samsøe. Test–retest reliability of trunk accelerometric gait analysis. *Gait & Posture*, 19(3):288–297, 2004.

[158] A. J. Flisher, J. Evans, M. Muller, and C. Lombard. Brief report: Test–retest reliability of self-reported adolescent risk behaviour. *Journal of Adolescence*, 27(2):207–212, 2004.

[159] A. Tzannes, A. Paxinos, M. Callanan, and G. A. C. Murrell. An assessment of the interexaminer reliability of tests for shoulder instability. *Journal of Shoulder and Elbow Surgery*, 13(1):18–23, 2004.

[160] W. Mendehall. *Statistics for the engineering and computer sciences*. Dellen Publishing., 1989.

[161] B. M. Ayyub and R. H. McCuen. *Probability, statistics, and reliability for engineers and scientists*. CRC press, 2011.

[162] I. H. Bernstein. *Applied multivariate analysis*. Springer Science & Business Media, 2012.

[163] A. Ainsworth. *Psychology 524: Applied Multivariate Statistics*, 2004 (accessed July 22, 2015). `http://www.csun.edu/~ata20315/psy524/docs/Psy524%20lecture%2011%20MANOVA2.pdf`.

[164] R. M. Warner. *Applied statistics: From bivariate through multivariate techniques*. Sage, 2008.

[165] L. C. Onyiah. *Design and analysis of experiments: classical and regression approaches with SAS*. CRC Press, 2008.

[166] P. Mallery. Spss for windows step by step: A simple guide and reference, 1999.

[167] L. S. Meyers, G. Gamst, and A. J. Guarino. *Applied multivariate research: Design and interpretation*. Sage, 2006.

[168] J. Nielsen and K. Pernice. *Eyetracking web usability*. New Riders, 2010.

[169] R. P. Harper and G. E. Cooper. Handling qualities and pilot evaluation. *Journal of Guidance, Control, and Dynamics*, 9(5):515–529, 1986.

[170] R. A. Zeller and E. G. Carmines. *Measurement in the social sciences: The link between theory and data*. CUP Archive, 1980.

[171] J. W. Osborne. *Best practices in quantitative methods*. Sage, 2008.

[172] J. A. Gliem and R. R. Gliem. Calculating, interpreting, and reporting cronbachs alpha reliability coefficient for likert-type scales. Midwest Research-to-Practice Conference in Adult, Continuing, and Community Education, 2003.

[173] R. D. Cook. *Concepts and applications of finite element analysis*. John Wiley & Sons, 2007.

[174] M. R. Gosz. *Finite element method: applications in solids, structures, and heat transfer*. CRC Press, 2005.

[175] C. T. F. Ross. *Finite element techniques in structural mechanics*. Elsevier, 1996.

[176] Grandt A. F. *Fundamentals of structural integrity: damage tolerant design and nondestructive evaluation*. John Wiley & Sons, 2003.

[177] J. A. Collins, H. R. Busby, and G. H. Staab. *Mechanical design of machine elements and machines: a failure prevention perspective*. John Wiley & Sons, 2010.

[178] F. Beer, E. Johnston, and J. DeWolf. Mechanics of materials, 2002, 2002.

[179] R. Shih. *Parametric Modeling with Autodesk Inventor 2014*. SDC Publications, 2013.

[180] MatWeb. *Material property database - SSAB Tunnplat Domex 420MC HSLA Steel*, 2015 (accessed July 27, 2015). `http://www.matweb.com/search/DataSheet.aspx?MatGUID=fe787d9e0a394e19a4586939687692c0`.

[181] Arcelormittal. *Material property database - SSAB Tunnplat Domex 420MC HSLA Steel*, 2015 (accessed July 27, 2015). `http://automotive.arcelormittal.com/saturnus/sheets/Recommended%20products_EN.html#`.

[182] J. Shaw, B. Engl, C. Espina, E. C. Oren, and Y. Kawamoto. Ulsab-advanced vehicle concepts-materials. Technical report, SAE Technical Paper, 2002.

[183] Tobii Pro. *Tobii Glasses 2*, 2015 (accessed July 27, 2015). `http://www.tobii.com/en/eye-tracking-research/global/`.

[184] CXC Simulation. *CXC Motion Pro II Motion Simulator*, 2015 (accessed July 27, 2015). `http://www.cxcsimulations.com/products/motion-pro/`.

[185] TNO Madymo. *Madymo (Active) Human Models*, 2015 (accessed July 27, 2015). `https://www.tassinternational.com/madymo-human-models`.

[186] Extreme Tech. *Jaguar concept car has transparent pillars*, 2015 (accessed July 27, 2015). `http://www.extremetech.com/extreme/195951-jaguar-concept-car-has-transparent-pillars-advanced-hud//-with-mario-kart-like-ghost-mode`.

[187] John T. *Process Planning: Human Simulation*, 2015 (accessed July 28, 2015). `http://www.industryweek.com/information-technology/process-planning-human-simulation`.

[188] J. R. Mkrkdtth and N. C. Surksh. Justification techniques for advanced manufacturing technologies. *International Journal of Production Research*, 24(5):1043–1057, 1986.

[189] N. Wilner, B. Koch, and T. Klammer. Justification of high technology capital investment-an empirical study. *The Engineering Economist*, 37(4):341–353, 1992.

[190] P. Van der Meulen and A. Seidl. Ramsis–the leading cad tool for ergonomic analysis of vehicles. In *Digital Human Modeling*, pages 1008–1017. Springer, 2007.

[191] T. Marler, J. Yang, S. Rahmatalla, K. Abdel-Malek, and C. Harrison. Validation methodology development for predicted posture. Technical report, SAE Technical Paper, 2007.

[192] D. Lämkull, L. Hanson, and R. Örtengren. Digital human models' appearance impact on observers' ergonomic assessment. Technical report, SAE Technical Paper, 2005.

[193] K. Abdel-Malek, J. Arora, J. Yang, T. Marler, S. Beck, C. Swan, L. Frey-Law, A. Mathai, C. Murphy, and S. Rahmatallah. Santos: A physics-based digital human simulation environment. In *Proceedings of the Human Factors and Ergonomics Society Annual Meeting*, volume 50, pages 2279–2283. SAGE Publications, 2006.

[194] A. Oudenhuijzen, J. Hudson, and G. Zehner. Verification of digital human modeling systems for cockpit accommodation studies. In *Proceedings of SAE International. Digital Human Modeling for Design and Engineering 2000, International Conference and Exposition, June*, pages 6–8, 2000.

[195] V. G. Duffy. *Handbook of digital human modeling: research for applied ergonomics and human factors engineering*. CRC press, 2008.

[196] R. L. Boring, J. C. Joe, and D. Mandelli. Human performance modeling for dynamic human reliability analysis. In *Digital Human Modeling. Applications in Health, Safety, Ergonomics and Risk Management: Human Modeling*, pages 223–234. Springer, 2015.

[197] M. P. Reed, J. Faraway, D. B. Chaffin, and B. J. Martin. The humosim ergonomics framework: A new approach to digital human simulation for ergonomic analysis. Technical report, SAE Technical Paper, 2006.

[198] Z. Zong and K. Y. Lam. Biodynamic response of shipboard sitting subject to ship shock motion. *Journal of Biomechanics*, 35(1):35–43, 2002.

[199] D. Bogosian, H. D. Avanessian, and W. Ashbery. Analytical and experimental studies to predict response of humans to blast-induced blunt trauma. Technical report, DTIC Document, 2001.

[200] W. Karwowski. Building sustainable human-centered systems: A grand challenge for the human factors and ergonomics discipline in the conceptual age. In *Corporate Sustainability as A Challenge for Comprehensive Management*, pages 117–128. Springer, 2008.

[201] K. Martin, S. Legg, and C. Brown. Designing for sustainability: ergonomics–carpe diem. *Ergonomics*, 56(3):365–388, 2013.

[202] V. G. Duffy. Improving sustainability through usability. In *Design, User Experience, and Usability. User Experience Design for Everyday Life Applications and Services*, pages 507–519. Springer, 2014.

[203] J. Peters, A. J. Hedley, C. M. Wong, T. H. Lam, S. G. Ong, J. Liu, and D. J. Spiegelhalter. Effects of an ambient air pollution intervention and environmental tobacco smoke on children's respiratory health in hong kong. *International journal of Epidemiology*, 25(4):821–828, 1996.

[204] C. C. Grant. Respiratory exposure study for fire fighters and other emergency responders. *Fire Technology*, 46(3):497–529, 2010.

[205] C. Grima-Olmedo, Á Ramírez-Gómez, L. Medic-Pejic, and J. García-Torrent. The penetration of respiratory protective devices by respirable solid particles. *Journal of Aerosol Science*, 74:36–41, 2014.

[206] G. Pahl and W. Beitz. *Engineering design: a systematic approach*. Springer Science & Business Media, 2013.

[207] J. D. Booker, M. Raines, and K. G. Swift. *Designing capable and reliable products*. Butterworth-Heinemann, 2001.

[208] N. J. Bahr. *System safety engineering and risk assessment: a practical approach*. CRC Press, 2014.

[209] N. Moray. Ergonomics and the global problems of the twenty-first century. *Ergonomics*, 38(8):1691–1707, 1995.

APPENDICES

APPENDIX A

APPROVED IRB FORM

Research Project Number __________

APPROVED
APR 03 2015
EXPIRES 2/23/2016
PURDUE UNIVERSITY
INSTITUTIONAL REVIEW BOARD

RESEARCH PARTICIPANT CONSENT FORM
A Human-in-the-loop Design Framework Based on Human Factors
Dr. Vincent G. Duffy, Associate Professor
Purdue University
Department of Industrial Engineering

What is the purpose of this study? The purpose of this research is to gather vision-of-sight data regarding obscuration created by automotive pillars. The collected data will be used to understand and evaluate the effects of pillar types and pillar models in driving safety. Design methodology proposed in this study will be used for ergonomic assessment of pillar models in computer environment.

What will I do if I chose to be in this study? Throughout this experiment you will be asked, with the help of the experimenter, to take a comfortable driving posture in front of a static driving simulator, and complete very short traffic object detection experiments. The driving simulator is composed of an adjustable seat, a large LCD monitor, an eye tracker device and cameras mounted on tripods. Before the experiment starts, you will be asked to work on a calibration task. This would include making a normal eye contact with an eye tracker device in front of the LCD monitor. Traffic object detection experiments include visual detection of traffic object that are projected to driver's perspective view. There will be three different pillar types (A, B and C/D pillars) associated with two different pillar models (Model I and II). You are asked to detect traffic objects that are hidden behind the pillar and projected in randomized order. After you complete each detection task, you are asked to fill the Object Detection form and a Cooper-Harper Test associated with each pillar type (A, B and C/D). Finally, you will be asked to complete a user experience questionnaire on pillar obscuration and two sets of questionnaires to assess pillar models.

The following procedure will be used to conduct experiments:

1. You will be asked to provide your height and weight on human subject log. This is intended both for screening for exclusions in the study and to construct your digital manikin on computer environment. (After subject data collection, the exact simulator environment will be replicated inside a computer as a post-process study. Your weight and height will be used as anthropometric inputs to create digital manikins.)
2. You will be asked to take a comfortable driving posture according to your seat adjustments. This includes raising-lowering and tilting the seat.
3. Experiment will start with eye-tracker calibration. This includes a step-by-step eye gazing to gather your eye motion behavior. Eye tracker will be only used for A-pillar tasks.
4. After eye tracker calibration is completed, you will work on various visual detection tasks. As the computer simulator turns on, you will be asked to make field-of-sight observations on a vehicle interior projected to the LCD monitor. During simulator experiment, there will be three different types of pillars corresponding to two different pillar models. There will be two different traffic objects projected behind the pillars. Traffic elements are

Initial: ______________ **Date:** ______________

Page 1

Figure A.1. Approved human participants form - Page 1.

Research Project Number __________

composed of what you could normally see on a public road (vehicles, pedestrians, bicycles). Pillar model, pillar type and traffic objects are randomized. And each task is repeated twice.

5. Each simulator task will take 3 seconds. You will be asked to stop the ongoing part of the experiment after three seconds passed.
6. Your input will be recorded on Traffic Object Detection Form before next simulation starts. It takes ~15 seconds to complete this form. Later, you will be asked to get ready for the next simulator task.
7. For Pillar Model – I, you will be asked to fill up a modified a Cooper-Harper test after completing A, B and C/D pillar tasks. It takes ~1-2 minutes to complete this test.
8. For Pillar Model – II, you will be asked to fill up a modified a Cooper-Harper test after completing A, B and C/D pillar tasks.
9. After completion of all simulator tasks, you will be asked to fill up three sets of small questionnaires. It takes ~9-15 minutes to complete all questionnaire.
10. After all simulator task and questionnaires are completed, you are required to sign off the human subject log, and exit the experiment.

How long will I be in this study? It is estimated that the total time (calibration, Obscuration Tasks, filling Object Detection Form, completing Modified Cooper-Harper Test and answering questionnaires) will take 1 hour or less (around 45-55 minutes). In this experiment, each subject is asked to finish a calibration (around 5 minutes) and work on object detection (obscuration test) experiment for two types of traffic objects for three pillar types (A, B and C/D) and two pillar modes (Type I and II). Therefore, each subject will go through 72 (2x3x2x2, corresponding to: pillar model x pillar type x traffic object x replication) obscuration tasks, which in total takes ~1.5 minutes (3 seconds per task). There will be in total of 72 Object Detection Forms (takes ~15 seconds), 6 Modified Cooper-Harper Test (takes ~1-2 minutes) and 3 questionnaires (takes ~3-5 minutes) are required to be completed.

What are the possible risk or discomforts? This research is of minimal risk to healthy individuals. You will be required to work on a visual detection task on a static driving simulator, making eye gaze over LCD monitor with minor neck movements. Though unlikely, you may feel eye-strain for a short period of time following the testing if you commonly do not stare at large LCD monitors. Breach of confidentiality is a risk, however every safeguard will be used to minimize this (please see Confidentiality section).

Are there any potential benefits? There are no direct benefits to you by participating in this study. Participants that are exposed to experiment may gain understanding about the engineering skills/knowledge that are applied on driving simulators, product development and analysis research. To society, this study aims to give further understanding of automobile pillar design and effects of pillar obscuration in field-of-view. This research would also extend the knowledge base of Digital Human Modeling research and would further help design/analyze products and workplaces which user discomfort is minimized.

Will I receive payment or other incentive? If you are taking IE 386 and/or IE 558 courses, you will receive extra credits, which are decided by the instructor, and extra credit will be maximum 3% of the student's overall grade. If you choose to quit before the experiment is completed, you will receive partial extra credits based on the amount of time that you have actually participated in the experiment. For students who do not want to participate the experiment, there will be an alternate assignment for same amount of extra credit.

Initial: ________________ **Date:** ________________

Page 2

Figure A.2. Approved human participants form - Page 2.

Research Project Number __________

Will information about my participation and me be kept confidential? The project's research records may be viewed by Prof. Vincent G. Duffy, H. Onan Demirel, School of Industrial Engineering, and by department at Purdue University for regulatory and research oversight.

To maintain confidentiality, you will be given an identification number at the start of testing which will be used in excel files and other files used to analyze the data. Your name will be kept on a sign-in sheet that will be stored in a locked cabinet for 3 years following the study and will not be kept with your data set. Your confidentiality will be maintained via the identification number mentioned above. Eye tracker data and all questionnaire feedback will be stored on a computer with an ECN login name and password in Wang Hall for 3 years following the study. Only Dr. Vincent G. Duffy and H. Onan Demirel will have access to this data and other subjects' collected information. This data may be used for future research purposes or for the publication of papers. The Purdue University Institutional Review Board or its designees to ensure that your rights are being protected may inspect the project's research records.

What are my rights if I take part in this study? Your participation in this study is voluntary. You may choose not to participate or, if you agree to participate, you can withdraw your participation at any time without penalty or loss of benefits to which you are otherwise entitled.

Who can I contact if I have questions about the study? If you have any questions, comments or concerns about this research project, you can talk H. Onan Demirel at (765) 409-9419.

If you have questions about your rights while taking part in the study or have concerns about the treatment of research participants, please call the Human Research Protection Program at (765) 494-5942, email (irb@purdue.edu)or write to:

Human Research Protection Program - Purdue University
Ernest C. Young Hall, Room 1032
155 S. Grant St.,
West Lafayette, IN 47907-2114

Documentation of Informed Consent

I have had the opportunity to read this consent form and have the research study explained. I have had the opportunity to ask questions about the research project and my questions have been answered. I am prepared to participate in the research project described above. I will receive a copy of this consent form after I sign it.

______________________________ ____________________

Participant's Signature Date

____

Participant's Name

______________________________ ____________________

Researcher's Signature Date

Initial: ______________ **Date:** ______________

Page 3

Figure A.3. Approved human participants form - Page 3.

APPENDIX B
QUICK SUMMARY

Apart from discussed limitations and weaknesses, human-in-the-loop design framework provides the method of systematically integrating human element early in the design process. It delivers tools as well as the capability of simulating numerous what-if scenarios without the need of excessive human-subject data collection. A concise 10-step summary is provided to systematically review goals, methodology and major findings of this study.

1. What is the purpose of this study (research ideas/questions)?
   The goal of this study is to introduce a human-in-the-loop design framework based on HFE methods and principles. The goal is to introduce human aspects early in the design framework.

2. What background supported (literature review)?
   An extensive literature review of Engineering Design, Industrial Design, Human Factors Engineering and System Engineering was provided. A through review of Automotive Design literature in terms of pillar obscuration zones are also explored. Theory and practice about current state-of-the-art human-centered design methods were reviewed.

3. Theoretical basis for analyzing questions/hypotheses?
   Theoretical foundations of human-in-the-loop design framework is based on Virtual Built Methodology. Hypotheses focus on validity and reliability of proposed methodology through experimental human subject data collection (eye-tracker), user-feedback (questionnaires) and simulations (FEA).

4. What are applicability/practical questions?

   The methodology and results provided in this study are directly applicable to engineering and industrial design domains, especially in automotive design. The framework introduced in this study can be applied to various HFE studies including: product design, safety, ergonomics and education.

5. What is the theoretical contribution?

   This study incorporates physical and some of the cognitive aspects of DHM theory and methods in product design. It includes human data collection, technology integration, data analysis and sketch-to-analysis type engineering design design theory.

6. What are the appropriate methodologies for carrying out the questions?

   A summary of variables, units and associated data analyses techniques were covered in Chapter 5 (Data Analysis).

7. What are the appropriate statistical analysis and assumptions?

   ANOVA and MANOVA analyses were executed to assess whether independent variables have significant effects on outcomes. Cronbach's Alpha analysis was included to check internal consistency of collected data. Reliability of repetitions (trials) were evaluated through Intra-class Correlation analysis.

8. How results are presented and what do they really mean?

   Human-in-the-loop design framework provides test-retest reliability with high fidelity. The proposed design idea (New Pillar design) provides better visualization performance with less mental workload in terms of detecting traffic objects. Subjects also rated New Pillar design higher than Old Pillar design in terms of overall visibility and visual safety. New Pillar design was within FMVSS roof-crush test limits.

9. What are the conclusions drawn: are they reasonable?

   Human-in-the-loop design framework demonstrates potential solutions to overcome issues related to human-centered design studies. It can reduce the time and cost associated with prototyping and detect safety and reliability related problems early in the design phase. Adaptation of this design methodology as a universal design framework requires further studies.

10. What are future work/research directions: any possibilities?

    There is a need for enhancing fidelity of DHM simulations and expanding the coverage of simulation tools. This study only covers a specific design problem (obscuration problem in automotive packaging). One could further develop simulation methods and tools to extend the theory and practice covered in human-in-the-loop design framework. These methods and tools could make connections to emerging technologies, sustainability, safety, quality...etc. A detailed review of future work regarding fidelity and expandability of DHM were covered in Chapter 9.1 and Chapter 9.2, under *'Fidelity'* and *'Expandability'* themes.

APPENDIX C
VEHICLE REFERENCE MODELS

C.1 Blueprint

Blueprint provided in Figure C.1 was used for construction vehicle CAD pillar model. Blueprint was taken from drawing database web resource [139]. (http://drawingdatabase.com/volkswagen-phaeton-2011/)

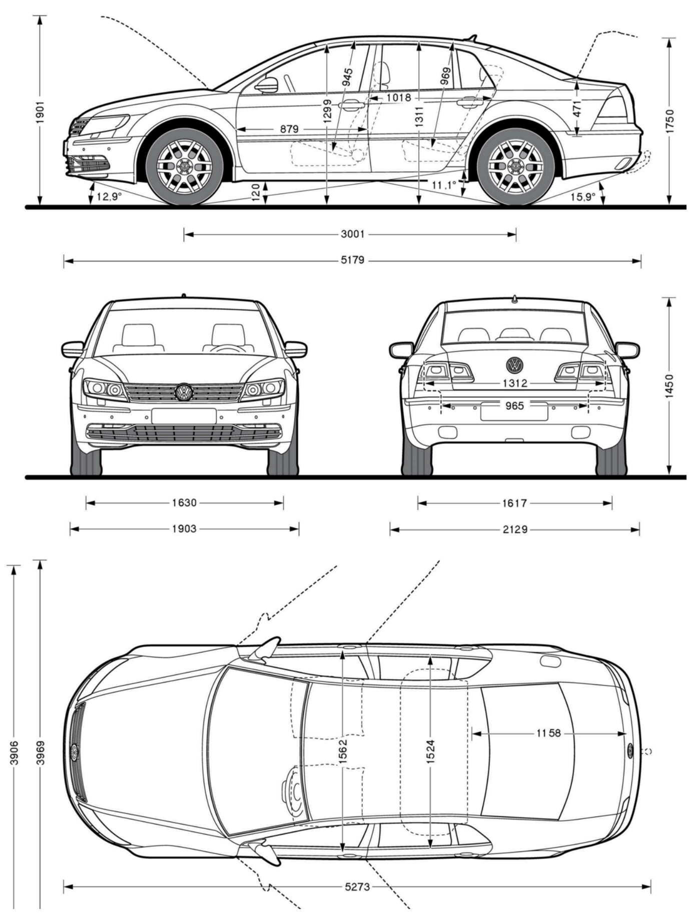

Figure C.1. A generic blueprint representation of VW Phaeton model [139].

C.2 Phaeton Model

Image credit goes to Caomengxing (https://grabcad.com/caomengxing-1/projects) from GrabCad open-source CAD community [140]. Some of the surfaces geometry and construction coordinates found on Phaeton surface model provided by Caomengxing (Figure C.2) were used as reference geometry/points during construction of CAD pillar model and representation of the vehicle.

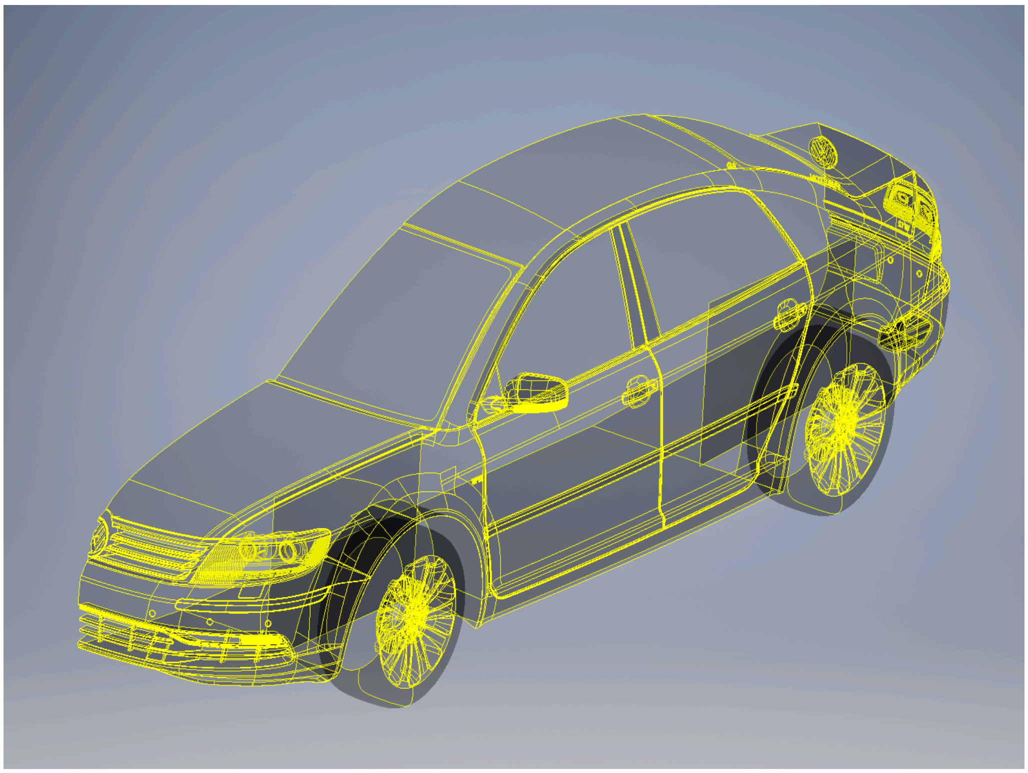

Figure C.2. VW Phaeton surface model was used inline with blueprint as reference geometry to construct CAD pillar models [140].

C.3 Body-in-white Vehicle Frame

Image credit of body-in-white geometry provided in (Figure C.3) goes both to Abhijatya Gupta (https://grabcad.com/abhijatya.gupta/projects) [141] and Sameer Bhardwaj (https://grabcad.com/sameer.bhardwaj-2/projects) [142] from GrabCad open-source CAD community. Reference points provided in Gupta's and Bhardwaj's body-in-white surface model were used as reference points, and modified to construct CAD vehicle frame.

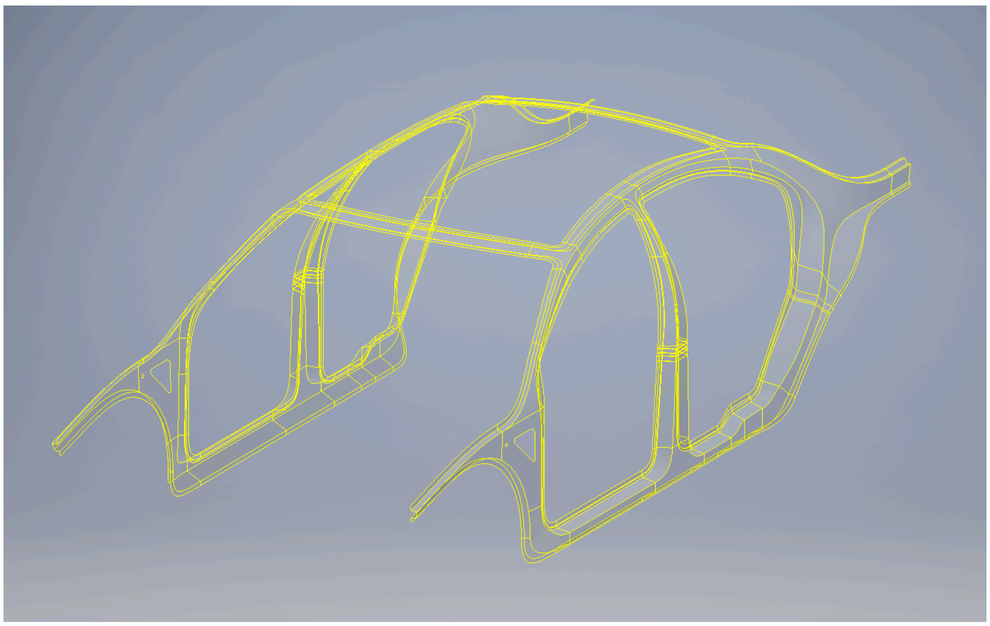

Figure C.3. A surface model representing a generic body-in-white frame of a 4-door sedan vehicle [141, 142]

.

VITA

VITA

Onan Demirel is a Ph.D. candidate under the supervision of Prof. Vincent G. Duffy in the school of Industrial Engineering at Purdue University, West Lafayette, Indiana. He received B.S and M.S degrees in Industrial Engineering from Purdue University.

In his research, Onan explores inter-dependencies and co-evolution of human element in engineering, natural and social systems. His research focuses on understanding and optimizing human performance and the well-being of the overall system. He currently works on developing a human-in-the-loop design framework, which uses Digital Human Modeling (DHM) to integrate Engineering Design, Human Factors and Systems Engineering. This framework allows visualization and scientific representation of humans in digital environment. It also embraces functional requirements (engineering design) with form aspects (industrial design), with human element at the center. His recent publications at HCII and IJIE focuses on sustainability, and representing strategies to evaluate adverse effects of indoor air quality.

He collaborated on cross-disciplinary DHM design research with companies such as Ford, Whirlpool and Cummins. He expects to begin employment as Assistant Professor at Oregon State University in the School of Mechanical, Industrial and Manufacturing Engineering.